Identifizierung und Charakterisierung von RTN-4/Nogo-Homologen in Amphibien und Fischen

Dissertation
zur Erlangung des akademischen Grades
des Doktors der Naturwissenschaften (Dr. rer. nat.)
an der Universität Konstanz
mathematisch-naturwissenschaftliche Sektion
Fachbereich Biologie
vorgelegt von Michael Klinger

Konstanz, Mai 2004

Dissertation der Universität Konstanz
Tag der mündlichen Prüfung: 15.7.2004
Referent: Prof. Dr. Claudia A. O. Stürmer
Referent: Prof. Dr. M. Groettrup

Table of Contents

1 Introduction

1.1 Regeneration in the mammalian central nervous system

Injuries to the adult mammalian central nervous system (CNS) are characterized by a failure of regrowth of transected axons, a phenomenon of broad and long lasting scientific as well as medical interest (Ramón y Cajal, 1928). Spinal cord injury in humans is the clearest example of a situation, in which the resulting axonal disconnection in the CNS leads to significant disability despite minimal neuronal death. In stark contrast to the situation in the CNS, sprouting and elongation of severed axons readily occur in the peripheral nervous system (PNS). The difference between CNS and PNS neurons in their ability to regenerate can in part be explained by the selective capacity of peripheral neurons to express neurite growth promoting proteins after axotomy (Bonilla et al., 2002; Neumann and Woolf, 1999). The lack of regeneration in the CNS, however, is due to a combination of internal and external factors and even PNS neurons show only limited growth if transplanted into the brain or spinal cord of adult vertebrates. Several lines of evidence suggest that reasons for the limited regeneration in the CNS are both cell-intrinic and non cell-autonomous. First of all, chondroitine sulfate proteoglycanes (CSPGs) that are produced by the astroglial scare at the damage site inhibit axonal growth locally (Fawcett and Asher, 1999). Indeed, functional recovery after spinal cord injury is promoted by the application of chondroitinase ABC that digests chondroitin sulfates at the site, where the astroglial scar forms (Bradbury et al., 2002). Besides the secretion of proteoglycanes, astrocytes themselves form a tight network that may provide a physical barrier to growing axons (Bandtlow and Oertle, 2002). In addition, prevention of axonal growth may be due to the expression of growth cone collapsing guidance cues like semaphorins in the regeneration zone that are normally involved in development (Pasterkamp et al., 1999).

Most prominently, factors associated with the axon sourrounding myelin sheath, made by oligodendrocytes, have been proposed to be an important source of axon growth inhibitors (Schwab and Caroni, 1988). Consistent with this view is the observation that CNS injuries in young animals, i.e. before the onset of axon myelination, are not deleterious for regeneration (Bandtlow and Oertle, 2002). The first characterized inhibitor from myelin was myelin-associated glycoprotein (MAG) (McKerracher et al., 1994; Mukhopadhyay et al., 1994). Although MAG inhibits axon growth *in vitro*, the MAG knock-out mouse did not display extensive regeneration capacities (Bartsch et al., 1995). This result prompted the search for additional myelin-associated inhibitory proteins. NI220/250, a protein that was purified from CNS myelin, was identified as the second potent inhibitor and the monoclonal antibody IN-1 raised against this protein promoted

axonal regeneration *in vitro* (Caroni and Schwab, 1988a; Caroni and Schwab, 1988b). Much interest has focused on the nature of this protein and its possible involvement in inhibition of axonal regeneration because of evidence that *in vivo* delivery of the antibody IN-1 can stimulate regeneration of axons, compensatory sprouting and enhance functional recovery in animal models of spinal cord injury (Bregman et al., 1995; Brosamle et al., 2000; Schnell and Schwab, 1990). Sequencing of the NI220/250 homologous protein from cow (Spillmann et al., 1998) resulted in six partial peptide sequences that served to clone the IN-1 antigen, now known as Nogo-A (Chen et al., 2000; GrandPré et al., 2000; Prinjha et al., 2000).

Based on sequence homology in the conserved carboxy terminal (C-terminal) part of the Nogo protein, Nogo is the fourth member of the reticulon (RTN) family, which comprises proteins that are ancored to the endoplasmatic reticulum (ER) by two transmembrane domains. Reticulon genes are widely distributed in plants, yeast and animals and for most of them the function is still elusive. In prokaryotes, no homologues have been identified so far, suggesting that RTNs emerged relatively recently in eukaryotes, potentially in paralell with the evolution of the endomenbrane system. Therefore, many RTNs might have more general functions related to the ER and be involved in intracellular trafficking, cell devision and apoptosis (Oertle and Schwab, 2003). There are four mammalian reticulon genes (RTN1-RTN4), each of which can give rise to a range of alternative transcripts by the use of different N-terminal exons. The tetralogs have similar gene structures with six conserved C-terminal exons and highly variable amino-termini (N-termini).

RTN4-A or Nogo-A, the largest of the different Nogo isoforms (Nogo-A, -B, -C, -D, -E, -F and -G) and the largest RTN protein at all, is enriched in oligodendrocytes and mostly associates with the endoplasmatic reticulum within these cells (Oertle et al., 2003d). However, Nogo-A has also been detected on the oligodendrocyte surface and on the innermost loop of the myelin membrane, where it could contact the axon (Huber et al., 2002; Wang et al., 2002c). Nogo-A has at least two inhibitory regions, one located in the A-spliceform specific N-terminus (amino-Nogo) and the other in the 66 aa loop between the two transmembrane domains of the C-terminus (Nogo-66) that is present in all Nogo transcripts (mainly Nogo-A, -B, -C; Oertle et al., 2003d). The topology of Nogo-A within the membrane is still under debate and therefore, the question which of the inhibitory sites are extra- or intracellular remains to be resolved. Nevertheless, it is conceivable that once myelin or oligodendrocytes are damaged by injury, both domains regardless of the protein-orientation at the cell surface and in the ER would become exposed to regenerating axons. *In vivo* experiments and mice lacking Nogo-A (Kim et al., 2003; Simonen et al., 2003), however, indicate that the Nogo-A N-terminus is essential.

Recently, a third myelin-associated inhibitor was identified, which, like MAG was recognized long before it was shown to be an inhibitor of axonal regeneration (Wang et al., 2002b). Oligodendrocyte myelin glycoprotein (OMgp) is a glycosylphosphatidylinositol-linked (GPI-linked) protein and, contrary to its name, is expressed not only by oligodendrocytes but also at high levels in various neurons (Habib et al., 1998). Like MAG and Nogo, OMgp induces growth cone collapse and inhibits neurite outgrowth *in vitro* (Wang et al., 2002b).

1.2 Axonal receptors for myelin related inhibitors

The identification of myelin inhibitors prompted the search for neuronal receptors that are able to transduce the inhibitory signal and to regulate axonal regeneration. Recent studies have revealed a pathway in which the three inhibitory components present in mammalian myelin, Nogo-66, MAG and OMgp interact with the same receptor complex found on neurons to prevent neurite outgrowth (Domeniconi et al., 2002; Fournier et al., 2001; Liu et al., 2002; Wang et al., 2002a; Wang et al., 2002b). This complex is currently thought to comprise three components, the Nogo-66 receptor (NgR) (Fournier et al., 2001), the p75 neurotrophin receptor, (Wang et al., 2002a) and LINGO-1 (Mi et al., 2004). Direct interaction of Nogo-66 with NgR is required to induce growth cone collapse and neurons that were unresponsive to Nogo-66 became responsive upon transfection with NgR encoding vectors (Fournier et al., 2001). In addition, interaction with NgR is essential for MAG and OMgp to exert their inhibitory effects. Since NgR is a GPI-anchored protein, the other components of the complex, p75 and LINGO-1 are required for the transduction of the signal across the membrane. Interestingly, amino-Nogo does not bind to NgR and blocking of NgR has no effect on the ability of amino-Nogo to induce growth cone collapse. This indicates that Nogo-A signals via a different, yet unknown receptor.

1.3 Regeneration in fish and amphibian

In contrast to mammals, CNS axons readily regenerate in the optic nerve and spinal cord of fish and urodeles (Gaze, 1970; Stuermer, 1988a; Stuermer, 1988b). Anura, like *Xenopus laevis*, take an intermediate position, in that retinal ganglion cell axons are capable of lifelong regeneration (Gaze, 1970) but spinal cord fiber tracts fail to regenerate after metamorphosis and axon myelination (Beattie et al., 1990).

In fish, special properties of glial cell as well as of neurons appear to contribute to the success of axonal regeneration after injury. At the morphological level, two differences in the reaction of the fish CNS compared to mammalian CNS are observed. Firstly, no glial scare comparable to that in

the mammalian CNS is formed (Bandtlow and Oertle, 2002). Oligodendrocytes dedifferentiate to elongated cells after the lesion of goldfish optic nerves and shut down the expression of myelin proteins (Ankerhold and Stuermer, 1999). These findings suggest an adaptive plasticity of goldfish oligodendrocytes beneficial to the repair of the visual pathway. The second morphological change following injury is the dramatic increase of the number of macrophages and microglia at the lesion site (Becker and Becker, 2001; Zupanc et al., 2003). As seen in the mammalian PNS, these cells can help to remove axon and myelin debris together with putative inhibitory proteins from the local environment. At the molecular level, both oligodendrocytes and most prominently neurons themselves re-express growth associated cell surface proteins (Stuermer et al., 1992; Stuermer, 1995). Goldfish oligodendrocytes re-express an L1- like adhesion protein (or E587) that has been shown to promote outgrowth of goldfish retinal axons regeneration *in vitro* (Ankerhold et al., 1998). Examples for molecules upregulated in regenerating neurons are L1, Neurolin, Thy1, Gap43, TAG-1 and many more. After transection of the optic nerve, the expression of Neurolin and E587 is upregulated in retinal ganglion cells (RGCs) (Paschke et al., 1992) and most or all RGC axons re-express Neurolin during their re-growth to the optic tectum.

As shown by *in vitro* assays, the most fundamental difference in the regeneration ability of coldblooded in contrast to warmblooded vertebrates lies in the absence of growth inhibitory molecules in the CNS of fish and in the optic nerves of frogs. Fish CNS myelin proved to possess rather growth permissive substrate properties for axons from fish, as well as for axons from amphibians, birds and mammals (Bastmeyer et al., 1991; Carbonetto et al., 1987; Lang et al., 1995; Wanner et al., 1995). However, a direct comparison of the growth cone collapsing effect exerted by mammalian oligodendrocytes *in vitro* to the effect of fish oligodendrocytes is not possible, because fish oligodendrocytes quickly dedifferentiate in cell culture and then support the growth of axons from mammals and fish (Bastmeyer et al., 1993). In cross species co-culture assays with rat oligodendrocytes, growth cones of fish retinal ganglion cell axons collaps upon contact (Bastmeyer et al., 1991; Lang and Stuermer, 1996). However, they cross the cells in the presence of IN-1, indicating that fish posess a receptor for mammalian neurite growth inhibitors although these proteins appear to be absent from fish CNS myelin.

Functional assays with CNS myelin and oligodendrocytes from frogs, i.e. *Xenopus laevis,* demonstrated that growth inhibitors comparable to the mammalian ones are present in the postmetamorphotic spinal cord where axons fail to regenerate. These inhibitors seemed to be absent from oligodendrocytes and CNS myelin of the adult *Xenopus* visual system since these axon are able to regenerate (Lang et al., 1995).

For both fish and frog, the evidence for absence of myelin associated inhibitors is indirect. Therefore, it is an intriguing question whether these organisms possess such inhibitors, i.e. RTN4-A/Nogo-A and if so, whether the gene structure, the expression pattern and the function of resulting alternative isoforms are similar to their mammalian ortologs.

1.4 Aims of this study

The primary goal of this study was to search for homologs of the mammalian neurite growth inhibitor RTN4/Nogo in frogs and fish. Phylogenetic methods were applied to examine the evolution of the whole RTN gene family and determine the evolutionary origin of the axon growth inhibitory regions within the third large exon, that is unique to RTN4-A/Nogo-A.

Expression of the various RTN4 transcripts in *Xenopus laevis* and of the different zebrafih RTN family members was analyed by RT-PCR and *Xenopus* specific antibodys were generated to examine the tissue distribution and subcellular localization of RTN-4.

Moreover, fish homologs of the mammalian NgR were cloned and analysed.

2 A reticular rhapsody: phylogenic evolution and nomenclature of the *RTN/Nogo* gene family

2.1 Abstract

RTN genes code for a family of proteins relatively recently described in higher vertebrates. The four known mammalian paralogues (RTN1, -2, -3, and -4/Nogo) have homologous C-termini with two characteristic large hydrophobic regions. Except for RTN4-A/Nogo-A, thought to be an inhibitor for neurite outgrowth restricting the regenerative capabilities of the mammalian CNS after injury, the functions of the other family members are largely unknown. The overall occurrence of RTNs in different phyla and the evolution of the RTN gene family have hitherto not been analysed. Here data is presented showing that the RTN family has arisen during early eukaryotic evolution potentially concertated to the establishment of the endomembrane system. Over 250 reticulon-like (RTNL) genes were identified in deeply diverging eukaryotes, fungi, plants and animals. A systematic nomenclature for all identified family members is introduced. The analysis of exon-intron arrangements and of protein homologies allowed to isolate key steps in the history of these genes. The data corroborate the hypothesis that present RTNs evolved from an intron-rich reticulon ancestor mainly by the loss of different introns in diverse phyla. Evidence that the exceptionally large RTN4-A-specific exon 3, which harbours a potent neurite growth inhibitory region, may have arisen *de novo* approx. 350 million years ago (MYA) during transition to land vertebrates is also presented.

These data emphasise on the one hand the universal role of reticulons in the eukaryotic system and on the other hand the acquisition of putative new functions through acquirement of novel N-terminal exons.

2.2 Introduction

The RTNs are a family of proteins, typically 200-1200 aa in length, relatively recently described in higher vertebrates (Chen et al., 2000; Moreira et al., 1999; Roebroek et al., 1998; van de Velde et al., 1994). They all share a C-terminal 150-201 aa reticulon-homology domain (Pfam PF02453) comprising two large hydrophobic regions with a ~66 aa loop in between. RTN1 was the first identified member (Roebroek et al., 1993), and is expressed in the CNS as well as in neuroendocrine cells (Senden et al., 1996; van de Velde et al., 1994). The functions of RTN1, RTN2 and RTN3 are unknown, yet all, including RTN4/Nogo, are enriched in endoplasmic reticulum membranes (Chen et al., 2000; Hamada et al., 2002; van de Velde et al., 1994). RTN

proteins are ubiquitously expressed in vertebrates and have also recently been described in *C.elegans* (Iwahashi et al., 2002). Their distribution among other metazoan phyla is still entirely undefined.

The fourth vertebrate family member, RTN4/Nogo, gives rise to a number of different isoforms both through alternative splicing and alternative promoter usage (Oertle et al., 2003a). The largest isoform, Nogo-A, has been described as a potent neurite outgrowth inhibitor of CNS myelin (Chen et al., 2000; GrandPré et al., 2000; Prinjha et al., 2000). In line with the more oligodendrocyte-restricted expression of Nogo-A (Huber et al., 2002) a stretch in the Nogo-A-specific region (NiG-Δ20, aa 544-725), which is strongly inhibitory for neurite outgrowth and cell spreading has been identified (Niederost et al., 2002; Oertle et al., 2003d). In addition, the loop region between the two C-terminal hydrophobic domains of the RHD (called Nogo-66) has been shown to induce collapse of neuronal growth cones (GrandPré et al., 2000) through interaction with a GPI-anchored receptor, NgR (Fournier et al., 2001; GrandPré et al., 2002), which simultaneously serves as a receptor for the myelin proteins OMgp (Wang et al., 2002b) and MAG (Domeniconi et al., 2002; Liu et al., 2002). Since Nogo-66 is present in all known Nogo splice-variants one would anticipate that they should all be restrictive for regenerative axons. Nogo-B, for instance, has a rather ubiquitous expression pattern (Huber et al., 2002; Li et al., 2001; Tagami et al., 2000) that is not compatible with earlier findings showing that adult CNS myelin is particularly enriched in neurite growth inhibitory factors (Schwab and Bartholdi, 1996). Because the adult CNS of lower vertebrates is able to regenerate after a lesion (Becker et al., 1998; Wood and Cohen, 1979), inhibitory components being largely absent (Bastmeyer et al., 1991; Wanner et al., 1995), a closer phylogenetic analysis of the *nogo* gene may elucidate the key evolutionary steps from lower to higher vertebrates that where required to give birth to its unique growth inhibitory function. In addition to the neurite outgrowth inhibitory character of Nogo, Nogo-B is thought to play a role in apoptosis, particularly in cancer cells (Li et al., 2001; Tagami et al., 2000), although some of the evidence is disputed (Oertle et al., 2003c).

Over 250 RTN and RTNL genes have been identified in eukaryotes. In addition, a systematic nomenclature for all the known members of the RTN family is present. Knowledge of the biological role of a shared protein in one organism can certainly illuminate, and often provide strong evidence of, its role in other organisms. The analysis is aimed not only to elucidate the evolutionary relationships between RTNs, but also to give insights into those residues that play critical roles for RTN structure and function.

2.3 Materials and methods

2.3.1 Sequences

Sequences were obtained from GenBank databases (see **Supplementary Tables 1A-G**). From expressed sequence tags (ESTs), contiguous sequences were established using SeqMan™II (DnaStar) and by non-computational analyses. Exon-intron structures were examined by comparing genomic sequences against cDNA sequences. Where possible, the GT-AG rule of splice donor and acceptor sites was respected.

2.3.2 Nomenclature

The RTN family nomenclature was performed based on the homology of the sequences (see Results). The suggested nomenclature has been approved by the HUGO Gene Nomenclature Committee, the Mouse Genomic Nomenclature Committee, the Zebrafish Nomenclature Committee, the Saccharomyces Genome Database and the Schizosaccharomyces pombe Genome Project.

2.3.3 Sequence analysis

Hydrophobicity plots were created using DAS (http://www.sbc.su.se/-miklos/DAS), TMHMM (http://www.cbs.dtu.dk/services/TMHMM-2.0/),TMPred (http://www.ch.embnet.org/software/TMPRED_form.html), and TopPred (http://bioweb.pasteur.fr/seqanal/interfaces/toppred.html) using the KD-, GVH- and GES-scale. A conservation plot (inverted Wu-Kabat variability plot) was calculated manually based on the protein sequences aligned with ClustalW and plotted using Prism. Sequence logos have been generated using GENIO/logo (http://genio.informatik.uni-stuttgart.de/GENIO/logo/logo.cgi). Bootstrap proportions and Neighbour-Joining Trees of protein sequences have been calculated using ClustalX (v.1.8) with the default parameters and ClustalW. Cladograms and trees have been drawn using TreeView (v.1.6).

2.3.4 Data deposition

The nucleotide sequences reported here have been submitted to the *GenBank*™/EBI Data Bank with accession numbers AY164656-AY164662, AY164697-AY164996, and AY262091-AY262105. They have been replaced by "Third Party Annotation" GenBank numbers (for details see revision history of each GenBank entry).

2.4 Results and discussion

2.4.1 *In silico and physical cloning of RTN and RNTL proteins*

Using the sequences of known RTN proteins, i.e. their C-terminal RHD, the public databases were searched for homologous proteins, messenger RNAs (mRNAs), genomic sequences and ESTs. In addition, RTN members from *R.norvegicus, B.taurus*, *G.gallus*, *X.laevis*, *C.auratus* and *D.rerio* were physically cloned from cDNA. From a total of 81 mRNA sequences, 48 genomic sequences, ~500 genomic traces, and ~7,500 ESTs contiguous strings were constructed encoding the total or partial sequences of 351 mRNA/proteins and isoforms arising from 272 *bona fide* independent genes from 94 different species (**Supplementary Tables 1 A-G**). Homologous genes could neither be identified in archaeal or bacterial species nor in the microsporid *Enzephalitozoon cuniculi*.

These results show that RTN-like genes are present in most eukarya and particularly in plants, where multiple duplication events led to an array of RTN paralogues in the same plant species (see **Supplementary Table 1 F**).

2.4.2 Nomenclature

The reticulon gene family is based on a cellular component ontology, i.e. proteins are considered to be members of the family if they contain at least part of an identifiable RHD (Pfam PF02453, http://www.sanger.ac.uk/cgi-bin/Pfam/getacc?PF02453) characterised by two large (>30 aa) hydrophobic regions and an about 60 aa spacer between the two regions (**Fig. 6A**). The two hydrophobic stretches are responsible for the association of RTN proteins to membranes, in particular those of the ER (Oertle et al., 2003c). The "functional" motif of RTNs and RTN-like proteins is therefore the RHD. A standardisation of the RTN nomenclature should help in the identification and understanding of new gene products and facilitate communication between scientists in different disciplines.

The following guidelines were developped: Proteins are considered to be members of the RTN or RTNL family if they contain at least part of an identifiable RHD (Pfam PF02453). "RTN" serves as the gene symbol for chordate reticulons and "RTNL" (RTN-like) for homologous proteins in non-chordate taxa. Reticulon-like genes in nonchordate metazoans are designated as RTNL, in fungi as RTNLA, in plants as RTNLB, and in protists as RTNLC. Paralogous sequences are arbitrarily numbered (1, 2, …) based on the species where the genome has been fully sequenced (*H. sapiens*, *D. melanogaster*, *C. elegans*, *S. cerevisiae*, *S. pombe*, *A. thaliana*). In distantly related species it was not always clear if a gene represents a direct orthologue or a homologue. In these cases, the gene received a separate number. If an orthologue has been duplicated in species, giving rise to two closely related paralogues, one of the two received the name of the putative ancestor orthologue and the other received a novel name (i.e. number). If the duplication is limited to a single species the novel paralogues share the same symbol and are distinguished by an additional number (.1, .2). Orthologues of different species can be distinguished by the prefixes: genus and species are indicated according to the identification codes proposed by SWISS-PROT with the exception of zebrafish (*Danio rerio*) that receives the identification code (DANRE) instead of (BRARE). Pseudogenes, if known, obtain the suffix PS and incomplete sequences the suffix w. Alternative transcripts are distingushed by a one letter suffix followed by numbers. The rule is that transcripts deriving from *different* promoters are distinguished by a different letter (e.g. -A, -B), while transcripts deriving from the *same* promoter but having different exon compositions due to splicing have the same letter but are distinguished by the following numbers (e.g. -A1, -A2). Due to historical reasons there are two exceptions from this rule: (a) RTN2-A and RTN2-B are alternative transcripts from the same promoter (and would thus be more correctly RTN2-A1 and –A2) and (b) RTN4-A and the RTN4-B transcripts are both driven by the *nogo* P1 promoter (Oertle et al., 2003a). Alternative usage of splice donor/acceptor sites within the same exon is shown by

lowercase letters (e.g. -Aa, -Ab). Some of the alternative splice-isoforms (e.g. skipping of an exon) are leading to premature translational stops due to incorrect phasing. The physiological significance of these transcripts is therefore questionable.

These nomenclature guidlines are the basis for the construction of a consistent expandable RTN nomenclature.

2.4.3 Phylogenic analysis

On the basis of the alignment of the RHD sequences from 226 distinct genes and 80 different species, a phylogenetic tree of the reticulon family has been inferred.

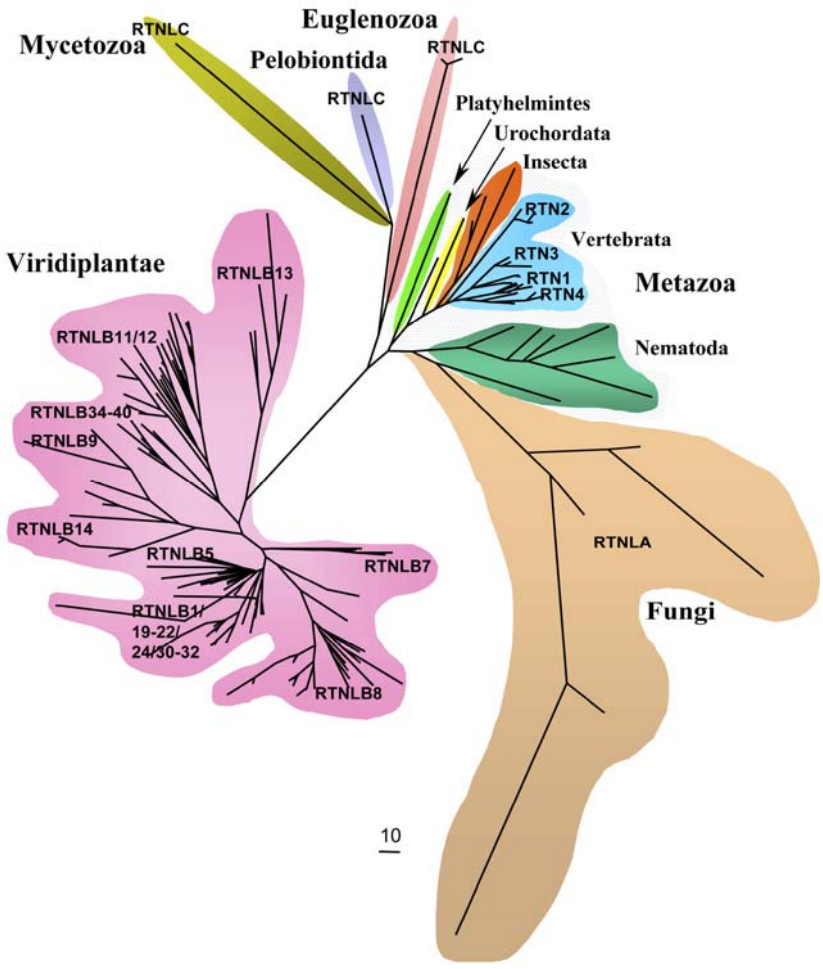

Fig. 1: *Tree diagram representing the taxonomic distribution of the RTN gene family based on alignement of the reticulon-homology domain*

RTNL genes are found in most eukaryotic kingdoms from protists to animals.

There is an excellent relationship between the clustering pattern of members in the family tree and taxonomic classification (**Fig. 1**). Similar to reticulons, many endomembrane-associated genes

have been found in most eukaryotic genomes while being absent in bacteria (Dacks and Doolittle, 2001).

In the following the different subfamilies will be discuss. First, the RTN genes and their splice isoforms are presented. Second, important evolutionary steps that happened within a subfamily are discussed. Third, known functional data of these RTN genes (e.g. protein-interaction partners), with the exception of the vertebrate reticulons where a large body of publications is already present covering these facets, will be briefly review. Finally, evolutionary features of the entire gene family as well as highly conserved residues will be exposed.

2.4.4 Chordate RTN subfamily

There are four major vertebrate reticulon paralogues, namely the previously identified *rtn1*, *rtn2*, *rtn3* and *rtn4/nogo* genes (**Fig. 2A**). All paralogues in fish, amphibians and mammals have six C-terminal exons encoding the RHD (**Fig. 2C**, **Fig. 5**; Klinger et al., 2002; Klinger et al., 2004a; Klinger et al., *submitted*).

Mammalian *rtn1* is formed by at least 10 exons and can give rise to 3 isoforms (RTN1-A, -B and –C) by alternative promoter usage (**Fig. 2C**, **Supplementary Table 1A**; Roebroek et al., 1996). *Rtn1* has been duplicated probably in euteleosts (generating the paralogue *rtn5;* Klinger et al., *submitted,* Klinger et al., 2002).

There are three known RTN2 mRNA variants (Roebroek et al., 1998) derived from 11 different exons (**Fig. 2C**). The analysis has revealed three additional minor splice variants in humans (**Supplementary Table 1A**). RTN2 is the most divergent of the mammalian tetralogues with 36 nucleotide insertions in exon 11.

The 9 exons of human *rtn3* can give rise to at least 5 isoforms (**Fig. 2C**, **Supplementary Table 1A**), from which only RTN3-A1 has so far been described in the literature (Hamada et al., 2002; Moreira et al., 1999). As previously published (Moreira et al., 1999) a RTN3 pseudogene (*rtn*3PS)exists in humans on chromosome 4. Since no intron sequences are present, this pseudogene represents a retronuon of the RTN3-A1 transcript (**Supplementary Fig. 1**).

Human *rtn4* is formed of 14 exons that can give rise to at least 10 splice-variants (**Fig. 2C**, **Supplementary Table 1A**). There is evidence that *rtn4* has been duplicated in *X.laevis* (Klinger et al., 2004a), while being present as a single gene in *S.tropicalis*, in conformity with the ancestral diploid karyotype of the genus.

In the urochordate *C.intestinalis* only a single RTN gene that can give rise to at least six different isoforms originating from both alternative splicing and the usage of three alternative

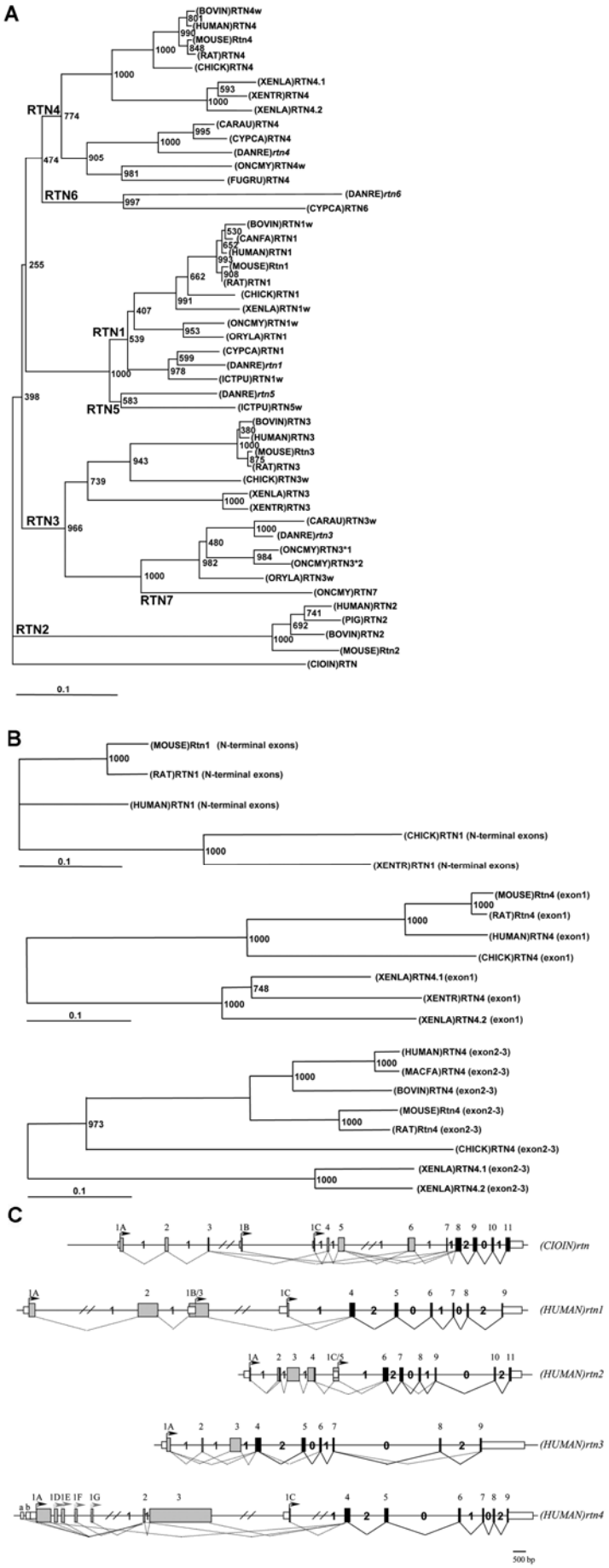

Fig. 2: *RTN-genes in chordates*

A) Cladogram displaying the different vertebrate RHDs. RTN1, -3 and -4/Nogo are the largest groups with orthologues from fish to mammals. RTN2 genes have been identified only in mammals. RTN1 and RTN3 have been duplicated in euteleosts giving rise to the RTN5 and RTN7 paralogues, respectively. The RTN6 paralogues present in euteleosts have relatively low homology to the other reticulon members. Based on cladistic analysis it is probably derived from a duplication of the RTN4/Nogo gene. Nogo has been duplicated recently in *X.laevis*. Numbers indicate the bootstrap (BS) values (for 1,000 replicate data sets). The tree is rooted taking the urochordate RHD as an outgroup.

B) Cladogram of the N-terminal exons of RTN1-A and RTN4-A. Note the higher nucleotide substitution rates in comparison to the RHD, proving non-homogeneous evolution of the reticulon genes. Numbers indicate BS values (1,000 replicates).

C) Exon-intron structure of the urochordate RTN gene and the four main mammalian RTN genes. In black are indicated exons coding for the RHD, in grey those coding for the paralogue-specific N-termini and in white boxes the untranslated regions (UTRs). Arrows are indicating the translation start sites. Numbers designate intron phasing. The exon sizes are matched according to the indicated line.

promoters was found (**Fig. 2C**, **Supplementary Table 1A**). The RHD of *C.intestinalis* is encoded by only four exons.

Vertebrate RTN1-4 are present on four different chromosomal loci, have conserved intron-exon boundaries and intron phasing of the RHD-encoding region (1-2-0-1-0-2), and are more similar to each other than to the invertebrate RTN members. The presence of a single *bona fide* RTN gene in invertebrates and the presence of the vertebrate tetralogues is in accordance with the hypothesis of genome quadruplication in amphioxus-like animals ~760-530 MYA before the cyclostome/gnathostome split (Abi-Rached et al., 2002; Spring, 1997).

Between the four vertebrate paralogues, no homology of the N-terminal exons could be identified. The divergence of the N-terminal exons within the same orthologues is also higher compared to the RHD exons demonstrating non-homogeneous evolution of the genes (**Fig. 2B**). Homologous ESTs to the N-terminal exons of *rtn1* could be identified down to *D.rerio*, while ESTs homologous to the N-terminal exon 1 of *nogo* were found in *S.tropicalis* and *X.laevis* (**Fig. 2B**). Homologous exons to the huge, 2400 bp long Nogo-A-specific exon 3 that encodes the neurite outgrowth and cell spreading inhibitory region of this protein could be found in *X.laevis*, but not in fish (**Fig. 2B**). Thus, some of the N-terminal exons seem to have arisen ~360 MYA during the transition to land vertebrates or have not yet been identified in the fish genomes. However, there are also more recent gains of exons, e.g. exon 1F of the *rtn4/nogo* gene has been newly acquired in primates after their divergence from rodents (100 MYA) (Oertle et al., 2003a).

These results demonstrate that all vertebrate RTN paralogues originated by gene duplication from an ancestor with the same RHD gene structure (see below section 2.4.11).

2.4.5 Insect RTN-like subfamily

Two RTN-like genes can be found in the *D.melanogaster* genome. The *rtnl1* gene is formed of 12 exons that can give rise to at least eleven splice-variants (**Fig. 3A**, **Supplementary Table 1B**). The RHD is formed by four C-terminal exons that are conserved in the *Anopheles gambiae* orthologue (**Fig. 3A**).

A *rtnl2* gene (formerly tropomyosin-like gene) has not been identified in the *Anopheles* genome and no ESTs originating from *rtnl2* could be found in public databases. Since the gene is in a single exon (thus lacking the typical reticulon exon-intron structure of insects) and its homology is relatively low to the other insect homologues one could speculate that this is a retronuon with pseudogene character. (DROME)Rtnl1 was trapped using a GFP-carried P1 element (it has not been recognised as a reticulon protein by the authors and was called G9). The given insertion point of the transposon would be exon 1D - according to the data presented here - and could

potentially be spliced into the -A, -B, -C isoforms of the gene. Based on these data these transcripts are expressed ubiquitously in early embryonic development and become CNS-specific late in embryogenesis (Kaushik et al., 2002). The fusion-protein is localised to the ER (Morin et al., 2001) and during cell division it is in a ring-like structure that surrounds the spindle rotating with it during neuroblasts division (Kaushik et al., 2002).

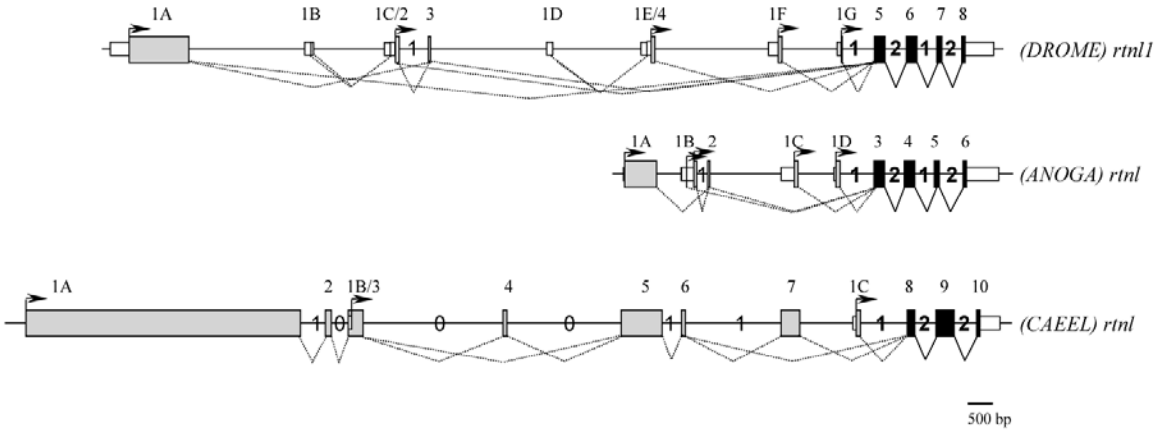

Fig. 3: *RTNL-genes in non-chordate animals*
A) Exon-intron structure of the RTNL gene of *Anopheles* and *Drosophila*.
B) Exon-intron structure of the RTNL gene of *Caenorhabditis*. Exon/intron representation as in **Fig. 2C**.

2.4.6 Nematode RTN-like subfamily

In the *C.elegans* genome one single RTN-like gene could be identified with 11 exons giving rise to at least five isoforms originating from three alternative promoter sites (**Fig. 3B**). Orthologous RTNL sequences were identified in a number of other nematodes (**Supplementary Fig. 2B**, **Supplementary Table 1C**). The RHD is formed by three C-terminal exons (**Fig. 3B**).
(CAEEL)RTNL-C (formerly nRTN-C) has been shown to be associated with ER membranes (Iwahashi et al., 2002). The protein is detectable almost exclusively during the late gastrulation stage of the embryo while mRNA is present in developing gonads and oocytes of larvae (Iwahashi et al., 2002). The N-terminal region specific for RTNL-C interacts with RME-1 (Iwahashi et al., 2002), a protein localised to the endocytic recycling compartment (ERC) and involved in the exit of proteins from ERC to the plasma membrane or to the *Trans*-Golgi network (Wendland, 2001).

2.4.7 Platyhelmints RTN-like subfamily

RTNL ESTs were identified in *S.mansoni*, a parasitic digenetic trematode belonging to the family of blood flukes (**Supplementary Table 1D**).

Although some vaccines against schistosomiasis are currently in human trials, none promises high efficacy so that the need for the identification of effective antigens for vaccination is strong (Pearce and MacDonald, 2002). Since (LEIIN)RTNLC has been successfully used as a vaccine against visceral leishmaniasis in hamster models (see below section 2.4.10) it would be of interest to envision vaccination with (SCHMA)RTNL against schistosomiasis in order to lower the T_H2 response of chronic infection.

2.4.8 Fungi RTN-like subfamily (RTNLA)

Despite otherwise stated (Iwahashi et al., 2002), RTN-like proteins could be identified both in the genome of *S.cerevisiae* as well as of *S.pombe* (**Fig. 1**, **Supplementary Fig. 2C**). In both cases single, intron-less genes encode the proteins (**Fig. 5**). *S.cerevisiae* is the only fungus where two separate genes were identified, suggestive for a separate gene duplication event consistent with previous findings (Wood et al., 2002). Orthologues were identified in different fungi, but the divergence between them is very high (**Supplementary Fig. 2C**, **Supplementary Table 1E**). The homology between (YEAST)RTN1 and (SCHPO)*rtn* is only around 25%, which is comparable to the homology between (YEAST)RTN1 and vertebrate reticulons. This is not uncommon (Sipiczki, 2000): there is evidence that yeast are generally fast-evolving organisms (Doolittle et al., 1996) and that *S.cerevisiae* and *S.pombe* diverged already 420-330 MYA (Sipiczki, 2000). Overexpression of (SCHPO)*rtn* (formerly *cwl*1+) has been shown to reduce the cell wall content (approx. 20%), to inhibit cell separation after division in the absence of thiamine, and to cause cell lysis in the absence of sorbitol (Winzeler et al., 1999). Fission and budding yeasts are viable and have no obvious phenotype after gene disruption (Burchett et al., 2002; Winzeler et al., 1999). (YEAST)RTN2 is induced by the G protein regulator Sst2 probably via a 5' stress-response element in its promoter region (Burchett et al., 2002), and is generally upregulated as a response to stressors (http://www.transcriptome.ens.fr/ymgv/).

It has been shown that (YEAST)RTN1 interacts with YOR285w and YDL089w, two genes of unknown function (Ito et al., 2001). Furthermore, RTN1 has been shown to interact with the H3/H4 histone acetyltransferase HAT2 (YEL056w), a yeast homologue of the human retinoblastoma binding protein 4 (Ho et al., 2002). (YEAST)RTN2 interacts with the inositol-1,4,5-trisposphate 5-phosphatase INP54, with the osmosensor SHO1, with karyopherin KAP104, with SEC27 involved in the ER-to-Golgi protein trafficking, and with YMR110c, an aldehyde dehydrogenase type III homologue (Ho et al., 2002; Ito et al., 2001). In conclusion, the data present not only new members of the RTN family but also new interaction partners pointing to possible functions.

2.4.9 Plant RTN-like subfamily (RTNLB)

In plants over 180 members of the RTNLB subfamily were identified (**Supplementray Fig. 3**, **Supplementary Table 1F**). *A.thaliana* has at least 15 RTNLB genes with conserved exon-intron structure and intron phasing (**Fig. 4**). The RHD domain for both *Arabidopsis* and *Oryza sativa* RTNLB genes is usually formed by four exons (generally exon 2-5) and the conserved intron phasing is 1-2-0-1. However, some exceptions exist: In *(ARATH)rtnlb5* intron IV is absent while in *(ARATH)rtnlb12* and *(ARATH)rtnlb13* intron III is absent and the two exons are fused. In *(ARATH)rtnlb6* exons 3 and 4 are non-homologous to the other paralogues, i.e. not encoding a RHD domain. The phasing of intron III in this gene is indeed different and might therefore represent an example of exon shuffling. *(ARATH)rtnlb14* lacks the last exon and *(ARATH)rtnlb15* lacks the first two exons of the RHD (**Fig. 4**). At least in two of the *A.thaliana* RTNLB genes (10 and 11) there is an additional, non-coding exon located 3' to the four RHD-encoding ones. The

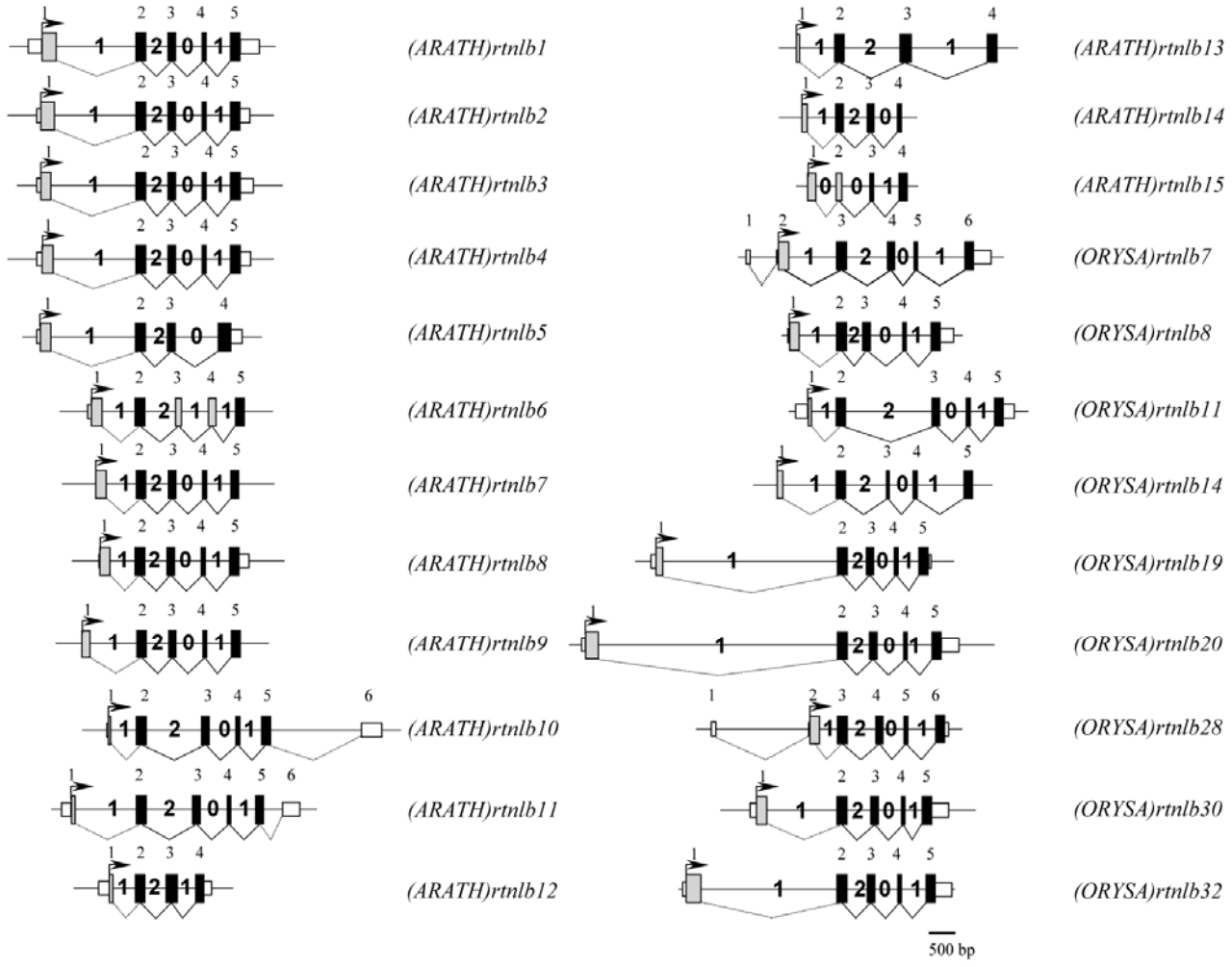

Fig. 4: *RTNLB-genes in plants*

Exon-intron structure of the RTNLB-genes identified in *Arabidopsis thaliana* and *Oryza sativa*. Exon/intron representation as in **Fig. 2C**.

phylogenetically most ancient group is probably represented by the *rtnlb10-12/18* orthologues, since they are the closest homologues of the fern *C.richardii* (*rtnlb34-35*) and the moss *P.patens* (*rtnlb36-40*) reticulons (**Fig. 1**, **Supplementary Fig. 3**).

The majority of the RTNLB genes have a single N-terminal exon with relatively low homology between the members.

2.4.10 RTN-like proteins in early-branching eukaryotes (RTNLC)

Beside the three eukaryotic kingdoms of metazoans, fungi and plants, RNTL genes were identified in euglenozoa (*Leishmania infantum* and *major*), in pelobiontida (*Mastigamoeba balamuthi*), and in mycetozoa (*Dictyostelium discoideum*) (**Fig. 1**, **Supplementary Table 1G**). Of these three subfamilies, (DICDI)RTNLC and (MASBA)RTNLC have the closest relationship in concordance with the literature (Bapteste et al., 2002). It is noteworthy that *Mastigamoeba* lack recognisable Golgi bodies. (LEIMA)RTNLC is encoded by a single, intron-less exon, while (DICDI)RTNLC is encoded by three exons (**Fig. 5**).

(LEIIN)RTNLC (formerly papLe22) has recently been described as a protein that potentially aggravates visceral leishmaniasis, that stimulates IL-10 release from patient-derived peripheral blood mononuclear cells *in vitro*, and that is found in nuclear fractions of the promastigote form (Suffia et al., 2000). The protein itself as well as anti-RTNLC antibodies have been detected in the serum of patients and specific IgG-titers correlated with the clinical status of the patients (Suffia et al., 2000). Intramuscular vaccination in hamster models with RTNLC cDNA downregulated the T_H2 response after *Leishmania* infection, and reduced episodes of *Leishmania* circulation by 50% (Fragaki et al., 2001).

2.4.11 Evolution of the intron-exon structure

Intron loss or gain represent critical steps in the divergence of expression patterns of individual gene family members, since introns are known to host regulatory elements. Intron loss can occur through an mRNA intermediate mechanism as processed retrotranscripts (Fink, 1987) or can be due to direct genomic deletion (Llopart et al., 2002). **Figure 5** shows the conservation of the intron-exon structure and intron phasing in different phyla. The most parsimonious scenario would propose an intron-rich reticulon ancestor (“Proto-Reticulon”) in early eukaryotes and multiple independent intron losses in distantly related lineages. The ancient exon-intron structure of the proto-reticulon would still be conserved in most plant genes and has been reacquired by urochordates after intron losses (**Fig. 5**).

The proposal would best fit with the intermediate view postulating that introns arose at the initiation of multicellularity. In different phyla extensive intron loss has therefore to be assumed.

However, two episodes of intron gain have also to be claimed in this model. A first phase 2 intron insertion occurred around the time period of the fungi-metazoan split. It is probable that the second insertion of the phase 0 intron antedates the tetraploidization event before the fish/tetrapode split (~500 MYA; Canestro et al., 2002) but took place after the urochordata-craniata split (**Fig. 5**). The absence of introns in yeast reticulons would fit with the theory of runaway reverse transcriptase leading to the loss of introns as a result of retroinsertions of spliced

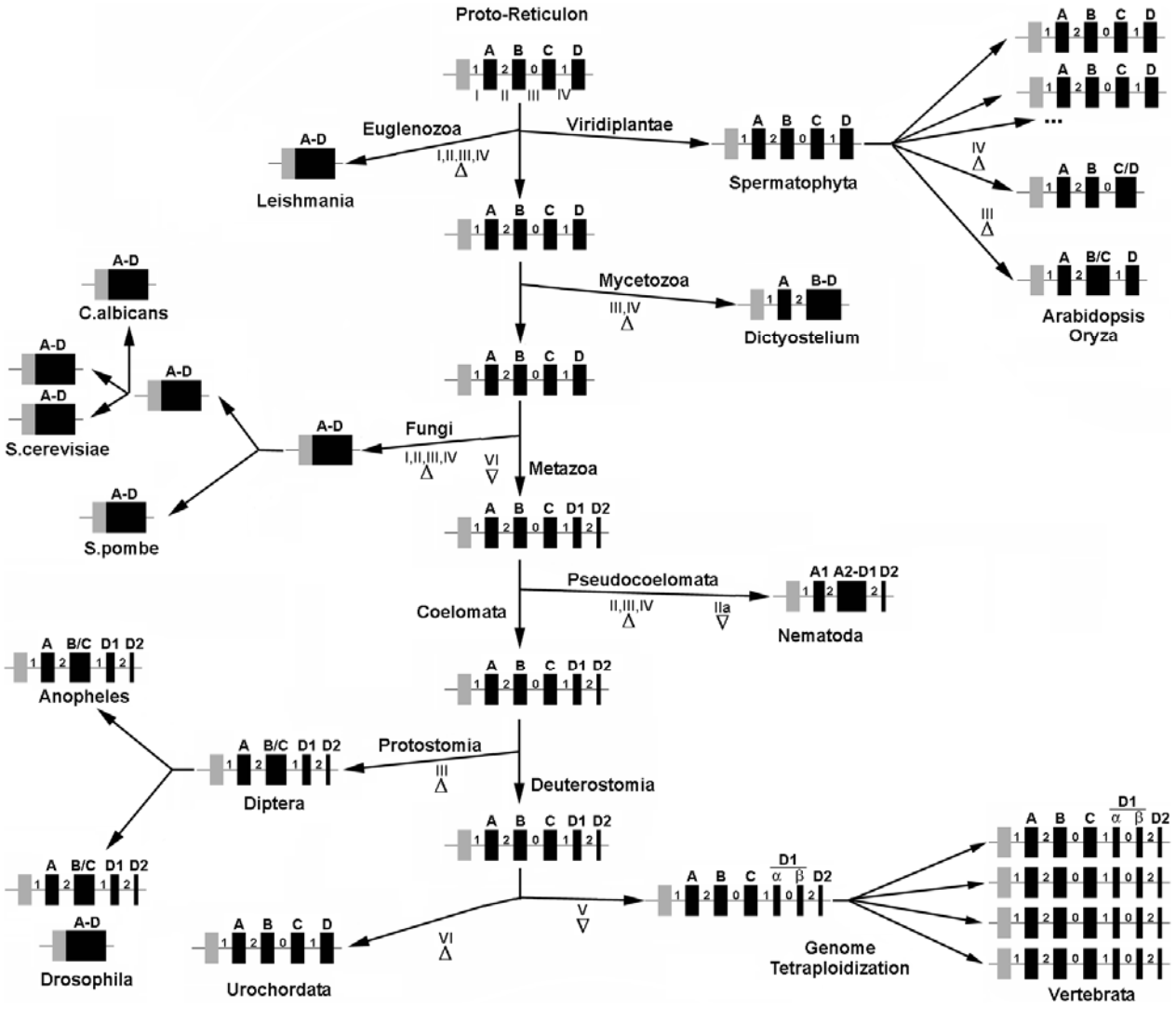

Fig. 5: *Evolution of the RTN gene family*

Most parsimonious scenario for the evolution of the RTN gene family intron-exon structure. RHD-coding exons are depicted in black. Alphabetical letters indicate exons, Latin numbers designate introns and Arabic numbers assign the intron phase. The assumed episodes of intron gains (▼) and intron losses (▲) are itemised.

messengers (Fink, 1987). Similarly, this could be the case for euglenozoa. The overrepresentation of phase 1 and 2 introns in respect to the mean percentage, as well as the overrepresentation of asymmetrical exons suggests that the proto-reticulon did not arise by classical exon shuffling

mechanisms (de Souza et al., 1998; Kolkman and Stemmer, 2001; Patthy, 1999). In contrast, the N-terminal exons are most probably newly acquired and are most often symmetrical 1-1 exons. The high rate of divergence of these N-terminal exons both between paralogues and orthologues suggest a low evolutionary pressure on these regions.

2.4.12 Variability and patterns of sequence conservation

The systematic approach allows to analyse the conservation of single amino acid residues within the RHD (**Fig. 6**). The functional importance of sites is generally believed to be inversely related to the evolutionary rate of amino acid replacement, i.e. sites of greatest functional significance are under the strongest selective constraints. Amino acids conserved in all orthologous sequences would point to the importance of such sites for a putative common function of these genes, while amino acids conserved in paralogues but different in orthologues would point to specific relevance of these sites for newly acquired functions. **Figure 6B** represents the graph for hyperconserved regions of the chordate RHD. Hyperconserved residues are concentrated in the calculated hydrophobic regions. Particularly the second putative transmembrane domain, shown to be *de rigueur* for ER-membrane association of the reticulon proteins (Oertle et al., 2003c), has highly conserved amino acids (**Fig. 6A, B**). Nine specific residues as well as five amino acid types within the canonical pattern of RHD are outstandingly conserved between *all* species of the various taxa (**Fig. 6B**). Two of them are prolines that might be critical structural residues, and five of them are aromatic amino acids that could represent essential functional residues. Proline is one of the most strongly conserved amino acids and occurs often in protein structures where the polypeptide backbone is required to adopt an unusual conformation, like the maintenance of short loops (de Prat Gay et al., 1994). The prolin at position 68 of the RHD could thus be crucial for the correct folding of the 66 aa loop. Future studies mutating these hyperconserved amino acids could give important insights into structure and function of the reticulons. Since Nogo-66 has been described as an inducer of growth cone collapse (GrandPré et al., 2000) via binding to NgR with residues 1-40 of the loop-region (NEP1-40; Fournier et al., 2001) and thus to be one of the responsible components for the lack of regeneration in the CNS of higher vertebrates, on could wondered if this unique feature is reflected by particular amino acid divergence in respect to lower vertebrates Nogo-66 and to the other RTN members, respectively.

While significant differences can be noted between Nogo-66 and the other RTN-66 regions, no major changes (i.e. amino acid substitution with different chemico-physical properties) from fish to higher vertebrates Nogo-66 can be *prime facie* observed that would allow to spot key mutations responsible for the putative gain of inhibitory activity (**Fig. 6C**).

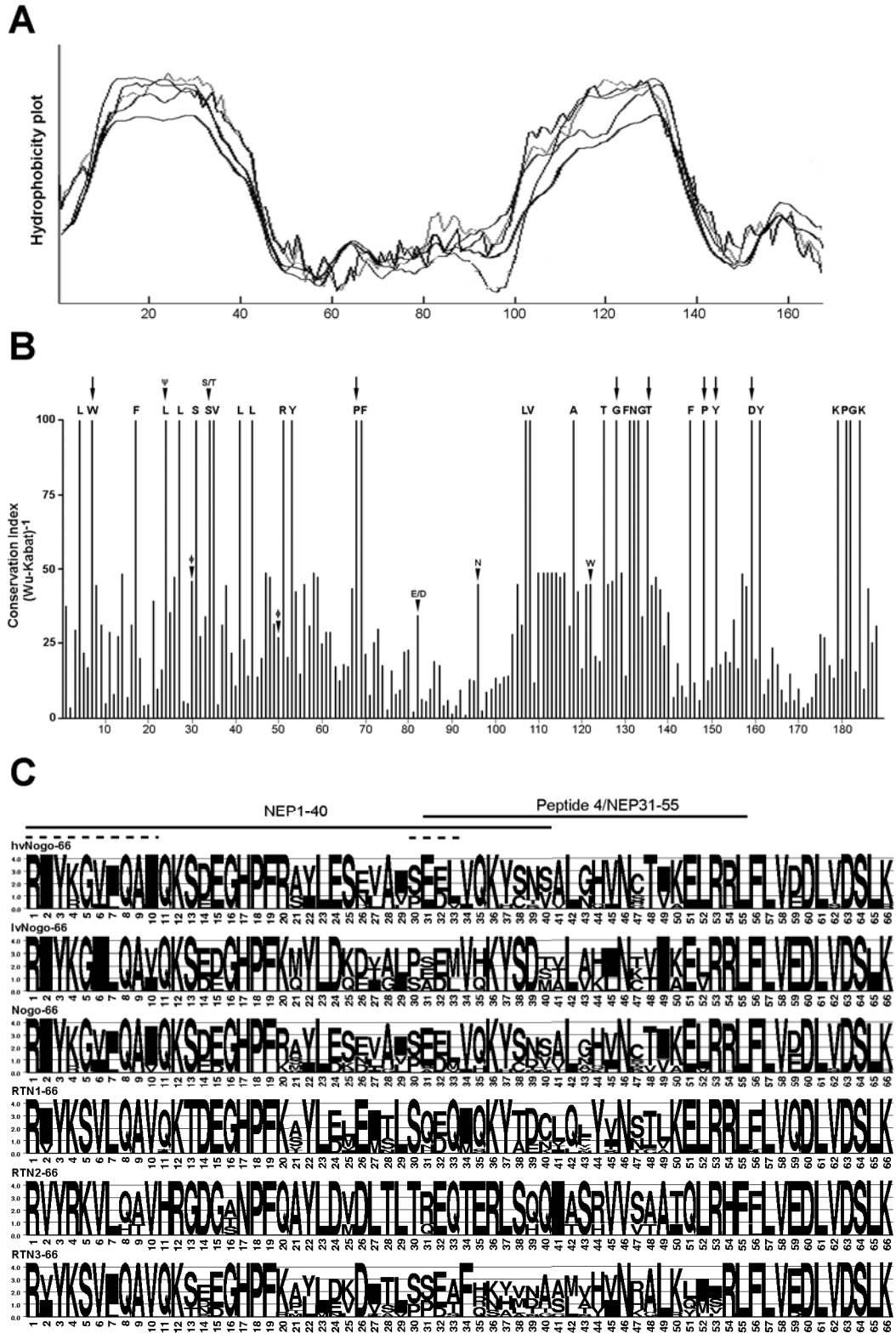

Fig. 6: *Hyperconserved regions within the reticulon-homology domain*

A) Hydrophobicity plot of the vertebrate RHD consensus sequence. The graph is an overlay of the plots calculated with the three TopPred2 scales (GvH, KD, GES), and with the algorithm based on TMbase offered by TMpred

B) Conservation plot of the RHD of all chordate members. For the residues that are 100% conserved the amino acids are displayed. The amino acids that are conserved in *all* known RTNL proteins are indicated

with arrows. Amino acid types conserved in most of the eukaryotic RTNL proteins are indicated by an arrowhead (ψ = hydrophobic residue; ϕ = aromatic residue).

C) Sequence logos of vertebrate 66-loop region. NEP1-40 is the peptide shown to bind to NgR particularly via residues 1-10 and 30-33 as indicated by dotted lines. Peptide4/NEP31-55, has been shown to be a relatively weak inducer of growth cone collapse despite its lack of binding affinity to NgR. This region is thought to be mainly responsible for the observed inhibitory properties of Nogo-66. Logos for hv-Nogo-66 (10 sequences), lv-Nogo-66 (3 sequences), Nogo-66 (13 sequences), RTN1-66 (9 sequences), RTN2-66 (4 sequences), and RTN3-66 (10 sequences) are shown (hv = higher vertebrates, i.e. amphibian to mammalian sequences; lv = lower vertebrates, i.e. fish sequences).

2.4.13 Evolution of Nogo/RTN4 in vertebrates

Concerning the evolution of RTN4/Nogo as a relevant inhibitor for neurite outgrowth it is of interest to consider if this function is in syntony with the data gathered in the present study. Nogo-66, which is part of the RHD, and NgR (Klinger et al., 2004b) are both present down to teleosts, were regeneration does occur. The Nogo-66 region is also present in all known Nogo splice variants and has therefore an almost ubiquitous tissue distribution that *strictu sensu* does not fit with the postulated constraint of inhibitors to the CNS. Sequence comparison did not allow to identify key evolutionary mutations that could have allowed Nogo-66 to become a potent inhibitory site in higher vertebrates, although the overall variability does of course not exclude an evolutionary gain of function (**Fig. 6**). Future studies will show if the orthologous fish Nogo-66 displays binding properties to and inhibitory activity via NgR and its fish orthologue or not. In contrast, the Nogo-A-specific 2400 bp long exon 3 seems to appear during the transition to land vertebrates. Both NiR-Δ2 and NiG-Δ20, shown to be inhibitory for neurite outgrowth and cell spreading (Oertle et al., 2003d), have so far no homologous counterpart in fish and are present with weak similarity in amphibians. This would be in concordance with the observation that the lack of regeneration during phylogeny was acquired during amphibian evolution and ontogenetically after metamorphosis (Beattie et al., 1990). However, based on ESTs, the amphibian Nogo-A orthologues are expressed already in embryos and tadpoles and not only after metamorphosis, similar to the situation in mammals, where Nogo-A is already present in the CNS before myelination and thus prior to the CNS-specific lack of axonal regeneration. Developmental regulation of the membrane topology and surface expression of Nogo-A might explain some of the discrepancies, but more in depth studies need to be performed on this issue. If this exceptionally long exon has originated *de novo* in amphibians, or if it has been acquired by horizontal gene transfer from a prokaryotic or viral entity can not be decided based on our current knowledge.

2.4.14 Final remarks

This study demonstrates that the evolution of the RTN genes, arisen probably during early eukaryote origin from an intron-rich ancestor, has been inhomogeneous. There is no evidence for evolutionary pressure on the highly variable N-termini of all subfamilies, in contrast to the conserved RHD. This is suggestive for a basal function of the common RHD – a function that might be shared by most of the identified members in the distinct taxa. Since the collective feature of RTNs is the association to ER membranes and in view of the fact that the RHD seems to be restricted to the eukaryotic world, on could speculate that the evolution of the RTNs was concomitant with the development of the endomembrane system approx. 1.7 billion years ago and that its function is related to it. Based on this hypothesis, the in depth study of simple model organisms might give important insights for the role of reticulons in other eukarya including plants and vertebrates, where the functions of most members are still elusive.

2.5 Acknowledgments

Thanks to Dr. A.Buss for reading the manuscript, and special thanks to Dr. H.Wain, HUGO Gene Nomenclature Committee, for excellent support, as well as Dr. L.Maltais (MGNC), Dr. K.Frazer (ZFIN), Dr. V.Wood (S.Pombe Genome Project) and Dr. S.Dwight (SGD) for collaboration on the gene nomenclature. T.O. and M.E.S were supported by the Swiss National Science Foundation (Grant No. 31-63633) and by the NCCR on Neural Plasticity and Repair, C.A.O.S. by the Deutsche Forschungsgemeinschaft (DFG, SPP) and M.K. by the "Stiftung der Deutschen Wirtschaft für Qualifizierung und Kooperation e.V.".

Published as:

Oertle, T., Klinger, M., Stuermer, C. A. O. and Schwab, M. E. (2003). A reticular rhapsody: phylogenic evolution and nomenclature of the RTN/Nogo gene family. *FASEB J.* **17**, 1238-1247.

2.6 Supplementary data

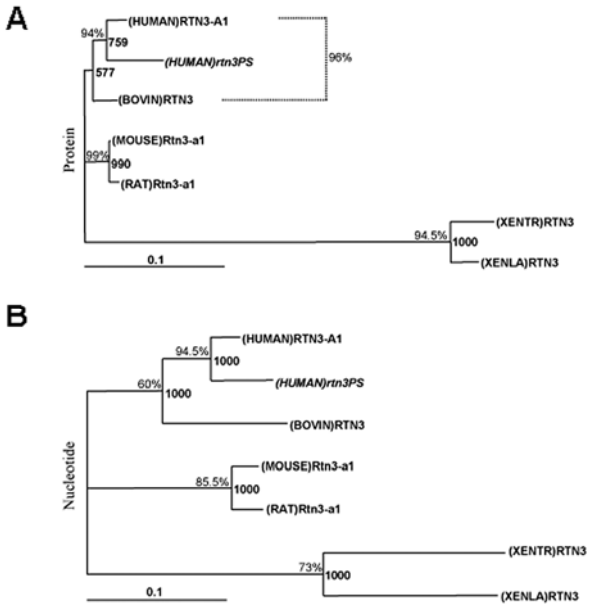

Supplementary Fig. 1: *Human rtn3PS formation*

Protein (**A**) and Nucleotide (**B**) comparison of mammalian RTN3. The nucleotide conservation of 94% suggests that the formation occurred relatively recently. The higher conservation of human to bovine RTN3 protein in comparison to human RTN3 to the translated *rtn3-PS* is suggestive for the lack of evolutionary pressure on the pseudogene coding region. Based on the nucleotide sequence comparison, the event of RTN3 reverse transcription followed by chromosomal insertion probably happened after the divergence of primates from rodents (100 MYA) and ruminants (65 MYA). In line with this hypothesis, the *rtn3* pseudogene could not be identified searching mouse genomic sequences. An indication that it is a real pseudogene, despite being still encoding a full-length reticulon protein, derives from the observation that 22% of the nucleotide substitutions between the human rtn3-A mRNA and the human chromosome 4 *rtn3PS* are due to mutations of CpG dinucleotides suggesting that they were methylated in the retronuon and that this gene was thus transcriptionally silence (data not shown). Percentages indicate the degree of identity between the sequences and numbers indicate bootstrap values (1,000 replicates). The tree is rooted taking *X.laevis* and *S.tropicalis* RTN3 as an outgroup.

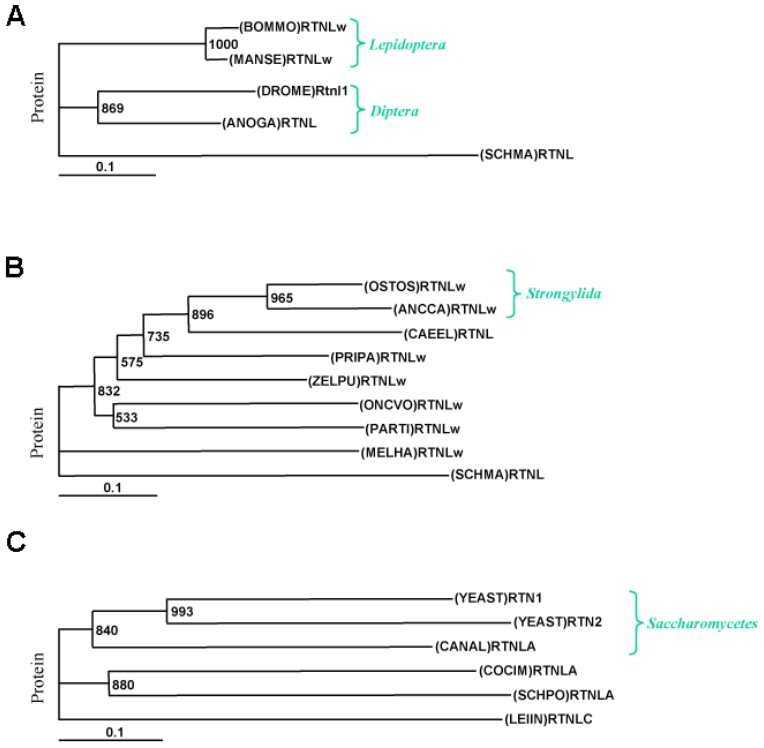

Supplementary Fig. 2: *Cladograms showing the relationship of members within specific subfamilies.*

A) Cladogram of the common region of insect RTNL proteins. Numbers indicate the bootstrap values (for 1,000 replicate data sets). The tree is rooted taking the *Schistosoma* RHD as an outgroup.

B) Cladogram of the common region of nematode RTNL proteins. Numbers indicate the bootstrap values (for 1,000 replicate data sets). The tree is rooted taking the *Schistosoma* RHD as an outgroup.

C) Cladogram of the common region of fungi RTNLA proteins. Numbers indicate the bootstrap values (for 1,000 replicate data sets). The tree is rooted taking the *Leishmania infantum* RHD as an outgroup.

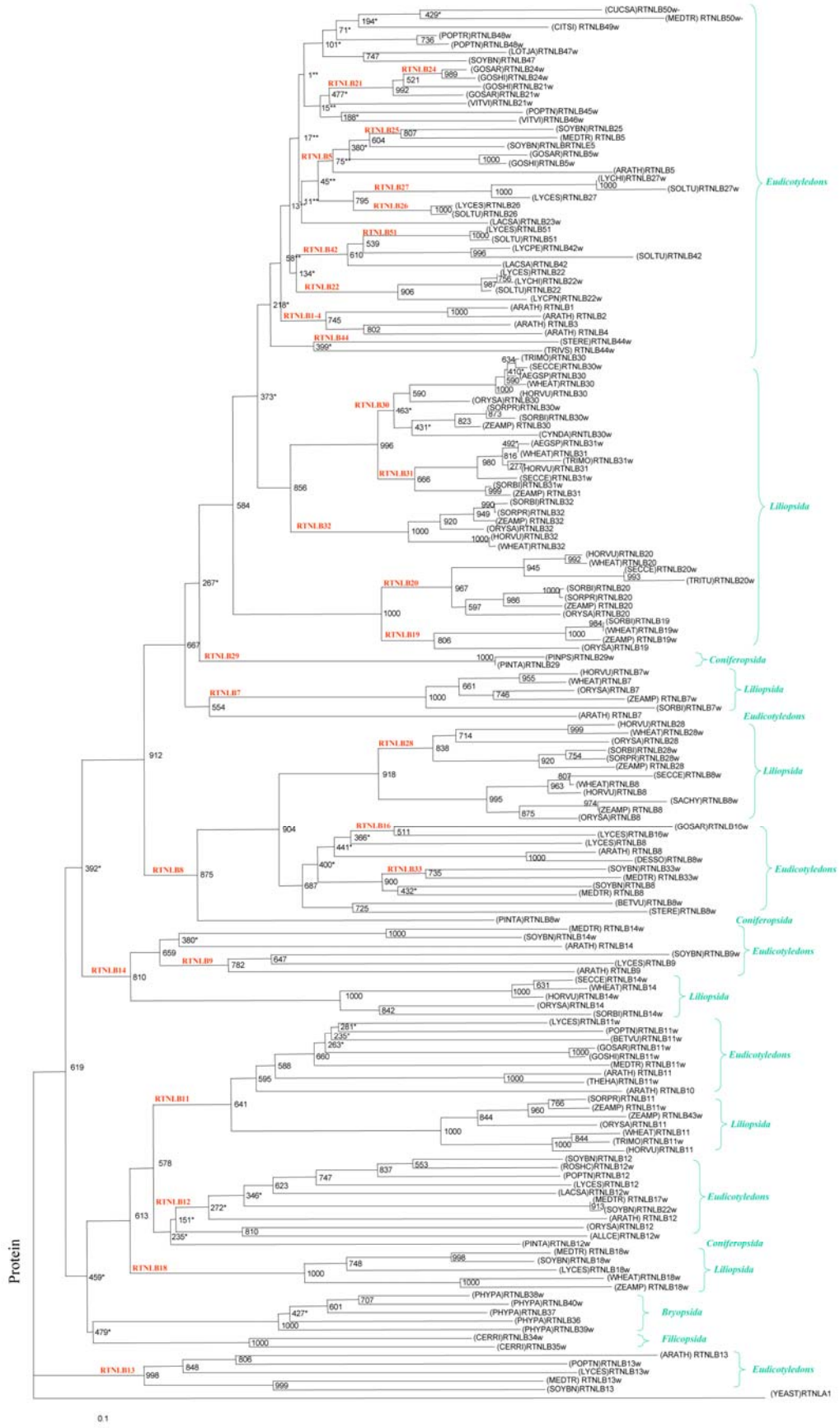

Supplementary Fig. 3: *Cladograms showing the relationship of plant RTNLB subfamily members*

Cladogram of the common region of RTNLB proteins from the phylum *Embryophyta*. The tree is rooted taking (YEAST)RTN1 RHD as an outgroup. Numbers indicate the bootstrap values (for 1,000 replicate data sets). * Indicate bootstrap proportions below 50% and ** indicate bootstrap proportions below 10%. In red some of the orthologous groups are indicated for clarity. In green the class of plant species to which the indicated reticulon members belong is indicated. Note the excellent cluster formation between the classes.

Supplementary Tables 1 A-G:

Systematic nomenclature for all the identified reticulon family members, subdivided into subfamilies (chordate, insects, nematodes, platyhelminthes, fungi, plants and protists). The nucleotide sequences reported in this paper have been submitted to the GenBank™/EBI Data Bank with accession numbers AY164656-AY164662, AY164697- AY164996, and AY262091-AY262105 They have been replaced by "Third Party Annotation" GenBank numbers (for details see revision history of each GenBank entry).

A) Chordate RTN-subfamily

B) Insect RTNL-subfamily

C) Nematode RTNL-subfamily

D) Platyhelminthes RTNL-subfamily

E) Fungi RTNLA-subfamily

F) Viridiplantae RTNLB-subfamily

G) Low-branching eukaryote RTNLC-subfamilies

Supplementary Table 1 A: *Chordate RTN subfamily*

Urochordate RTN								
Species	Gene	Transcript	Alternate symbols	Genbank Accession	Chromoso-mal locus	Number of dbESTs*	Exons	Pu-blished
Ciona intestinalis	(CIOIN)RTN			AY164660 (n)		74		
		(CIOIN)RTN-A1		AY164756		10	1A, 2, 3, 4, 5, 8, 9, 10, 11	
		(CIOIN)RTN-A2		AY164755		1	1A, 2, 3, 8, 9, 10, 11	
		(CIOIN)RTN-B1		AY164757		8	1B, 6a, 8, 9, 10, 11	
		(CIOIN)RTN-B2		AY164760		1	1B, 6b, 8, 9, 10, 11	
		(CIOIN)RTN-C1		AY164759		1	1C, 4, 5, 7, 8, 9, 10, 11	
		(CIOIN)RTN-C2		AY164758		1	1C, 4, 5, 6a, 8, 9, 10, 11	
Vertebrate RTN								
Species	Gene	Transcript	Alternative symbols	Genbank Accession	Chromoso-mal locus	Number of dbESTs*	Exons	Pu-blished
Homo sapiens	(HUMAN)RTN1		neuroendocrine-specific protein (nsp)	NT_025892, AY164662	14q21-22 (a)	approx. 320		1, 2
		(HUMAN)RTN1-A	Nsp-A	L10333, NM_021136.1		15	1A, 2, 3, 4, 5, 6, 7, 8, 9	3
		(HUMAN)RTN1-B	Nsp-B	L10334		0	1B, 3, 4, 5, 6, 7, 8, 9	3
		(HUMAN)RTN1-C	Nsp-C	L10335, BC003003		116	1C, 4, 5, 6, 7, 8, 9	3
	(HUMAN)RTN2		nspl1, nsp2	NT_011109, **AY164661**	19q13.32 (b)	approx. 190		4
		(HUMAN)RTN2-A1	Nspl1-A, RTN2-A	AF004222, **AY164714**		11	1A, 2b, 3, 4a, 5, 6, 7, 8, 9, 10, 11	4
		(HUMAN)RTN2-A2 (¢)		AY164717		2	1A, 2a, 2b, 3, 4a, 5, 6, 7, 8, 9, 10, 11	
		(HUMAN)RTN2-B1	Nspl1-B	**AY164715**		2	1A, 2b, 3, 4a, 6, 7, 8, 9, 10, 11	4
		(HUMAN)RTN2-B2		AY164718		2	1A, 2b, 3, 4a, 4b, 6, 7, 8, 9, 10, 11	
		(HUMAN)RTN2-C	Nspl1-C	AF004224, **AY164713**			1C, 6, 7, 8, 9, 10, 11	4
		(HUMAN)RTN2-D8 (¢)		AY164716		1	1A, 2b, 3, 4a, 5, 6, 7, 9, 10, 11	
	(HUMAN)RTN3		Nspl2, nsp3	NT_033241; NT_009984 (m)	11q13 (c)	approx. 700		5
		(HUMAN)RTN3-A1	RTN-3	NM_006054, AF059524, **AY164701**		approx. 280	1A, 4, 5, 6, 7, 8, 9	5
		(HUMAN)RTN3-A2		AY164704		8	1A, 2, 4, 5, 6, 7, 8, 9	
		(HUMAN)RTN3-A3 (¢)		AY164703		4	1A, 3, 4, 5, 6, 7, 8, 9	
		(HUMAN)RTN3-D5 (¢)		AY164702		1	1A, 4, 6, 7, 8, 9	
		(HUMAN)RTN3-D8 (¢)		AY164705		2	1A, 4, 5, 6, 7, 9	
	(HUMAN)RTN3PS			NT_016606	4q31.21	0		5
	(HUMAN)RTN4		nspl3, nogo, nsp-c-like	AY102285	2p16 (d)	approx. 1600		6, 7, 8
		(HUMAN)RTN4-A	Nogo-A, RTN-xL, KAIA0886	AY102279, AB020693, AB040462, AF148537		85	1A, 2, 3, 4, 5, 6, 7, 8, 9	6, 7, 9, 10
		(HUMAN)RTN4-Aa		AY123245		0	1Aa, 2, 3, 4, 5, 6, 7, 8, 9	6
		(HUMAN)RTN4-Ab		AY123246		0	1Ab, 2, 3, 4, 5, 6, 7, 8, 9	6
		(HUMAN)RTN4-B1	Nogo-B, ASY, RTN-xs, foocen-m, RTN4-B	AY102277, AB015639, AF132047, AF148538		16	1A, 4, 5, 6, 7, 8, 9	6, 9, 10
		(HUMAN)RTN4-B2		AY102278		1	1A, 2, 4, 5, 6, 7, 8, 9	6
		(HUMAN)RTN4-C	Nogo-C, vp20, foocen-s, nspc-like	AY102276, AF077050, AF087901		approx. 270	1C, 4, 5, 6, 7, 8, 9	6, 9, 10, 11

		(HUMAN)RTN4-D		AY123247		0	1D, 2, 3, 4, 5, 6, 7, 8, 9	6
		(HUMAN)RTN4-E	reticulon 5	AY123248, AF333336		0	1E, 2, 3, 4, 5, 6, 7, 8, 9	6, 12
		(HUMAN)RTN4-F		AY123249		0	1F, 2, 3, 4, 5, 6, 7, 8, 9	6
		(HUMAN)RTN4-G		AY123250		0	1G, 2, 3, 4, 5, 6, 7, 8, 9	6
Ateles belzebuth chamek	(ATEBE)RTN1					0		
		(ATEBE)RTN1-Aw	NSP	AF029167, AY164729		0		
Macaca fascicularis	(MACFA)RTN4					0		
		(MACFA)RTN4-Aw				0		13
		(MACFA)RTN4-C		AB049853, AY164742		0		
Mus musculus	(MOUSE)Rtn1		nsp	NW_000053	12 (e)	approx. 250		
		(MOUSE)Rtn1-a		AB074899, BC030455, **AY164731**		18	1A, 2, 3, 4, 5, 6, 7, 8, 9	
		(MOUSE)Rtn1-c		AK002997, AK014358, XM_127007, AY164730		17	1C, 4, 5, 6, 7, 8, 9	
	(MOUSE)Rtn2		nspl1		7 (f)	approx. 60		14, 15
		(MOUSE)Rtn2-b		NM_013648, AY164711		13	1A, 2, 3, 4, 6, 7, 8, 9, 10, 11	14
		(MOUSE)Rtn2-c		NM_013648, AY164712		4	1C, 6, 7, 8, 9, 10, 11	14
	(MOUSE)Rtn3		AW558451	NW_000139	19 (g)	approx. 650		16
		(MOUSE)Rtn3-a1	RTN3	NM_053076, **AY164700**		approx. 120	1A, 4, 5, 6, 7, 8, 9	
		(MOUSE)Rtn3-a2		AY164699		6	1A, 2, 4, 5, 6, 7, 8, 9	
	(MOUSE)Rtn4		nogo	AY102286, NW_000035	11 (h)	approx. 500		6
		(MOUSE)Rtn4-a	Nogo-A	AY102284		44	1A, 2, 3, 4, 5, 6, 7, 8, 9	6
		(MOUSE)Rtn4-b1	Nogo-B	AY102281		17	1A, 4, 5, 6, 7, 8, 9	6
		(MOUSE)Rtn4-b2		AY102282		2	1A, 2, 4, 5, 6, 7, 8, 9	6
		(MOUSE)Rtn4-c	Nogo-C	AY102283, NM_024226		14	1C, 4, 5, 6, 7, 8, 9	6
		(MOUSE)Rtn4-d		AY102280		0	1D, 2, 3, 4, 5, 6, 7, 8, 9	6
Rattus norvegicus	(RAT)Rtn1				6 (i)	23		
		(RAT)Rtn1-a	rS-Rex-b	NM_053865.1, U17604, **AY164728**		0	1A, 2, 3, 4, 5, 6, 7, 8, 9	17, 18
		(RAT)Rtn1-c	rS-Rex-s, C1-13	U17603, X52817, **AY164727**		0	1C, 4, 5, 6, 7, 8, 9	17, 18, 19
	(RAT)Rtn2				(j)	14		
		(RAT)Rtn2w		AY164710		14		
	(RAT)Rtn3				(k)	52		
		(RAT)Rtn3-a1	RTN3	AY164698		52	1A, 4, 5, 6, 7, 8, 9	
	(RAT)Rtn4				(l)	60		
		(RAT)Rtn4-a	Nogo-A	AJ242961		15	1A, 2, 3, 4, 5, 6, 7, 8, 9	20
		(RAT)Rtn4-b1	Nogo-B, foocen-m1	AJ242962, AF132046, AY164740		0	1A, 4, 5, 6, 7, 8, 9	20
		(RAT)Rtn4-b2	foocen-m2	AF132045, AY164741		0	1A, 2, 4, 5, 6, 7, 8, 9	
		(RAT)Rtn4-c	Nogo-C, Glut4 vesicle 20 kD protein	AJ242963, AF051335		0	1C, 4, 5, 6, 7, 8, 9	11, 20
		(RAT)Rtn4-a D				1	1AD, 2, 3, 4, 5, 6, 7, 8, 9	
Bos taurus	(BOVIN)RTN1					2		
		(BOVIN)RTN1-Cw		AY164734		2		
	(BOVIN)RTN2					37		
		(BOVIN)RTN2-Aw				2		
		(BOVIN)RTN2-C		AY164719		37		
	(BOVIN)RTN3					26		
		(BOVIN)RTN3		AY164707		26		
	(BOVIN)RTN4					29		
		(BOVIN)RTN4-Aw	bNI-220, Nogo-A	AY164744		2		21
Sus scrofa	(PIG)RTN1					4		
		(PIG)RTN1w (#)		AY164726		4		
	(PIG)RTN2					8		
		(PIG)RTN2-Aw		AY164709		2		
		(PIG)RTN2-C		AY164708		3		
	(PIG)RTN4					13		
		(PIG)RTN4-Aw		AY164739		1		
Canis familiaris	(CANFA)RTN1					6		
		(CANFA)RTN1-Aw		AY164733		1		
		(CANFA)RTN1-C		AY164732		3		
	(CANFA)RTN3					2		
		(CANFA)RTN3w		AY164706		2		
	(CANFA)RTN4					1		
		(CANFA)RTN4-Cw		AY164743		1		
Capra hircus	(CAPHI)RTN3					2		
		(CAPHI)RTN3w (#)				2		
Gallus gallus	(CHICK)RTN1					17		
		(CHICK)RTN1-A	chS-Rex-b	U17606, AY164724		0		18
		(CHICK)RTN1-C	chS-Rex-s	U17605, AY164723		14		18
	(CHICK)RTN3					13		
		(CHICK)RTN3w		AY164697		13		
	(CHICK)RTN4					20		
		(CHICK)RTN4-Aw				2		22
		(CHICK)RTN4-B1				0		
		(CHICK)RTN4-B2				1		
		(CHICK)RTN4-C		AY164737		2		
Columba livia	(COLLI)RTN1					2		
		(COLLI)RTN1w (#)		AY164725		2		
Xenopus laevis	(XENLA)RTN1					11		
		(XENLA)RTN1-C		AY164721		11		
	(XENLA)RTN3					12		
		(XENLA)RTN3		AY164749		12		

	(XENLA)RTN4-1					approx. 60		
		(XENLA)RTN4-1-A1				6	1A, 3, 4, 5, 6, 7, 8, 9, 10	23
		(XENLA)RTN4-1-A2				0	1A, 2, 3, 4, 5, 6, 7, 8, 9, 10	23
		(XENLA)RTN4-1-A3				0	1A, 4, 5, 6, 7, 8, 9, 10	23
		(XENLA)RTN4-1-B1				9	1A, 5, 6, 7, 8, 9, 10	23
		(XENLA)RTN4-1-B2				1	1A, 3, 5, 6, 7, 8, 9, 10	23
		(XENLA)RTN4-1-C				0	1C, 5, 6, 7, 8, 9, 10	23
		(XENLA)RTN4-1-N				8	1N, 5, 6, 7, 8, 9, 10	23
	(XENLA)RTN4-2					11		
		(XENLA)RTN4-2-A1				4	1A, 3, 4, 5, 6, 7, 8, 9, 10	23
		(XENLA)RTN4-2-A2				0	1A, 2, 3, 4, 5, 6, 7, 8, 9, 10	23
		(XENLA)RTN4-2-A3				0	1A, 4, 5, 6, 7, 8, 9, 10	23
		(XENLA)RTN4-2-B1				0	1A, 5, 6, 7, 8, 9, 10	23
		(XENLA)RTN4-2-B2				0	1A, 3, 5, 6, 7, 8, 9, 10	23
		(XENLA)RTN4-2-B3				0	1A, 2, 5, 6, 7, 8, 9, 10	23
		(XENLA)RTN4-2-C				0	1C, 5, 6, 7, 8, 9, 10	23
		(XENLA)RTN4-2-N				0	1N, 5, 6, 7, 8, 9, 10	23
Silurana tropicalis	(XENTR)RTN1					1		
		(XENTR)RTN1-Aw		AY164722		1		
	(XENTR)RTN3					12		
		(XENTR)RTN3		AY164750		12		
	(XENTR)RTN4					22		
		(XENTR)RTN4-B		AY164736		4		
		(XENTR)RTN4-N		AY164735		6		
Carassius auratus	(CARAU)RTN3					0		
		(CARAU)RTN3w		AY164748		0		
	(CARAU)RTN4					0		
		(CARAU)RTN4-M		AY164754		0		25
Danio rerio	(DANRE)*rtn1*				LG. 20	8		24
		(DANRE)*rtn1-a*				1		
		(DANRE)*rtn1-c*				7		24
	(DANRE)*rtn3*				LG. 7	11		24
		(DANRE)*rtn3*				11		24
	(DANRE)*rtn4*				LG. 6	approx. 65		24
		(DANRE)*rtn4-l1*				22	1La, 2, 3, 4, 5, 6, 7	24
		(DANRE)*rtn4-l2*				2	1Lb, 2, 3, 4, 5, 6, 7	24
		(DANRE)*rtn4-m*				0	1M, 2, 3, 4, 5, 6, 7	24
		(DANRE)*rtn4-n*				10	1N, 2, 3, 4, 5, 6, 7	24
	(DANRE)*rtn5*					approx. 80		24
		(DANRE)*rtn5-a*				1		
		(DANRE)*rtn5-b*				approx. 80		24
	(DANRE)*rtn6*					2		24
Takifugu rubripres	(FUGRU)RTN1			(Scaffold_753)		0		
		(FUGRU)RTN1w				0		
	(FUGRU)RTN3					1		
		(FUGRU)RTN3w		(JGI_17875), AY164745		1		
	(FUGRU)RTN4			(T008603 Scaffold_8604)		1		
		(FUGRU)RTN4w		(JGI_24887), AY164753		1		
Ictalurus punctatus	(ICTPU)RTN1					3		
		(ICTPU)RTN1		AY164720		3		
	(ICTPU)RTN5					3		
		(ICTPU)RTN5-Aw		AY164752		1		
		(ICTPU)RTN5-Bw		AY164751		2		
Paralichthys olivaceus	(PAROL)RTN3					4		
		(PAROL)RTN3		AY164746		4		
Oryzias latipes	(ORYLA)RTN3					1		
		(ORYLA)RTN3w		AY164747		1		

(a) LocusID: 6252
(b) LocusID: 6253
(c) LocusID: 10313
(d) LocusID: 57142
(e) LocusID: 66093
(f) LocusID: 20167
(g) LocusID: 20168
(h) LocusID: 68585
(i) LocusID: 116644
(j) LocusID: 29537
(k) LocusID: 140945
(l) LocusID: 83765
(m) Genomic contig from locus 13q13.3 probably contaminated from Chr. 11
(n) Genomic contig derived from 114 Trace sequences
(¢) Truncated protein predicted
(#) Only non-coding regions (UTR)

(1) Roebroek et al., 1996
(2) Kools et al., 1994
(3) Roebroek et al., 1993
(4) Roebroek et al., 1998
(5) Moreira et al., 1999
(6) Oertle et al., 2003
(7) Yang et al., 2000
(8) Nagase et al., 1998
(9) GrandPré et al., 2000
(10) Prinjha et al., 2000
(11) Morris et al., 1999
(12) Zhang et al., 2002
(13) Barske et al., unpublished
(14) Geisler et al., 1992
(15) Stubbs et al., 1996
(16) Hamada et al., 2002
(17) Baka et al., 1996
(18) Ninkina et al., 1997
(19) Wieczorek and Hughes, 1992
(20) Chen et al., 2000
(21) Spillmann et al., 1998
(22) Lecoq, E., Leiteritz, D., unpublished
(23) Klinger et al., in preparation
(24) Klinger et al., in preparation
(25) Simonen, Leiteritz, Lecoq, E., unpublished data

Supplementary Table 1 B: *Insecta RTNL subfamily*

Species	Gene	Transcript	Alternative symbols	Genbank Accession	Chromoso-mal locus	Number of dbESTs*	Exons	Pu-blished
Drosophila melanogaster	(DROME)Rtnl1		CG8895, G9	AY164658, AE003608, AC008233, AC009749	2L (25B9-25B10) (a)	approx. 200		
		(DROME)Rtnl1-a1		AY164765		approx. 90	1A, 5, 6, 7, 8	
		(DROME)Rtnl1-a2		AY164773		1	1A, 3, 5, 6, 7, 8	
		(DROME)Rtnl1-b1	CG8895, CT41192	AE003608, FBgn0031666, AAF52194/97, AY164774		25	1B, 2, 3, 5, 6, 7, 8	
		(DROME)Rtnl1-b2		AAF52194/97, AY164772		2	1Ba, 2, 3, 5, 6, 7, 8	
		(DROME)Rtnl1-b3		AAF52194/97, AY164771		1	1Bb, 2, 3, 5, 6, 7, 8	

		(DROME)Rtnl1-c1	CG8895, CT25554	AE003608, FBgn0031666, AAF52194/97, AY164770		9	1C, 3, 5, 6, 7, 8	
		(DROME)Rtnl1-c2		AY164768		1	1C, 5, 6, 7, 8	
		(DROME)Rtnl1-d	CG8895, CT25548	AE003608, FBgn0031666, AAF521968, AY164769		26	1D, 4, 5, 6, 7, 8	
		(DROME)Rtnl1-e		AAF521968, AY164767		4	1E, 5, 6, 7, 8	
		(DROME)Rtnl1-f	CG8895, CT25544	AE003608, FBgn0031666, AAF52195, AY164766		21	1F, 5, 6, 7, 8	
		(DROME)Rtnl1-g	CG8895, CT26268	AE003608, FBgn0031666, AAF52196, AY164775		2	1G, 5, 6, 7, 8	
	(DROME)Rtnl2		CG1279, TML84D	U51048, AE003671, AAF54008, FBgn0015831, AY164764	3R (84D9) (b)	0		
Anopheles gambiae	(ANOGA)RTNL			AY164659, AAAB01008964		36		
		(ANOGA)RTNL-A		AY164776		7	1A, 2, 3, 4, 5, 6	
		(ANOGA)RTNL-B1		AY164779		3	1Ba, 2, 3, 4, 5, 6	
		(ANOGA)RTNL-B2		AY174777		1	1Bb, 3, 4, 5, 6	
		(ANOGA)RTNL-C		AY164778		8	1C, 3, 4, 5, 6	
		(ANOGA)RTNL-D	agCP11339	EAA12900, AY164780		9	1D, 3, 4, 5, 6	
Bombyx mori	(BOMMO)RTNL					3		
		(BOMMO)RTNLw		AY164762		3		
Antheraea yamamai	(ANTYA)RTNL					1		
		(ANTYA)RTNLw		AY164763		1		
Manduca sexta	(MANSE)RTNL					1		
		(MANSE)RTNLw		AY164761		1		

* EST numbers in the row for genes represent the total number of ESTs found for this gene; EST numbers in the row of transcripts represent transcript-specific ESTs
(a) LocusID: 33721 (b) LocusID: 40903

Supplementary Table 1 C: *Nematoda RTNL subfamily*

Species	Gene	Transcript	Alternative symbols	Genbank Accession	Chromosomal locus	Number of ESTs*	Exons	Published
Caenorhabditis elegans	(CAEEL)RTNL		ret-1	AY164657	V (14,831,787. .14,846,845)	48		
		(CAEEL)RTNL-A1	W06A7.3A, Histone H4-like, nRTN-A	Z78066, CAB01522, AY164786		2	1A, 2, 3, 4, 5, 6, 7, 8, 9, 10	
		(CAEEL)RTNL-A2	W06A7.3C, nRTN-B	Z78066, CAB51467, AY164788		"	1A, 2, 3, 4, 5, 6, 8, 9, 10	
		(CAEEL)RTNL-B1		AY164789		12	1B, 4, 5, 6, 8, 9, 10	
		(CAEEL)RTNL-B2		AY164787		"	1B, 5, 6, 8, 9, 10	
		(CAEEL)RTNL-C	W06A7.3B, nRTN-C	Z78066, CAB01523, AY164790		3	1C, 8, 9, 10	1
Caenorhabditis briggsae	(CAEBR)RTNL					0		
Pristionchus pacificus	(PRIPA)RTNL	(PRIPA)RTNLw		AY164793		2		
Zeldia punctata	(ZELPU)RTNL	(ZELPU)RTNLw		AY164792		1		
Parastrongyloides trichosuri	(PARTI)RTNL	(PARTI)RTNLw		AY164791		3		
Ancylostoma caninum	(ANCCA)RTNL	(ANCCA)RTNLw		AY164785		4		
Ostertagia ostertagi	(OSTOS)RTNL	(OSTOS)RTNLw		AY164783		2		
Onchocerca volvulus	(ONCVO)RTNL	(ONCVO)RTNLw		AY164782		1		
Brugia malayi (a)						0		
Meloidogyne hapla	(MELHA)RTNL	(MELHA)RTNLw		AY164781		1		
Ascaris suum	(ASCSU)RTNL	(ASCSU)RTNLw		AY164794		1		
Necator americanus	(NECAM)RTNL	(NECAM)RTNLw		AY164784		2		

* EST numbers in the row for genes represent the total number of ESTs found for this gene; EST numbers in the row of transcripts represent transcript-specific ESTs
(a) TIGR Brugia malayi DB (1) Iwahashi et al., 2002

Supplementary Table 1 D: *Platyhelminthes RTNL subfamily*

Species	Gene	Transcript	Alternative symbols	Genbank Accession	Chromosomal locus	Number of ESTs	Exons	Published
Schistosoma mansoni	(SCHMA)RTNL	(SCHMA)RTNL		AY164795		43		

Supplementary Table 1 E: *Fungi RTNLA subfamily*

Species	Gene	Transcript	Alternative symbols	Genbank Accession	Chromosomal locus	Number of dbESTs	Exons	Published
Saccharomyces cerevisiae	(YEAST)RTN1	(YEAST)RTN1	YDR233c, (YEAST)RTNLA1 (ç)	NP_010519, S59439, Q04947, Z48612, AY164798	IV (930348-929461)	3		
	(YEAST)RTN2	(YEAST)RTN2	YDL204w, (YEAST)RTNLA2 (ç)	NP_010077, S67763, CAA98782, Q12443, Z74252, AY164797	IV (94606-95787)	1		

Schizosaccharomyces pombe	(SCHPO)*rtn*	(SCHPO)*rtn*	*cwl1*, SPBC31A8.01c, (SCHPO)RTNLA (ç)	CAA64219, T40196, S71746, CAB37609, P53694, AY164796	II (1183303-1182377)	0		1
Candida albicans	(CANAL)RTNLA		IPF14247	AY164799		0		
Coccidioides immitis	(COCIM)RTNLA	(COCIM)RTNLAw		AY164800		4		

(1) Godoy et al., 1996; Wood et al., 2002

(ç) For S.cerevisiae and S.pombe the official name was adapted according to the Saccharomyces and Schizosaccharomyces Nomenclature Committee Guidelines. As alternative symbol the symbol which would be in line with the Reticulon Nomenclature Guidelines is presented.

Supplementary Table 1 F: *Viridiplantae RTNLB subfamily*

Species	Gene	Transcript	Alternative symbols	Genbank Accession	Chromosomal locus	Number of ESTs	Exons	Published
Arabidopsis thaliana	(ARATH)RTNLB1		F9D16.100, AT4G23630	AL161559	4			
		(ARATH)RTNLB1		AL035394, CAA23029, CAB79318, AY050321, AAK91338, T05595, NP_194094, AY164888		65		
	(ARATH)RTNLB2		F8L21.10, At4g11220	AL096882	4			
		(ARATH)RTNLB2		CAB51406, AL161531, CAB81223, AY057606, AAL14401, AY034901, AAK59408, AAK82535, T13013, NP_192861, AY164887		11		
	(ARATH)RTNLB3		F22C12.15	AC007764	1			
		(ARATH)RTNLB3		AAF24576, AAL36421.1, NP_176592, AY164886		13		
	(ARATH)RTNLB4		MBK23.13	AB005233	5			
		(ARATH)RTNLB4		BAB11466, AY057638, AAL15269, AY035169, AAK59673, NP_198975, AY164885		13		
	(ARATH)RTNLB5		At2g46170	AC005397	2			
		(ARATH)RTNLB5		AAC62889, AY053421, AAK96651, AAL69534, NP_566065, AY164884		6		
	(ARATH)RTNLB6		F2A19.160	AL132962	3			
		(ARATH)RTNLB6		CAB71086, T47948, NP_191715, AY164883		1		
	(ARATH)RTNLB7		AT4G01230	AL161491	4			
		(ARATH)RTNLB7		CAB80932, NP_192032, AY164882		0		
	(ARATH)RTNLB8		F14w13.14	AC009400	3			
		(ARATH)RTNLB8		AAF02816, AY045830, AAK76504, AAM14307, NP_566371, AY164881		11		
	(ARATH)RTNLB9		MIE15.4	AP000414	3			
		(ARATH)RTNLB9		AY087239, AAM64795, BAB01175, NP_566604, AY164880		0		
	(ARATH)RTNLB10		At2g15280	AC007267	2			
		(ARATH)RTNLB10		AAD26905, NP_179130, AY164894		2		
	(ARATH)RTNLB11		MLD14.20, At3g19460	NC_003074	3			
		(ARATH)RTNLB11		AAD26905, AB025624, AY097614, AAM65155, BAB02471, NP_566635, AY164893		3		
	(ARATH)RTNLB12		F24B22.80	AL132957	3			
		(ARATH)RTNLB12		CAB70986, T47571, NP_190980, AY164892		2		
	(ARATH)RTNLB13		At2g23640	AC004482	2			
		(ARATH)RTNLB13		AAC17096, T01153, AAM14868, NP_565555, AY164891		0		
	(ARATH)RTNLB14		T22E19.14	AC016447	1			
		(ARATH)RTNLB14		AAG52605, NP_176990, AY164890		0		
	(ARATH)RTNLB15		At2g01240	AC006200	2			
		(ARATH)RTNLB15		AAD14524, NP_178233, AY164889		0		
Brassica rapa	(BRARP)RTNLB3 (£)	(BRARP)RTNLB3w (£)		AY164877		1		
	(BRARP)RTNLB5	(BRARP)RTNLB5w		AY164876		1		
	(BRARP)RTNLB6 (£)	(BRARP)RTNLB6w (£)		AY164879		1		
	(BRARP)RTNLB8 (£)	(BRARP)RTNLB8w (£)		AY164875		1		
	(BRARP)RTNLB22 (£)	(BRARP)RTNLB22w (£)		AY164878		1		
Citrus sinensis	(CITSI)RTNLB22 (£)	(CITSI)RTNLB22 (£)		AY164873		1		
	(CITSI)RTNLB49 (£)	(CITSI)RTNLB49w (£)		AY164874		4		
Cucumis sativus	(CUCSA)RTNLB50	(CUCSA)RTNLB50w (£)		AY164872		2		
Descurainia sophia	(DESSO)RNTLE8	(DESSO)RTNLB8w		AY164871		2		
Euphorbia esula	(EUPES)RTNLB22 (£)	(EUPES)RTNLB22w (£)		AY164870		1		
Glycine max	(SOYBN)RTNLB5	(SOYBN)RTNLB5		AY164859		29		
	(SOYBN)RTNLB8	(SOYBN)RTNLB8		AY164858		14		
	(SOYBN)RTNLB9	(SOYBN)RTNLB9w		AY164857		4		
	(SOYBN)RTNLB12	(SOYBN)RTNLB12		AY164868		4		

	(SOYBN)RTNLB13	(SOYBN)RTNLB13		AF004806, AAD01540, AY164867		0		
	(SOYBN)RTNLB14	(SOYBN)RTNLB14w		AY164866		1		
	(SOYBN)RTNLB18	(SOYBN)RTNLB18w		AY164865		3		
	(SOYBN)RTNLB22	(SOYBN)RTNLB22w		AY164869		4		
	(SOYBN)RTNLB25	(SOYBN)RTNLB25*1		AY164862		24		
		(SOYBN)RTNLB25*2		AY164861		10		
	(SOYBN)RTNLB33	(SOYBN)RTNLB33w		AY164860		7		
	(SOYBN)RTNLB47	(SOYBN)RTNLB47*1		AY164864		24		
		(SOYBN)RTNLB47*2		AY164863		20		
Gossypium arboreum	(GOSAR)RTNLB5	(GOSAR)RTNLB5w		AY164852		3		
	(GOSAR)RTNLB11	(GOSAR)RTNLB11		AY164856		2		
	(GOSAR)RTNLB16	(GOSAR)RTNLB16w		AY164855		2		
	(GOSAR)RTNLB21	(GOSAR)RTNLB21w		AY164854		2		
	(GOSAR)RTNLB24	(GOSAR)RTNLB24w		AY164853		1		
Gossypium hirsutum	(GOSHI)RTNLB5	(GOSHI)RTNLB5w		AY164848		3		
	(GOSHI)RTNLB11	(GOSHI)RTNLB11w		AY164851		1		
	(GOSHI)RTNLB21	(GOSHI)RTNLB21w		AY164850		1		
	(GOSHI)RNTLE24	(GOSHI)RTNLB24w		AY164849		1		
Lotus japonicus	(LOTJA)RTNLB47	(LOTJA)RTNLB47w		AY164847		25		
Manihot esculenta	(MANES)RTNLB22 (£)	(MANES)RTNLB22w (£)		AY164846		1		
Medicago truncatula	(MEDTR)RTNLB5	(MEDTR)RTNLB5 (£)		AY164934		4		
	(MEDTR)RTNLB8	(MEDTR)RTNLB8		AY164933		8		
	(MEDTR)RTNLB11	(MEDTR)RTNLB11w		AY164941		3		
	(MEDTR)RTNLB13	(MEDTR)RTNLB13w		AY164940		3		
	(MEDTR)RTNLB14	(MEDTR)RTNLB14w		AY164939		6		
	(MEDTR)RTNLB17	(MEDTR)RTNLB17w		AY164938		1		
	(MEDTR)RTNLB18	(MEDTR)RTNLB18w		AY164937		1		
	(MEDTR)RTNLB33	(MEDTR)RTNLB33w		AY164935		4		
	(MEDTR)RTNLB50 (£)	(MEDTR)RTNLB50w		AY164936		4		
Populus balsamifera (trichocarpa)	(POPTR)RTNLB22	(POPTR)RTNLB22w		AY164932		4		
	(POPTR)RTNLB48	(POPTR)RTNLB48w		AY164931		3		
Populus tremula	(POPTN)RTNLB11	(POPTN)RTNLB11w		AY164930		1		
	(POPTN)RTNLB12	(POPTN)RTNLB12		AY164929		4		
	(POPTN)RTNLB13	(POPTN)RTNLB13w		AY164928		2		
	(POPTN)RTNLB22	(POPTN)RNTLE22w		AY164927		3		
	(POPTN)RTNLB45 (£)	(POPTN)RTNLB45w (£)		AY164924		1		
	(POPTN)RTNLB48	(POPTN)RTNLB48*1w		AY164926		3		
		(POPTN)RTNLB48*2w		AY164925		5		
Ricinus communis	(RICCO)RTNLB23 (£)	(RICCO)RTNLB23w (£)		AY164923		1		
Robinia pseudoacacia	(ROBPS)RTNLB11	(ROBPS)RTNLB11w		AY164922		1		
Rosa hybrid cultivar	(ROSHC)RTNLB12	(ROSHC)RTNLB12w		AY164921		1		
Thellungiella halophila	(THEHA)RTNLB11	(THEHA)RTNLB11w		AY164920		1		
Vitis vinifera	(VITVI)RTNLB21 (£)	(VITVI)RTNLB21w (£)		AY164919		3		
	(VITVI)RTNLB46 (£)	(VITVI)RTNLB46w (£)		AY164918		7		
Beta vulgaris	(BETVU)RTNLB8	(BETVU)RTNLB8w		AY164803		1		
	(BETVU)RTNLB11	(BETVU)RTNLB11w		AY164802		3		
Mesembryanthemum crystallinum	(MESCR)-RTNLB29	(MESCR)RTNLB29w		AY164801		2		
Avicennia marina	(AVIMR)RTNLB1 (£)	(AVIMR)RTNLB1w (£)		AY164832		2		
Triphysaria versicolor	(TRIVS)RTNLB44	(TRIVS)RTNLB44w		AY164804		2		
Lycopersicon esculentum	(LYCES)RTNLB8	(LYCES)RTNLB8		AY164819		7		
	(LYCES)RTNLB9	(LYCES)RTNLB9w		AY164818		1		
	(LYCES)RTNLB11	(LYCES)RTNLB11w		AY164827		1		
	(LYCES)RTNLB12	(LYCES)RTNLB12		AY164826		3		
	(LYCES)RTNLB13	(LYCES)RTNLB13w		AY164825		2		
	(LYCES)RTNLB16	(LYCES)RTNLB16w		AY164824		7		
	(LYCES)RTNLB18	(LYCES)RTNLB18w		AY164823		2		
	(LYCES)RTNLB22	(LYCES)RTNLB22		AY164822		9		
	(LYCES)RTNLB26	(LYCES)RTNLB26		AY164821		15		
	(LYCES)RTNLB27	(LYCES)RTNLB27		AY164820		17		
	(LYCES)RTNLB51	(LYCES)RTNLB51		AY164828		approx. 45		
Lycopersicon hirsutum	(LYCHI)RTNLB1 (£)	(LYCHI)RTNLB1w (£)		AY164817		1		
	(LYCHI)RTNLB22	(LYCHI)RTNLB22w		AY164816		1		
	(LYCHI)RTNLB27	(LYCHI)RTNLB27w		AY164815		3		
Lycopersicon pennelli	(LYCPN)RTNLB22	(LYCPN)RTNLB22w		AY164814		5		
	(LYCPN)RTNLB26 (£)	(LYCPN)RTNLB26w (£)		AY164813		1		
	(LYCPN)RTNLB42	(LYCPN)RTNLB42w		AY164812		15		

Solanum tuberosum	(SOLTU)RTNLB22	(SOLTU)RTNLB22		AY164810		7		
	(SOLTU)RTNLB26	(SOLTU)RTNLB26		AY164809		13		
	(SOLTU)RTNLB27	(SOLTU)RTNLB27w		AY164808		3		
	(SOLTU)RTNLB42	(SOLTU)RTNLB42w		AY164807		2		
	(SOLTU)RTNLB51	(SOLTU)RTNLB51		AY164811		22		
Lactuca sativa	(LACSA)RTNLB12	(LACSA)RTNLB12w		AY164830		3		
	(LACSA)RTNLB23	(LACSA)RTNLB23w		AY164829		1		
	(LACSA)RTNLB42	(LACSA)RTNLB42		AY164831		2		
Stevia rebaudiana	(STERE)RTNLB8	(STERE)RTNLB8w		AY164805		1		
	(STERE)RTNLB44	(STERE)RTNLB44w		AY164806		1		
Pinus taeda	(PINTA)RTNLB8	(PINTA)RTNLB8w		AY164833		1		
	(PINTA)RTNLB12	(PINTA)RTNLB12w		AY164836		3		
	(PINTA)RTNLB29	(PINTA)RTNLB29		AY164835		16		
	(PINTA)RTNLB41 (£)	(PINTA)RTNLB41w (£)		AY164834		35		
Pinus pinaster	(PINPS)RTNLB29	(PINPS)RTNLB29w		AY164837		2		
Cryptomeria japonica	(CRYJA)RTNLB41 (£)	(CRYJA)RTNLB41w (£)		AY164838		1		
Aegilops speltoides	(AEGSP)RTNLB30	(AEGSP)RTNLB30p		AY164917		3		
	(AEGSP)RTNLB31	(AEGSP)RTNLB31w		AY164916		2		
Allium cepa	(ALLCE)RTNLB12	(ALLCE)RTNLB12w		AY164915		1		
Cynodon dactylon	(CYNDA)RTNLB30	(CYNDA)RTNLB30w		AY164914		1		
Hordeum vulgare	(HORVU)RTNLB7	(HORVU)RTNLB7w		AY164906		3		
	(HORVU)RTNLB8	(HORVU)RTNLB8		AY164905		14		
	(HORVU)RTNLB11	(HORVU)RTNLB11		AY164913		7		
	(HORVU)RTNLB14	(HORVU)RTNLB14w		AY164912		1		
	(HORVU)RTNLB20	(HORVU)RTNLB20		AY164911		28		
	(HORVU)RTNLB28	(HORVU)RTNLB28		AY164910		9		
	(HORVU)RTNLB30	(HORVU)RTNLB30		AY164909		approx. 65		
	(HORVU)RTNLB31	(HORVU)RTNLB31		AY164908		27		
	(HORVU)RTNLB32	(HORVU)RTNLB32		AY164907		14		
Oryza sativa	(ORYSA)RTNLB7			AAAA01005909 ($)				
		(ORYSA)RTNLB7		AY164904		2		
	(ORYSA)RTNLB8		OSJNBA0091J19.7	AC084320	3			
		(ORYSA)RTNLB8		AAK09242.1, AY164895		4		
	(ORYSA)RTNLB11			AAAA01000481 ($)				
		(ORYSA)RTNLB11		AY164903		1		
	(ORYSA)RTNLB12			AAAA01020689 ($)				
		(ORYSA)RTNLB12w		AY164902		1		
	(ORYSA)RTNLB14		P0442D08.33	AP003250	1			
		(ORYSA)RTNLB14		BAB64153, AY164901		0		
	(ORYSA)RTNLB19			AAAA01005829 ($)				
		(ORYSA)RTNLB19		AY164900		3		
	(ORYSA)RTNLB20			AAAA01002108 ($)				
		(ORYSA)RTNLB20		AY164899		11		
	(ORYSA)RTNLB28			AAAA01016437 ($)				
		(ORYSA)RTNLB28		AY164898		1		
	(ORYSA)RTNLB30			AP003218	1			
		(ORYSA)RTNLB30		AP003218, BAB89453, AY164897		54		
	(ORYSA)RTNLB32		P0492F05.25	AP002902	1			
		(ORYSA)RTNLB32		BAB32723.1, AY164896		16		
Saccharum sp.	(SACHY)RTNLB8	(SACHY)RTNLB8w		AY164973		1		
Secale cereale	(SECCE)RTNLB8	(SECCE)RTNLB8w		AY164969		1		
	(SECCE)RTNLB14	(SECCE)RTNLB14w		AY164971		1		
	(SECCE)RNTLE20	(SECCE)RNTLE20w		AY164972		4		
	(SECCE)RTNLB30	(SECCE)RTNLB30		AY164970		7		
	(SECCE)RTNLB31	(SECCE)RTNLB31w		AY262092		4		
Sorghum bicolor	(SORBI)RTNLB7	(SORBI)RTNLB7w		AY164960		2		
	(SORBI)RTNLB14	(SORBI)RTNLB14w		AY164968		2		
	(SORBI)RTNLB19	(SORBI)RTNLB19		AY164967		4		
	(SORBI)RTNLB20	(SORBI)RTNLB20		AY164966		23		
	(SORBI)RTNLB28	(SORBI)RTNLB28*1		AY164965		9		
		(SORBI)RTNLB28*2		AY164964		1		
	(SORBI)RTNLB30	(SORBI)RTNLB30w		AY164963		3		
	(SORBI)RTNLB31	(SORBI)RTNLB31		AY164962		4		
	(SORBI)RTNLB32	(SORBI)RTNLB32		AY164961		10		
Sorghum halepense	(SORHL)RTNLB8 (£)	(SORHL)RTNLB8w (£)		AY164959		2		
Sorghum propinquum	(SORPR)RTNLB11	(SORPR)RTNLB11		AY164958		6		
	(SORPR)RTNLB20	(SORPR)RTNLB20		AY164957		4		
	(SORPR)RTNLB28	(SORPR)RTNLB28w		AY164956		1		
	(SORPR)RTNLB30	(SORPR)RTNLB30w		AY164955		7		
	(SORPR)RTNLB32	(SORPR)RTNLB32		AY164954		10		
Triticum aestivum	(WHEAT)RTNLB7	(WHEAT)RTNLB7		AY164942		4		
	(WHEAT)RTNLB8	(WHEAT)RTNLB8*1		AY164992		3		
		(WHEAT)RTNLB8*2		AY164991		9		
	(WHEAT)RTNLB11	(WHEAT)RTNLB11w		AY164953		3		
	(WHEAT)RTNLB14	(WHEAT)RTNLB14w		AY164952		2		
	(WHEAT)RTNLB18	(WHEAT)RTNLB18		AY164951		4		
	(WHEAT)RTNLB19	(WHEAT)RTNLB19w		AY164950		2		

	(WHEAT)RTNLB20	(WHEAT)RTNLB20*1		AY164949		20		
		(WHEAT)RTNLB20*2		AY164948		19		
	(WHEAT)RTNLB28	(WHEAT)RTNLB28		AY164947		3		
	(WHEAT)RTNLB30	(WHEAT)RTNLB30*1		AY164946		11		
		(WHEAT)RTNLB30*2		AY164945		7		
	(WHEAT)RTNLB31	(WHEAT)RTNLB31		AY164944		14		
	(WHEAT)RTNLB32	(WHEAT)RTNLB32		AY164943		12		
Triticum monococcum	(TRIMO)RTNLB11	(TRIMO)RTNLB11w		AY164990		1		
	(TRIMO)RTNLB30	(TRIMO)RTNLB30		AY164989		5		
	(TRIMO)RTNLB31	(TRIMO)RTNLB31w		AY164988		3		
Triticum turgidum	(TRITU)RTNLB20	(TRITU)RTNLB20w		AY164987		2		
Zea mays	(ZEAMP)RTNLB7	(ZEAMP)RTNLB7w		AY164977		4		
	(ZEAMP)RTNLB8	(ZEAMP)RTNLB8		AY164976		16		
	(ZEAMP)RTNLB9	(ZEAMP)RTNLB9w		AY164975		2		
	(ZEAMP)RTNLB11	(ZEAMP)RTNLB11w		AY164984		8		
	(ZEAMP)RTNLB18	(ZEAMP)RTNLB18w		AY164986		2		
	(ZEAMP)RTNLB19	(ZEAMP)RTNLB19w		AY164974		1		
	(ZEAMP)RTNLB20	(ZEAMP)RTNLB20*1		AY164983		7		
		(ZEAMP)RTNLB20*2		AY164982		5		
	(ZEAMP)RTNLB28	(ZEAMP)RTNLB28		AY164981		8		
	(ZEAMP)RTNLB30	(ZEAMP)RTNLB30*1		AY164980		11		
		(ZEAMP)RTNLB30*2		AY164979		22		
	(ZEAMP)RTNLB31	(ZEAMP)RTNLB31w		AY262091		7		
	(ZEAMP)RTNLB32	(ZEAMP)RTNLB32		AY164978		25		
	(ZEAMP)RTNLB43	(ZEAMP)RTNLB43w		AY164985		4		
Ceratopteris richardii	(CERRI)RTNLB34	(CERRI)RTNLB34w		AY164840		2		
	(CERRI)RTNLB35	(CERRI)RTNLB35w		AY164839		1		
Physcomitrella patens	(PHYPA)RTNLB36	(PHYPA)RTNLB36		AY164845		13		
	(PHYPA)RTNLB37	(PHYPA)RTNLB37		AY164844		10		
	(PHYPA)RTNLB38	(PHYPA)RTNLB38w		AY164943		4		
	(PHYPA)RTNLB39	(PHYPA)RTNLB39w		AY164842		2		
	(PHYPA)RTNLB40	(PHYPA)RTNLB40w		AY164841		3		

£: Sequence not well aligneable; no clear position within phylogenetic tree; nomenclature unclear $: Sequence from Rice Genome DataBank at Torrey Mesa Research Institute

Viridiplantae RTN-like domain containing genes; no clear position within phylogenetic tree; exon-intron structure dissimilar from known RTNLB genes								
Species	Gene	Transcript	Alternative symbols	Genbank Accession	Chromosomal locus	Number of ESTs	Exons	Published
Arabidopsis thaliana								
			At2g20590	NC_003071	2			
				AAD21707, NM_127620, NP_179649		nd		
			At4g28430	NC_003075	4			
				AAM63049, AY085834, NM_118985, NP_567809		nd		
			At1g78895, F9K20.31	NC_003070	1			
				AAM61731, AY085180, NM_106538, NP_565194		nd		
			At5g58000	NC_003076	5			
				NM_125185, NP_200608		nd		
			MTI20.26	AB013396	5			
				AB013396, BAB08870		nd		
Hordeum vulgare	(HORVU)RTNs1	(HORVU)RTNs1w				6		
Triticum aestivum	(WHEAT)RTNs2	(WHEAT)RTNs2w				2		
Sorghum propinquum	(SORPR)RTNs3	(SORPR)RTNs3w				1		
Sorghum bicolor	(SORBI)RTNs4	(SORBI)RTNs4w				1		

Supplementary Table 1 G: *Euglenozoa RTNLC subfamily*

Species	Gene	Transcript	Alternative symbols	Genbank Accession	Chromosomal locus	Number of dbESTs	Exons	Published
Leishmania infantum	(LEIIN)RTNLC	(LEIIN)RTNLC	papLe22	AF123892, AY164995		0		1
Leishmania major	(LEIMA)RTNLC			LM31_BIN-Contig2025/26 (a)		0		
		(LEIMA)RTNLC		AY164996		0		

Mycetozoa RTNLC subfamily								
Species	Gene	Transcript	Alternative symbols	Genbank Accession	Chromosomal locus	Number of ESTs	Exons	Published
Dictyostelium discoideum	(DICDI)RTNLC			AY164656, 44689 (b), DICTY6P2_0002 (c)				
		(DICDI)RTNLC		AY164994		approx. 130		

Pelobiontida RTNLC subfamily								
Species	Gene	Transcript	Alternative symbols	Genbank Accession	Chromosomal locus	Number of ESTs	Exons	Published
Mastigamoeba balamuthi	(MASBA)RTNLC	(MASBA)RTNLCw		AY164993		1		

(a) Wellcome Trust Sanger Institute (b) DictyConsortium (c) EUDICT_contigs (1) Suffia et al., 2000

3 Analysis of the reticulon gene family demonstrates the absence of Nogo-A in fish

3.1 Abstract

RTNs are a family of conserved proteins that might have evolved in eukaryotes along with the endomembrane system. Four RTN paralogs (RTN1, RTN2, RTN3, RTN4) are present in the ER of land vertebrates. While the exact functions of RTN1 - RTN3 are unknown, mammalian RTN4-A/Nogo-A was shown to inhibit the regeneration of severed CNS axons via two distinct regions, one within the Nogo-A specific N-terminus and the other in the conserved RHD. In contrast to mammals, fish are capable of CNS axon regeneration. To determine whether fish might express an rtn4 ortholog, we performed detailed analyses of fish rtns. Seven rtn genes were identified in zebrafish, six in pufferfish and 30 in 8 additional fish species. Phylogenetic and syntenic relationships indicate that the identified fish rtn genes are orthologs of mammalian RTN1, RTN2, RTN3 and RTN4 and that several paralogous fish genes (e.g. rtn4 and rtn6) resulted from genome duplication events early in actinopterygian evolution. Accordingly, sequences homologous to the conserved RTN4/Nogo RHD are present in two fish genes, rtn4 and rtn6, whereas the large N-terminal exon of mammalian Nogo-A and its inhibitory function is absent in zebrafish. This result is in accordance with earlier functional data showing that axon growth inhibitory molecules are absent from fish oligodendrocytes and CNS myelin.

3.2 Introduction

The reticulon gene family codes for proteins that all contain a highly conserved carboxy-terminal RHD (Pfam PF02453) and a variable amino-terminus. The RHD domain is 150-201 amino acids (aa) in length and is characterized by two large (>30 aa) hydrophobic regions with a ~66-aa loop in between. The two hydrophobic stretches are responsible for the association of RTN proteins to membranes (Oertle et al., 2003c; van de Velde et al., 1994). RTNs are ubiquitously expressed in vertebrates and have been identified in other metazoan phyla such as insects, nematodes, fungi and plants (Oertle et al., 2003b). In mammals, four reticulon family members are known. RTN1 (formerly NSP1), RTN2 and RTN3 are enriched in membranes of the endoplasmic reticulum (van de Velde et al., 1994), but their exact functions have not been elucidated so far. The gene of the fourth vertebrate family member, RTN4/Nogo, gives rise to a number of different isoforms (Nogo-A, -B and -C as main transcripts) both through alternative splicing and alternative promoter usage (Chen et al., 2000; Oertle et al., 2003a). The largest isoform, RTN4-A/Nogo-A,

has been described as a potent neurite outgrowth inhibitor of mammalian CNS myelin (Chen et al., 2000; GrandPré et al., 2000; Prinjha et al., 2000). *In vitro* assays with recombinant peptides allowed to map the inhibitory function to two different regions of the Nogo-A protein (Oertle et al., 2003d). One domain provoking growth cone collapse is encoded by a stretch of the Nogo-A specific exon (NiGΔ20) (Oertle et al., 2003d) and antibodies against this region promote *in vivo* CNS regeneration in rats. Another N-terminal site, NiRΔ2 is involved in the inhibition of fibroblast spreading, but not in growth cone collapse (Oertle et al., 2003d). The second region that induces growth cone collapse is the 66-aa loop between the two C-terminal hydrophobic domains of the RHD (Nogo-66). Nogo-66 is identical in all RTN4/Nogo isoforms and signals through an interaction with the GPI-linked NgR receptor (Fournier et al., 2001; GrandPré et al., 2002).

In contrast to mammals, lesioned axons readily regenerate in the fish CNS and re-establish appropriate connections with their targets (Stuermer, 1988a; Stuermer, 1988b). This success of axonal regeneration depends on intrinsic properties of fish neurons and on a growth-promoting environment for regenerating axons (Stuermer et al., 1992). Fish CNS myelin is a permissive substrate for the growth of axons of fish and mammals and does not induce collapse of growth cones of either species (Ankerhold et al., 1998; Bastmeyer et al., 1991; Wanner et al., 1995). These findings suggested the absence of myelin-associated neurite growth inhibitors from the fish CNS. In this context, it is an intriguing question whether fish posses an rtn4/nogo orthologous gene with aa stretches similar to the aforementioned inhibitory sites of mammalian RTN4-A/Nogo-A. Given the high conservation in the RHD of the rtn gene family and against the background of the proposed fish-specific genome duplication (Taylor et al., 2003), phylogenetic and syntenic relationships within the entire rtn gene family were determined to unequivocally confirm the presence of rtn4 orthologs in fish. In a second step, the genomic organization of all fish rtn genes were analysed in order to compare exon compositions and isoform variations of their N-termini to those of the respective human ortholog. The results in combination with the dissection of sequence homologies argue for fundamental differences in the evolution of rtn1-rtn3 and rtn4: the specific N-termini of fish and mammalian rtn1, rtn2 and rtn3, respectively, evolved from a common ancestor, whereas the rtn4 N-termini must have been acquired independently. Finally, the presence of exons homologous to the N-terminal region of mammalian Nogo-A in zebrafish was excluded by aligning the relevant genomic region to the orthologous mammalian sequences. To substantiate this finding that rtn4 transcripts with functions similar to mammalian Nogo-A are absent in zebrafish, we performed extensive RT-PCR analyses and demonstrate that none of the fish rtn4 isoforms is expressed in a pattern comparable to the neurite growth inhibitory Nogo-A.

3.3 Materials and methods

3.3.1 Nomenclature of fish rtn transcripts

Zebrafish and fugu transcripts were named according to the nomenclature guidelines for reticulon genes (Oertle et al., 2003b). In brief, rtn serves as a gene symbol for chordate reticulons. Paralogous rtn sequences are arbitrarily numbered. To distinguish rtn genes of various species, a prefix according to the identification code proposed by SWISS-PROT is used (e.g. (FUGRU)rtn4). Alternative transcripts generated by alternative promoter usage receive different letters (e.g. (FUGRU)rtn4-l, (FUGRU)rtn4-n), while alternatively spliced transcripts derived from a single promoter have the same letter but are distinguished by consecutive numbering (e.g. (FUGRU)rtn4-l1, (FUGRU)rtn4-l2).

3.3.2 Cloning and sequence analysis of zebrafish and fugu rtn genes

Zebrafish and fugu rtn genes and transcripts were uncovered by a combination of library screening, database searches for fish ESTs and mRNAs with known human RTN protein sequences, RT-PCR and RACE (**Supplementary Table 1A**). To isolate zebrafish rtn cDNAs, two rounds of library screening were performed at the RZPD (Deutsches Ressourcenzentrum für Genomforschung GmbH, Heidelberg Germany). The RZPD first screened high density filters of an adult zebrafish retina library and of a late somitogenesis library using ^{33}P-labeled bp 2-490 of (DANRE)rtn4-n. In a subsequent approach, the same libraries plus an adult brain library were probed with ^{33}P-labeled bp 1739-2422 of (DANRE)rtn1-a1 and bp 1624-3157 of (DANRE)rtn6-a1. Obtained clones are listed in **Supplementary Table 1A**.
In addition, zebrafish and fugu cDNA and genomic sequences were obtained using blast algorithms (Altschul et al., 1997) at NCBI (www.ncbi.nlm.nih.gov/BLAST/), Ensembl (www.ensembl.org/Danio_rerio/blastview; www.ensembl.org/Fugu_rubripes/blastview) and the Doe Joint Genome Institute (aluminum.jgi-psf.org/prod/bin/runBlast.pl?db=fugu6) web pages. Exon-intron structures were examined by comparing genomic against cDNA sequences, respecting the GT-AG rule of splice donor and acceptor sites. For fugu rtn genes, without any ESTs or cDNA information available exon sequences were deduced from the genomic sequences by comparison with the zebrafish cDNAs. In total, we uncovered 13 different zebrafish and fugu rtn genes with 37 mRNA variants. The sequences surrounding the putative start methionines of most fish rtn transcripts comply with the consensus motif for translation initiation (gccAcc**ATG**G) at least at one of the two most important positions (a G following the ATG and a purine at position –3 (Kozak, 1996). In addition, an upstream stop codon in most sequences ensures that the identified start methionines corresponds to the respective N-terminus of the protein (**Supplementary Table 1A**). The predicted proteins have a more or less conserved dilysine ER membrane retention motif at their C-terminus and the N-termini of the long splice forms (-a and -l variants) are remarkably acidic (**Supplementary Table 1A**).
We used the exon-intron information and the deduced cDNA sequences to amplify zebrafish rtn splice variants from various adult tissues (see RT-PCR section 3.4.5) and fugu rtn transcripts from liver and brain cDNA with specific primers (**Supplementary Table 1A, B**). Sequences were completed performing 5'- and 3'-RACE, respectively. In brief, we extracted mRNA from a pool of 48 hours post fertilization (hpf) zebrafish embryos (FastTrack™ 2.0 kit; Invitrogen) and used 0.9 µg/reaction as template for the synthesis of either first-strand 5'-Ready cDNA using 5'-CDS and SMART II oligonucleodides or of 3'-Ready cDNA using 3'-CDS primer, according to the manufacturer's instructions (SMART RACE cDNA Amplification Kit; BD Clontech). All PCR fragments were directly subcloned into the pCRII cloning vector (Invitrogen) and plasmid DNA was prepared using the QIAprep® 8 Miniprep Kit (Qiagen). Both DNA strands were sequenced using the Abi Prism® BigDye™ Terminator Cycle Sequencing Kit (Applied Biosystems) and analyzed on an AbiPrism 3100 Genetic Analyzer. Single sequences were assembled using SeqMan™II of the DnaStar software package (GATC Biotech). Specific informations for the cloning strategy of each gene are available upon request. Sequences were deposited in GenBank and accession numbers are listed in **Supplementary Table 1D**.

3.3.3 Sequence alignments and phylogenetic analyses

GenBank accession numbers of sequences used for the different alignments are listed in **Supplementary Table 1D**. 46 partial or complete RTN mRNAs were uncovered by database searches in addition to the ones already described (Baka et al., 1996; Geisler et al., 1998; GrandPré et al., 2000; Hamada et al., 2002; Klinger et al., 2004a; Kools et al., 1994; Moreira et al., 1999; Morris et al., 1999; Nagase et al., 1998; Ninkina et al., 1997; Oertle et al., 2003a; Prinjha et al., 2000; Roebroek et al., 1996; Roebroek et al., 1998; Roebroek et al., 1993; Stubbs et al., 1996; Yang et al., 2000; Zhang et al., 2002). The single RTN gene of the urochordate *Ciona intestinalis* was used as an outgroup.
Nucleotide sequences of the RHDs were translated using BioEdit (Hall, 1999) and aligned as aa using ClustalW (Thompson et al., 1994). The alignment was edited by hand and then converted back into nucleotides to produce a codon alignment that was 642 nucleotides long. Due to length variations in the RTN2 genes all other sequences contain a C-terminal gap of up to 60 nucleotides. Eighteen of the 86 sequences used for the analyses were incomplete

either at the N- or C-terminus producing alignment-gaps of different length. Phylogenies of reticulon sequences were reconstructed using neighbour joining (NJ) methods with *MEGA* version 2.1 (Kumar et al., 2001) and pair-wise deletion of the aforementioned gaps. Support for nodes in the NJ tree was assessed using 1000 bootstrap reiterations (Felsenstein, 1985).
Molecular evolutionary analyses were conducted using *MEGA* version 2.1 (Kumar et al., 2001). In brief, sequences of the RHDs were aligned at the amino acid level by the ClustalW program and gaps were pair-wise deleted. Numbers of nonsynonymous substitutions (aa altering) per nonsynonymous site (d_N) and synonymous substitutions (silent) per synonymous site were estimated (Nei and Gojobori, 1986) for each fish paralogue in separate comparisons to the respective human rtn sequence.

3.3.4 Percent identity plots of rtn4

The zebrafish clone BX324134 from nucleotides 1 to 112195 (LG6), covering the entire (DANRE)rtn4 gene as well as the orthologous genomic sequences of the MTIF2 and RPS27A, was aligned against 1 megabase (nucleotides 33'841'399 to 34'841'398) of the corresponding human region on chromosome 2p16 from the genomic contig NT_022184.13/Hs2_22340 using the minus strand sequence. In addition, both sequences were aligned against 400 kilobases (nucleotides 26'300'000 to 26'700'000) of the orthologous mouse sequence on chromosome 11 from the genomic contig NT_039515.2/Mm11_39555_32 as previously described in (Oertle et al., 2003a). Using a newly generated exon mask for the human genes MTIF2, RPS27A, FLJ31438 and RTN4, and a mask for repetitive sequences using the RepeatMasker software (http://repeatmasker.genome.washington.edu/cgi-bin/RepeatMasker), the percent-identity-plots (PIPs) were generated using MultiPipMaker (http://bio.cse.psu.edu/cgi-bin/multipipmaker) and the dot plot was generated using Advanced PipMaker (http://bio.cse.psu.edu/cgi-bin/pipmaker?advanced) according to the published method (Schwartz et al., 2000). The output was modified as in (Oertle et al., 2003a). The same procedure was adopted using the mVista Software (http://www.gsd.lbl.gov/vista/index.shtml) according to the published methodology (Mayor et al., 2000) with comparable results to the plots generated by PipMaker.

3.3.5 Radiation hybrid mapping and synteny analysis

A conserved synteny is defined by two or more genes located on the same chromosome in fish and their orthologs located on a single chromosome in human (Barbazuk et al., 2000). Therefore, zebrafish rtns were mapped on the LN54 radiation hybrid panel using standard conditions (Hukriede et al., 1999) and the respective web interface (http://mgchd1.nichd.nih.gov:8000/zfrh/beta.cgi). Since no unequivocal result was obtained for rtn5 and rtn6 on this panel, these rtns were mapped on the Goodfellow T51 radiation hybrid panel (Research Genetics, Inc.) by instant mapping at http://134.174.23.167/zonrhmapper/instantMapping.htm.
For synteny analysis (Woods et al., 2000), other zebrafish genes and ESTs already mapped on the LN54 and T51 radiation hybrid panels (http://zfin.org/cgi-bin/mapper_select.cgi) were assigned to putative human orthologs by BlastX searches (Altschul et al., 1997) against the NCBI human non-redundant (nr) protein sequence database (http://www.ncbi.nlm.nih.gov/blast/blast.cgi). For EST clones that have been sequenced at the 5' and 3' ends, both sequences were used for BlastX searches. If the results of these searches had expect scores (*E* values) of ≤-5, the putative orthologs were further tested with reciprocal searches against the zebrafish subset of nr sequences and dbESTs. A human ortholog was confirmed if the original zebrafish gene or EST (or a gene or EST that showed highly significant overlap with the original sequence) was in the top 15 matches of the reciprocal search by tBlastN. Fugu synteny data were retrieved with MartView (http://www.ensembl.org/Fugu_rubripes/martview) for all scaffolds, on which other genes could be predicted in the vicinity of the fugu rtns.

3.3.6 RT-PCR

100 zebrafish embryos (appr. 100 mg) for each stage or 50 mg of various adult tissues were used for preparation of total RNA with the RNeasy Mini Prep Kit (Qiagen) following manufacturer's instructions. Muscle tissue was additionally subjected to proteinase K digestion (200 µg/30 mg tissue). First-strand cDNA was synthesized under standard conditions with the Superscript First-Strand Synthesis System (Invitrogen) using oligo$(dT)_{12\text{-}18}$ primer. Zero-transcriptions (without Superscript II in the reaction) were performed in parallel, to control for genomic DNA contaminations in subsequent PCRs. Amount and quality of the different cDNA samples were evaluated comparing the expression level of the housekeeping gene actin. Informations on primer sequences and PCR conditions are listed in **Supplementary Tables 1B, C**.

3.4 Results

3.4.1 Phylogenetic analysis of fish rtns

To proof the existence of true rtn4 orthologs in fish, we classified newly identified fish rtns by phylogenetic analysis of the vertebrate RTN gene family. Characterization of all fish rtn family members avoided conceivable misidentification due to high conservation of the RHD and ensured the detection of paralogous rtn genes resulting from the proposed fish-specific genome duplication. We physically cloned seven rtn family members from zebrafish (*Danio rerio*) and five from pufferfish (*Takifugu rubripes*) by library screening, RT-PCR and RACE (**Supplementary Table 1A**). Database searches uncovered a sixth rtn gene within the fugu genome and 46 new partial or complete vertebrate RTN mRNAs (**Supplementary Table 1D**) compared to the ones already described (Oertle et al., 2003b). We produced an unambiguous alignment of all 86 vertebrate RTN sequences, representing the conserved RHD (**Supplementary Fig. 1**). Phylogenetic reconstruction produced a tree comprised of distinct, well-supported RTN1, RTN2, RTN3 and RTN4 clades (**Fig. 1**). Each clade included human, mouse, rat and several other tetrapod sequences, at least one zebrafish and one fugu sequence and a variable number of other fish species, indicating that gene duplication events producing RTN1, RTN2, RTN3 and RTN4 occurred before the divergence of ray-finned fish (actinopterygians) and tetrapods (sarcopterygians). Therewith, this is the first evidence for the presence of RTN2 sequences in 'lower vertebrates' like fish and amphibians. The assignement of four distinct RTN clades was supported by the identification of aa residues unique to one subfamily of rtn genes (**Supplementary Fig. 2**). The RTN1 and RTN2 subfamilies are each defined by two unique and derived (not ancestral) aa substitutions. RTN3 proteins have one diagnostic and derived residue, whereas no diagnostic residues could be identified for the RTN4 subfamily (**Supplementary Fig. 2**).

All clades exept RTN3 contained two zebrafish genes and the RTN2 and RTN3 clade included two fugu genes (**Fig. 1**). Consequently, the zebrafish and fugu genes were named (DANRE)rtn1-rtn4 and (FUGRU)rtn1-rtn4, respectively and additional fish genes were consecutively numbered according to the nomenclature guidelines for reticulon genes (Oertle et al., 2003b), i.e. (DANRE)rtn5, rtn6, rtn8 and (FUGRU)rtn7 and rtn8. Fish sequences within one clade did not cluster according to species, but subdivided into two subclades each containing one of the duplicated zebrafish and/or fugu genes (**Fig. 1**). The relationships in the resulting subclades are similar, e.g the zebrafish genes are closely related to carp (**Fig. 1**, (CYPCA)rtn1, 3, 4, 5, 6) and goldfish (**Fig. 1**, (CARAU)rtn3, 4) and fugu genes are closely related to medaka (**Fig. 1**,

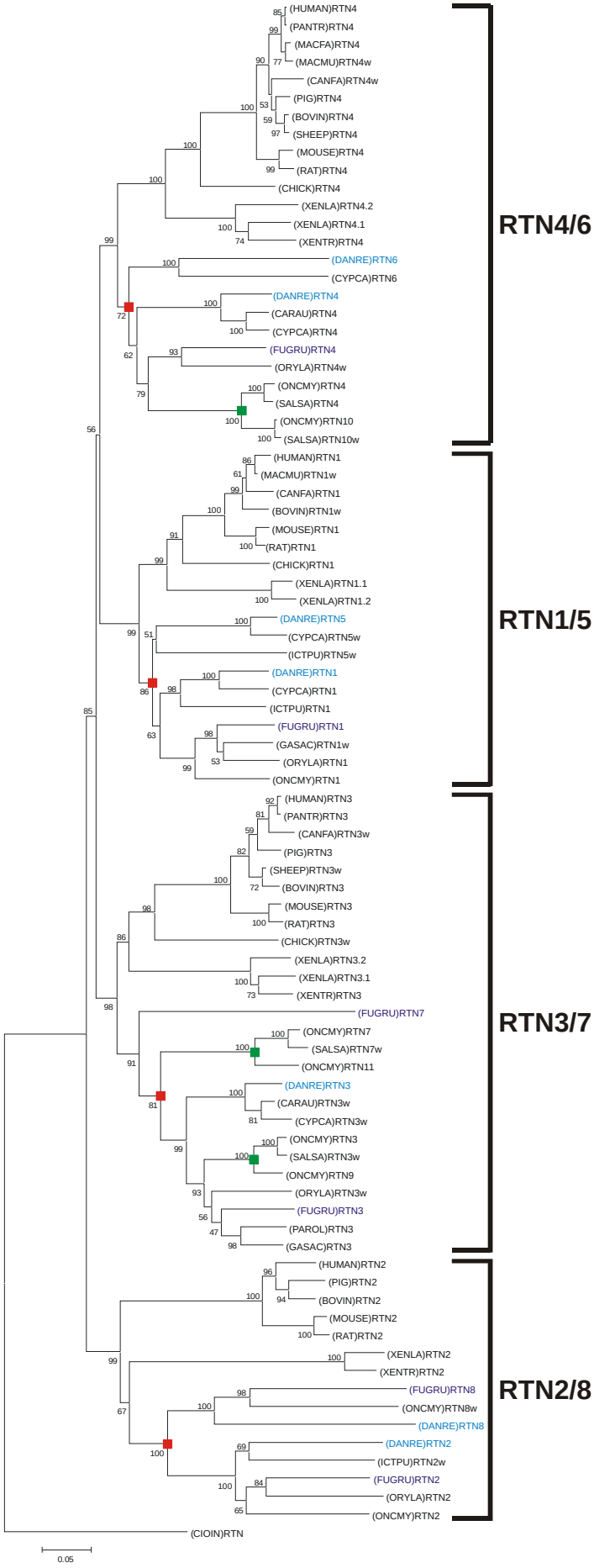

Fig. 1: *Evolutionary relationships among vertebrate RTN genes*

Pylogenetic relationships of vertebrate RTN sequences as determined by neighbor joining methode with 1000 bootstrap reiterations based on a 642 bp long alignement of the RHDs. *Ciona intestinalis* was used as an outgroup. Nodes that reflect genome duplication early during fish evolution and nodes that reflect the salmonid genome duplication are highlighted in red and green, respectively. Zebrafish and fugu sequences are shown in blue. Sequences that did not comprise the full RHD received the suffix 'w'. Scale represents 5% nucleotide sequence divergence.

BOVIN, Bos taurus; CANFA, Canis familiaris; CARAU, Carassius auratus; CHICK, Gallus gallus; CIOIN, Ciona intestinalis; CYPCA, Cyprinus carpio; DANRE, Danio rerio; FUGRU Takifugu rubripres; GASAC, Gasterosteus aculeatus; ICTPU, Ictalurus punctatus; HUMAN, Homo sapiens; MACMU, Macaca mulatta; MACFA, Macaca fascicularis; MOUSE, Mus musculus; ONCMY, Oncorhynchus mykiss; ORYLA, Oryzias latipes; PANTR, Pan troglodytes; PAROL, Paralichthys olivaceus; PIG, Sus scrofa; RAT, Rattus norvegicus; SHEEP, Ovis aries; SALSA, Salmo salar; XENLA Xenopus laevis; XENTR, Silurana tropicalis

(ORYLA)rtn2, 3, 4, 8). This topology is consistent with the hypothesis that the duplicates of rtn1-rtn4 were produced before the ancestors of zebrafish and fugu diverged. Moreover, the relationships between the 13 trout and salmon sequences included in this study argue for an additional, salmonidae-specific genome duplication.

To examine whether one of the two zebrafish or fugu paralogs ((DANRE)rtn1/5, rtn2/8, rtn4/6 and (FUGRU)rtn2/8, rtn3/7) evolved faster and is therefore more distantly related to the respective human RTN, we calculated the rates of synonymous (silent) and nonsynonymous (aa altering) nucleotide substitutions (d_S and d_N; Nei and Gojobori, 1986). All zebrafish and fugu rtns accumulated similar numbers of silent nucleotide changes, but aa altering substitutions were retained to a different extent (**Supplementary Table 1E**). In particular, twice as many changes were fixed in zebrafish rtn6 compared to rtn4, indicating that the rtn6 duplicate has evolved faster and is therefore more distantly related to human RTN4.

Taken together, our phylogenetic analysis served to assign the identified fish genes to the correct RTN subfamily and provided evidence for the existence of orthologous rtn4 genes in fish. In addition, we found duplications for all mammalian RTN tetralogues in zebrafish (rtn1/5, rtn2/8, rtn4/6) and/or in fugu (rtn2/8, rtn3/7) resulting in two paralogous genes in the respective species.

3.4.2 Conserved syntenies of fish and human rtns

To unequivocally confirm the identity of the fish rtn genes by a second non-bioinformatical method, syntenic relationships were analysed. Zebrafish rtn1, rtn2, rtn3, rtn4 and rtn8 were mapped on LG20, LG15, LG7, LG6 and LG21, respectively. Rtn5 and rtn6 both lie on LG13. The chromosomal positions of the mapped zebrafish rtn genes was then compared to the locations of human RTNs (**Fig. 2**, **Supplementary Table 2 A-F**).

(DANRE)rtn1 together with 15 additional ESTs and the genes *e(r)* and *esr2a* on LG20 and (DANRE)rtn5 with ten ESTs on LG13 both extend existing syntenies with the same region (14q22-14q33) of human chromosome 14 (**Fig. 2A**, **B**; Woods et al., 2000). This indicates that zebrafish rtn1 and rtn5 result from a fish-specific duplication of this segment and are therefore both orthologous to human RTN1. (DANRE)rtn2 together with five ESTs (**Fig. 2F**) and (DANRE)rtn8 together with EST fi30c01 (**Fig. 2E**) both define so far unrecognized small syntenic groups with the region around RTN2 on human Chr. 19. Mapping of (DANRE)rtn3, twelve additional ESTs and the two genes *fth1* and *men1* confirmed the large syntenic region between zebrafish LG7 and human Chr. 11 (**Fig. 2C**) (Yoder and Litman, 2000). (DANRE)rtn4 belongs to a known syntenic group on zebrafish LG6 and human Chr. 2; Woods et al., 2000); **Fig. 2D**), supported by 15 additional ESTs and the gene *chma1*. (DANRE)rtn6 and eight other ESTs

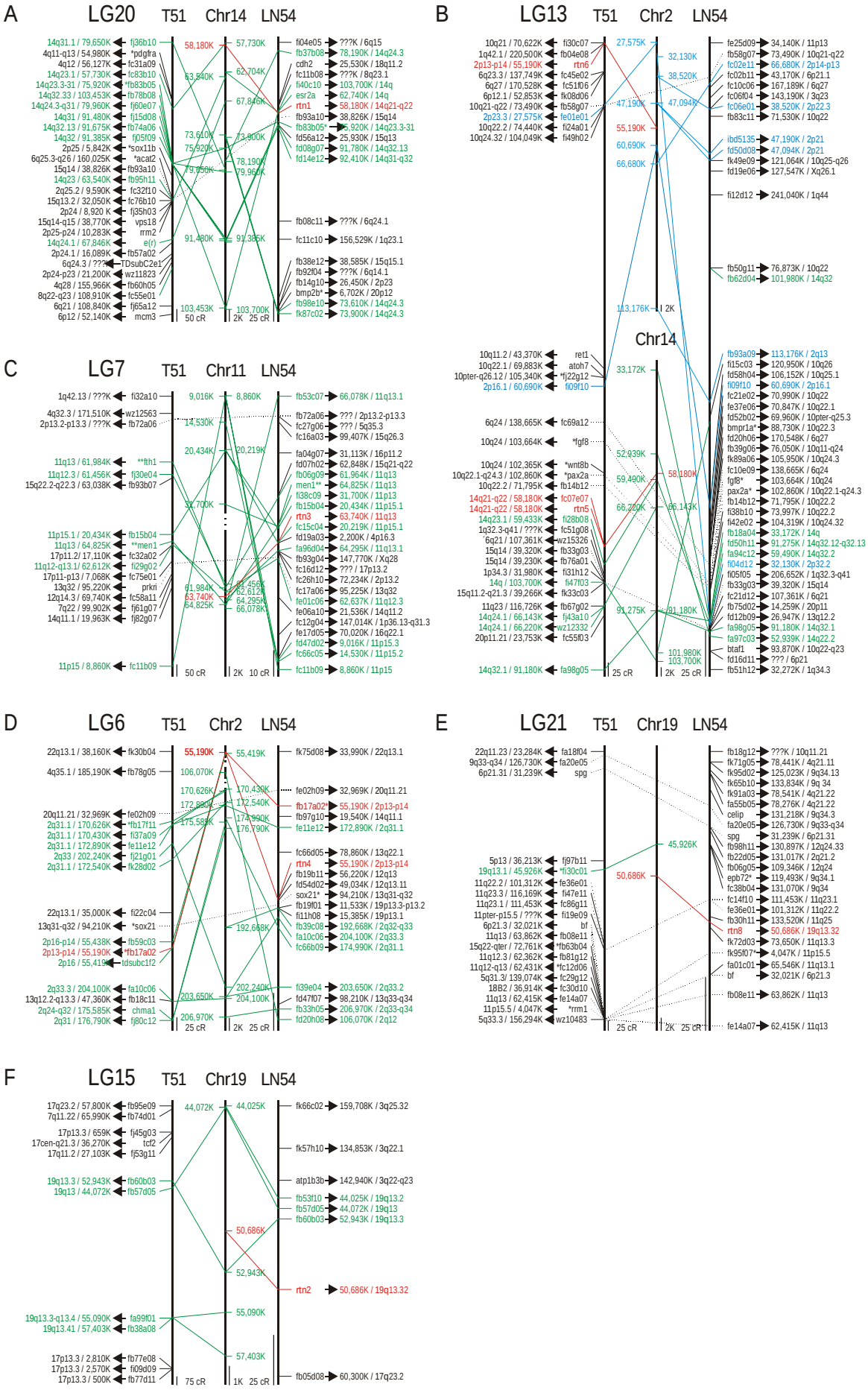
A
LG20
T51
Chr14
LN54
B
LG13
T51
Chr2
LN54
Chr14
C
LG7
T51
Chr11
LN54
D
LG6
T51
Chr2
LN54
E
LG21
T51
Chr19
LN54
F
LG15
T51
Chr19
LN54

Fig. 2: *Analyses of zebrafish and human syntenic relationships (previous page)*

Map locations of ESTs and genes in the radiation hybrid panels T51 and LN54 were obtained from ZFIN. The relative chromosomal locations of the human orthologs were deduced from data in LocusLink. Markers that are syntenic to rtn1, rtn3, rtn4 and rtn5 (red), respectively, are shown in green. ESTs supporting a synteny of rtn6 and human Chr. 2 are shown in blue. Markers present on more than one zebrafish panel are connected by dotted lines.

A) Conserved synteny of zebrafish linkage group (LG) 20 and human Chr. 14 defined by (DANRE)rtn1 (red).

B) Conserved synteny of zebrafish LG13 and human Chr. 14 defined by (DANRE)rtn5 (red) and conserved synteny of zebrafish LG13 and human Chr. 2 defined by (DANRE)rtn6 (red).

C) Conserved synteny of zebrafish LG7 and human Chr. 11 defined by (DANRE)rtn3 (red).

D) Conserved synteny of zebrafish LG6 and human Chr. 2 defined by (DANRE)rtn4 (red).

E) Conserved synteny of zebrafish LG21 and human Chr. 19 defined by (DANRE)rtn8 (red).

F) Conserved synteny of zebrafish LG15 and human Chr. 19 defined by (DANRE)rtn2 (red).

cR, centiray; K, kilobasepairs, * EST and genes have been published by Woods et al., 2000, .** EST and genes have been published by Yoder and Litman, 2000.

on LG13 are also syntenic to human Chr. 2 (**Fig. 2B**), providing additional evidence that (DANRE)rtn6 resulted from a fish specific duplication and is therefore a second ortholog of human RTN4.

The six fugu rtn genes were identified within the genomic sequences of scaffolds 188 (rtn1), 257 (rtn2), 346 (rtn3), 2616 (rtn4), 2117 (rtn8), 3887 (rtn7; all scaffolds Ensembl release 19.2.1) and 6658 (rtn7, NCBI). Predicted genes in the vicinity of the fugu rtns were compared with the chromosomal localization of their respective mammalian ortholog. Again conserved syntenies were revealed for genes near rtn1 and human Chr14, for rtn2 and human Chr19 and for rtn3 and human Chr11 (**Supplementary Table 2G**).

Summarized, the comparative mapping results in both species support the phylogenetic classification of fish rtns in four RTN subfamilies (RTN1, RTN2, RTN3 and RTN4) and the fish specific duplications leading to rtn5, rtn8, rtn7 and rtn6. Both methods emphasize that two zebrafish orthologs of human RTN4 have been identified.

3.4.3 Non-homogeneous evolution of rtn genes

Having ascertained the presence of orthologous rtn4 genes in fish (based on the conserved RHD), we determined the genomic organization and the N-terminal sequences of all fish rtn genes in comparison to the respective human orthologs to analyze the evolution of the variable N-termini and to examine whether domains homologous to the growth inhibitory regions in the N-terminus of mammalian Nogo-A (i.e. NiGΔ20) are present in fish.

Zebrafish rtn1 and rtn5 are formed by at least ten exons that can give rise to several isoforms (rtn1-a, rtn1-c and rtn5-a, rtn5-c, respectively) by alternative promoter usage (**Fig. 3A**). For rtn1-a

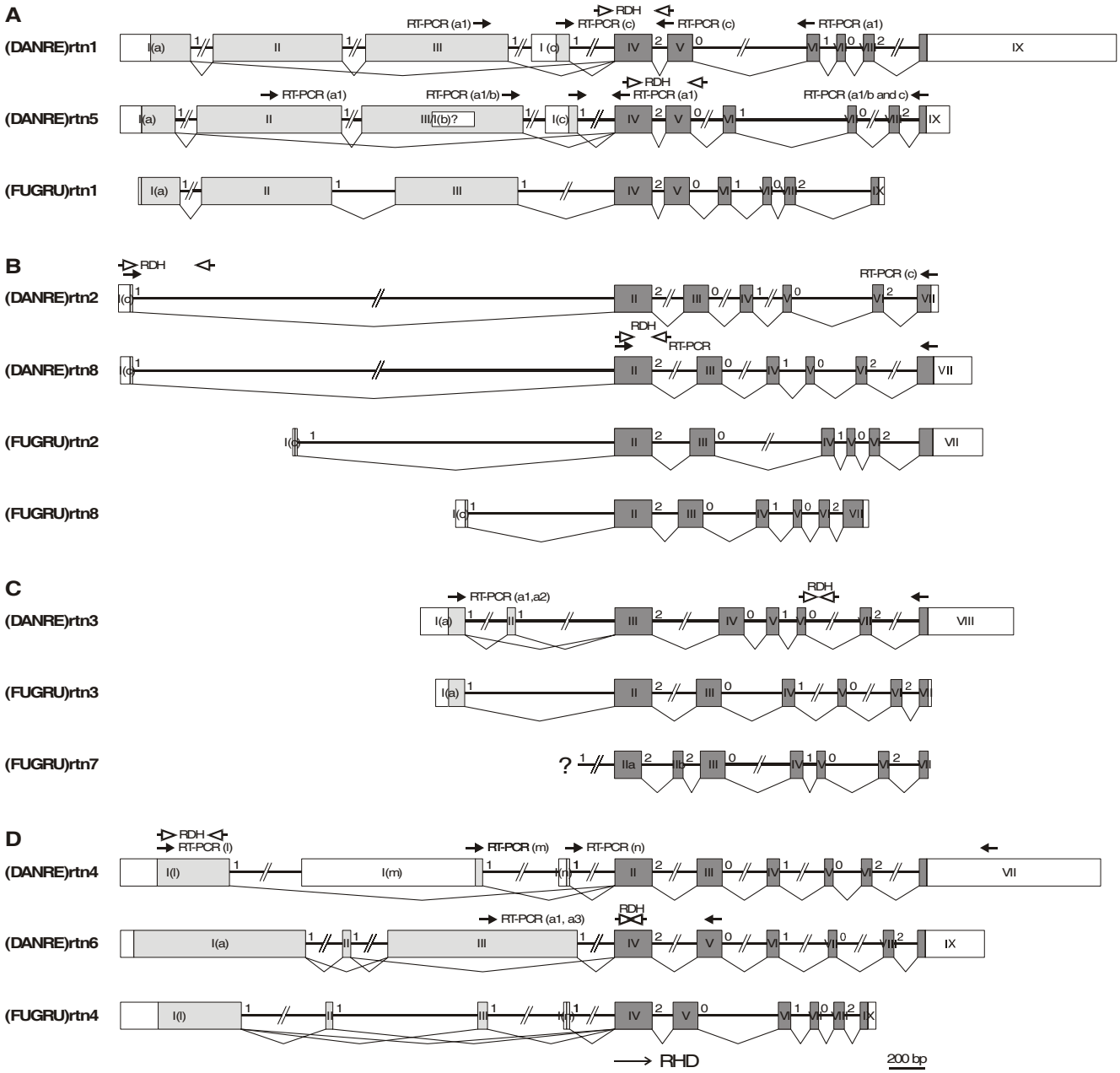

Fig. 3: *Analysis of zebrafish and pufferfish rtn genes*

A-D) Exon-intron arrangements are schematically shown. Exons are drawn as Roman numbered boxes. The coding regions for paralog-specific amino-termini are shaded light grey and exons of the RHDs are shaded dark grey. UTRs are depicted as open boxes. Intron phases are specified with Arabic numbers. Localizations of primers used for analyses of the zebrafish genes/transcripts are indicated by closed (RT-PCR) and open (radiation hybrid mapping (RDH)) arrows, respectively.

A) Exon-intron arrangements of (DANRE)rtn1, (DANRE)rtn5 and (FUGRU)rtn1 genes.

B) Exon-intron arrangements of (DANRE)rtn8, (FUGRU)rtn2 and (FUGRU)rtn8 genes.

C) Exon-intron arrangements of (DANRE)rtn3, (FUGRU)rtn3 and (FUGRU)rtn7 genes.

For fugu (FUGRU)rtn7, the specific N-terminal exon could not be identified within the genomic sequences (marked with ?).

D) Exon-intron arrangements of (DANRE)rtn4, (DANRE)rtn6 and (FUGRU)rtn4 genes.

and rtn5-a, two splice forms each were detected, either with (-a1) or without (-a2) exons II + III. Cryptic splicing generated additional rtn5-a1 variants (**Supplementary Fig. 3C**). In the fugu genome, the one rtn1 ortholog is comprised of nine exons coding for the -a isoform (**Fig. 3A**).

RTN2 is the most divergent of the RTN tetralogues with a longer RHD due to nucleotide insertions in the last exon. We found two paralogs each in zebrafish and fugu (rtn2 and rtn8). Based on sequence analyses one could speculate that the insertions present in mammalian RTN2 (36 or 39 bp) and fish rtn2/8 (33 to 66 bp) occurred independently (**Supplementary Fig. 1**). All identified fish rtn2 and rtn8 genes are built by at least seven exons and the resulting transcripts (zebrafish and fugu rtn2-c and rtn8-c) bear only a short specific N-terminus of four aa in both species (**Fig. 3B, Supplementary Figure 6**).

The eight exons of (DANRE)rtn3 can give rise to two different splice variants (**Fig. 3C**), encompassing either all exons (rtn3-a2) or lacking exon II (rtn3-a1). In fugu, only the rtn3-a1 transcript was found (**Fig. 3C**). The sequence of the second paralog, (FUGRU)rtn7 was deduced from genomic scaffolds, since no transcripts could be found in databases or amplified from liver and brain cDNA. Therefore, we can not exclude the possibility that it represents a nontranscribed pseudogene. Interestingly, (FUGRU)rtn7 is the only vertebrate reticulon identified so far, in which the first exon of the RHD is subdivided by an extra intron.(**Fig. 3C**).

Rtn4 is formed by at least nine exons in zebrafish and eight exons in fugu. In zebrafish, three different mRNAs (-l, -m, -n) are generated by alternative promoter usage, each consisting of one specific exon and the RHD with six exons (**Fig. 3D**). From fugu cDNA, only the -l and -n transcripts were isolated. Fugu rtn4-l differs by the presence of two additive small exons (**Fig. 3D**), leading to three splice variants (rtn4-l1, rtn4-l2 and rtn4-l3). The second zebrafish rtn4 ortholog, (DANRE)rtn6, comprises nine exons and three alternative splice forms (-a1, -a2 and -a3) are produced by inclusion or exlusion of exon II or exon III (**Fig. 3D**). Zebrafish rtn4 and rtn6 mRNA variants spliced at cryptic donor and acceptor sites were detected by RT-PCR (**Supplementary Fig. 3A**, **B**).

These extensive analyses of the genomic organisation revealed that all identified zebrafish and fugu rtns genes share the same exon-intron structure in the C-terminal RHD (**Fig. 3**, **Supplementary Table 3**), which is also conserved in mammals and reflects the high degree of sequence similarity in this region (**Supplementary Fig. 1**). The RHDs are each encoded by 6 exons of identical sizes (208, 139, 70, 47, 59 and 40/43/49 bp, respectively), except for rtn2 orthologs which have a longer last exon and for (FUGRU)rtn7 which has an additional intron in the first RHD exon. Intron phases between the RHD encoding exons show a consistent pattern of

2-0-1-0-2, whilst the amino-terminal exons are all symmetrical 1-1 exons (**Fig. 3**, **Supplementary Table 3**).

In contrast, the N-terminal sequences of rtn1-rtn8 are less conserved compared to the RHD and show no homology between the tetralogs (rtn1/5 to rtn2/8 to rtn3/7 to rtn 4/6). However, the fish N-termini of rtn1/5-a, rtn1/5-c, rtn2/8-c and rtn3/7-a1 and rtn3/7-a2 are each orthologous to their mammalian counterparts. First of all, the exon-intron arrangements for the aforementioned transcripts are comparable to those of the respective mammalian isoforms (**Fig. 3A-C** and Oertle et al., 2003b). For example, both N-termini of (DANRE)rtn1-a1 and (HUMAN)RTN1-A consist of three exons each, with similar size. The same holds true for rtn3-a2, in which particularly exon 2 is conserved. (**Fig. 3C**, **Supplementary Fig. 7**). Secondly, although the N-terminal sequences have diverged between different species, at least stretches of conserved aa can be identified, demonstrating a common predecessor of these N-termini (**Supplementary Fig. 4-7**).

Interestingly, the N-termini of mammalian RTN4 and fish rtn4/6 show no indication for a common ancestor. Stretches of conserved aa could neither be identified between the two fish paralogs (rtn4, rtn6) nor between either of the fish duplicates (rtn4/6) and mammalian rtn4 (**Supplementary Fig. 8-9**). Moreover, the exon-intron arrangement of the fish rtn4 gene markedly differs from mammalian RTN4. Three alternative N-termini (-l, -m, -n) are generated by the use of three different promoters and are each encoded by a single specific exon whereas the N-termini of mammalian RTN4 (-A, -B, -C, -D, -E, -F, -G) are represented by one to three exons (**Fig. 3D**; Oertle et al., 2003a).

Taken together, the N-terminal parts of the rtns show higher divergence compared to the RHD, demonstrating non-homogeneous evolution of the reticulon family genes. Although not all rtn splice forms present in mammals were found in fish, detailed genomic and sequence analyses indicate that the specific N-termini of fish and mammalian rtn1/5, rtn2/8 and rtn3/7, respectively, evolved from a common ancestor. In contrast, the rtn4/6 N-termini are completely different and must have been acquired independently. Stretches of aa comparable to the mammalian neurite growth inhibitory region NiG-Δ20 were neither found in the three alternative N-termini of zebrafish rtn4 (-l, -m, -n) nor in rtn6-a1.

3.4.4 Absence of exons homologous to mammalian Nogo-A

To unequivocally exclude the presence of exons homologous to the N-terminal region of mammalian Nogo-A in zebrafish, we had to compare the genomic region of (DANRE)rtn4 against the orthologous human and mouse genomic regions. This required an ungapped alignment of zebrafish versus mammalian genomic sequences ranging at least from the nearest common gene

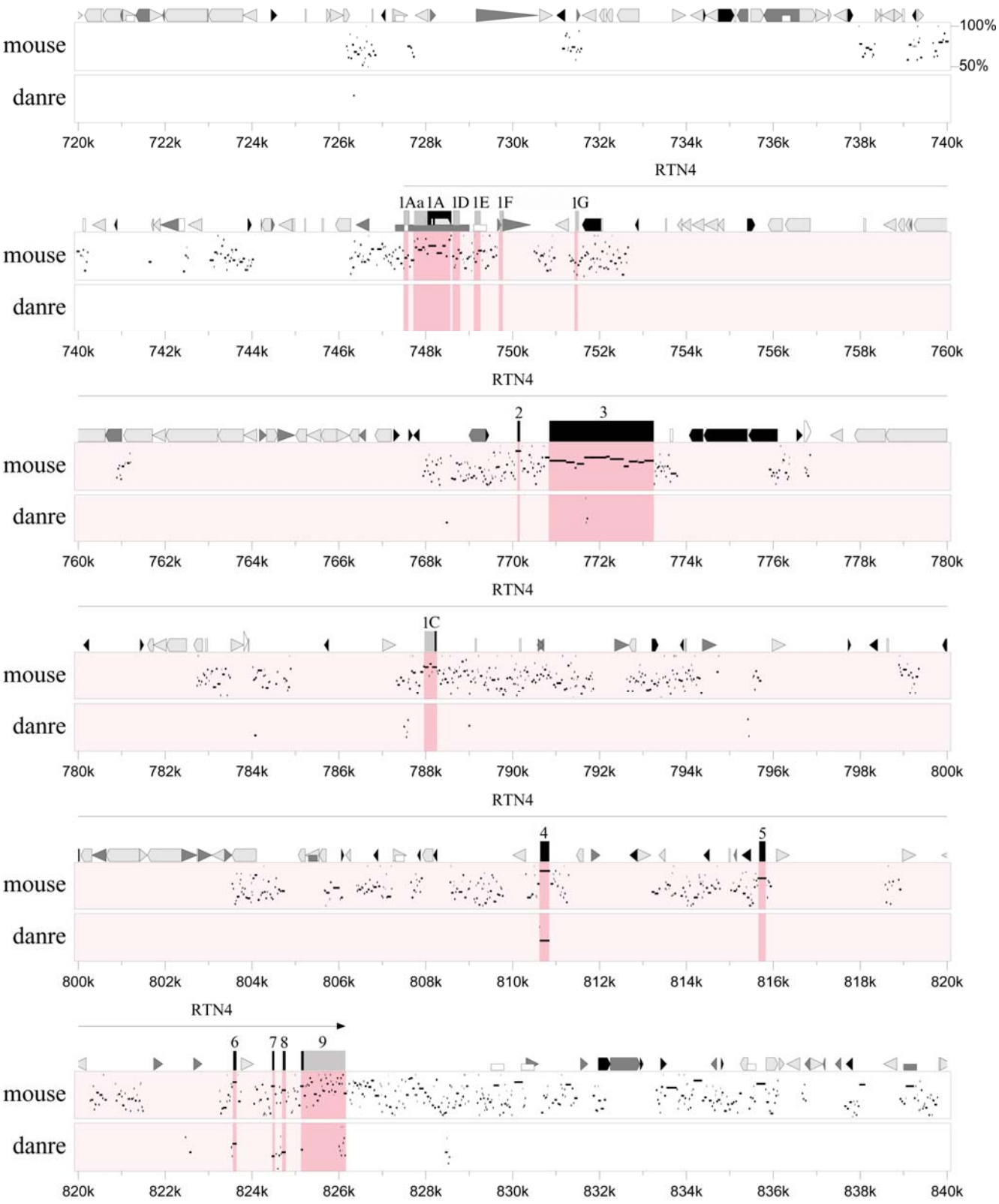

Fig. 4: *Comparison of the human, mouse and zebrafish rtn4 gene locus*

Graphical representation of pair-wise comparisons between the human-mouse (mouse) and human-zebrafish (danre) rtn4 gene locus using a percent-identity plot (PIP) in which the percent identity (from 50% to 100%) in each gap-free aligning segment is plotted using the coordinates of the human sequence. The human exons are numbered according to (Oertle et al., 2003a) and marked in darker colour. Note that while the N-terminal exons 1A, 2 and 3 are strongly conserved in the murine orthologous region, no homology could be identified in zebrafish. In contrast, the exons coding for the conserved C-terminal RHD domain (exons 4-9) are also conserved in the fish orthologous locus. The ungapped alignment from the MTIF2 gene to RTN4, unequivocally proving the absence of sequences orthologous to the N-termini of mammalian RTN4 isoforms in zebrafish, is shown in **Supplementary Fig. 10**. For the analysis and explanation of the interspersed repetitive elements please refer to the PIP in (Oertle et al., 2003a).

lying 5' to RTN4 on the same coding strand to the six exons encoding the RHD which are present in mammals as well as fish (**Supplementary Fig. 10**). We identified the mitochondrial translation initiation factor 2 (MTIF2) (Bonner et al., 1998) as the nearest gene lying 5' to rtn4 on the same coding strand in zebrafish, mouse and human. The two genes FLJ31438 and RPS27A are in fact closer located to rtn4 but an orthologous FLJ31438 gene is not present in zebrafish and RPS27A is encoded by the complementary strand. As shown in the percent identity plot (PIP; **Supplementary Fig. 10A**, **B**), the coding exons of the MTIF2 gene and the six exons of the rtn4 RHD are well conserved in both mammals and zebrafish. However, within the genomic region 5' of the RHD, no stretches homologous to the N-terminal exons of mammlian Nogo-A (human RTN4 exons 1A, 2, 3, 1C and 1D-G) could be identified in zebrafish (**Fig. 4**, **Supplementary Fig. 10**). Consequenctly, the ungapped alignment from the MTIF2 gene to RTN4 unequivocally proved the absence of any known human isoforms in zebrafish. Thus, the neurite outgrowth inhibitory regions of the N-terminus of Nogo-A (NiR-Δ2, NiG-Δ20; Oertle et al., 2003d) are not present in zebrafish.

3.4.5 RT-PCR analyses of zebrafish rtn expression

The finding that rtn4 transcripts with functions similar to mammalian Nogo-A are absent in zebrafish would be substantiated by the verification of dissimilar expression patterns of fish rtn4-l, -m and -n in comparison to mammalian RTN4-A/Nogo-A. In addition, transcription of the other fish rtn mRNAs during zebrafish development and in different adult tissues was examined (**Fig. 5A-L**) not only to characterize each rtn splice form, but to compare the expression of recently duplicated gene paralogs (e.g. rtn4 - rtn6) and to obtain information about potential subfunctionalizations. The observed temporal expression patterns of the rtns can be assigned to three distinct groups. In zebrafish embryos and larvae (**Fig. 5**; **right panel**), many rtn cDNAs are ubiquitously expressed without temporal variations (rtn1-a1, rtn5-b, rtn5-c, rtn3-a1, rtn4-l and rtn4-n). Four transcripts show no (rtn5-a1, rtn2-c) or less (rtn4-m, rtn6-a1) expression at early developmental stages whereas quite dynamic patterns are observed for rtn1-c and rtn8. All

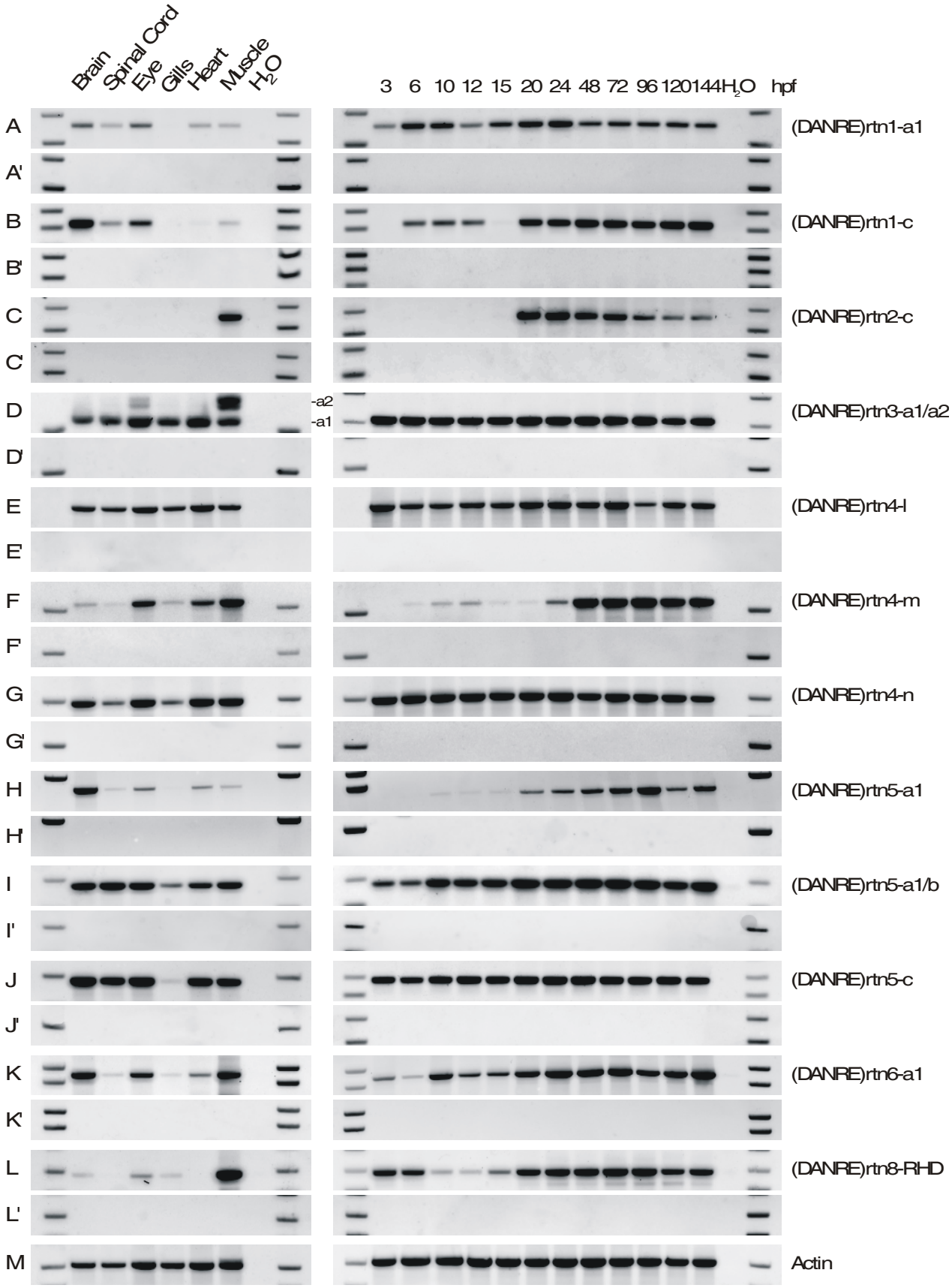

Fig. 5: *RT-PCR analyses of zebrafish rtn mRNA expression*

Expression of zebrafish rtn mRNAs was examined by RT-PCR (**A-L**). A reverse transcriptase negative control (without SuperscriptII enzyme) was performed with each primer pair (**A'-L'**). RT-PCR with actin-specific primers (Actin) served as a positive control and to ensure that equal amounts of cDNA template were put into each reaction (**M**).

During development (3 hpf to 144 hpf; **right panel**), rtn1-a1, rtn5-b, rtn5-c, rtn3-a1, rtn4-l and rtn4-n are ubiquitously expressed (**A**, **I**, **J**, **D**, **E**, **G**). Rtn5-a1, rtn2-c, rtn4-m and rtn6-a1 show less expression at early developmental stages (**H**, **C**, **F**, **K**). Rtn1-c expression is quite dynamic with repeatedly low mRNA levels at 3 hpf and 15 hpf (**B**). The level of rtn8 mRNA is significantly decreased between 6 hpf and 20 hpf (**L**). Note that the rtn8 RT-PCR detects the RHD and is not specific for a single isoform, but only rtn8-c is known so far.

In the adult tissues analyzed (**left panel**), rtn1-a1, rtn5-b, rtn5-c, rtn3-a1, rtn4-l, rtn4-n and rtn6-a1 are omnipresent, but some show varying expression levels (**A**, **I**, **J**, **D**, **E**, **G**, **K**). Rtn1-c, rtn5-a1, rtn2-c, rtn8, rtn3-a2, rtn4-m are rather tissue-specifically expressed (**B**, **H**, **C**, **L**, **D**, **F**).

Note that rtn5 RT-PCRs with a sense primers located either in exon II or at the 3'-end of exon III (**Fig. 1A**) give totally different patterns (**H**, **I**). We therefore propose the existence of a third alternative promoter giving rise to a transcript that we call rtn5-b (**Fig. 1A**).

hpf, hours post fertilization; H_2O, no template control.

transcripts that are omnipresent during zebrafish development are also ubiquitously expressed in various adult tissues (rtn1-a1, rtn5-b, rtn5-c, rtn3-a1, and rtn4-l) with the exception that rtn1-a1 and rtn5-c are hardly detectable in gill (**Fig. 5**, **left panel**). Rtn4-n and rtn6-a1 transcripts were found in all tissues analyzed, but to a varying degree. Six of the analysed zebrafish rtn transcripts show rather tissue-specific expression (rtn1-c, rtn5-a1, rtn2-c, rtn8, rtn3-a2, rtn4-m).

Overall, the extensive RT-PCR analyses revealed differences in the spatial and/or temporal expression patterns of corresponding paralogous transcripts (rtn1-a1/5-a1; rtn1-c/5c). For example, onset of rtn5-a1 transcription is delayed with respect to rtn1-a1, meaning that only rtn1-a1 is present at early developmental stages. High level rtn5-c in contrast to low rtn1-c expression in muscle and heart reveals tissue specific discrimination. Since the structure of the paralogous rtn4 and rtn6 genes differ for the N-terminal exons (three alternative promoters for rtn4 compared to one promoter, but alternative splicing of three exons for rtn6; **Fig. 1D**), the resulting transcripts are not orthologous and therefore not directly comparable. Nevertheless, the expression patterns of neither rtn4-l, -m or -n is similar to rtn6-a1. These divergences in the expression of duplicated genes indicate a potential subfunctionalization. We therefore conclude that none of the gene copies is redundant and that in particular the paralogous rtn4 and rtn6 proteins exert different functions in fish. Moreover, none of the patterns of the four fish rtn4-homologous transcripts (rtn4-l, -m, -n and rtn6-a1) fits to the expression of the axon growth inhibitory mammalian RTN4-A/Nogo-A in neurons and oligodendrocytes (Oertle and Schwab, 2003). This provides additional evidence that the identified fish rtn4 transcripts do not exert neurite growth inhibitory functions similar to mammalian Nogo-A.

3.5 Discussion

The rtn gene family member RTN4/nogo has been widely described as a potent inhibitor of axon regeneration in mammals (Brittis and Flanagan, 2001; Chen et al., 2000; GrandPré et al., 2000; Prinjha et al., 2000). Within this protein, two different regions mediate the axon growth inhibitory effect: one located in the RTN4-A/Nogo-A specific N-terminus and the other (Nogo-66) in the RHD which is the C-terminal part of all RTN4/Nogo isoforms (Oertle et al., 2003d). Whereas no Nogo-A-specific receptor has been identified yet, the inhibitory effect of Nogo-66 is mediated through an interaction with the NgR-p75 receptor complex (Fournier et al., 2001; Hunt et al., 2002a). Interestingly, fish express an NgR ortholog (Klinger et al., 2004b), although fish are capable of regeneration. In this context, it is important to clarify whether fish possess an rtn4 ortholog with one or both inhibitory sites present.

Since rtn4 is a member of a large gene family with a highly conserved C-terminal domain, (Oertle et al., 2003b) phylogenetic analyses of all vertebrate rtn members coupled with gene mapping and synteny data are necessary for the correct assignment of a true fish rtn4 ortholog. We therefore cloned seven zebrafish and five pufferfish rtn genes and uncovered 30 additional rtn genes in eight different fish species by database searches. Our phylogenetic analyses based on the conserved RHD indicate that the four subgroups of the vertebrate RTN family (RTN1-4) arose by duplication events before the divergence of tetrapods (sarcopterygians) and ray-finned fish (actinopterygians) and that we identified at least one zebrafish and fugu ortholog for each subgroup. The presence of additional genes for each of the tetralogs RTN1-4 either in zebrafish and/or pufferfish, that can also be seen in other fish species (e.g. carp rtn1/5 and carp rtn4/6) is consistent with the prediction of the fish-specific genome duplication hypothesis (Amores et al., 1998; Taylor et al., 2003). The phylogenetic relationships of the rtn genes identified in salmonidae, however, cannot solely be explained by this 2R hypothesis, but an additional genome duplication leading to possibly 16 different rtn genes (**Fig. 6**) has to be proposed in this fish subgroup (Brunelli et al., 2001; Rise et al., 2004). Assuming the validity of the genome duplications early in actinopterygian evolution and in salmonidae, several zebrafish, fugu and salmon rtn genes have yet to be discovered or specific gene losses have to be postulated (**Fig. 6**). The differences in gene expression of duplicated rtn genes and in some cases the rapid sequence divergence of duplicated genes potentially generating alternative functional properties (see e.g the relatively low sequence homology of rtn4 and rtn6) could explain why highly related paralogs were maintained in the zebrafish genome and were not rapidly mutated to pseudogenes (Meyer and Schartl, 1999).

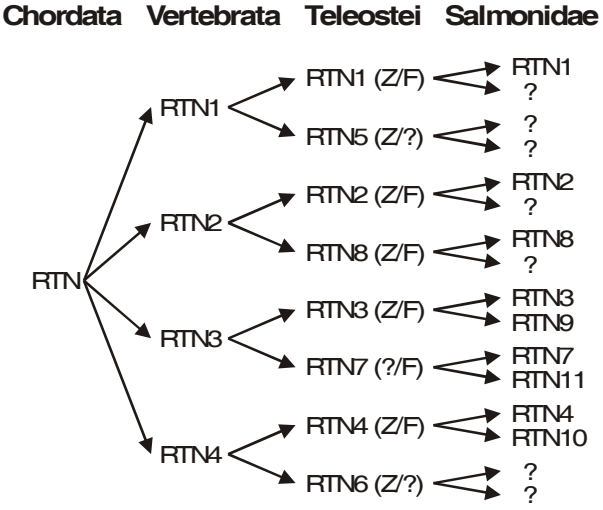

Fig. 6: *Schematic overview of duplicated fish rtn genes*

A single rtn gene is present in the urochordate *Ciona intestinalis*. The divergenc of the rtn family in fish was produced by separate duplication events in the ancestors of vertebrates and early in actinopterygian evolution, leading to rtn1 to rtn8 in teleostei. For salmonidae, an additional genome duplication has to be postulated.

Z, the respective rtn gene has been identified in zebrafish; F, the respective rtn gene has been identified in fugu; ?, the respective rtn gene has yet to be identified or has specifically been lost.

The identity of the zebrafish rtn orthologs was confirmed by radiation hybrid mapping and synteny analyses. All seven zebrafish rtn genes are positioned within syntenic gene clusters, i.e. genes in the vicinity of a given rtn are the same on the zebrafish and the respective human chromosomes. Similar results were obtained for three of the six fugu genes. Moreover, our phylogenetic result of duplication of RTN1-4 in zebrafish is substantiated by the synteny data that zebrafish paralogs map to regions syntenic with the same human chromosome, e.g. zebrafish rtn1 and rtn5 both with human chromosome 14. Although rtn5 and rtn6 both map to the same zebrafish chromosome (LG13), it is unlikely that these genes are the result of a tandem duplication. The distance between rtn5 and rtn6 is rather large and each gene is located in a region that is syntenic to a different human chromosome (chromosomes 14 and 2, respectively). Taken together, our detailed phylogenetic and syntenic analyses clearly demonstrate that a true fish ortholog of the mammalian rtn4/nogo gene exists and that the fish gene has been duplicated, leading to the two paralogs rtn4 and rtn6. However, these data do not provide evidence whether the fish orthologs could exert a similar, axon growth inhibitory function as the mammalian gene.

Indications for a shared function of fish and mammalian rtn4 could be obtained by the identification of homologous aa stretches that have been shown to exert the inhibitory function (i.e. NiG-Δ20 and Nogo-66). We therefore analyzed the N-termini of fish rtn4 and rtn6 for the presence of a comparable NiG-Δ20 region and compared their evolution with the evolution of the rtn1-3 N-termini. The N-termini of all rtn genes are far more divergent than their RHDs, but for rtn1/5, rtn2/8 und rtn3/7 the genomic structures of the fish and the respective mammalian genes are comparable and stretches of conserved aa are detectable within these N-termini. Consequently, the N-termini of fish and of most mammalian rtn1-3 isoforms are orthologous and derived from a common ancestor. These findings are comparable with the non-homogenous evolution of different

parts of the annexin proteins, which has also led to evolutionary conserved C-termini and highly variable N-termini. The annexin N-termini show recognizable homology only in functionally important domains, e.g. phosphorylation sites (Farber et al., 2003). In contrast to rtn1-3, neither conserved genomic organisations nor stretches of similar aa argue for common ancestors of the various alternative fish and mammalian rtn4/6 N-termini. Moreover, examination of the genomic region upstream of the zebrafish rtn4 gene proofs the absence of exons homologous to the mammalian RTN4-A/B specific exons 1A, 2 and 3 (Oertle et al., 2003a). Thus, the N-termini of fish and mammalian rtn4 have a different evolutionary origin and the neurite outgrowth inhibitory region NiG-Δ20 of mammalian Nogo-A is not present in zebrafish. This result is consistent with the observation that the ability for axon regeneration was lost during the transition from fish to land vertebrates (Stuermer et al., 1992). Therefore, yet unidentified functions not related to axonal growth inhibition are expected for the N-termini of fish rtn4. Owing to the fact that orthologous N-termini for mammalian Nogo-A have been identified in amphibian and avian organisms (Klinger et al., 2004a; Oertle et al., 2003b) future studies will have to concentrate on the evolutionary origin of this region in organism linking the transition between fish and amphibians. An interesting question remains if the appearance of Nogo-A-specific regions correlates with the incapacity to regenerate axons after a lesion.

The question of a functional orthologous Nogo-66 domain in fish, however, is much harder to resolve by molecular analyses because the sequence conservation throughout the whole RHD is rather high. No changes in key residues nor differing domains within either the tetrapods or the fish rtn4/6 RHD could be identified that could explain the growth inhibitory function of nogo-66 on one side (tetrapods) and the lack of inhibiton on the other (fish) supporting our previous analysis on this topic (Oertle et al., 2003b). The widespread expression of all zebrafish rtn4/6 transcripts including a variety of non-neuronal tissues rather contradicts an axon growth inhibitory function. Since rtn4 transcripts are also present in goldfish oligodendrocytes (M. Klinger. unpublished results) and fish express the corresponding receptor NgR (Klinger et al., 2004b), a functional receptor-ligand interaction is conceivable. In contrast to mammals (Fournier et al., 2001; GrandPré et al., 2002), however, this interaction obviously does not lead to inhibition of axon growth in fish, since fish grow over isolated fish oligodendrocytes *in vitro* (Bastmeyer et al., 1991; Stuermer et al., 1992) and readily regenerate *in vivo* (Stuermer et al., 1992). Therefore, an assumed Nogo-66-NgR interaction in fish is supposed to be coupled to a different intracellular signaling cascade than in mammals. Alternatively, the homologous fish nogo-66 region might not be exposed to the extracellular surface of fish oligodendrocytes and therefore not be accessible for an interaction with NgR. Future studies will have to show if a molecular interaction between fish

Nogo-66 and NgR is indeed possible and mediates any inhibitory activity. This could shed light on the physiological importance of Nogo-66 as an inhibitor of axonal regeneration also in mammals. In this context, it is worth noticing that NgR is also a member of a larger receptor family with yet unidentified ligands (Klinger et al., 2004b). A hypothesis would be that rtn1-3 might bind to these other NgR-like receptors. Since the fish-specific whole genome duplication increased the number of both rtn and NgR genes in comparison to mammals, the zebrafish is a potent model organism to study the evolution of receptor-ligand interactions after the sequence divergence of two sibling paralogs.

3.6 Acknowledgements

This work was supported by grants of the Deutsche Forschungsgemeinschaft (DFG) and of the Fonds der Chemischen Industrie (FCJ) to C.A.O.S.. M.K. was supported by the "Stiftung der Deutschen Wirtschaft für Qualifizierung und Kooperation e.V. (sdw) and H.-M.P. by the DFG (DFG PO807/1-1). We thank M.-A. Cahill for technical assistance, C. Haenisch for her help in the RT-PCR analysis, A.Y. Loos for fish care and J.S. Taylor for critical reading of the manuscript.

Submitted as:

Klinger, M., Diekmann, H., Oertle, T., Pogoda, H.-M.,. Schwab, M. E˙ and Stuermer C. A. O. Analysis of the reticulon gene family demonstrates the absence of Nogo-A in fish (2004)

3.7 Supplementary data

```
HUMAN)RTN1     AIDLLYWRDIKQTGIVFGSFLLLLFSLTQFSVVSVVAYLALAALSATISFRIYKSVLQAVQKTD-EGHPFKAYLELEITL 79
MACMU)RTN1w    AIDLLYWRDIKQTGIVFGSFLLLLFSLTQFSVVSVVAYLALAALSATISFRIYKSVLQAVQKTD-EGHPFKAYLELEITL 79
BOVIN)RTN1w    AIDLLYWRDIKQTGIVFGSFLLLLFSLTQFSVVSVVAYLALAALSATISFRIYKSVLQAVQKTD-EGHPFKAYLELEITL 79
MOUSE)RTN1     AIDLLYWRDIKQTGIVFGSFLLLLFSLTQFSVVSVVAYLALAALSATISFRIYKSVLQAVQKTD-EGHPFKAYLELEITL 79
RAT)RTN1       AIDLLYWRDIKQTGIVFGSFLLLLFSLTQFSVVSVVAYLALAALSATISFRIYKSVLQAVQKTD-EGHPFKAYLELEITL 79
CANFA)RTN1     AIDLLYWRDIKQTGIVFGSFLLLLFSLTQFSVVSVVAYLALAALSATISFRIYKSVLQAVQKTD-EGHPFKTYLELEITL 79
CHICK)RTN1     AINLLYWRDIKQTGIVFGSLLLLLFSLTQFSVVSVVAYLALAGLSATISFRIYKSVLQAVQKTD-EGHPFKAYLDMEMNL 79
XENLA)RTN1.1   AIDLLYWRDIKQTGIVFGSVLLMLFSLIQFSVVSVMAYLALAALSATISFRIYKSVLQAVQKTD-EGHPFKSYLDMEISL 79
XENLA)RTN1.2   AIDLLYWRDVKQTGIVFGSILLMLFSLTLFSVVSVIAYLALAALSATISFRIYKSVLQAVQKTD-EGHPFKSYLDIEISL 79
DANRE)RTN1     AMELLYWRDLKKSGLVFGSLLLMLFSLTQFSVVSVVAYLALASLSATISFRVYKSVLQAVQKTD-EGHPFKVYLDVEMSL 79
FUGRU)RTN1     AIDLLYWRNVKQSGAVFSSVLLLLFSLTQFSVVSVGAYLALAALSATISFRIYKSVLQAVQKTD-EGHPFKSYLEMEITL 79
ICTPU)RTN1     AMELLYWRDVKQTGLVFSSVLLLLFSLTQFSVVSVVATLALAALSATISFRVYKSVLQAVQKTD-EGHPFKSYLEIEMSL 79
CYPCA)RTN1     VMELLYWRNLKQSGLVFGSFLLLLFSLTQFSVVSVVAYLALAALSATISFRIYKSVLQAVQKTD-EGHPFEAYLEVEMSL 79
GASAC)RTN1w    ----------------------------------------LSASISFRIYKSVLQAVQKTD-EGHPFKAYLEVEIAL 36
ONCMY)RTN1     AIDLLYWRNVKQSGAVFGSVLLLLFSLTQFSVVSVGAYLTLAALSASISFRIYKSVLQAVQKTD-EGHPFKSYLEVEISL 79
ORYLA)RTN1     AIDLLYWRNVKQSGAVFSSVLLLLFSLTQFSVVSVGAYLALAALSATISFRIYKSVLQAVQKTD-EGHPFKAYLEMEIAL 79
DANRE)RTN5     VVDLVHWRDLKQSGLVFGSVLLLLFSLTQFSVVSVIAYLALAVLSATISFRVYKSVLQAVQKTD-EGHPFKSYLEVEISL 79
CYPCA)RTN5w    ------------------------------------------------------------------------------- 1
ICTPU)RTN5w    VVELLRWRDVKQTAVLFSSVLLLLFSLTQFSVVSVIAYLALAALSTTISFRVYKSVLQAVQKTD-DGHPFKVYLEKEIAL 79
HUMAN)RTN2     VADLLYWKDTRTSGVVFTGLMVSLLCLLHFSIVSVAAHLALLLLCGTISLRVYRKVLQAVHRGD-GANPFQAYLDVDLTL 79
MOUSE)RTN2     VADLLYWKDTRTSGAVFTGLMASLLCLLHFSIVSVAAHLALLGLCATISLRVYRKVLQAVHRGD-GTNPFQAYLDMDLTL 79
RAT)RTN2       VADLLYWKDTRTSGAIFTGLMASLLCLLHFSIVSVAAHLALLGLCATISLRVYRKVLQAVHRGD-GTNPFQAYLDMDLTL 79
BOVIN)RTN2     VVDLLHWKDAKTSGVVFTCLMVSLLSLLHFSIVSVAAHVALLLLCGTISLRVYRKVLQAVHRGD-GANPFQAYLDVDLTL 79
PIG)RTN2       VADLLYWKDTXTSGVVFTGLMVSLLSLLHFSIVSVAAHVALLLLCGTISLRVYRKVLHTVHRGD-GSNPFQAYLDVDLTL 79
XENLA)RTN2     VKDLLYWRDTLLSTGCLTGVTLSLLCLSQFSVISVFAYGCLIILSVTLTLRLYTKLLHALKRGN-GANPFQYYLDTDLKL 79
XENTR)RTN2     VKDLLYWRDILLSAGCLTGVTLSLLCLSQFSVISVFAYGCLIILSVTLTLRLYTKLLHALKRGN-GANPFQYYLDADLKL 79
FUGRU)RTN2     VVDLIYWKDTERTGMVLTGLVVGLLSLFQLSIITVFSTVSLAIVCCTISVRIYYGLIHALKWGD-GEHPFKTYLDLDISF 79
ICTPU)RTN2w    VMDLIYWKDTERTGMVFTSLVVGLLFLFQLSIITVLATVSLAIVCFTISVRIYCKLLHALQLRD-AAHPFQTYLDVDIGL 79
FUGRU)RTN8     LMDLVYWRDVRKTGVVFTGLVISLASVFQLSVITVFSHICLVAMCATFPLRLYYKLLELLRWNP-GVHPYQSYLDYDSSL 79
DANRE)RTN2     VMDLVYWKDMERTGMVLTGLVVALLSLFQLSIITVVSTLSLAILCFTISVRIYYKLLHVLQLGD-GVHPFQSYLDLDISL 79
DANRE)RTN8     VLDLIYWRNLATTGVVFTGLVVGLASLFQLSAITILSNLGLSIMAFTLPVRLLYKAMTVTRLND-GSHPFQSYLDEDHTL 79
ONCMY)RTN8w    VMDLIYWRDVGKTGLVVTGLVIGLASLFQFSSVTMLSYLCISIMCLTFPLRLYYKLLELIRKIPEGVHPFQSYIGDDSSL 80
ONCMY)RTN2     VMDLIYWKDTERTGMVFTGLMVGLLSLFQLSIITVISTISLGALCFTVSVSLYYKILHVLNMGD-GVPPFKAYLDLDISF 79
ORYLA)RTN2     VMDLIYWKDMERSGMVLTGLVVGLLSLFQLSIITVVSTVSLAVMCFTISVRTYYQFLYVLSWGD-GEHPFKSYLDLDISF 79
HUMAN)RTN3     VHDLIFWRDVKKTGFVFGTTLIMLLSLAAFSVISVVSYLILALLSVTISFRVYKSVIQAVQKSE-EGHPFKAYLDVDITL 79
MOUSE)RTN3     VHDLIFWRDVKKTGFVFGTTLIMLLSLAAFSVISVVSYLILALLSVTISFRVYKSVIQAVQKSE-EGHPFKAYLDVDITL 79
RAT)RTN3       VHDLIFWRDVKKTGFVFGTTLIMLLSLAAFSVISVVSYLILALLSVTISFRVYKSVIQAVQKSE-EGHPFKAYLDVDITL 79
CANFA)RTN3w    VHDLIFWRDVKKTGFVFGTTLIMLLSLAAFSVISVXSYLILAXXXXXXXXXXXXXXXXXXXXXX-XXXXXXXXXXXXXX 79
SHEEP)RTN3w    GHDLIFWRDVKKTGFVFGTTLIVLLSLAAFSVISVVSYLILALLSVTISFRVYKSVIQAVQKSE-EGHPFKAYLDVDITL 79
BOVIN)RTN3     VHDLIFWRDVKKTGFVFGTTLIMLLSLAAFSVISVVSYLILALLSVTISFRVYKSVIQAVQKSE-EGHPFKAYLDVDITL 79
PIG)RTN3       VHDLIFWRDVKKTGFVFGTTLIMLLSLAAFSVISVVSYLILALLSVTISFRVYKSVIQAVQKSE-EGHPFKAYLDVDITL 79
PANTR)RTN3     VHDLIFWRDVKKTGFVFGTTLIMLLSLAAFSVISVVSYLILALLSVTISFRIYKSVIQAVQKSX-EGHPFKAYLDVDITL 79
CHICK)RTN3w    VHDLIFWRDVRRSGAVFASSLLLLLSLAAFSVVSVVAYLVLALLSVTISFRVYKSVIQAVQKSE-EGHPFRAYLELDXTL 79
XENLA)RTN3.1   VRDLLYWRDVKQSGMVFGGTMVLLLSLAAFSIISVISYLVLSLLTVTISYRVYKSVLQAVQKTD-EGHPFKPLLEKDITL 79
XENLA)RTN3.2   VRDLLYWRDVKQSGMVFGGTMVLLLSLAAFSIISVISYLVLSLLSVTISFRVYKSVLQAVQKTE-EGHPFKPLLEKDIAL 79
XENTR)RTN3     VQDLLYWRDVKQSGMVFGGTMVLLLSLAAFSIISVISYLVLSLLAVTISYRVYKSVLQAVQKTD-EGHPFKPLLEKDIAL 79
PAROL)RTN3     VKDLIHWRDPKKSGLVFGLSMLMLLSLAAFSVISVASYLLLALLCVTISFRIYKSVIQAVQKSS-DGHPFKTLIDKDVSI 79
DANRE)RTN3     VNDLVHWRDPKKSGVVFGVSLLLLLSLAAFSVISVVSYLLLSLLCVTISFRIYKSVIQAVQKSN-EGHPFKALMDKDVTV 79
CARAU)RTN3w    ----------------------------------------------------YKSVIQAVQKSN-EGHPFKALMEKDVTV 27
CYPCA)RTN3w    ------------------------------------------------------------------------------- 1
FUGRU)RTN3     VKDLIHWRDPKKSGLAFGLSMLLLLSLAAFSVISVASYLLLALLCVTITFRIYKSVIQAVQKSS-DGHPFKSLIEKDVSI 79
GASAC)RTN3     VKDLIHWRDPKKSGVVFGLSLLLLLSLAAFSFISVASYLLLALLCVTITFRIYKSVVQAVQKSS-DGHPFKTLIEKDVSI 79
SALSA)RTN3w    ----------KSGVVFGLSLLTLLSLAAFSVISVISYLLLALLCVTITFRIYKSVVQAVQKSN-DGHPFKALMEKDVSI 68
ORYLA)RTN3w    VKDLIHWRDPKKSGVVFGLSLLMLLSLAAFSVISVASYLLLALLIVTISFRIYKSVLQAVQKSN-DGHPFKMLINKDVSI 79
ONCMY)RTN9     VKDLVHWRDPKKSGVVFGLSLLTLLSLAAFSVISVVSYLLLALLCVTISFRIYKAVVQAVQKSD-DGHPFKALMEKDVSV 79
ONCMY)RTN3     VKDLVHWRDPKKSGVVFGLSLLTLLSLAAFSVISVISYLLLALLCVTISFRIYKSVVQAVQKSN-DGHPFKALMEKDVSI 79
FUGRU)RTN7     VLQLVHWKEPKKTAAAFSGSLLVLVSVATLSIISVVSYSLLTCLCVTITFRVYKSVIQAVQKSD-EGHPFRSLLDRDISV 79
ONCMY)RTN7     VMELVYWRDPKKSAVAFGMSLLVLLSLATFSVISVVSYMLLALLCVTITFRVYKSVIQAVQKSE-EGHPFKALMEKDLTV 79
ONCMY)RTN11    VMELVYWRDPKKSAVAFGMSLLVLLSLAIFSIISVLSYLLLALLCVTITFRIYKSVIQAVQKSG-EGHPFKGLMEQDLTV 79
SALSA)RTN7w    ----------------------------------------ALLCVTITFRVYKSVIQAVQKSE-EGHPFKALMEKDLTV 38
HUMAN)RTN4     VVDLLYWRDIKKTGVVFGASLFLLLSLTVFSIVSVTAYIALALLSVTISFRIYKGVIQAIQKSD-EGHPFRAYLESEVAI 79
MACFA)RTN4     VVDLLYWRDMKKTGVVFGASLFLLLSLTVFSIVSVTAYIALALLSVTISFRIYRGVIQAIQKSD-EGHPFRAYLESEVAI 79
MACMU)RTN4w    VVDLVYWRDMKKTGVVFGASLFLLLSVTVFSIVSVTAYIALALLSVTISFRRYRGVIQAIQKSD-EGHPFRAYLESEVAI 79
MOUSE)RTN4     VVDLLYWRDIKKTGVVFGASLFLLLSLTVFSIVSVTAYIALALLSVTISFRIYKGVIQAIQKSD-EGHPFRAYLESEVAI 79
RAT)RTN4       VVDLLYWRDIKKTGVVFGASLFLLLSLTVFSIVSVTAYIALALLSVTISFRIYKGVIQAIQKSD-EGHPFRAYLESEVAI 79
BOVIN)RTN4     VVDLLYWRDIKKTGVVFGASLFLLLSLTVFSIVSVTAYIALALLSVTISFRIYKGVIQAIQKSD-EGHPFRAYLESEVAI 79
SHEEP)RTN4     VVDLLYWRDIKKTGVVFGASLFLLLSLTVFSIVSVTAYIALALLSVTISFRIYKGVIQAIQKSD-EGHPFRAYLESEVAI 79
PIG)RTN4       VVDLLYWRDIKKTGVVFGASLFLLLSLTVFSIVSVTAYIALALLSVTISFRIYKGVIQAIQKSD-EGHPFRAYLESEVAI 79
CANFA)RTN4w    VVDLLYWRDIKKTGVVFGASLFLLLSLTVFSIVSVTAYIVLALLSVTISFRIYKGVIQAIQKSD-EGHPFRAYLESEVAI 79
PANTR)RTN4     VVDLLYWRDIKKTGVVFGASLFLLLSLTVFSIVSVTAYIALALLSVTISFRIYKGVIQAIQKSD-EGHPFRAYLESEVAI 79
CHICK)RTN4     VVDLLYWRDIKKTGVVFGASLFLLLSLTVFSIVSVTAYIALALLSVTISFRIYKGVIQAIQKSD-EGHPFRAYLESDVAV 79
XENLA)RTN4.1   VVDLIYWRDIKRSGVVFGASLFLLLSLSVFSIVSVLAYIALALLSVTISLRIYKGILQAIQKSE-EGHPFRSILESNLAV 79
XENLA)RTN4.2   VVDLIYWRDIKRSGVVFGASLFLLLSLSVFSIVSVLAYIALALLSVTISFRIYKGVLQAIQKSE-EGHPFRSILESNLAL 79
XENTR)RTN4     VVDLVYWRDIKKSGAVFGASLFLLLSLSVFSIVSVLAYIALALLSVSISFRIYRGVLQAIQKSD-EGHPFRSILESNLAV 79
```

```
CARAU)RTN4     VVDLLYWRDLQRTGVVFGASLLLLLSLSVCSIISVISYVALALLSVTISFRIYKGILQAVQKSE-DGHPFKMYLDKDIGI 79
DANRE)RTN4     LVELLYWRDLQRTGVVFGAGLFLLLSLSMCSIISVLSYVALALLSVTVSFRIYKGILQAVQKSE-DGHPFKMYLDKDTAL 79
FUGRU)RTN4     LVDLVYWRDVKTTGVVFGAALLLLLSLMACSIVSVISYIGLALLSVTISFRIYKGILQAIQKSD-EGHPFKQYLDQEVAL 79
ONCMY)RTN4     VVELLYWRDVKTSGVVFGASLSLLLSLTLCSIVSVSSYIGLALLSVTICFRIYKGILQAIQKSD-EGHPFKLYLDQDVAL 79
ONCMY)RTN10    VVELLYWRDVKTSGVVFGAGLSLLLSLTLCSIVSVSSYITLVLLSVTICFRIYKGILQAIQKSD-EGHPFKLYLDQDVGL 79
SALSA)RTN4     VVELLYWRDVKTSGVVFGASLSLLLSLTLCSIVSVSSYIGLALLSVTICFRIYKGILQAIQKSD-EGHPFKLYLDQDVAL 79
SALSA)RTN10w   ----------------------------------------XICXRIYKGILQAIQKSD-EGHPFKLYLNQDVGL 33
ORYLA)RTN4w    ------------------------------------------------------------------------------- 1
CYPCA)RTN4     VVDLLYWRDLQRTGVVFGASLFLLLSLSVCSIISVISYVALALLSVTISFRIYKGILQAVQKSE-DGHPFKMYLDKDIGI 79
CYPCA)RTN6     VLELLYWRDVRASGLVLGCSLFLLLSLLSCSIISVLSYSSLALLSLTLSFRTYRGVLQAIQKSD-EGHPFKRYLAQDIFL 79
DANRE)RTN6     VLQLLYWRDVRASALVLGSLLLLLFLSCCSVISVLSYSALCLLTLTLSTRVFTAVLQAMRKTE-DGHPFRQYLERDVLL 79
CIOIN)RTN      VKDLLYWRDIKVSGVVFGLTLLVLLSLCCFSVVSVISYLTLSLLTVTVAFRLYKLVLQTLNGTQ-QPNPFQSLLDMEVTL 79

HUMAN)RTN1     SQEQIQKYTDCLQFYVNSTLKELRRLFLVQDLVDSLKFAVLMWLLT-YVGALFNGLTLLLMAVVSMFTLPVVYVKHQAQI 158
MACMU)RTN1w    SQEQIQKYTDCLQFYVNSTLKELRRLFLVQDLVDSLKFAVLMWLLT-YVGALFNGLTLLLMAVVSMFTLPVVYVKHQAQI 158
BOVIN)RTN1w    SQEQIQKYTDCLQFYVNNTLKELRRLFLVQDLVDSLKFAVLMWLLT-YVGALFNGLTLLLMAXVXMFTLPVVYXXXXXXX 158
MOUSE)RTN1     SQEQIQKYTDCLQLYVNSTLKELRRLFLVQDLVDSLKFAVLMWLLT-YVGALFNGLTLLLMAVVSMFTLPVVYVKHQAQV 158
RAT)RTN1       SQEQIQKYTDCLQLYVNSTLKELRRLFLVQDLVDSLKFAVLMWLLT-YVGALFNGLTLLLMAVVSMFTLPVVYVKHQAQV 158
CANFA)RTN1     SQEQIQKYTDCLQFYVNNTLKELRRLFLVQDLVDSLKFAVLMWLLT-YVGALFNGLTLLLMAVVSMFTLPVVYVKHQAQI 158
CHICK)RTN1     SQDQIQKYTDCLQLYVNSTVKELRRLFLVQDLVDSLKFAVLMWLLT-YVGALFNGLTLLIMAVVSMFTLPVVYDKYQAQI 158
XENLA)RTN1.1   SQEQIQKYTDCLQVYTNSIAKELRRLFLVQDLVDSLKFAVLMWLLT-YVGALFNGLTLLIMAVVSMFSLPVVYDKYQAQI 158
XENLA)RTN1.2   SQEQIQKYTGCFQLYTNSIAKELRRLFLVQDLVDSLKFAVLMWLLT-YVGALFNGLTLLIMAVVSMFSLPVVYDKYQAQI 158
DANRE)RTN1     SHDQMQKYAENVQYYINSTLKELRRLFLVQDLVDSLKFAVLMWLLT-YVGALFNGLTLLIMVVVCMFSMPVVYEKYQAQI 158
FUGRU)RTN1     SQDQISKYADKILLYSNTCVKELRRLFLVQDLVDSLKFAVLMWLLT-YVGALFNGLTLLILAVVSMFTMPVVYEKHQAQI 158
ICTPU)RTN1     SNDQMQKYAENTQNYINNTLKELRRLFLVQDLVDSLKFAVVMWLLT-YVGALFNGLTLLIMAVVSMFTMPVVYEKYQAQI 158
CYPCA)RTN1     SHDQMQKYAENAQYYINSTLKELRRLFLVQDLVDSLKFAXLMWLLT-YVGALFNGLTLLIMVXVSMFSMPVVYEKYQAQI 158
GASAC)RTN1w    SQDQISKYADKILLYTNTCMKELRRLFLVQDLIDSLKFAVLMWLLT-YVGALFNGLTLLILAVVSMFSMPVVYEKHQAQI 115
ONCMY)RTN1     SQDQIGKYADKALLYANTCMKELRRLFLVQDLIDSLKFAVLMWLLT-YVGALFNGLTLLILAVVSMFSMPIVYEKNQAQI 158
ORYLA)RTN1     SQDQITKYADKILLYTNTCMKELRRLFLVQDLVDSLKFAVLMWLLT-YVGALFNGLTLLILVVVSMFTMPVVYEKHQAQI 158
DANRE)RTN5     SADQISKYVDKTQLYINTTMKELRRLFLVQDLVDSIKFAVLMWLLT-YVGALFNGLTLLILAVISMFSVPVVYEKYQTQI 158
CYPCA)RTN5w    SADQISKYVEKTQLYINSTMKELRRLFLVQDLVDSIKFAVLMWLLT-YVGALFNGLTLLILAVVSMFTVPLVYEKYQTQI 79
ICTPU)RTN5w    SPEQISKYVEKVQLYVNYTLKELRRLFLVQDLVDTLKFAVLMWLLT-YVGALFNGLTLLLLAVVCVFTVPLVYEKIPEQI 158
HUMAN)RTN2     TREQTERLSHQITSRVVSAATQLRHFFLVEDLVDSLKLALLFYILT-FVGAIFNGLTLLILGVIGLFTIPLLYRQHQAQI 158
MOUSE)RTN2     TREQTERLSQQIASHVVSTATQLRHFFLVEDLVDSLKLALLFYILT-FVGAIFNGLTLVILGVVALFTVPLLYRQHQAQI 158
RAT)RTN2       TREQTERLSQQIASHVVSTATQLRHFFLVEDLVDSLKLALLFYILT-FVGAIFNGLTLVILGVVALFTVPLLYRQHQAQI 158
BOVIN)RTN2     TQEQTERLSQQIASRVVSAAIQLRHFFLVEDLVDSLKLALLFYILT-FVGAVFNGLTLLILGVIGVFTVPLLYRQHQAQI 158
PIG)RTN2       TREQTERLSQQIASRVVVAATQLRHFLLVEDLVDSLKLALLFYILT-FVGAVFNGLTLLILGVIGLFTVPLLYRQHQAQI 158
XENLA)RTN2     TTKQAEEIVARAFSLASTTLCTLRSLFLVEELKDSLKFLVIVYLLT-YVGAVFNGITVLLLCVIGAFTFPILYKQHQTQV 158
XENTR)RTN2     TTKQAEEITARVLSLLSTTICTLRSLFLVEELKDSLKFLVIIYLLT-YVGAVFNGITVLLLCVIGAFTFPILYKQHQTQV 158
FUGRU)RTN2     SGEEAERCTQKAIVMFLSAIDSLKGLFFVKSLFESLKFLVLMYLVT-YLGRLCNGLTVLIIGVIAVFSLPLFYKRHQEKV 158
ICTPU)RTN2w    SGDQAEHYMQRAIFLCFAAVDTLKRLVFVASLFDSLKFLLLMYLVT-YLGALCNGLTLLVIGVIAVFSVPLFYSRHQETL 158
FUGRU)RTN8     TDRETVMLVEEVVLLITFAITELKRLIFIGSITDSIKFVVLLYLLT-YVGALTNGLTLVISAVIGLFSIPLLYKKQQVRL 158
DANRE)RTN2     SGEEAEHCLQRAIVLSCSALETLRNLIFVGNLFSSLKFWLLMYVVT-FLGNLCNGLTLIIIGVIAVFSVPLFYTRHQDKV 158
DANRE)RTN8     TDEDTVRMAEQMVLLIATAVSELKRLFFIDSIMDSVKFIVFLYLLT-YVGVQANGLTLVMSGVICAFSLPLLYKLQQERI 158
ONCMY)RTN8w    TDEETVLVVEEVVLMMAFAITEIKRLLFIDSIMDSIKFVVLLYVLT-YMGITTNGLTLVIVGVICVFSLPLFYKQMQGRM 159
ONCMY)RTN2     SGELADQYTQKVIVAVVSAANSLKNLFLVGNLFDSLKLLALMYLVT-FLGDLCNGLTVLIIGVIALFSLPLVYRQHQAKV 158
ORYLA)RTN2     SGEQADLYXQKVIVSTLSAVDALKKLFFVGNLFDSLKFLFLLYLVT-YLGDLCNGLTLLIISVIAVFSLPLFYKXRQEEV 158
HUMAN)RTN3     SSEAFHNYMNAAMVHINRALKLIIRLFLVEDLVDSLKLAVFMWLMT-YVGAVFNGITLLILAELLIFSVPIVYEKYKTQI 158
MOUSE)RTN3     SSEAFHNYMNAAMVHVNKALKLIIRLFLVEDLVDSLKLAVFMWLMT-YVGAVFNGITLLILAELLVFSVPIVYEKYKTQI 158
RAT)RTN3       SSEAFHSYMNAAMVHVNKALKLIIRLFLVEDLVDSLKLAVFMWLMT-YVGAVFNGITLLILAELLVFSVPIVYEKYKTQI 158
CANFA)RTN3w    XXEAFHNYVNAAMVHINRALKLIIRLFLVEDLVDSLKLAVFMWLMT-YVGAVFNGITLLILAELLIFSVPIVYEKYKTQI 158
SHEEP)RTN3w    SSEAFHNYVNAAMVHINRALKLIIRLFLVEDLVDSLKLAVFMWLMT-YVGAVFNGITLLILAELLVFSVPIVYX------ 152
BOVIN)RTN3     SSEAFHNYVNAAMVHINRALKLIIRLFLVEDLVDSLKLAVFMWLMT-YVGAVFNGITLLILAELLVFSIPIVYEKYKTQI 158
PIG)RTN3       SSEAFHNYVNAAMVHINKALKLIIRLFLVEDLVDSLKLAVFMWLMT-YVGAVFNGITLLILAELLIFSVPVVYEKYKTQI 158
PANTR)RTN3     SSEAFHNYMNAAMVHINRALKLIIRLFLVEDLVDSLKLAVFMWLMT-YVGAVFNGITLLILAELLIFSVPIVYEKYKTQI 158
CHICK)RTN3w    SPEAFQSHATAAMAHVNHALRLLLRLFLVEDLVDSLKLAVAMWLMT-YVGAVFNGITLLILAELLAFTLPPVXEKNKVQI 158
XENLA)RTN3.1   SSDSFQKALTASLAHVNHALKYIVRLFLVDDLVDSLKLALLMWLMT-YVGAVFNGITLLILGVLLTFTAPIVYEKYKVQI 158
XENLA)RTN3.2   SSDSFQKGLSSSLAHVNHALKSIVRLFLVEDLVDSLKLALLMWLMT-YIGAVFNGITLLILGVLLAFTTPLVYEKYKVQI 158
XENTR)RTN3     SSDAFQKALSTSLAHVNHALKYIVRLFLVEDLVDSLKLALLMWLMT-YVGAVFNGITLLILGVLLAFTAPIVYEKYKVQI 158
PAROL)RTN3     PPETFRKHVDASLTYINRALKQMSRLFLVEDLVDSLKLAVVMWLLT-YVGAVFNGITILILADILLFAVPPVYEKNKTQI 158
DANRE)RTN3     PPETFRKHVDGCLSHVNRALKQMSRLFLVEDLVDSLKLAVVMWLLT-YVGAVFNGITILILADILLFSVPPIYEKNKTQI 158
CARAU)RTN3w    PPETFRKHVDVCLTHVNRALKQMSRLFLVEDLVDSLKLAVVMWLMT-YVGAVFNGITILILADILLFSVPPIYEKNKTQI 106
CYPCA)RTN3w    ---------------------------------LKLAVVMWLLT-YVGAVFNGITVLILADILLFSVPLIYEKNKTQI 44
FUGRU)RTN3     PPETFRKHVDCGLSYINRALKQMSRLFLVEDLVDSLKLAVIMWLFT-YVGAVFNGITILILANILLFAVPPVYEKNKTQI 158
GASAC)RTN3     PPETFRKHVDSSLTHINRALKQMSRLFLVEDLVDSLKLAVVMWLFT-YVGAVFNGITILILADILLFAVPPVYEKNKTQI 158
SALSA)RTN3w    PPETFHKHVDVSLTYINRFLKQMSKLFLVEDLIDSLKLAVVMWLLT-YVGAVFNGITVLILADILLFAVPPFYEKNKTQI 147
ORYLA)RTN3w    PPETFRKHVDASLTYINRGLKQMSRLFLVEDLVDSLKLAVVMWLLT-YVGAVFNGITLLILADILLFAVPPVYEKNKTQI 158
ONCMY)RTN9     PPETFRKHVDASLTHINRLLKQLRKLFLVEDLIDSLKLAVVMWLLT-YVGAVFNGITILILADILLFAVPPFYEKNKTQI 158
ONCMY)RTN3     PPETFHKHVDVSLTYINRFLKQMSKLFLVEDLIDSLKLAVVMWLLT-YVGAVFNGITILILADILLFAVPPFYEKNKTQI 158
FUGRU)RTN7     SSEWIRSLAGQSLVHVNCFISQTRRLMLVEDLVDSMKVTAVMWVMT-YVGAIFNGITLLIIADILCFTAPLIYQRKKTQI 158
ONCMY)RTN7     QPEILRKYVDVCLTYVNLAITQARHLLLVEDLVDSLKLAGFMWLLT-YVGAVFNGITILILTDIIFFSTPLVYERNKTQI 158
ONCMY)RTN11    QPETFRKYVDVFLTYVNRAVKQIKHLLLVEDLVDSLKLAGFMWLMT-YVGAVFNGITILILADVILFSTPPVYDKNKTQI 158
SALSA)RTN7w    QPEIFRKYVDVCLTYVNRAIKQARHLLLVEDLVDSLKLAGFMWLLT-YVGAVFNGITILILTDIIFFSTPLVYERNKIQI 117
HUMAN)RTN4     SEELVQKYSNSALGHVNCTIKELRRLFLVDDLVDSLKFAVLMWVFT-YVGALFNGLTLLILALISLFSVPVIYERHQAQI 158
MACFA)RTN4     SEELVQKYSNSALGHVNCTIKELRRLFLVDDLVDSLRFAVLMWVFT-YVGALFNGLTLLILALISLFSVPVIYERHQAQI 158
MACMU)RTN4w    SEELVQKYSNSALGHVNCTIKELRRLFLVDDLVDSLKFAVLMWVFT-YVGALFNGLTLLILALISLFSVPVIYEPHQAQI 158
MOUSE)RTN4     SEELVQKYSNSALGHVNSTIKELRRLFLVDDLVDSLKFAVLMWVFT-YVGALFNGLTLLILALISLFSIPVIYERHQAQI 158
```

```
RAT)RTN4       SEELVQKYSNSALGHVNSTIKELRRLFLVDDLVDSLKFAVLMWVFT-YVGALFNGLTLLILALISLFSIPVIYERHQVQI 158
BOVIN)RTN4     SEELVQKYSNSALGHVNCTIKELRRLFLVDDLVDSLKFAVLMWVFT-YVGALFNGLTLLILALISLFSVPVIYERHQAQI 158
SHEEP)RTN4     SEELVQKYSNSALGHVNCTIKELRRLFLVDDLVDSLKFAVLMWVFT-YVGALFNGLTLLILALISLFSVPVIYERHQAQI 158
PIG)RTN4       SEELVQKYSNSALGHVNCTIKELRRLFLVDDLVDSLKFAVLMWVFT-YVGALFNGLTLLILALISLFSVPVIYERHQAQI 158
CANFA)RTN4w    SEELVQKYSNSALGHVNCTIKELRPSFLVDDLSDSLKFAVLMWVFT-YVGX---------------------------- 129
PANTR)RTN4     SEELVQKYSNSALGHVNCTIKELRRLFLVDDLVDSLKFAVLMWVFT-YVGALFNGLTLLILALISLFSVPVIYERHQAQI 158
CHICK)RTN4     SEDLIQKYSSVVLGHINGTVKELRRLFLVDDLVDSLKFAVLMWVFT-YVGALFNGLTLLILALISLFSVPVIYERHQAQI 158
XENLA)RTN4.1   PEDLVQKYCNVALNHVNCTVKELRHLFLVEDLVDSLKFAVLMWVFT-YIGALFNGLTLLIVALISLFSIPVIYERHQTQV 158
XENLA)RTN4.2   PEDVVQKHCTVALNQVNRTVAELRRLFLVEDLVDSLKFAVLMWVFT-YIGALFNGLTLLIVALISLFSIPVIYERHQTQV 158
XENTR)RTN4     PEDLVQKYCNVALNHVNCTVKELRRLFLVEDLVDSLKFAVLMWVFT-YIGALFNGLTLLILALISLFSIPVIYERHQTQV 158
CARAU)RTN4     SSELVQKYSDTALAHINCVIKELRRLFLVEDLVDSLKFAVFMWILT-YVGALFNGLTLLIMGLIGTFSWPVIYEKHQAQI 158
DANRE)RTN4     PAEMVHKYSDSTLVHINTVIKELRRLFLVEDLVDSLKFAVLMWILT-YVGALFNGLTLIILGFIGAFSCPVIYEKHQAQI 158
FUGRU)RTN4     PEDMVHKYSDMVLAKLNKTIAEVRRLFLVEDLVDSIKFAVLMWILT-YVGALFNGLTLLILGLIAVFSCPIVYEKHQAQI 158
ONCMY)RTN4     SEGTVHKYSDCVLARFNTTVTELRRLFLVEDLVDSLKFAVLMWILT-YVGALFNGLTLFILGLVGMFSCPIVYEKYKVQI 158
ONCMY)RTN10    SEETVHKYSDCALARFNTTVIELRRLFLVEDLVDSLKFAVLMWILT-YVGALFNGLTLLILGLVGMFSFPIIYEKYKVQI 158
SALSA)RTN4     SEETVHKYSDCVLTRFNTTVTELRRLFLVEDLVDSLKFAVLMWILT-YVGALFNGLTLFILGLVGMFSCPIVYEKYKVQI 158
SALSA)RTN10w   SKETVHKYSDCALARFNTTVIELRRLFLVEDLVDSLKFAVLMWILT-YVGALFNGLTLLILGLVGMFSFPIIYEKYKVQI 112
ORYLA)RTN4w    ------------FG----TRGELRRVFLVEDLVDSIKFAVLMWILT-YVGAFFNGLTLIILGLIAAFTCPIVYEKHQAQI 63
CYPCA)RTN4     SSELVHKYSDTTLAHINCVIKELRRLFLVEDLVDSLKFAVLMWILT-YVGALFNGLTLLILGLIGTFSWPVIYEKHQAQI 158
CYPCA)RTN6     SKDVVQRHSDMVLSRINGALKELRRLFLVEDLIDSLKFAAFLWVLT-YVGAWFNGLTLLILGLIGAFNGPIVYERHQTQI 158
DANRE)RTN6     SADAVHTHSEALLRRINTALVELRRLFLVEDLVDSLKLAVGLWLLT-YVGSWFNGLTLLIIALIGAFSGPIAYERHQSEI 158
CIOIN)RTN      SKDQIHKYADVILDHLNCTLVCTRDLVLVKNMVASLKFAVFMWLLT-YIGCCFNGLTLLILGVIAAFVLPPIYEKYQVPI 158

HUMAN)RTN1     DQYLGLVR-THINAV-VAKIQAKIPGAKR-------------------HAE-* 189
MACMU)RTN1w    DQYLX------------------------------------------------ 163
BOVIN)RTN1w    XXXXXXXX-XXXXXX-XXXXXXKIPGAKR-------------------HTE-* 189
MOUSE)RTN1     DQYLGLVR-THINTV-VAKIQAKIPGAKR-------------------HAE-* 189
RAT)RTN1       DQYLGLVR-THINTV-VAKIQAKIPGAKR-------------------HAE-* 189
CANFA)RTN1     DQYLGLVR-THINTV-VAKIQAKIPGAKR-------------------HAE-* 189
CHICK)RTN1     DQYLGLVR-THINTV-VAKIQAKIPGAKR-------------------KAE-* 189
XENLA)RTN1.1   DQYLGLVR-TNMNTI-MTKIQAKIPGTKQ-------------------K-E-* 188
XENLA)RTN1.2   DQYLGLVR-TNMNII-VTKIQAKIPGTKQ-------------------K-E-* 188
DANRE)RTN1     DQYVDLIR-TQVNSV-VAKIQEKVPGTKR-------------------KAE-* 189
FUGRU)RTN1     DQYVGLIR-THVNSV-VGKIQAKIPGAKR-------------------KEE-* 189
ICTPU)RTN1     DQYVGLIR-TQVNTV-VGKIQEKIPGAKR-------------------KAE-* 189
CYPCA)RTN1     DQYLALIR-TQVNSV-VGKIQEKIPGAKR-------------------KAE-* 189
GASAC)RTN1w    DQYVGLIR-THVNSV-VGKIQAKIPGAKR-------------------KEE-* 146
ONCMY)RTN1     DQYVGLIR-TQVNSV-VGKIQAKIPGAKR-------------------KEE-* 189
ORYLA)RTN1     DQYVGLIR-TQVNSV-VGKIQAKIPGTKR-------------------KEE-* 189
DANRE)RTN5     DQYLGLVR-TQVNSV-MGKIREKVPGAKK-------------------K-E-* 188
CYPCA)RTN5w    DQYLGLVR-TQVNSI-MGKIREKVPGAKK-------------------K-E-* 109
ICTPU)RTN5w    DQYLGLVR-TQVNSV-M-----------------------------------X 174
HUMAN)RTN2     DQYVGLVT-NQLSHI-KAKIRAKIPGTGALASAAAAVS-------GSKAKAE-* 202
MOUSE)RTN2     DQYVGLVT-NQLSHI-KAKIRAKIPGTGTLAP-TASVS-------GSKAKAE-* 201
RAT)RTN2       DQYVGLVT-SQLSHI-KAKIRAKIPGTGTLAP-AASVS-------GSKAKAE-* 201
BOVIN)RTN2     DQYVGLVT-NQLSHI-KAKIRAKIPGTGALASVAAAVS-------GPKAKAE-* 202
PIG)RTN2       DQYVGLVT-NQLSHI-KAKIRAKIPGTGALASAAAAVS-------GSKAKAE-* 202
XENLA)RTN2     DHYVSLVS-KKVNAF-RSKFQGAAKKPPA-------------------KQK-* 189
XENTR)RTN2     DHYVSLVS-KKVNAF-RSKIQGTVKKPPA-------------------KQK-* 189
FUGRU)RTN2     DGFFAKIQAHVDNIKDIFQRLAQGGGPPPDSTP-----------GGAKPKNQ-* 200
ICTPU)RTN2w    DNWVAKVQAHVDNIHDILKRLAQGGRPP-------------------------X 187
FUGRU)RTN8     RRTVRTVKGFVKKIRNLCLSLYHSIRPSLVPEPASKPAPAAAPSLRQKAKAK-* 211
DANRE)RTN2     DSCIVAVQAQIDNIKDFFYRLTQGGGPPPDPTP-----------GGAKPKAH-* 200
DANRE)RTN8     DKIIKAVQLLVEKITEMVDLVVSLAKPPPAPAPPPAPA------LKHKQKTK-* 205
ONCMY)RTN8w    KRISKAVRGLLRKIKNLFKMLYSKLRPSPATTSATT-----------------X 196
ONCMY)RTN2     DGFVAGIQANVDNAKDILHRIAQGGGPTPDTTP-----------GGAKPKTQ-* 200
ORYLA)RTN2     DSFVAKIQAKLDSIKDTLQRLAQGGGPPPDPTP-----------GGAKPKLQ-* 200
HUMAN)RTN3     DHYVGIAR-DQTKSI-VEKIQAKLPGIAKK-------------------KAE-* 190
MOUSE)RTN3     DHYVGIAR-DQTKSI-VEKIQAKLPGIAKK-------------------KAE-* 190
RAT)RTN3       DHYVGIAR-DQTKSI-VEKIQAKLPGIAKK-------------------KAE-* 190
CANFA)RTN3w    DHYVGIAR-DQTKSI-VEKIQAKLPGIAKK-------------------KAE-* 190
SHEEP)RTN3w    ------------------------------------------------------ 152
BOVIN)RTN3     DHYVGIAR-DQTKSI-VEKIQAKLPGIAKK-------------------KAE-* 190
PIG)RTN3       DHYVGIAR-DQTKSI-VEKIQAKVPGIAKK-------------------KAE-* 190
PANTR)RTN3     DHYVGIAR-DQTKSI-VEKIQAKLPGIAKK-------------------KAE-* 190
CHICK)RTN3w    DHYVSIAR-EQX--------------------------------------- 169
XENLA)RTN3.1   DHYVSLVH-SQVKSI-TEKIQAKLPGALKK-------------------KSE-* 190
XENLA)RTN3.2   DHYVSLVH-SQVKSI-TEKIQAKLPGALKK-------------------KSE-* 190
XENTR)RTN3     DHYVSLVH-SHVKSI-TEKIQAKLPGALKK-------------------KSE-* 190
PAROL)RTN3     DQYIDVAR-TQVNTT-MAKLQEKLPGAMKAQ-----------------KTE-* 191
DANRE)RTN3     DHYIDIAR-TQFNTT-VAKLQEKLPGAMKRC-----------------KAE-* 191
CARAU)RTN3w    D------------------------------------------------------ 107
CYPCA)RTN3w    DRYIDIAR-TQFNTT-VAKLQEKLPGSMKRC-----------------KAE-* 77
FUGRU)RTN3     DKYMDLVR-TQVNTT-MAKLQEKLPGAVKSN-----------------KTE-* 191
GASAC)RTN3     DQYIDVIR-TQINTT-MAKLQEKLPGAVKRC-----------------KTE-* 191
SALSA)RTN3w    DRYMEIAR-TQVNTT-MAKLQEKLPGAVKRT-----------------KAE-* 180
ORYLA)RTN3w    DQYIDVVR-TQVNAT-VAKLQEKLPG---------------------------- 182
```

```
ONCMY)RTN9     DHYMEIAR-TQVNTT-MAKLQEKLPGAIKRT-----------------KAE-* 191
ONCMY)RTN3     DRYMEIAR-TQVNTT-MAKLQEKLPGAVKRT-----------------KAE-* 191
FUGRU)RTN7     DQYIALIK-SRVEET-KYQLQDRLPGAVKKV-----------------KAE-* 191
ONCMY)RTN7     DQYIXLIR-TRVEVT-LAKLQDKLPGAVKRT-----------------KAE-* 191
ONCMY)RTN11    DQYIELIR-TRVEVT-LAKLQDKLPGALKRT-----------------KAE-* 191
SALSA)RTN7w    DKYIELIR-TRVEVT-LAKLQDKLPGAVKRT-----------------KAE-* 150
HUMAN)RTN4     DHYLGLAN-KNVKDA-MAKIQAKIPGLKR-------------------KAE-* 189
MACFA)RTN4     DHYLGLAN-KNVKDA-MAKIQAKIPGLKR-------------------KAE-* 189
MACMU)RTN4w    DHYLGLAN-KNVKDA-MAKIQAKIP--------------------------X 182
MOUSE)RTN4     DHYLGLAN-KSVKDA-MAKIQAKIPGLKR-------------------KAE-* 189
RAT)RTN4       DHYLGLAN-KSVKDA-MAKIQAKIPGLKR-------------------KAD-* 189
BOVIN)RTN4     DHYLGLAN-KNVKDA-MAKIQAKIPGLKR-------------------KAE-* 189
SHEEP)RTN4     DHYLGLAN-KNVKDA-MAKIQAKIPGLKR-------------------KAE-* 189
PIG)RTN4       DHYLGLAN-KNVKDA-MAKIQAKIPGLKR-------------------KTE-* 189
CANFA)RTN4w    ------------------------------------------------------ 129
PANTR)RTN4     DHYLGLAN-KNVKDA-MAKIQAKIPGLKR-------------------KAE-* 189
CHICK)RTN4     DHYLGLVN-KNVKDA-MAKIQAKIPGLKR-------------------KTE-* 189
XENLA)RTN4.1   DHYLALVN-KNLKST-SDLILSKVPGLKR-------------------KAE-* 189
XENLA)RTN4.2   DHYLALIN-KNLKNT-SDLILAKVPGLKR-------------------KSE-* 189
XENTR)RTN4     DHYLALIN-KNVKST-SDLILSKVPGLKR-------------------KAE-* 189
CARAU)RTN4     DHYYGLVN-KQIKDV-MGKIQAKIPGAKP-------------------KTE-* 189
DANRE)RTN4     DHYYGLVN-KQFKDV-VGKIQAKIPGAKP-------------------KTE-* 189
FUGRU)RTN4     DHYLSLVN-NQVKDI-VGKIQAKVPGMKR-------------------KTE-* 189
ONCMY)RTN4     DHYVGMAN-KHVKDI-IATVQSKVPGLKRV------------------KAE-* 190
ONCMY)RTN10    DHYVGMAN-KQVKDI-IATVQAKVPGLKRV------------------KAD-* 190
SALSA)RTN4     DHYVGMAN-KQVKDI-IATVQAKVPGLKRV------------------KAE-* 190
SALSA)RTN10w   DHYVGMAN-KQVKDI-IATVQAKVPGLKRV------------------KAD-* 144
ORYLA)RTN4w    DHYVALVN-NQVKDV-VGKIQAKVPGMKR-------------------KAE-* 94
CYPCA)RTN4     DHYYGLLN-KQITDV-LGKIQAKIPGAKP-------------------KTD-* 189
CYPCA)RTN6     DQFHFQTEEPGVGSH-RATITAKVPWSKI-------------------KNPK* 191
DANRE)RTN6     DQFISMIN-TQMREA-LGKVLAMVPGGKK-------------------KSD-* 189
CIOIN)RTN      DNHYNLVA-QKFAQV-ANAVRSKIPGAKP-------------------KTQ-* 189
```

Supplementary Fig. 1: *BioEdit alignment of RHD sequences*

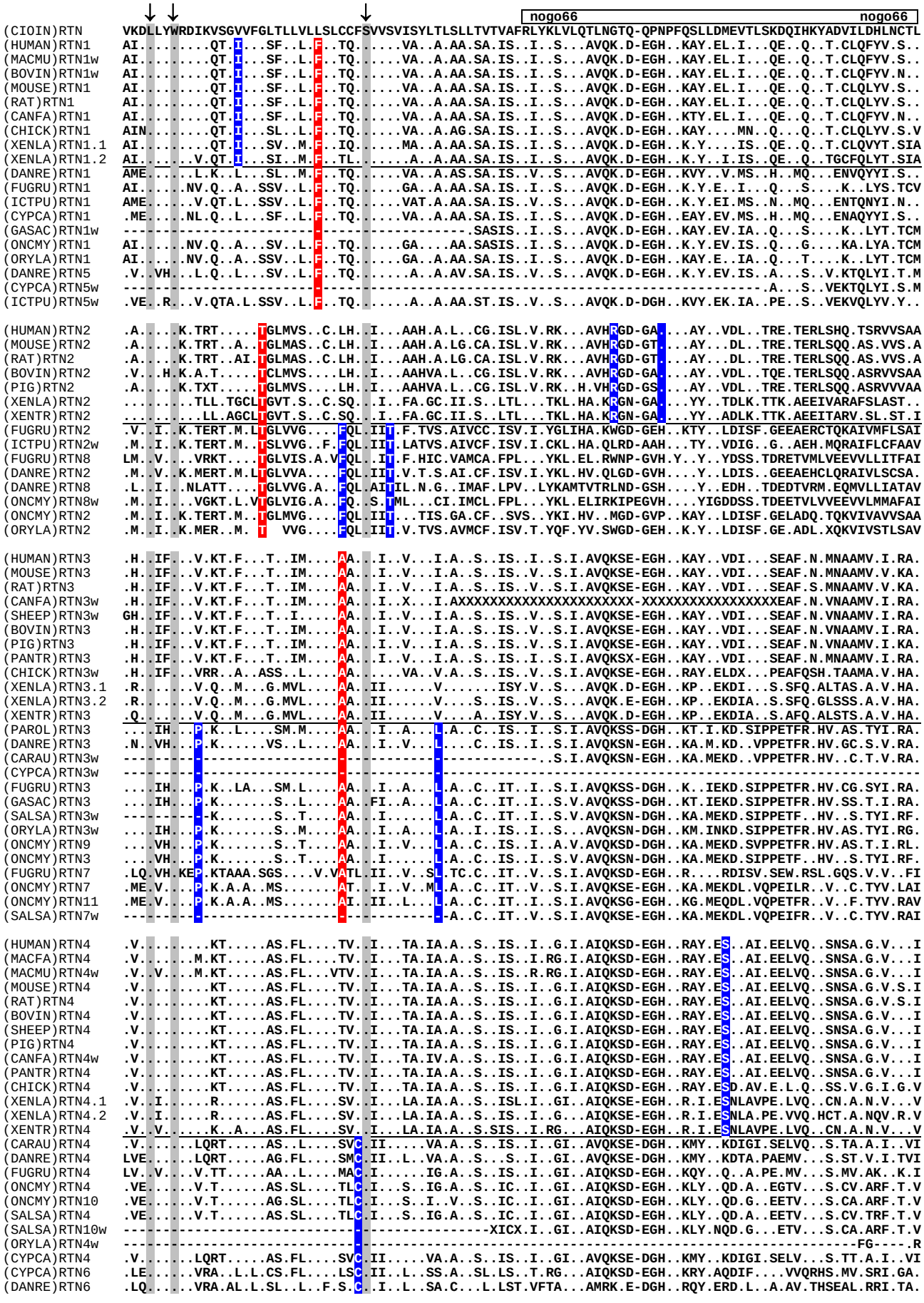
nogo66
nogo66
(CIOIN)RTN
(HUMAN)RTN1
(MACMU)RTN1w
(BOVIN)RTN1w
(MOUSE)RTN1
(RAT)RTN1
(CANFA)RTN1
(CHICK)RTN1
(XENLA)RTN1.1
(XENLA)RTN1.2
(DANRE)RTN1
(FUGRU)RTN1
(ICTPU)RTN1
(CYPCA)RTN1
(GASAC)RTN1w
(ONCMY)RTN1
(ORYLA)RTN1
(DANRE)RTN5
(CYPCA)RTN5w
(ICTPU)RTN5w
(HUMAN)RTN2
(MOUSE)RTN2
(RAT)RTN2
(BOVIN)RTN2
(PIG)RTN2
(XENLA)RTN2
(XENTR)RTN2
(FUGRU)RTN2
(ICTPU)RTN2w
(FUGRU)RTN8
(DANRE)RTN2
(DANRE)RTN8
(ONCMY)RTN8w
(ONCMY)RTN2
(ORYLA)RTN2
(HUMAN)RTN3
(MOUSE)RTN3
(RAT)RTN3
(CANFA)RTN3w
(SHEEP)RTN3w
(BOVIN)RTN3
(PIG)RTN3
(PANTR)RTN3
(CHICK)RTN3w
(XENLA)RTN3.1
(XENLA)RTN3.2
(XENTR)RTN3
(PAROL)RTN3
(DANRE)RTN3
(CARAU)RTN3w
(CYPCA)RTN3w
(FUGRU)RTN3
(GASAC)RTN3
(SALSA)RTN3w
(ORYLA)RTN3w
(ONCMY)RTN9
(ONCMY)RTN3
(FUGRU)RTN7
(ONCMY)RTN7
(ONCMY)RTN11
(SALSA)RTN7w
(HUMAN)RTN4
(MACFA)RTN4
(MACMU)RTN4w
(MOUSE)RTN4
(RAT)RTN4
(BOVIN)RTN4
(SHEEP)RTN4
(PIG)RTN4
(CANFA)RTN4w
(PANTR)RTN4
(CHICK)RTN4
(XENLA)RTN4.1
(XENLA)RTN4.2
(XENTR)RTN4
(CARAU)RTN4
(DANRE)RTN4
(FUGRU)RTN4
(ONCMY)RTN4
(ONCMY)RTN10
(SALSA)RTN4
(SALSA)RTN10w
(ORYLA)RTN4w
(CYPCA)RTN4
(CYPCA)RTN6
(DANRE)RTN6

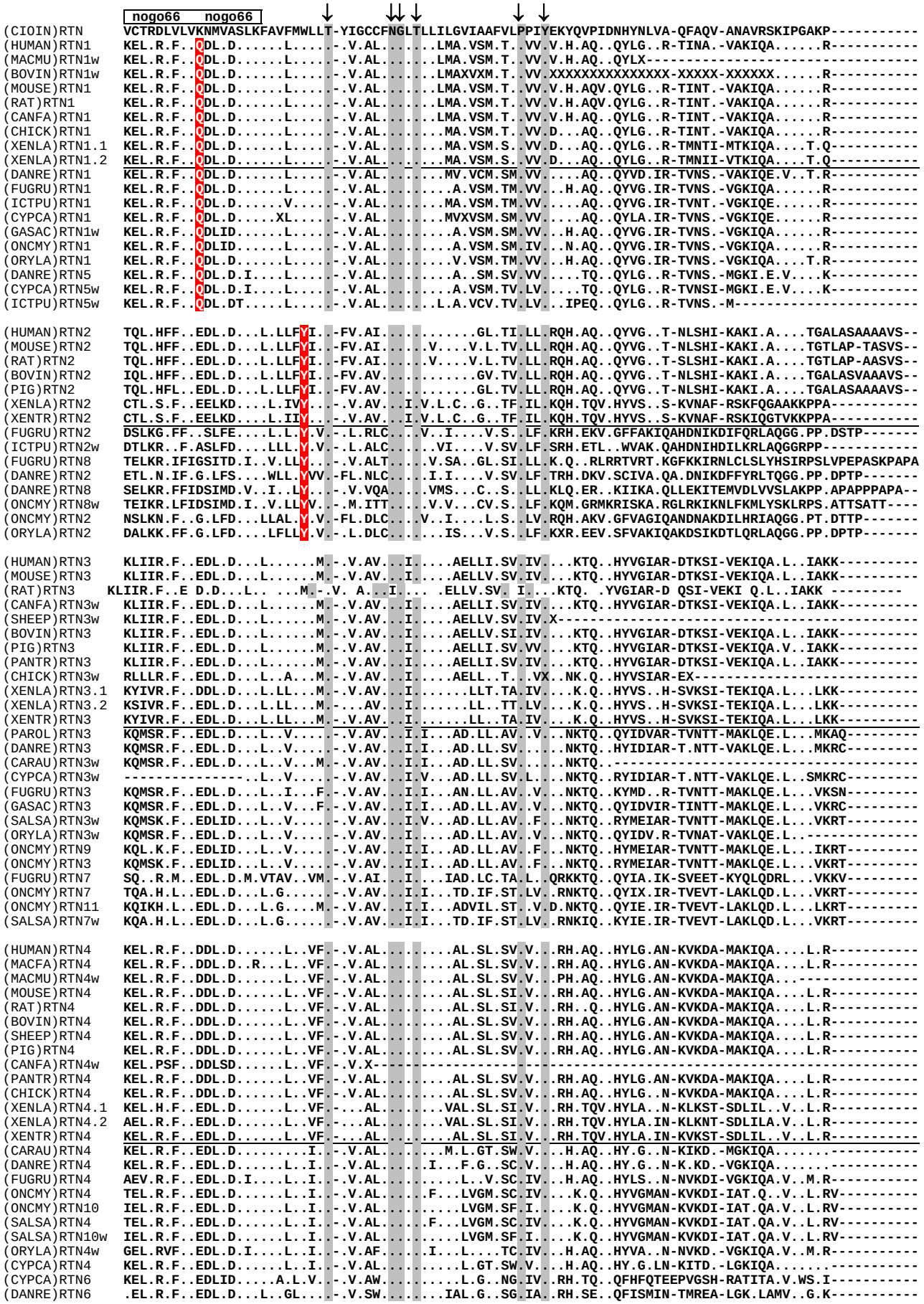
nogo66
nogo66
(CIOIN)RTN
(HUMAN)RTN1
(MACMU)RTN1w
(BOVIN)RTN1w
(MOUSE)RTN1
(RAT)RTN1
(CANFA)RTN1
(CHICK)RTN1
(XENLA)RTN1.1
(XENLA)RTN1.2
(DANRE)RTN1
(FUGRU)RTN1
(ICTPU)RTN1
(CYPCA)RTN1
(GASAC)RTN1w
(ONCMY)RTN1
(ORYLA)RTN1
(DANRE)RTN5
(CYPCA)RTN5w
(ICTPU)RTN5w
(HUMAN)RTN2
(MOUSE)RTN2
(RAT)RTN2
(BOVIN)RTN2
(PIG)RTN2
(XENLA)RTN2
(XENTR)RTN2
(FUGRU)RTN2
(ICTPU)RTN2w
(FUGRU)RTN8
(DANRE)RTN2
(DANRE)RTN8
(ONCMY)RTN8w
(ONCMY)RTN2
(ORYLA)RTN2
(HUMAN)RTN3
(MOUSE)RTN3
(RAT)RTN3
(CANFA)RTN3w
(SHEEP)RTN3w
(BOVIN)RTN3
(PIG)RTN3
(PANTR)RTN3
(CHICK)RTN3w
(XENLA)RTN3.1
(XENLA)RTN3.2
(XENTR)RTN3
(PAROL)RTN3
(DANRE)RTN3
(CARAU)RTN3w
(CYPCA)RTN3w
(FUGRU)RTN3
(GASAC)RTN3
(SALSA)RTN3w
(ORYLA)RTN3w
(ONCMY)RTN9
(ONCMY)RTN3
(FUGRU)RTN7
(ONCMY)RTN7
(ONCMY)RTN11
(SALSA)RTN7w
(HUMAN)RTN4
(MACFA)RTN4
(MACMU)RTN4w
(MOUSE)RTN4
(RAT)RTN4
(BOVIN)RTN4
(SHEEP)RTN4
(PIG)RTN4
(CANFA)RTN4w
(PANTR)RTN4
(CHICK)RTN4
(XENLA)RTN4.1
(XENLA)RTN4.2
(XENTR)RTN4
(CARAU)RTN4
(DANRE)RTN4
(FUGRU)RTN4
(ONCMY)RTN4
(ONCMY)RTN10
(SALSA)RTN4
(SALSA)RTN10w
(ORYLA)RTN4w
(CYPCA)RTN4
(CYPCA)RTN6
(DANRE)RTN6

```
(CIOIN)RTN      ---------KTQ-
(HUMAN)RTN1     ---------HAE-
(MACMU)RTN1w    ----------
(BOVIN)RTN1w    ---------H.E-
(MOUSE)RTN1     ---------HAE-
(RAT)RTN1       ---------HAE-
(CANFA)RTN1     ---------HAE-
(CHICK)RTN1     ---------.AE-
(XENLA)RTN1.1   ---------.-E-
(XENLA)RTN1.2   ---------.-E-
(DANRE)RTN1     ---------.AE-
(FUGRU)RTN1     ---------.EE-
(ICTPU)RTN1     ---------.AE-
(CYPCA)RTN1     ---------.AE-
(GASAC)RTN1w    ---------.EE-
(ONCMY)RTN1     ---------.EE-
(ORYLA)RTN1     ---------.EE-
(DANRE)RTN5     ---------.-E-
(CYPCA)RTN5w    ---------.-E-
(ICTPU)RTN5w    ----------X

(HUMAN)RTN2     -----GSKA.AE-
(MOUSE)RTN2     -----GSKA.AE-
(RAT)RTN2       -----GSKA.AE-
(BOVIN)RTN2     -----GPKA.AE-
(PIG)RTN2       -----GSKA.AE-
(XENLA)RTN2     ---------.QK-
(XENTR)RTN2     ---------.QK-
(FUGRU)RTN2     ----GGAKP.N.-
(ICTPU)RTN2w    ----------X
(FUGRU)RTN8     AAPSLRQKA.AK-
(DANRE)RTN2     ----GGAKP.AH-
(DANRE)RTN8     ----LKHKQ..K-
(ONCMY)RTN8w    ----------X
(ONCMY)RTN2     ----GGAKP...-
(ORYLA)RTN2     ----GGAKP.L.-

(HUMAN)RTN3     ---------.AE-
(MOUSE)RTN3     ---------.AE-
(RAT)RTN3       ---------.AE-
(CANFA)RTN3w    ---------.AE-
(SHEEP)RTN3w    ----------
(BOVIN)RTN3     ---------.AE-
(PIG)RTN3       ---------.AE-
(PANTR)RTN3     ---------.AE-
(CHICK)RTN3w    ----------
(XENLA)RTN3.1   ---------.SE-
(XENLA)RTN3.2   ---------.SE-
(XENTR)RTN3     ---------.SE-
(PAROL)RTN3     ---------..E-
(DANRE)RTN3     ---------.AE-
(CARAU)RTN3w    ----------
(CYPCA)RTN3w    ---------.AE-
(FUGRU)RTN3     ---------..E-
(GASAC)RTN3     ---------..E-
(SALSA)RTN3w    ---------.AE-
(ORYLA)RTN3w    ----------
(ONCMY)RTN9     ---------.AE-
(ONCMY)RTN3     ---------.AE-
(FUGRU)RTN7     ---------.AE-
(ONCMY)RTN7     ---------.AE-
(ONCMY)RTN11    ---------.AE-
(SALSA)RTN7w    ---------.AE-

(HUMAN)RTN4     ---------.AE-
(MACFA)RTN4     ---------.AE-
(MACMU)RTN4w    ----------X
(MOUSE)RTN4     ---------.AE-
(RAT)RTN4       ---------.AD-
(BOVIN)RTN4     ---------.AE-
(SHEEP)RTN4     ---------.AE-
(PIG)RTN4       ---------..E-
(CANFA)RTN4w    ----------
(PANTR)RTN4     ---------.AE-
(CHICK)RTN4     ---------..E-
(XENLA)RTN4.1   ---------.AE-
(XENLA)RTN4.2   ---------.SE-
(XENTR)RTN4     ---------.AE-
(CARAU)RTN4     ---------..E-
(DANRE)RTN4     ---------..E-
(FUGRU)RTN4     ---------..E-
(ONCMY)RTN4     ---------.AE-
(ONCMY)RTN10    ---------.AD-
(SALSA)RTN4     ---------.AE-
(SALSA)RTN10w   ---------.AD-
(ORYLA)RTN4w    ---------.AE-
(CYPCA)RTN4     ---------..D-
(CYPCA)RTN6     ---------.NPK
(DANRE)RTN6     ---------.SD-
```

Supplementary Fig. 2: *Diagnostic residues of vertebrate RTN subfamilies*

The nine residues conserved (monomophic) in all vertebrates RTN1-RTN4 sequences and *Ciona* RTN are shaded in grey and marked by an arrow above the alignment. Residues unique to one RTN subfamily (RTN1, 2, 3 or 4) are highlighted in red. Residues within each RTN1-RTN4 subfamily that are unique to either land vertebrate or fish proteins are highlighted in blue. All residues conserved with the respective *Ciona* residue (ancestral) are represented by dots. Sequences that did not comprise the full RHD received the suffix 'w'.The 66 aa loop between the two transmembrane regions of the RHD is denoted above the alignement (nogo-66).

BOVIN, Bos taurus; CANFA, Canis familiaris; CARAU, Carassius auratus; CHICK, Gallus gallus; CIOIN, Ciona intestinalis; CYPCA, Cyprinus carpio; DANRE, Danio rerio; FUGRU Takifugu rubripres; GASAC, Gasterosteus aculeatus; ICTPU, Ictalurus punctatus; HUMAN, Homo sapiens; MACMU, Macaca mulatta; MACFA, Macaca fascicularis; MOUSE, Mus musculus; ONCMY, Oncorhynchus mykiss; ORYLA, Oryzias latipes; PANTR, Pan troglodytes; PAROL, Paralichthys olivaceus; PIG, Sus scrofa; RAT, Rattus norvegicus; SHEEP, Ovis aries; SALSA, Salmo salar; XENLA Xenopus laevis; XENTR, Silurana tropicalis.

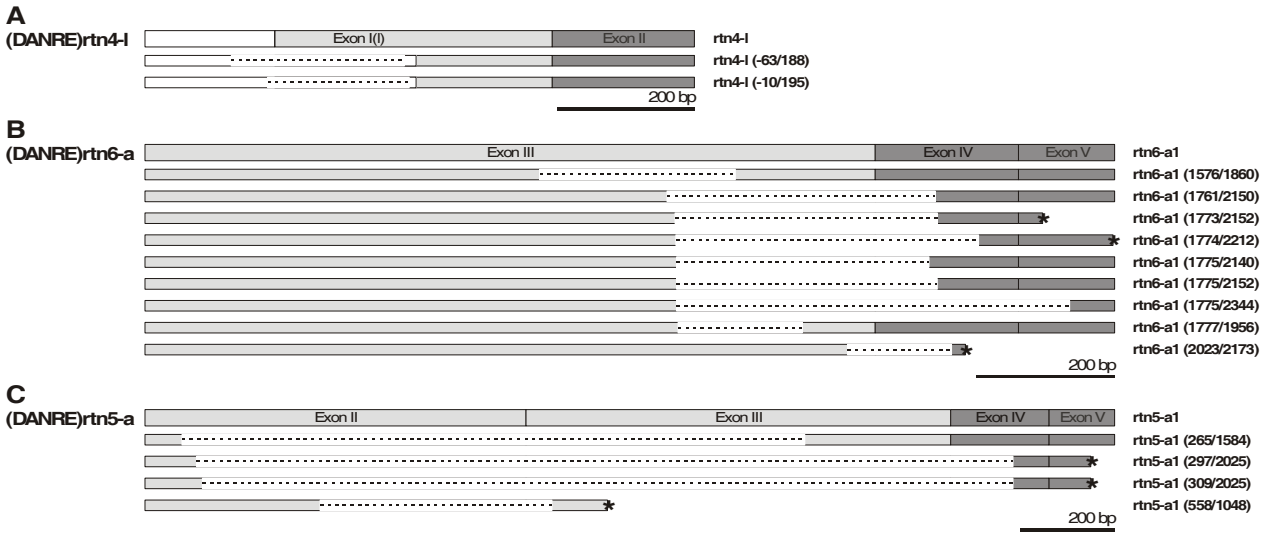

Supplementary Fig. 3: *Cryptic splice variants of (DANRE)rtn4, rtn5 and rtn6*

Schematic drawing of mRNA variants that result from internal splicing at cryptic donor and acceptor sites.

A) Two minor rtn4–I spliceforms due to internal splicing of the first exon were amplified from cDNA. The start codon of these transcripts would shift to a new position.

B) Internal splicing in exons II and III of rtn6-a1 lead to either internal, in frame deletions or to premature stops (*).

C) Internal splicing in exons II, III and IV of rtn5-a1.

```
HUMAN)RTN1-A    MAAPGDPQDELLPLAGPGSQWLRHRGEGENEAVTPKGATPAPQAGEPSPGLG-ARAREAASREAGSGPARQS-PVAMETA 78
RAT)RTN1-A      MAAPPDLQDEPLSPANPGSQLFGGRGEGE-EATP-KGARPAQQDGEPAWGSG-AGAGVVSSRGLCSGPARSP-PVAMETA 76
MOUSE)Rtn1-A1   MAAPPDLQDEPLSLGSPGSQWFGGRGDGEDEATAVMGARPAQQDGEPAWGSG-AGAGVTSSRELCSGPARSP-PVAMETA 78
MOUSE)RTN1-A2   MAAPPDLQDEPLSLGSPGSQWFGGRGDGEDEATAVMGARPAQQDGEPAWGSG-AGAGVTSSRELCSGPARSP-PVAMETA 78
CHICK)RTN1-A    MSAPPDPQD--LLLAGTAERWAAAGADEYAAGAALRDGDGAQQREQLAFGS--AR-------------EHP-PVAMATA 61
FUGRU)RTN1-A1   MSA---EEL------GSEGRWFGDDYERNGLFG-NAPTQFGELREDFKPRGSEVSSDLDQQFHPYQDDGQRPS-VTMETA 69
DANRE)RTN1-A2   MSE--KPEA------DSEGSWYGEDFEKIDRFGRTSSARRDVLGEERQTRDWEDESSVEKQFSSHPESDRQPLPVVMETA 72
DANRE)RTN1-A1   MSE--KPEA------DSEGSWYGEDFEKIDRFGRTSSARRDVLGEERQTRDWEDESSVEKQFSSHPESDRQPLPVVMETA 72
DANRE)RTN5-A1   MSANSNEGP------GLDGKWFEEEEEKNGMFG-SAGPHFDEMRDDLRAP--------KQQFHPFEGTG-----VAMETA 60

HUMAN)RTN1-A    STGVAGVSSAMDHTFSTTSKDGEGSCYTSLISDICYPP--QEDSTYFTGILQKENGHVTISESPEELGTPGPS---LPDV 153
RAT)RTN1-A      STGVAAVPDALDHSSSPTLKDGEGACYTSLISDICYPP--REDSAYFTGILQKENGHITTSESPEELGTPGPS---LPEV 151
MOUSE)Rtn1-A1   STGMAAVPDALDHSPSSTLKDGEGACYTSLISDVCYPP--REDSAYFTGILQKENGHITTSESPEEPETPGPS---LPEV 153
MOUSE)RTN1-A2   ST---------------------------------------------------------------------------- 80
CHICK)RTN1-A    SPGVTASSRLFDYG-SSSANGADSSFYTSLISDVHYTT--PRDNTYFTGVYQQENSPIPCSGSTEGFNALGHP---VQDV 135
FUGRU)RTN1-A1   STDDSMSGLARKSM--ND----DGDVYTSLLSGQSFAS--GQGSSSYLS-------DSLKASETSLGSSG----------L 124
DANRE)RTN1-A2   ST---------------------------------------------------------------------------- 74
DANRE)RTN1-A1   STDKSTS-SIQKSS--DD----RDDLYTSLLSNQHYSS--HEDTSYFSG------SLSKSADKHTTHTD---------- 126
DANRE)RTN5-A1   STGDSLSDMFMKSS--PV----EGDLYTSLLSSKSSSNPFNDGASLFSSEGNRSPPAPTGTDSGIGMTPGDPSDHQTTLQ 134

HUMAN)RTN1-A    PGIESRGLFSSDSGIEMTPAES-TEVNKILADPLDQMKAEAYKYIDITRPEEVKHQE--QHHPELEDKDLDFKNKDTDIS 230
RAT)RTN1-A      PGTEPHGLLSSDSGIEMTPAES-TEVNKILADPLDQMKAEACKYIDITRPQEAKGQE--EQSPGLEDKDLDFKDKDSEVS 228
MOUSE)Rtn1-A1   PGMEPQGLLSSDSGIEMTPAES-TEVNKILADPLDQMKAEAYKYIDITRPQEAKGQE--EQHPGLEDKDLDFKDKDTEVS 230
MOUSE)RTN1-A2   ---------------------------------------------------------------------------- 80
CHICK)RTN1-A    TGFESRGLFSLDSGIEMTPAES-AEVDKSLTDP---MKVEGYKYMDISRPEEIKYQE--KHDPDSEDESPDLIDEYRGTP 209
FUGRU)RTN1-A1   GDFSSDSYSFSSN----IKMAS-GLADDMPKSLFSSDKTESYNYMDISHGDERHDQR--LGDKGSK--GHD--SLGGYID 193
DANRE)RTN1-A2   ---------------------------------------------------------------------------- 74
DANRE)RTN1-A1   -DFISGSYSVTFSSDSSNKIKTSTDQIDSSHSTERAFG-SSYNYMDISGKDDSRSSQRPLEDRSMS--GLSEPSLYTKLE 202
DANRE)RTN5-A1   GSHKSDHYSYMDMGGDLCDFGSMGNAKNKQQPPMSGYGDEEDEEDDDEDEDDIQDFKPKIEERGSKESSHDPFDLGRYLE 214
```

```
HUMAN)RTN1-A    IKPEGVRE--------PDKPAPVEGKIIKDHLLEESTFAPYIDDLSEEQRRAPQITTPVKITLTEIEP-----SVETTTQ 297
RAT)RTN1-A      TKPEGVHA--------PNQPSPVEGKLIKDNLFEESTFAPYIDELSDEQHRMSLVTAPVKITLTEIGP-----PVMTATH 295
MOUSE)Rtn1-A1   TKAEGVRA--------PNQPAPVEGKLIKDHLFEESTFAPYIDELSDEQHRVSLVTAPVKITLTEIEP-----PLMTATQ 297
MOUSE)RTN1-A2   -------------------------------------------------------------------------------- 80
CHICK)RTN1-A    IGSGHAAE--------PQRTTASEAIKAPK---EQD---PLEDKSFRDQHNASVVTAPVKITLTETPG-----AREATSK 270
FUGRU)RTN1-A1   KNPGGDEDDEEEEEEEEENLGPALGSHSFPYVEEPSDEELSDYRSYRNLGGTPQTASPVKITLTESQPTSARPDVHPAPP 273
DANRE)RTN1-A2   -------------------------------------------------------------------------------- 74
DANRE)RTN1-A1   KSPSPVEVD-----ADEFGSAGLLDTQTFPYVEEPSDEELSDYQPYRSP-GTGSSASPVRITLTEIPPTSVSPTTIQHSP 276
DANRE)RTN5-A1   KSPLGSED-----TEVKTSTGSAGGQHAFPYVEDPSDEEMADFRSYRRM-ETPQSASPVKITVTTESHSTASEPVR-VSP 287

HUMAN)RTN1-A    EKTPEKQDICLKPSPDTVPTVTVSEPEDDSPGSITPP---SSGTEPSAAESQGKGSISEDELITAIKEAKGLSYETAENP 374
RAT)RTN1-A      ETIPEKQDLCLKPSPDTVPTVTVSEPEDDSPGSVTPP---SSGTEPSAAESQGKGSVSEDELIAAIKEAKGLSYETTESP 372
MOUSE)Rtn1-A1   ETIPEKQDLCLKPSPDTVPTVTVSEPEDDSPGSVTPP---SSGTEPSAAESQGKGSVSEDELIAAIKEAKGLSYETTESP 374
MOUSE)RTN1-A2   -------------------------------------------------------------------------------- 80
CHICK)RTN1-A    EASVTQPKSGLKPSHEVVPTVMVSEPEDDSPGSVTPP---SSGTEPSGSESQGKGSLSEDELISAIKEAKGFSFETSEVQ 347
FUGRU)RTN1-A1   PVSVSERENILSVGLQGVPTVTLSEPEDDSPAS-------SPNASPTQKEFRSDDMFKDDAVKPPACKGP----SS---- 338
DANRE)RTN1-A2   -------------------------------------------------------------------------------- 74
DANRE)RTN1-A1   TVTVSEKESILSLGLEGMPTVTLSEPEDDSPESSTPPTEDSESPMDPNIQAGETELMNSIPDSTQVSPIPPAQPASKKDS 356
DANRE)RTN5-A1   QGGMSERDSVLSFGQQGLPTVTLSEPEDDSAASSA---NHSPNHSPTGRESPSDVLFHPAGMKSMSSTQDSSSISSHPNP 364

HUMAN)RTN1-A    RPVGQLADRPEVKARSGPPTIPSPLDHEASSAESGDSEIELVSEDP--------------------MAAEDALPSGYVS 433
RAT)RTN1-A      RPVGQAADRPKVKARSGLPTIPSSLDQEASSAESGDSEIELVSEDP--------------------MASEDALPSGYVS 431
MOUSE)Rtn1-A1   RPVGQVADKPKTKTRSGLPTIPSPLDQEASSAESGDSEIELVSEDP--------------------MASEDALPSGYVS 433
MOUSE)RTN1-A2   -------------------------------------------------------------------------------- 80
CHICK)RTN1-A    QSPAVSAEKQEQKMKPGRPAVPSPLDNEASSAESGDSEIELVSEDP--------------------LAAEEVLHSNYMT 406
FUGRU)RTN1-A1   --------------TNAG-----GREQDGSSAESGDSEIELVSEEP-----------PKASG------NPFAQPPKSKGT 382
DANRE)RTN1-A2   -------------------------------------------------------------------------------- 74
DANRE)RTN1-A1   SPV-------ENISAPKSTLPPTSQGFEGNSAESGDSEIELVSEEP--------SPRAPSSGYMSFSKTPATAPSTIVAS 421
DANRE)RTN5-A1   PPI-------HDIKTSAKPSSPWAQDLQGSGDESGDSEIEQVAEELDSPLHDLTSKTPPAKGGFSPTSNPFE-PPSYTSA 436

HUMAN)RTN1-A    FGHVGGPPPSPAS-----------------------PSIQYSILREEREAELDSELIIESCDASSASEESPKREQDSPPM 490
RAT)RTN1-A      FGHVSGPPPSPAS-----------------------PSIQYSILREEREAELDSELIIESCDASSASEESPKREQDSPPM 488
MOUSE)Rtn1-A1   FGHVSGPPPSPAS-----------------------PSIQYSILREEREAELDSELIIESCDASSASEESPKREQDSPPM 490
MOUSE)RTN1-A2   -------------------------------------------------------------------------------- 80
CHICK)RTN1-A    FSHIGGPPPSPAS-----------------------PSIQYSILREEREAELDSELIIESCDASSASEESPKREQDSPLM 463
FUGRU)RTN1-A1   VSQPNNPFDSPP----AAPGGCGLAG-------NHAPPTAYSILREEREAELDSDLFIES-----ASEESPKREQGFGGL 446
DANRE)RTN1-A2   -------------------------------------------------------------------------------- 74
DANRE)RTN1-A1   TAPVPSSTTAIP-----------------------KSLALQYSILREEREAELDSELALESC-----GEESPKRLTHGSSK 474
DANRE)RTN5-A1   TDKASNPFDKPQTNKVSASNPFDLSAGSKMGFGQSSNPPLYSLLREEREAELDSDLLIES-----ASEESPKREQEYSAP 511

HUMAN)RTN1-A    KPSALDAIREETGVRA----------EERAPSRRGLAEPGSFLDYPS-TEPQPGPELPPGDGALEPETP-MLPRKPEEDS 558
RAT)RTN1-A      KPGVLDAIREETSSRAT---------EERAPSHQGPVEPDPILSFTP-VTLQSRPEPSSGDGAPVPEPPKSQQQKPEEEA 558
MOUSE)Rtn1-A1   KPGALDAIREETGSRAT---------EERAPSHQGPVEPDPMLSFAPAAALQSRPEPSSGDGASVPEPPRSQQQKPEEEA 561
MOUSE)RTN1-A2   -------------------------------------------------------------------------------- 80
CHICK)RTN1-A    KPMVMDIIKEENSSRASASDYEASKTTESRMNRENLADSASYLKSSF-VAPKVSSEPPTSAVSTEELKERIILKKPIEET 542
FUGRU)RTN1-A1   KQGVSPPSPLVPSVVSPR------STSEAVPAAAAATERVKTPVKSEEDYPAKPKPPTAAV------PPEIRSERPQKDD 514
DANRE)RTN1-A2   -------------------------------------------------------------------------------- 74
DANRE)RTN1-A1   GYKEIPQAVKKPTSPTSAT-----KEPFVTSTTPSTTILAPTSALKEKMSTMEEKPKHSTILSPG--LPELKVEHPAGEV 547
DANRE)RTN5-A1   KP-PEPSSPLITDNMSSKP-----ITTSSVSSSPFTEPRVVSAQKEPEKEKEKEKEKAAPIEKPKPQPEDSWSTKPRPAV 585

HUMAN)RTN1-A    -SSNQSPAATKGPGPLGPGAPP---------------PLLFLNKQK 588
RAT)RTN1-A      VSSSQSPAATEIPGPLGSDLVP---------------PLPFFNKQK 589
MOUSE)Rtn1-A1   VSSSQSPTATEIPGPLGSGLMP---------------PLPFFNKQK 592
MOUSE)RTN1-A2   ------------------------------------------- 80
CHICK)RTN1-A    -VVNQSKVSSKDSGKRSPLALP---------------LLPFLNKQK 572
FUGRU)RTN1-A1   MHENASEGKGDPGKPTAS-------------------IFPGLNKQK 541
DANRE)RTN1-A2   ------------------------------------------- 74
DANRE)RTN1-A1   HKKERRRSSQARRGSEKTSAPP--------------AVFQGFSREK 579
DANRE)RTN5-A1   MGTSTVTPEKQPSQETESKSKSSIVSSSTEKEADLSLLLHGFSRQK 631
```

Supplementary Fig. 4: *BioEdit alignement of rtn1-a / 5-a N-termini*

```
HUMAN)RTN1-C   MQAT----ADSTKMDCVWSNWKSQ 20
MACMU)RTN1-C   MQAT----ADSTKMDCVWSNWKSQ 20
BOVIN)RTN1-C   MQAT----ADSTKMDCVWSNWKSQ 20
CANFA)RTN1-C   MQAT----ADFTKMDCVWSNWKSQ 20
MOUSE)RTN1-C   MQAT----ADSTKMDCVWSNWKSQ 20
RAT)RTN1-C     MQAT----ADSTKMDCVWSNWKSQ 20
CHICK)RTN1-C   MQAS----ADSTKMDCLWSNWKCQ 20
XENLA)RTN1.1-  MQAS----ADSTRMECLWSNWKCQ 20
XENLA)RTN1.2-  MQAS----PDSARMECLWSNWKCQ 20
ORYLA)RTN1-C   MQAT----ADQTKKESSWSSWKGQ 20
ONCMY)RTN1-C   MQAT----ADGIKKECSWSSWKGQ 20
ICTPU)RTN1-C   MQSSTTAAADSTKMEGFWSNWECQ 24
CYPCA)RTN1     MQASTMAAADSTKKEGFWSNWKCQ 24
DANRE)RTN1-C   MQASTMAAADSTKMEGFWSSWKCQ 24
ICTPU)RTN5-B   MDCE--------KKECPWSGWKGH 16
DANRE)RTN5-C   MDKG--------KKECTWSSWRGQ 16
```

Supplementary Fig. 5: *BioEdit alignement of rtn1-c / 5-c N-termini*

```
HUMAN)RTN2-C  MGSK  4
BOVIN)RTN2-C  MGSK  4
PIG)RTN2-C    MGSK  4
MOUSE)RTN2-C  MGSK  4
XENLA)RTN2-C  MNKT  4
XENTR)RTN2-C  MNKA  4
DANRE)RTN8-C  MASK  4
FUGRU)RTN8-C  MASK  4
FUGRU)RTN2-C  MASK  4
ICTPU)RTN2-C  MASK  4
ONCMY)RTN2-C  MANIN 5
ONCMY)RTN8-C  MAIK  4
ORYLA)RTN2-C  MASK  4
DANRE)RTN2-C  MSSK  4
```

Supplementary Fig. 6: *BioEdit alignement of rtn2-c / 8-c N-termini*

```
XENLA)RTN3.1-  MAETS-GPQSSHISSS---------------SV-GEKGSG-----CA------------------ 25
XENLA)RTN3.2-  MAETS-GPQSSHISSS---------------SA-GDKGSG-----CA------------------ 25
XENTR)RTN3-A1  MADTS-GPQSSHISSS----------------A-GEKGSG-----CA------------------ 24
CHICK)RTN3-A1  MADP-AA-QSPFVSSSS---APSEPAG----P-ACTRHGTPA----CA------------------ 34
HUMAN)RTN3-A1  MAEPSAATQSHSISSSSFGAEPSAPGGGG-SPGACPALGTKSCSSSCA------------------ 47
BOVIN)RTN3-A1  MAEPSAATQSPSVSSSSSGAESSAPGGGSGSPGACPALGTKSCGSSCA------------------ 48
PIG)RTN3-A1    MAELSAATQSPSVSSSS-GAESSAPGGGGGSPGACPALGAKSCGSSCA------------------ 47
CANFA)RTN3-A1  MAEPSAATQSPSVSSSSSGAEPAAPGGG--SPGACPALGAKSCGSSCA------------------ 46
PANTR)RTN3-A1  MAEPSAATQSHSISSSSFGAEPSAPGGGG-SPGACPALGTKSCSSSCA------------------ 47
RAT)RTN3-A1    MAESSAATQSPSVSSSSSGAEPSTLGGGG-SPGACPALGAKSCGSSCA------------------ 47
MOUSE)RTN3-A1  MAESSAATQSPSVSSSSSGAEPSALGGGGGSPGACPALGAKSCGSSCA------------------ 48
HUMAN)RTN3-A2  MAEPSAATQSHSISSSSFGAEPSAPGGGG-SPGACPALGTKSCSSSCADSFVSSSSSQPVSLFSTSQ 66
MOUSE)RTN3-A2  MAESSAATQSPSVSSSSSGAEPSALGGGGGSPGACPALGAKSCGSSCADSFVSSSSSQPVSIFSTSQ 67
ONCMY)RTN9-A2  MADSM--TQSAQISSSQ-----GLADG----QNSVAAKDSKMS-----DSFLSSS---PVSLIQSPE 48
GASAC)RTN3-A2  M-DPM--TQSAQISSSQ-----GLADG----QNS-AAKESKLS-----DSFLSSS---PVSLIQSPQ 46
DANRE)RTN3-A2  MADPM--TQSSQISSSQ-----GLNDG----HSA-ASKDSKFS-----DSFFSS----PVSLIQSPQ 46
ONCMY)RTN3-A2  MADPM--TQSAQISSSQ-----GLADG----QNSVAAKDSKMS-----DSFLSSS---PVSLIQSSQ 48
PAROL)RTN3-A1  M-DPM--TQSAQISSSQ-----GLADG----QNS-AAKDSKLS------------------------ 30
ORYLA)RTN3-A1  M-DSM--TQSAQISSSQ-----GFADG----QNS-AAKESKLS------------------------ 30
ONCMY)RTN9-A2  MADSM--TQSAQISSSQ-----GLADG----QNSVAAKDSKMS------------------------ 32
ONCMY)RTN3-A1  MADPM--TQSAQISSSQ-----GLADG----QNSVAAKDSKMS------------------------ 32
FUGRU)RTN3-A1  M-DSM--TQSSQISSSH-----GFADG----QNA-AAKESKLS------------------------ 30
DANRE)RTN3-A1  MADPM--TQSSQISSSQ-----GLNDG----HSA-ASKDSKFS------------------------ 31
GASAC)RTN3-A1  M-DPM--TQSAQISSSQ-----GLADG----QNS-AAKESKLS------------------------ 30
ONCMY)RTN7-A1  MADPT--TQSAQISCA--------------MNASSTKESTYY------------------------ 26
ONCMY)RTN11-A  MADPM--TQSGQISSS--------------LNASSTKESTYS------------------------ 26
```

Supplementary Fig. 7: *BioEdit alignement of rtn3-a / 7-a N-termini*

```
HUMAN)RTN4-A   MEDLDQSPLVSSS-DSPPRPQ-PAFKYQFVREPEDEEEEEEEE-EEDEDEDLEELEVLERKPAAGLSAAPVPTAPAAGAP 77
MOUSE)RTN4-A   MEDIDQSSLVSSSADSPPRPP-PAFKYQFVTEPEDEEDEEDEE-EEEDDEDLEELEVLERKPAAGLSAAPVP--P-AAAP 75
RAT)RTN4-A     MEDIDQSSLVSSSTDSPPRPP-PAFKYQFVTEPEDEEDEEEEEDEEEDDEDLEELEVLERKPAAGLSAAAVP--PAAAAP 77
CHICK)RTN4-Aw  MDELDQSPLISSS--GPPRPQQPQFNYQFVLDDEKEEDEEEEE-EEEDEDFDEQLEVMERKPIVATQEWPSP--P----- 70
XENLA)RTN4.1-  MDE--QSPDISSS------------------HSGDERREPAQ-PGERKPWDDLDDVLDLTGGAGQFSQPFS-------- 50
XENLA)RTN4.2-  MEA--QSSDISSS------------------HE----------PGDTKPWEDLDDVLDLTGGAGQFSPTFP-------- 41
DANRE)RTN6-A1  MEDTERASSAALG--------------SAPHEESGNEASAAGKTRADEPLLDAEETRDEQVTEVTSTQQIT-------- 57
DANRE)RTN4-L   ------------------------------------------------------------------------------- 1
FUGRU)RTN4-L2  ------------------------------------------------------------------------------- 1
FUGRU)RTN4-L3  ------------------------------------------------------------------------------- 1
ONCMY)RTN4-L   ------------------------------------------------------------------------------- 1
SALSA)RTN4-Lw  ------------------------------------------------------------------------------- 1

HUMAN)RTN4-A   LMDFGNDFVPPAPRGPLPAAPPVAPERQPSWDPSPVSSTVPAPSPLSAAAVSPSKLPEDDEPPARPPPPPPASVSPQAEP 157
MOUSE)RTN4-A   LLDFSSDSVPPAPRGPLPAAPPTAPERQPSWERSPAAS---APSLPPAAAVLPSKLPEDDEPPAR--PPAPAGASPLAEP 150
RAT)RTN4-A     LLDFSSDSVPPAPRGPLPAAPPAAPERQPSWERSPAAP---APSLPPAAAVLPSKLPEDDEPPARPPPPPPAGASPLAEP 154
CHICK)RTN4-Aw  -QDRSSPAEPPRPAAPEPAPEPLQP---AWCLPQPAAS-----SSSSSAASTPS--PGTERP---------A--PPQPEP 128
XENLA)RTN4.1-  -GSHPARDIEEEEE---DEEEERGA-WKDSLEPSPVEE-----EPGSIDSISPVS-PHSPAVPS----------APMEEP 109
XENLA)RTN4.2-  -VSYPARHMEEKEEENEDEEEDEKS-WKESLEASPVLE-----DPGSTSGSSPT--PHSPPEPS----------APTEEP 102
DANRE)RTN6-A1  -EVN--TAPQTAEVTSAEQITEVTSAEQTSLTPTTEVN-----TAQQTAEVTLTN--VSAEQIT---------------- 111
DANRE)RTN4-L   ------------------------------------------------------------------------------- 1
FUGRU)RTN4-L2  ------------------------------------------------------------------------------- 1
FUGRU)RTN4-L3  ------------------------------------------------------------------------------- 1
ONCMY)RTN4-L   ------------------------------------------------------------------------------- 1
SALSA)RTN4-Lw  ------------------------------------------------------------------------------- 1

HUMAN)RTN4-A   VWTPPAPAPAAPPSTPAAPKRRGSSGSVDETLFALPAASEPVIRSSAEN-MDLKEQPGNTISAGQEDFPSVLLETAASLP 236
MOUSE)RTN4-A   ---------AAPPSTPAAPKRRGS-GSVDETLFALPAASEPVIPSSAEKIMDLKEQPGNTVSSGQEDFPSVLFETAASLP 220
RAT)RTN4-A     ---------AAPPSTPAAPKRRGS-GSVDETLFALPAASEPVIPSSAEKIMDLMEQPGNTVSSGQEDFPSVLLETAASLP 224
CHICK)RTN4-Aw  ------------------RRRVSSSGSADETLFALPATSEPLMHSSAEKVVDLQEQPGSAKSLGQEDFTAVPLDTAASLL 190
XENLA)RTN4.1-  ------------ERPPAPCTAPS-GSVDENLFTLPAASAHLMHASADK----IMEPYSTVSTGQEEFASVLLQSTASLS 171
XENLA)RTN4.2-  ------------ERPPATCTAPS-SSLDENLFPLPAASAHLMHLSADK----IMEPSSTVSTGQEDFASVLLQSTASLS 164
DANRE)RTN6-A1  ------------EADPQITEQTDISLTQTTVVTSPEQVTEVTSTSPEHVTEVKADPHITEVTQITEDTSLTLPTEATSP 178
DANRE)RTN4-L   ------------------------------------------------------------------------------- 1
FUGRU)RTN4-L2  ------------------------------------------------------------------------------- 1
FUGRU)RTN4-L3  ------------------------------------------------------------------------------- 1
ONCMY)RTN4-L   ------------------------------------------------------------------------------- 1
SALSA)RTN4-Lw  ------------------------------------------------------------------------------- 1

HUMAN)RTN4-A   SLSPLSAASFKEHEYLGNLSTVLPTEGTLQENVSEASKEVSEKAKTLLIDR-DLTEFSELEYSEMGSSFSVSPKAESAVI 315
MOUSE)RTN4-A   SLSPLSTVSFKEHGYLGNLSAVASTEGTIEETLNEASRELPERATNPFVNR-ESAEFSVLEYSEMGSSFNGSPKGESAML 299
RAT)RTN4-A     SLSPLSTVSFKEHGYLGNLSAVSSSEGTIEETLNEASKELPERATNPFVNR-DLAEFSELEYSEMGSSFKGSPKGESAIL 303
CHICK)RTN4-Aw  SFSPLSADPFKEHAAFDSVSDALPARGIYKESASEVCKEAMENVRNPFLAEGNKRDISEMKYSEMEPSFT---KAEAATI 267
XENLA)RTN4.1-  SLPSLSTDSSKEHAETVAFPTGLAATEALQEPTDNMYSVSRITSHLPLSDN---LESKALDQVKEEVIFS---E-KGYVV 244
XENLA)RTN4.2-  SLPSLS---SKEHVQTVAFSTGLAANEALQEPTDNTYSASRS-----LIDT---LETKALDQFKEEVIFS---D-KGYVV 229
DANRE)RTN6-A1  EQ-------VTEVRVDPQITEVTSSTQVTEETSLTQITEVTSPEQVSELKPDPQISEETLTQTAGVTSVSPEPITEITSA 251
DANRE)RTN4-L   ------------------------------------------------------------------------------- 1
FUGRU)RTN4-L2  ------------------------------------------------------------------------------- 1
FUGRU)RTN4-L3  ------------------------------------------------------------------------------- 1
ONCMY)RTN4-L   ------------------------------------------------------------------------------- 1
SALSA)RTN4-Lw  ------------------------------------------------------------------------------- 1

HUMAN)RTN4-A   VANPREEIIVKNKDEEEKLVSNNILHNQQELPTALTKLVKEDEVVSSEK--AKDSFNEKRVAVEAPMREEYADFKPFERV 393
MOUSE)RTN4-A   VENTKEEVIVRSKDKED-LVCSAALHNPQESPATLTKVVKEDGVMSPEK--TMDIFNEMKMSVVAPVREEYADFKPFEQA 376
RAT)RTN4-A     VENTKEEVIVRSKDKED-LVCSAALHSPQESP-----VGKEDRVVSPEK--TMDIFNEMQMSVVAPVREEYADFKPFEQA 375
CHICK)RTN4-Aw  FQAEEMQLEGPKELCDLEKMPAQPLIMSPETPEDLFEKNEEDIFSSKDKGRDGDSGDKKALKEDAIRREEYVDFKQYEPV 347
XENLA)RTN4.1-  DHPTSQQETISEEHAKLYSQSAKEMFSGMLQS------------VAPPH---------EEFTDIKEVYDPYVDFKPFMSS 303
XENLA)RTN4.2-  EHPTSQQETISEEHAKLYSQSAKEMFSGMLQS------------VAPPH---------EEFTDIKEVDYQYVDFKPFISS 288
DANRE)RTN6-A1  EQTSEETSLTQISEDVTEETSVPPVSGPPPPP-------------------------PHHPAAAAPPPDRSLAPCNAR 304
DANRE)RTN4-L   ------------------------------------------------------------------------------- 1
FUGRU)RTN4-L2  ------------------------------------------------------------------------------- 1
FUGRU)RTN4-L3  ------------------------------------------------------------------------------- 1
ONCMY)RTN4-L   ------------------------------------------------------------------------------- 1
SALSA)RTN4-Lw  ------------------------------------------------------------------------------- 1

HUMAN)RTN4-A   WEVKDS---KEDS-DMLAAGGKIESNLESKVDKKCFADSLE-QTNHEKDSESSNDDTSFPSTPEGIKDRSGAYITCAPFN 468
MOUSE)RTN4-A   WEVKDT---YEGSRDVLAAR----ANMESKVDKKCFEDSLE-QKGHGKDSESRNENASFPRTPELVKDGSRAYITCDSFS 448
RAT)RTN4-A     WEVKDT---YEGSRDVLAAR----ANVESKVDRKCLEDSLE-QKSLGKDSEGRNEDASFPSTPEPVKDSSRAYITCASFT 447
CHICK)RTN4-Aw  WEVEGAGHGLSGLREDIESN--IDAKLETSLDEKYGEDKLSVLKDYERDSEGSAEDLSFPNSPEAVKEPSQNYITCTKFE 425
XENLA)RTN4.1-  KSGDVG-YEVSDVAEKFQVD---VGRLNLESAVKHEEKSSE-----EMEIDSISDDIS-PLTPELLPDST-DYDMFATVE 372
XENLA)RTN4.2-  NSRDIG-YEVKDVAEKLHV-----GRLNLESTAKHEEKSSE-----EKEMD-ISDDIS-PLTPEVLSDST-DYEMFATVE 354
DANRE)RTN6-A1  PPEPCG----EPHSELPPAG-------EPEVSVSVFQTLPS------------ERCRSLVSSAGLAMDAFGR-------- 353
DANRE)RTN4-L   ----------------------------------------------------------MDDQI--------- 5
FUGRU)RTN4-L2  ----------------------------------------------------------MADNV--------- 5
FUGRU)RTN4-L3  ----------------------------------------------------------MADNV--------- 5
ONCMY)RTN4-L   ----------------------------------------------------------MEDS---------- 4
SALSA)RTN4-Lw  ----------------------------------------------------------MEDS---------- 4
```

```
HUMAN)RTN4-A   PAAT-ESIATNIFPLLGDPTSENKTD-EKKIEEKKAQIVTEKNTSTKTSNPFLVAAQDSETDYVTTDNLTKVTEEVVANM 546
MOUSE)RTN4-A   -SAT-ESTAANIFPVLEDHTSENKTD-EKKIEERKAQIITEK-TSPKTSNPFLVAIHDSEADYVTTDNLSKVTEAVVATM 524
RAT)RTN4-A     -SAT-ESTTANTFPLLEDHTSENKTD-EKKIEERKAQIITEK-TSPKTSNPFLVAVQDSEADYVTTDTLSKVTEAAVSNM 523
CHICK)RTN4-Aw  SSVTPDGSKVKSICPIEEDTSENRTDDEKKIAEMKAQNTEQG----DFSSQAIGKQEGLEADDAKTGSISTLLSDTAASM 501
XENLA)RTN4.1-  QNIP--------FSFGGGHVAGNKTD-EKKIEDIEAQKTSVGFGLKVATVNPFYNESAQESEYVTT-----HVATHVSTK 438
XENLA)RTN4.2-  HSYP--------FSLGGSRVAGNKTD-EKKIEDFEAQKTSVGFGLKVATVNPFYDESAQESEYVTTG----ATRVQVSTK 421
DANRE)RTN6-A1  ----------------EPSATSDPDLLSPSDDDLMLEMKSSAG---------------------------------- 380
DANRE)RTN4-L   ------------------SSTTPSYD--VHHDDEGEFRAEKQANS---------------------------------- 30
FUGRU)RTN4-L2  ----------------EHEVSSTTPFYTEEVHHYQAEPEPQP----------------------------------- 31
FUGRU)RTN4-L3  ----------------EHEVSSTTPFYTEEVHHYQAEPEPQP----------------------------------- 31
ONCMY)RTN4-L   ----------------EQVVSSTTPS-EDEMRSYRQFGNHYG---------------------------------- 29
SALSA)RTN4-Lw  ----------------EQVVSSTTPS-EDEMRSYRQFGNHYG---------------------------------- 29

HUMAN)RTN4-A   PEGLTPDLVQEACESELNEVTGTKIAYETKMDLVQTS-EVMQESLYPAAQLCPSFEESEATPSPVLPDIVMEAPLNSAVP 625
MOUSE)RTN4-A   PEGLTPDLVQEACESELNEATGTKIAYETKVDLVQTS-EAIQESIYPTAQLCPSFEEAEATPSPVLPDIVMEAPLNSLLP 603
RAT)RTN4-A     PEGLTPDLVQEACESELNEATGTKIAYETKVDLVQTS-EAIQESLYPTAQLCPSFEEAEATPSPVLPDIVMEAPLNSLLP 602
CHICK)RTN4-Aw  PEGLTPDLVQEAYESEMHDAACTKLAYETKIDLVQTS-ESVQETLKPVTQLCPSFEDSEAAPSPVLPDIVMEAPLSSGTA 580
XENLA)RTN4.1-  PEGPTPDIVQEAYESEAYDTGIPKQKYESNIDLVQTAANSVQEKVSPTAQAPARLEETDSVSSPVLPDIVMEAPLAS--- 515
XENLA)RTN4.2-  AEGPTPDIVQEAYESEAYDTGISKLNYEPNIDLVQTAATSMQEKVSPTAQVPALLED--SVSSPVLPDIVMEAPLASTL- 498
DANRE)RTN6-A1  ------------------LEESRSVSDSPSPDLLQDAYEDLQTPGALSAAEPPNPEQ----RPVALPDILQSSPLNPEKL 438
DANRE)RTN4-L   -------LMDEDFSS--SEAQAHVPEVEGILDLAGGAKDALERHRSTMPRKEEPLLD---------FG------------ 80
FUGRU)RTN4-L2  ------------------DPPKQDLFSLDDIVDLVGGAHDALNRHIAED-NASHEFTET--HPADSVSEVP---------- 81
FUGRU)RTN4-L3  ------------------DPPKQDLFSLDDIVDLVGGAHDALNRHIAED-NASHEFTET--HPADSVSEVP---------- 81
ONCMY)RTN4-L   ----------------N-EATAKVGKDDIVDLVGGAQDAIERHMASCPDDLKEFTEE--AKEQLTNEVISDITPSD--- 86
SALSA)RTN4-Lw  ----------------N-EATAKVGKDDILDLVGGAQDAIERHMASYPDDLKEFTEE--AKEQLTKKVISDITPSD--- 86

HUMAN)RTN4-A   SAGASVIQPSSSPLEASS--VNYESIKHEPENPPPYEEAMSVSLKKVS-GIKEEIKEPEN---INAALQETEAPYIS--- 696
MOUSE)RTN4-A   STGASVAQPSASPLEVPSP-VSYDGIKLEPENPPPYEEAMSVALKTS--DSKEEIKEPES---FNAAAQEAEAPYIS--- 674
RAT)RTN4-A     SAGASVVQPSVSPLEAPPP-VSYDSIKLEPENPPPYEEAMNVALKAL--GTKEGIKEPES---FNAAVQETEAPYIS--- 673
CHICK)RTN4-Aw  GAEASTVQLETSQLGTFVTTASYENVKKEAEKPPLYQEAVNMPLTQAQ-EAKEELTLKKADRESSTSPEDLETPYIS--- 656
XENLA)RTN4.1-  ALETVALKPDISPVGIKPP-ARVEKTKAEPEKPPSYEEAVTEVLQNQD--LAAALGGSKQ----GAVVEETETPYIS--- 585
XENLA)RTN4.2-  CLETMALKPDISPVRIEPP-ARDEKTKAEPEKPPSYEEAVTEVLQDQGPAAAADLGDSKQ----GAVVKEAEAPYISPYI 573
DANRE)RTN6-A1  DSGSSEGSPDCSPAHRCSP---------NPPLSAAGSPDSRILLLR-------------------EMVEETEARAVEK-- 488
DANRE)RTN4-L   -------EP-------------------EPEPSSTIKPE------P-------------------------EAP------ 97
FUGRU)RTN4-L2  -------EP------------G------PDSTSYSFLPDTSEVVAP-----------------------KAEPES--- 108
FUGRU)RTN4-L3  -------EP------------G------PDSTSYSFLPDTSEVVAP-----------------------KAEPES--- 108
ONCMY)RTN4-L   -------EE------------Q------EEEVTDTFSEAQPVILNPL---------------------DADYLP--- 114
SALSA)RTN4-Lw  -------EE------------Q------EEEVTDTFSEAEPVIVNPL---------------------EADYLP--- 114
HUMAN)RTN4-A   -IACDLIKETKLSAE-PAPDFSDYS---EMAKVEQPVPDHSELVEDSSPDSEPVDLFSDDSIPDVPQKQDETVMLVKESL 771
MOUSE)RTN4-A   -IACDLIKETKLSTE-PSPEFSNYS---EIAKFEKSVPDHCELVDDSSPESEPVDLFSDDSIPEVPQTQEEAVMLMKESL 749
RAT)RTN4-A     -IACDLIKETKLSTE-PSPDFSNYS---EIAKFEKSVPEHAELVEDSSPESEPVDLFSDDSIPEVPQTQEEAVMLMKESL 748
CHICK)RTN4-Aw  -IACDLIKETKVSGESASPSLTDYSTTPITEHLSQDVSEHKELAEKLSPQFGKCDLFSRQVMPDFPGNR----------- 724
XENLA)RTN4.1-  -IACDLIKGTESVAS----GFTEFS----KLKQNEFESQFMEPSDESSPDSECSEPSYKQWDSEVVQKEAFS--IKTESV 654
XENLA)RTN4.2-  SIACDLIKGTQSAAS----DFTEFS----KFKQHEFDSQFMEPSDESSPDSELSEPSYKQWDSEVVRKETFT--IKTESA 643
DANRE)RTN6-A1  -VQQDVQQEVQQEAQ----------------------AQLEKQVQQESQQGCTVLDLLQEAPAHTQTLPPP--------- 536
DANRE)RTN4-L   -------KPAPISS-------------------------FG--DASPKQAKPEEKEEKPTVAPYKCNSSCS-------- 134
FUGRU)RTN4-L2  ----AKIEPEPLSAP---------E------------SDALPVVEPWKAAPAPAEAAERPAVTEEPSAPS---------- 153
FUGRU)RTN4-L3  ----AKIEPEPLSAP---------E------------SDALPVVEPWKAAPAPAEAAERPAVTEEPSAPS---------- 153
ONCMY)RTN4-L   ----ELIRPDPPKAAQ--------E------------KEPAPVVESAPVEAAPVAEVLPEAAPEKEAIAAPP-------- 162
SALSA)RTN4-Lw  ----ELIRPDPPKAPQ--------E------------EAPAPVVESA-----PVVEVLPEAAPEKEAI------------ 153

HUMAN)RTN4-A   TETSFESMIEYENKEKLSALPPEGGKPYLESFKLSLDNTKDTLLPDEVSTLSKKEKIPLQMEELSTAV-YSNDDLFISKE 850
MOUSE)RTN4-A   TEVS-ETVTQHKHKERLSASPQEVGKPYLESFQPNLHITKDAAS-NEIPTLTKKETISLQMEEFNTAI-YSNDDLLSSKE 826
RAT)RTN4-A     TEVS-ETVAQHK-EERLSASPQELGKPYLESFQPNLHSTKDAAS-NDIPTLTKKEKISLQMEEFNTAI-YSNDDLLSSKE 824
CHICK)RTN4-Aw  ---------------------------------------------------------------------------- 724
XENLA)RTN4.1-  NAQS-IIIPEQKQVFDQKSEESSPSKSYLDSFQPEICVSKATS-------------DLFAKGLTTLL---QEKPLQMEE 716
XENLA)RTN4.2-  MAQS-FVIPEQKPGIDQKSEESSPSKPYLASFQPEIYVSKAT--------------DLFAKGLDTEISIPQERHLHMEE 707
DANRE)RTN6-A1  ------------------------------------P---------------------------------QQQTDAP 544
DANRE)RTN4-L   ---------------------------------------------------------------------------- 134
FUGRU)RTN4-L2  ------------------------------------S-----------------------------------CALIGW 160
FUGRU)RTN4-L3  ------------------------------------S-----------------------------------YVTSPS 160
ONCMY)RTN4-L   ---AP-------------------------------S-----------------------------------RVLQRW 171
SALSA)RTN4-Lw  ---------------------------------------------------------------------------- 153

HUMAN)RTN4-A   AQIRETETFSDSSPIEIIDEFPTLISSKTDSFSKLAREYTDLEVSHKSEIANAPDGAGSLPCTELPHDLSLKNIQPKVEE 930
MOUSE)RTN4-A   DKMKESETFSDSSPIEIIDEFPTFVSAKDDSP----KEYTDLEVSNKSEIANVQSGANSLPCSELPCDLSFKNTYPKDEA 902
RAT)RTN4-A     DKIKESETFSDSSPIEIIDEFPTFVSAKDDSPK-LAKEYTDLEVSDKSEIANIQSGADSLPCLELPCDLSFKNIYPKDEV 903
CHICK)RTN4-Aw  ---------------------------------------------------------------------------- 724
XENLA)RTN4.1-  LDEGLSLEKIPCTKYSPVSESPEPRPSP-----------VPEDLSSKLGDIQKEVLIAKQPEDKVQKNRSNLDFVPENIE 785
XENLA)RTN4.2-  FDEGLYSSKLPGSKYSPVSESPEFRLS-------------PEELTSKHEEIQ--THIAKHPEDKLQKNKDKLDFLPENIE 772
DANRE)RTN6-A1  AELLQGLQFSSGPHVELWDSSPSADSFS-----------PVLDAEQQKHSENTHSHTHIDAADEEQEPSSSEEFEFVERP 613
DANRE)RTN4-L   ---------------------------------------------------------------------------- 134
FUGRU)RTN4-L2  KLKLNSR------------------------------------------------------------------------ 167
FUGRU)RTN4-L3  KAQPLPLMQFPT---------------------------------------------------------------------- 172
ONCMY)RTN4-L   NIDKRDEHFLPSTPLQPLMQFPK------------------------------------------------------------ 194
SALSA)RTN4-Lw  ---------------------------------------------------------------------------- 153
```

```
HUMAN)RTN4-A    KISFSDDFSKNGSATSKVLLLPPDVSALATQAEIESIVKPKVLVKEAEKKLPSDTEKEDRSPSAIFSAELSKTS 1004
MOUSE)RTN4-A    HVS--DEFSKSRSSVSKVPLLLPNVSALESQIEMGNIVKPKVLTKEAEEKLPSDTEKEDRSLTAVLSAELNKTS 974
RAT)RTN4-A      HVS--DEFSENRSSVSKASISPSNVSALEPQTEMGSIVKSKSLTKEAEKKLPSDTEKEDRSLSAVLSAELSKTS 975
CHICK)RTN4-Aw   -------------------------------------------------------------------------- 724
XENLA)RTN4.1-   FTPAVQKPDDSGKAVSDTFGGLDTTTKGGSAVHEVKVDKPKPPSKEDDGSKLPKKESKA---STVSSSDFMNS- 855
XENLA)RTN4.2-   FTPIVQKADDFGKAASATHGGVDTTAKGASEVHEEKVTKPEPPSKKDEVSKLPKKESKAPS-STVPSSDFRNS- 844
DANRE)RTN6-A1   AAGAAEEFVELQDGLTSITAPPPEAAEAPEQKQSSTCLLSPAEGGGPADGEERSDVQQTCPAGHTAGAPADPTA 687
DANRE)RTN4-L    -------------------------------------------------------------------------- 134
FUGRU)RTN4-L2   -------------------------------------------------------------------------- 167
FUGRU)RTN4-L3   -------------------------------------------------------------------------- 172
ONCMY)RTN4-L    -------------------------------------------------------------------------- 194
SALSA)RTN4-Lw   -------------------------------------------------------------------------- 153
```

Supplementary Fig. 8: *BioEdit alignement of mammalian rtn4-a and fish rtn4-l / 6-a N-termini*

```
HUMAN)RTN4-C    ---MDGQKKNWKDK 11
MACMU)RTN4-C    ---MDGQKKNWKDR 11
MACFA)RTN4-C    ---MDGQKKNWKDK 11
BOVIN)RTN4-C    ---MDGQKKNWKDK 11
PIG)RTN4-C      ---MDGQKKNWKDK 11
PANTR)RTN4-C    ---MDGQKKNWKDK 11
MOUSE)RTN4-C    ---MDDQKKRWKDK 11
RAT)RTN4-C      ---MDGQKKHWKDK 11
CHICK)RTN4-C    ---MDSQPSGWKDK 11
XENLA)RTN4.1-   ---MACLPSSWKEK 11
XENLA)RTN4.2-   ---MACVPSSWKEK 11
XENTR)RTN4-C    ---MACLPSSWKEK 11
XENLA)RTN4.1-   ---MDSKA        5
XENLA)RTN4.2-   ---MDSKA        5
XENTR)RTN4-N    ---MDSKA        5
DANRE)RTN4-N    ---MDSKQ        5
FUGRU)RTN4-N    ---MDAKR        5
CYPCA)RTN4-N    MSEMDSKQ        8
ONCMY)RTN4-N    ---MDAKR        5
ONCMY)RTN10-N   ---MDAER        5
```

Supplementary Fig. 9: *BioEdit alignement of mammalian rtn4-c and fish rtn4-n N-termini*

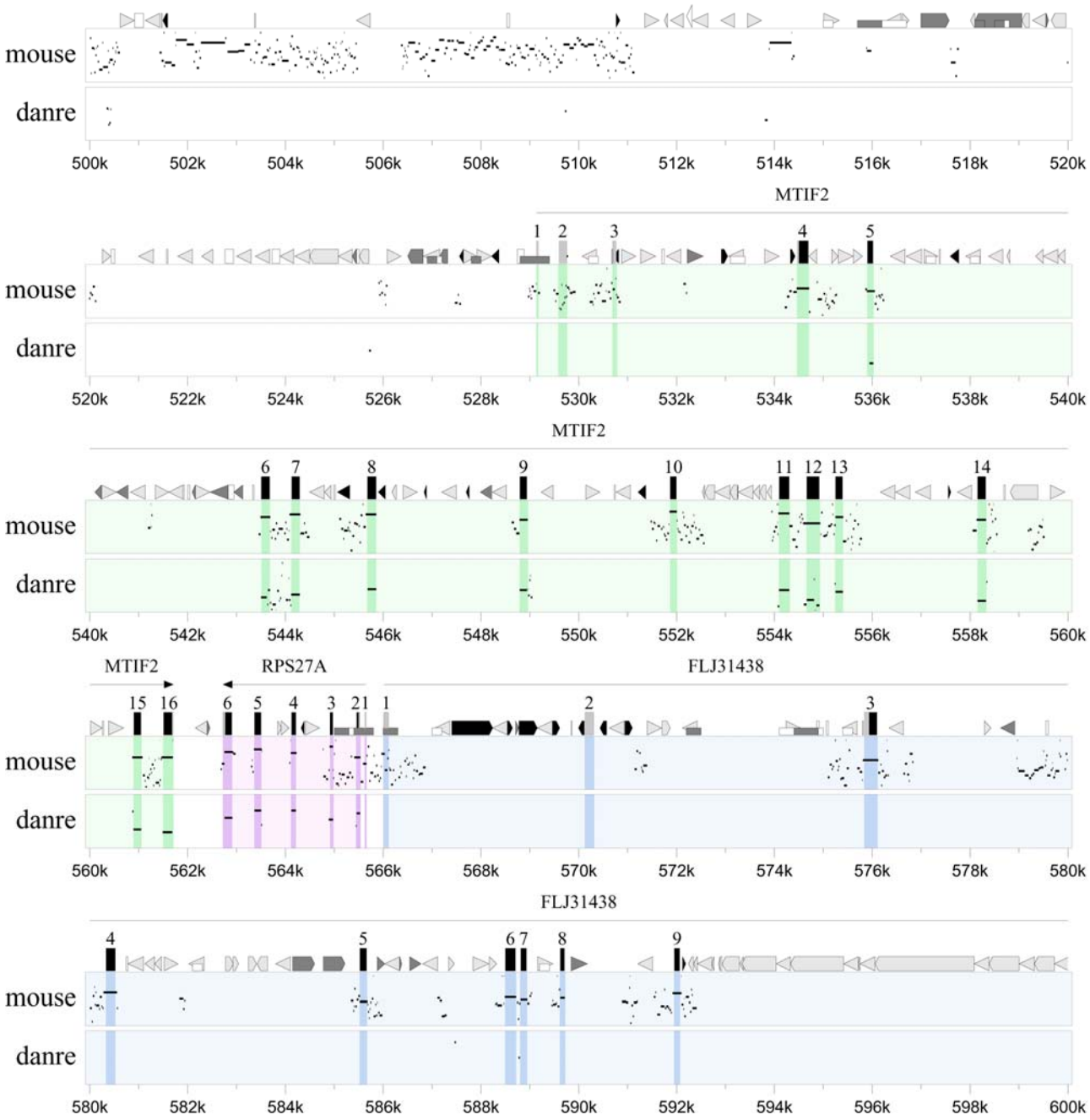
mouse
danre
500k 502k 504k 506k 508k 510k 512k 514k 516k 518k 520k
MTIF2
1 2 3 4 5
mouse
danre
520k 522k 524k 526k 528k 530k 532k 534k 536k 538k 540k
MTIF2
6 7 8 9 10 11 12 13 14
mouse
danre
540k 542k 544k 546k 548k 550k 552k 554k 556k 558k 560k
MTIF2
RPS27A
FLJ31438
15 16 6 5 4 3 21 1 2 3
mouse
danre
560k 562k 564k 566k 568k 570k 572k 574k 576k 578k 580k
FLJ31438
4 5 6 7 8 9
mouse
danre
580k 582k 584k 586k 588k 590k 592k 594k 596k 598k 600k

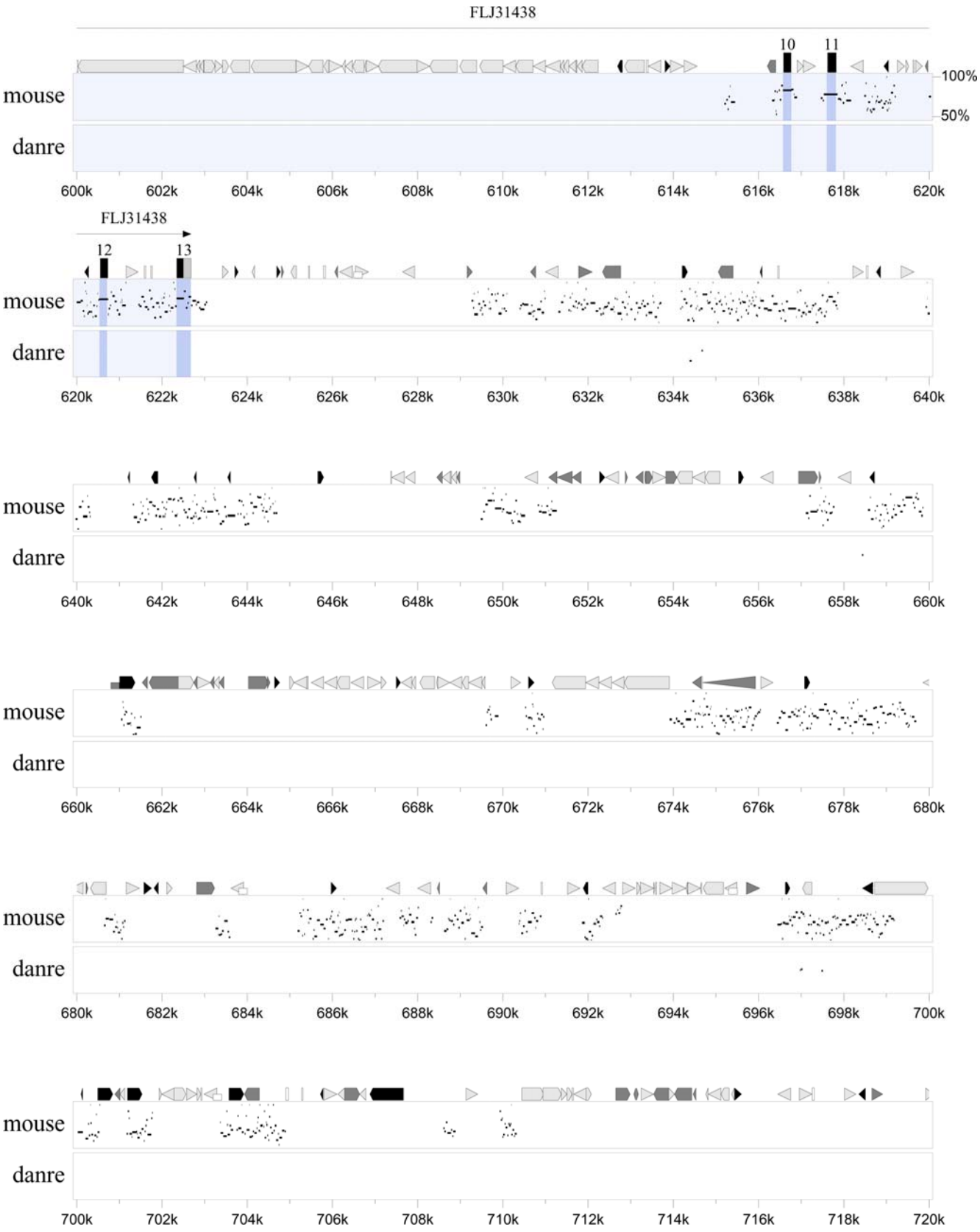
FLJ31438
10
11
100%
50%
mouse
danre
600k 602k 604k 606k 608k 610k 612k 614k 616k 618k 620k
FLJ31438
12
13
mouse
danre
620k 622k 624k 626k 628k 630k 632k 634k 636k 638k 640k
mouse
danre
640k 642k 644k 646k 648k 650k 652k 654k 656k 658k 660k
mouse
danre
660k 662k 664k 666k 668k 670k 672k 674k 676k 678k 680k
mouse
danre
680k 682k 684k 686k 688k 690k 692k 694k 696k 698k 700k
mouse
danre
700k 702k 704k 706k 708k 710k 712k 714k 716k 718k 720k

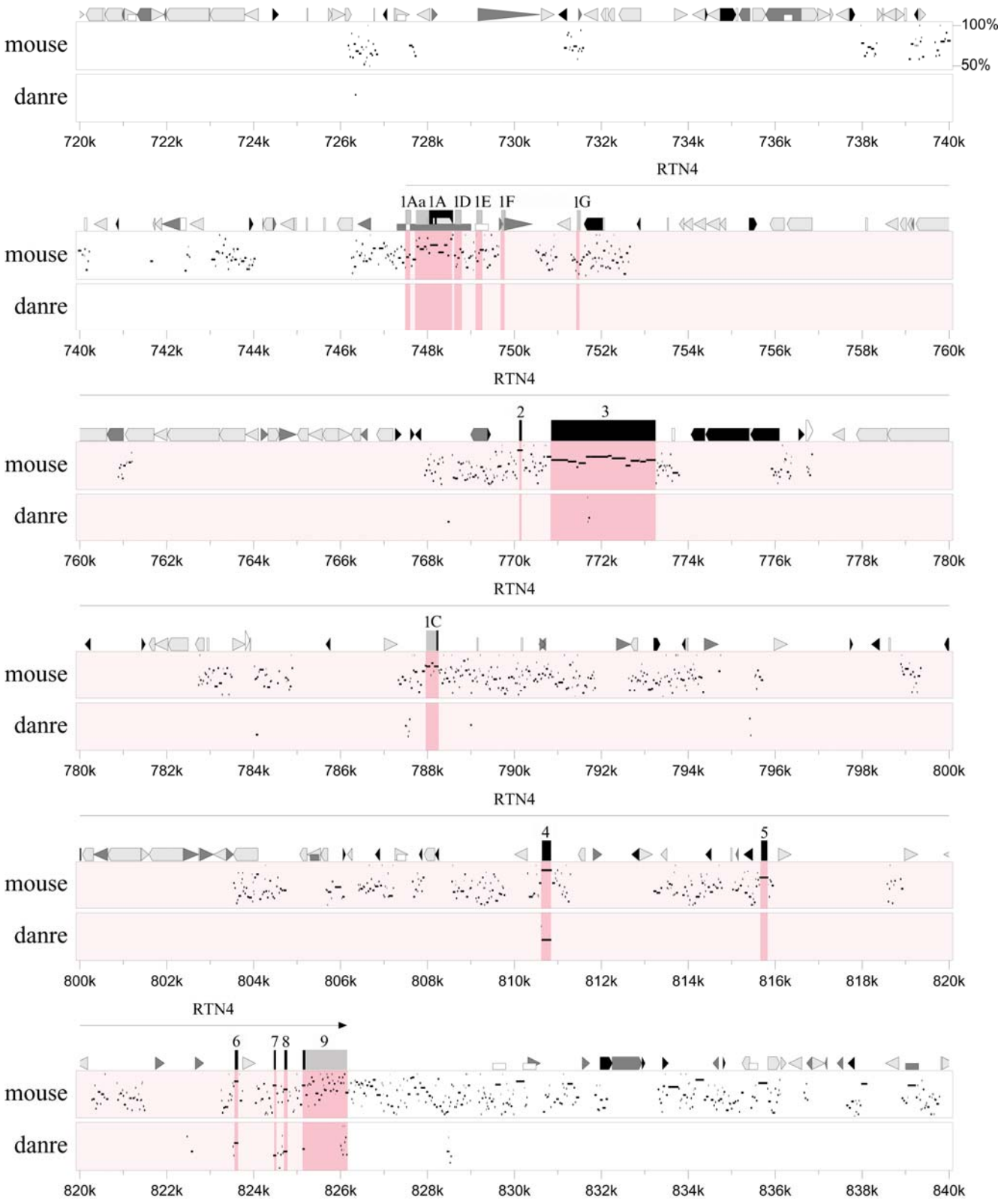

Supplementary Fig. 10: *Comparison of the human, mouse and zebrafish rtn4 gene locus*

Graphical representation of pair-wise comparisons between the human-mouse (mouse) and human-zebrafish (danre) mtif2 to rtn4 gene locus using a percent-identity plot (PIP) in which the percent identity

(from 50% to 100%) in each gap-free aligning segment is plotted using the coordinates of the human sequence. The entire alignement is represented by three consecutive parts (**A**, **B** and **C**). The human rtn4 exons (**C**) are numbered according to Oertle et al., 2003a, while the exons of human MTIF2 (**A**), RPS27A (**A**) and FLJ31438 (**A**, **B**) have been consecutively numbered from 5' to 3'. The MTIF2 gene region is shown in green, RPS27A (encoded on the reverse strand) in purple, FLJ31438 in blue and RTN4 (**C**) in red. Exons are marked in darker colour. Coding exons are shown as black boxes above the alignement while untranslated exonic regions (UTRs) are depicted as grey boxes. Almost all coding exons of MTIF2 and RPS27A are strongly conserved in human, mouse and zebrafish (**A**). The FLJ31438 gene (**A**, **B**), however, is present in human and mouse but absent in zebrafish, suggesting that this gene has been acquired at a later evolutionary stage in vertebrate phylogeny. Almost the entire genomic region between RPS27A and exon 4 of RTN4 shows no or very low homologies in zebrafish (**A**-**C**). Note that while the N-terminal exons 1A, 2 and 3 are strongly conserved in the murine orthologous region, no homology could be identified in zebrafish. In contrast, the exons coding for the conserved C-terminal RHD domain (exons 4-9) are also conserved in the fish orthologous locus. The ungapped alignment from the MTIF2 gene to RTN4 is unequivocally proving the absence of sequences orthologous to the N-termini of mammalian RTN4 isoforms in zebrafish. For the analysis and explanation of the interspersed repetitive elements please refer to the PIP in Oertle et al., 2003a.

Gene	Transcripts	Exons	Identification	size of identified 5'UTR (bp)	position of upstream stop codon (bp)	Kozak Consensus (gccAccATGG)	ORF (bp)	size of identified 3'UTR (bp)
(DANRE)**rtn1**	rtn1-a1	I(a), II, III, IV-IX	5'race, library screen[1]	168	-93 to -91	tccAaa**ATG**T	2304	1055
	rtn1-a2	I(a), IV-IX	RT-PCR			tccAaa**ATG**T	789	
	rtn1-c	I(c), IV-IX	5'race, library screen[1]	138	-120 to -118	cctAgt**ATG**C	639	1055
(DANRE)**rtn2**	rtn2-c	I(c), II-VII	RT-PCR	65	-42 to -40	tccAaa**ATG**A	612	41
(DANRE)**rtn3**	rtn3-a1	I(a), III-VIII	RT-PCR, ESTs	156	-114 to -112	caaAaa**ATG**G	666	473
	rtn3-a2	I(a), II, III-VIII	RT-PCR			caaAaa**ATG**G	711	
(DANRE)**rtn4**	rtn4-l	I(l), II-VII	5'race, ESTs, library screen[1]	206	-33 to -31	gcaAca**ATG**G	969	970
	rtn4-l(-63/188)	I(l) -63/188, II-VII	RT-PCR, ESTs, library screen[1]			tccAca**ATG**C	765	
	rtn4-l(-10/195)	I(l) -10/195, II-VII	RT-PCR	89	-6 to -4	tccAca**ATG**C	765	
	rtn4-m	I(m), II-VII	5'race			tgaCcg**ATG**C	639	
	rtn4-n	I(n), II-VII	ESTs, library screen[1]	48	-18 to-16	agcGag**ATG**G	582	970
(DANRE)**rtn5**	rtn5-a1	I(a), II, III, IV-IX	5'race, library screen[1]	118	-51 to -53	gcaAgc**ATG**T	2457	132
	rtn5-a2	I(a), IV-IX	RT-PCR			gcaAgc**ATG**T	750	
	rtn5-a1(265/1584)	I(a), II , III , IV-IX	RT-PCR			gcaAgc**ATG**T	1137	
	rtn5-a1(297/2025)	I(a), II ,IV -IX	RT-PCR			gcaAgc**ATG**T	462	
	rtn5-a1(309/2025)	I(a), II , III, IV-IX	RT-PCR			gcaAgc**ATG**T	474	
	rtn5-a1(558/1048)	I(a), II , III, IV-IX	RT-PCR			gcaAgc**ATG**T	678	
	rtn5-c	I(c), IV-IX	library screen 1	175	-75 to -73	acaGac**ATG**G	612	132
(DANRE)**rtn6**	rtn6-a1	I(a), II, III, IV-IX	ESTs, library screen[1]	284	-102 to -100	ctcCcg**ATG**G	2628	321
	rtn6-a2	I(a), II, IV-IX	RT-PCR			ctcCcg**ATG**G	1569	
	rtn6-a3	I(a), III, IV-IX	ESTs			ctcCcg**ATG**G	2583	
	rtn6-a1(337/555)	I(a) , II, III, IV-IX	EST			ctcCcg**ATG**G	2409	
	rtn6-a1(1576/1860)	I(a), II, III , IV-IX	RT-PCR			ctcCcg**ATG**G	2343	
	rtn6-a1(1761/2150)	I(a), II, III , IV -IX	RT-PCR			ctcCcg**ATG**G	2238	
	rtn6-a1(1773/2152)	I(a), II, III , IV -IX	RT-PCR			ctcCcg**ATG**G	1926	
	rtn6-a1(1774/2212)	I(a), II, III , IV -IX	RT-PCR			ctcCcg**ATG**G	1968	
	rtn6-a1(1775/2140)	I(a), II, III , IV -IX	RT-PCR			ctcCcg**ATG**G	2262	
	rtn6-a1(1775/2152)	I(a), II, III , IV -IX	RT-PCR			ctcCcg**ATG**G	2250	
	rtn6-a1(1775/2344)	I(a), II, III , V -IX	RT-PCR			ctcCcg**ATG**G	2058	
	rtn6-a1(1777/1956)	I(a), II, III , IV-IX	RT-PCR			ctcCcg**ATG**G	2448	
	rtn6-a1(2023/2173)	I(a), II, III , IV -IX	RT-PCR			ctcCcg**ATG**G	2043	
(DANRE)**rtn8**	rtn8-c	I(c), II-VII	5'race, RT-PCR, EST	53	-36 to -34	gcaGaa**ATG**G	627	213

Gene	Transcripts	Exons	Identification	size of identified 5'UTR (bp)	position of upstream stop codon (bp)	Kozak Consensus (gccAccATGG)	ORF (bp)	size of identified 3'UTR (bp)
(FUGRU)**rtn1**	rtn1-a1	I(a), II, III, IV-IX	RT-PCR	16	-6 to -4	tagAcc**ATG**T	2190	32
(FUGRU)**rtn2**	rtn2-c	I(c), II-VII	genomic, 3'race			actAaa**ATG**G	612	277
(FUGRU)**rtn3**	rtn3-a1	I(c), II-VII	RT-PCR	72	-15 to -13	aatAca**ATG**G	663	18
(FUGRU)**rtn4**	rtn4-l1	I(l), IV-IX	RT-PCR, ESTs	210	-73 to -75	acgAaa**ATG**G	1029	28
	rtn4-l2	I(l), II, IV-IX	RT-PCR			acgAaa**ATG**G	1068	
	rtn4-l3	I(l), III, IV-IX	RT-PCR			acgAaa**ATG**G	1083	
	rtn4-n	I(n), IV-IX	RT-PCR, ESTs	17		ttcAag**ATG**G	682	44
(FUGRU)**rtn7**		IIa, IIb, III-VII	genomic					
(FUGRU)**rtn8**	rtn8-c	I(c), II-VII	RT-PCR, ESTs	76	-43 to -45	gctGaa**ATG**G	645	32

[1]Library screening was performed at the RZPD (Deutsches Ressourcenzentrum für Genomforschung GmbH, Heidelberg Germany) and for the different zebrafish rtn genes, the following clones were identified:

rtn1: embryo library: ICRFp524P1647Q8
brain library: UCDMp611H0866Q2, UCDMp611K0437Q2, UCDMp611L1236Q2, UCDMp611C2452Q2, UCDMp611E0247Q2, UCDMp611I0110Q2, UCDMp611D2082Q2, UCDMp611L0217Q2, UCDMp611M1391Q2, UCDMp611B1010Q2, UCDMp611M2385Q2, UCDMp611F1912Q2, UCDMp611B1221Q2, UCDMp611M1173Q2

rtn4: embryo library: ICRFp524H215808, ICRFp524N0372Q8, ICRFp524M1514508, ICRFp524E1950Q8, ICRFp524J2089Q8, ICRFp524M0310708, ICRFp524N1114608, ICRFp524I0216Q1, ICRFp524G2016Q8, ICRFp524N1511008, ICRFp524O0124Q8, ICRFp524K1013508
retina library: UWS_p760C0818Q2, UWS_p760F0665Q2, UWS_p760G2345Q2, UWS_p760N0712Q2
rtn5: retina library: UWS_p760O0115Q2
rtn6: embryo library: ICRFp524L0812608, ICRFp524L0812626Q8, ICRFp524A0107Q8
brain library: UCDMp611B2213Q2

Supplementary Tabel 1A: *Overview of cloned zebrafish and fugu rtns*

(DANRE)rtn1		
No	Sequence	Project
1	GTC TAA ATA AAC TGG AAG TTG CTG AGA C	RDH mapping sense primer
2	CAT GGG ACA GTG ACA TCT CCA CAT CC	RDH mapping antisense primer
3	GAA AAG ATG TCC ACC ATG	RT-PCR sense primer (-a1 splice form)
4	ATA AGA GCT CCA ACA TAG G	RT-PCR antisense primer (-a1 splice form)
5	ATG CAG GCC AGC ACC ATG	RT-PCR sense primer (-c splice form)
2	CAT GGG ACA GTG ACA TCT CCA CAT CC	RT-PCR antisense primer (-c splice form)
(DANRE)rtn2		
No	Sequence	Project
6	GGG TTT CAG AGA TCA GG	RDH mapping sense primer
7	ACT GCT ATG TGG GAC TTC	RDH mapping antisense primer
8	CGG TCC ATG AAG ACT C	RT-PCR sense primer (c splice form)
9	GAG TGA CAG CGC ATG G	RT-PCR antisense primer (c splice form)
(DANRE)rtn3		
No	Sequence	Project
10	GCT CTT CAG TGT ACC GCC CAT CTA TG	RDH mapping sense primer

11	GCC ATT GAG ACA CCG CGG ACA CC	RDH mapping antisense primer
12	ATG GCA GAC CCA ATG ACC	RT-PCR sense primer (-a1 and -a2 splice forms)
13	GGA TCA TTC TGC TTT ACA GC	RT-PCR antisense primer (-a1 and -a2 splice forms)
(DANRE)rtn4		
No	Sequence	Project
14	ATG GAT GAT CAA ATA AGC TC	RDH mapping sense primer
15	GTT ACA TTT ATA TGG CGC TAC TGT TGG C	RDH mapping antisense primer
14	ATG GAT GAT CAA ATA AGC TC	RT-PCR sense primer (-l splice form)
16	CCT GAC TGG ATA TAT GAC C	RT-PCR sense primer (-m splice form)
17	ATG AGC GAG ATG GAT TCC	RT-PCR sense primer (-n splice form)
18	GAA ATG AAT CCA AAT GGC C	RT-PCR antisense primer (-l, -m and -n splice forms)
(DANRE)rtn5		
No	Sequence	Project
19	GTT TGG CAG TGT GCT GCT GCT GCT C	RDH mapping sense primer
20	GGA ATC GTG ACT ATT CCA GTT TCG CGC	RDH mapping antisense primer
21	TGA GGA TGA AGA TGA CAT CC	RT-PCR sense primer (-a1 splice form)
22	GGT TAA AGA GAA GAG CAG C	RT-PCR antisense primer (-a1 splice form)
23	GGC TGA TCT GTC CTT GC	RT-PCR sense primer (-a1/b splice form)
24	ATG GAT AAA GGG AAG AAA GAG	RT-PCR sense primer (-c splice form)
25	GAA GTG AAG AGT TTA TTC CTT C	RT-PCR antisense primer (-a1/b and -c splice forms)
(DANRE)rtn6		
No	Sequence	Project
26	TGC TGC AGC TGC TGT ACT GGC G	RDH mapping sense primer
27	GCA TGG CCT GTA GCA CCG CCG TG	RDH mapping antisense primer
28	AAA AGC AGG TGC AGC AG	RT-PCR sense primer (-a1/a3 splice form)
29	ACT GCC AAC TTC AGC GAG	RT-PCR antisense primer (-a1/a3 splice form)
(DANRE)rtn8		
No	Sequence	Project
30	GGA TCT GAT ATA CTG GCG	RDH mapping sense primer
31	TTC CTG TTG TTA CAG TTA CC	RDH mapping antisense primer
30	GGA TCT GAT ATA CTG GCG	RT-PCR sense primer (RHD)
32	GTG AGC TCC ACA TTT CTC	RT-PCR antisense primer (RHD)
Actin		
No	Sequence	Project
33	GCT CAC CAT GGA TGA TGA TAT CGC	RT-PCR sense primer
34	GGA GGA GCA ATG ATC TTG ATC TTC	RT-PCR antisense primer

Supplementary Tabel 1B: *Primer used for RT-PCR und RHD mapping*

(DANRE)rtn1					
Primer sense	Primer antisense	Annealing Temp.	Elongation Time	Number of Cycles	Ampified Splice Form
3	4	51 °C	35 sec	35	(DANRE)rtn1-a1
5	2	59 °C	30 sec	35	(DANRE)rtn1-c
(DANRE)rtn2					
Primer sense	Primer antisense	Annealing Temp.	Elongation Time	Number of Cycles	Ampified Splice Form
8	9	54 °C	45 sec	35	(DANRE)rtn2-c
(DANRE)rtn3					
Primer sense	Primer antisense	Annealing Temp.	Elongation Time	Number of Cycles	Ampified Splice Form
12	13	58 °C	45 sec	35	(DANRE)rtn3-a1 and -a2
(DANRE)rtn4					
Primer sense	Primer antisense	Annealing Temp.	Elongation Time	Number of Cycles	Ampified Splice Form
14	18	56 °C	90 sec	35	(DANRE)rtn4-l
16	18	60 °C	40 sec	35	(DANRE)rtn4-m
17	18	59 °C	70 sec	35	(DANRE)rtn4-n
(DANRE)rtn5					
Primer sense	Primer antisense	Annealing Temp.	Elongation Time	Number of Cycles	Ampified Splice Form
21	22	58 °C	120 sec	35	(DANRE)rtn5-a1
23	25	60 °C	50 sec	35	(DANRE)rtn5-a1/b
24	25	55 °C	45 sec	35	(DANRE)rtn5-c
(DANRE)rtn6					
Primer sense	Primer antisense	Annealing Temp.	Elongation Time	Number of Cycles	Ampified Splice Form
28	29	63 °C	60 sec	35	(DANRE)rtn6-a1
(DANRE)rtn8					
Primer sense	Primer antisense	Annealing Temp.	Elongation Time	Number of Cycles	Ampified Splice Form
30	32	59 °C	20 sec	35	(DANRE)rtn8-RHD
Actin					
Primer sense	Primer antisense	Annealing Temp.	Elongation Time	Number of Cycles	Ampified Splice Form
33	34	50 °C	90 sec	25	(DANRE)Actin

Supplementary Tabel 1C: *RT-PCR conditions*

Urochordate RTN					
Species	Gene	Transcript	GenBank Accession for newly identified RTN Genes	GenBank Accession for previously identified RTN Genes [a]	Published
Ciona intestinalis	(CIOIN)RTN			BK001680 (AY164660)	24
		(CIOIN)RTN-A1		BK001675 (AY164756)	24
		(CIOIN)RTN-A2		BK001674 (AY164755)	24
		(CIOIN)RTN-B1		BK001678 (AY164757)	24
		(CIOIN)RTN-B2		BK001677 (AY164760)	24
		(CIOIN)RTN-C1		BK001676 (AY164759)	24
		(CIOIN)RTN-C2		BK001679 (AY164758)	24
Vertebrate RTN					
Species	Gene	Transcript	GenBank Accession for newly identified RTN Genes	GenBank Accession for previously identified RTN Genes	Published
Homo sapiens	(HUMAN)RTN1			NT_025892, **AY164662**	1, 2, 24
		(HUMAN)RTN1-A		L10333, NM_021136.1	3
		(HUMAN)RTN1-B		L10334	3
		(HUMAN)RTN1-C		L10335, BC003003	3
	(HUMAN)RTN2			NT_011109, **AY164661**	4
		(HUMAN)RTN2-A1		BK001687 AF004222, **(AY164714)**	4, 24
		(HUMAN)RTN2-A2 (¢)		BK001690 (AY164717)	24
		(HUMAN)RTN2-B1		**BK001688 (AY164715)**	4, 24
		(HUMAN)RTN2-B2 (¢)		BK001691 (AY164718)	24
		(HUMAN)RTN2-C		BK001686 AF004224, **(AY164713)**	4, 24
		(HUMAN)RTN2-Δ8 (¢)		BK001689 (AY164716)	24
	(HUMAN)RTN3			NT_033241; NT_009984 (m)	5
		(HUMAN)RTN3-A1		BK001681 NM_006054, AF059524, **(AY164701)**	5, 24
		(HUMAN)RTN3-A2		BK001684 (AY164704)	24
		(HUMAN)RTN3-A3 (¢)		BK001683 (AY164703)	24
		(HUMAN)RTN3-Δ5 (¢)		BK001682 (AY164702)	24
		(HUMAN)RTN3-Δ8 (¢)		BK001685 (AY164705)	24
		(HUMAN)RTN3-A4		BK001696	
	(HUMAN)RTN3PS			NT_016606	5
	(HUMAN)RTN4			AY102285	6, 7, 8
		(HUMAN)RTN4-A		**AY102279**, AB020693, AB040462, AF148537	6, 7, 9, 10
		(HUMAN)RTN4-Aa		AY123245	6
		(HUMAN)RTN4-Ab		AY123246	6
		(HUMAN)RTN4-B1		**AY102277**, AB015639, AF132047, AF148538	6, 9, 10
		(HUMAN)RTN4-B2		AY102278	6
		(HUMAN)RTN4-C		**AY102276**, AF077050, AF087901	6, 9, 10, 11
		(HUMAN)RTN4-D		AY123247	6
		(HUMAN)RTN4-E		**AY123248**, AF333336	6, 12
		(HUMAN)RTN4-F		AY123249	6
		(HUMAN)RTN4-G		AY123250	6
Pan troglodytes	(PANTR)RTN1				
		(PANTR)RTN1w	BK003953		24
	(PANTR)RTN3				
		(PANTR)RTN3-A1	BK003954		24
	(PANTR)RTN4				
		(PANTR)RTN4-C	BK001700		24
Ateles belzebuth chamek	(ATEBE)RTN1				
		(ATEBE)RTN1-Aw		BK001692 AF029167, (AY164729)	24
Macaca mulatta	(MACMU)RTN1				
		(MACMU)RTN1-Cw	BK001697		24
	(MACMU)RTN3				
		(MACMU)RTN3w	BK003957		24
	(MACMU)RTN4				
		(MACMU)RTN4-Cw (Part1)	BK003948		24
		(MACMU)RTN4-Cw (Part2)	BK003949		24
Macaca fascicularis	(MACFA)RTN4				
		(MACFA)RTN4-Aw			13
		(MACFA)RTN4-C		BK001695 AB049853, (AY164742)	24
Mus musculus	(MOUSE)Rtn1			NW_000053	
		(MOUSE)Rtn1-a1		BK001694 AB074899, BC030455, **(AY164731)**	24
		(MOUSE)Rtn1-a2	BK001698		24
		(MOUSE)Rtn1-c		**BK001693**, AK002997, AK014358, XM_127007, **(AY164730)**	24
		(MOUSE)Rtn1-d	BK001699		24
	(MOUSE)Rtn2				14, 15
		(MOUSE)Rtn2-b		BK001789 NM_013648, (AY164711)	14, 24
		(MOUSE)Rtn2-c		BK001790 NM_013648, (AY164712)	14, 24
	(MOUSE)Rtn3			NW_000139	16
		(MOUSE)Rtn3-a1		NM_053076, **AY164700**	24
		(MOUSE)Rtn3-a2		BK001796 (AY164699)	24
		(MOUSE)Rtn3-a4		BK003955	24
	(MOUSE)Rtn4			**AY102286**, NW_000035	6
		(MOUSE)Rtn4-a		AY102284	6
		(MOUSE)Rtn4-b1		AY102281	6
		(MOUSE)Rtn4-b2		AY102282	6
		(MOUSE)Rtn4-c		**AY102283**, NM_024226	6
		(MOUSE)Rtn4-d		AY102280	6

Rattus norvegicus	(RAT)Rtn1				
		(RAT)Rtn1-a		NM_053865.1, U17604, **AY164728**	17, 18, 24
		(RAT)Rtn1-c		U17603, X52817, **AY164727**	17, 18, 19, 24
	(RAT)Rtn2				
		(RAT)Rtn2-B		BK001788 (AY164710)	24
	(RAT)Rtn3				
		(RAT)Rtn3-a1		AY164698	24
	(RAT)Rtn4				
		(RAT)Rtn4-a		AJ242961	20
		(RAT)Rtn4-b1		AJ242962, AF132046, **AY164740**	20, 24
		(RAT)Rtn4-b2		AF132045, **AY164741**	24
		(RAT)Rtn4-c		AJ242963, AF051335	11, 20
Bos taurus	(BOVIN)RTN1				
		(BOVIN)RTN1-Cw		AY164734	24
		(BOVIN)RTN1-Cw (Part1)		BK003967	24
		(BOVIN)RTN1-Cw (Part2)		BK003968	24
	(BOVIN)RTN2				
		(BOVIN)RTN2-B	BK001798		24
		(BOVIN)RTN2-C		BK001791 (AY164719)	24
	(BOVIN)RTN3				
		(BOVIN)RTN3		BK001797 (AY164707)	24
	(BOVIN)RTN4				
		(BOVIN)RTN4-C		AY164744	21, 24
Sus scrofa	(PIG)RTN1				
		(PIG)RTN1w (#)		BK001792 (AY164726)	24
	(PIG)RTN2				
		(PIG)RTN2-Aw		BK001798 (AY164709)	24
		(PIG)RTN2-C		BK001787 (AY164708)	24
	(PIG)RTN3				
		(PIG)RTN3-A1	BK003952		24
	(PIG)RTN4				
		(PIG)RTN4-Aw		AY164739	24
		(PIG)RTN4-Aw (Part1)		BK003964	24
		(PIG)RTN4-Aw (Part2)		BK003965	24
		(PIG)RTN4-Aw (Part3)		BK003966	24
		(PIG)RTN4-C		BK001795 (AY164739)	24
Canis familiaris	(CANFA)RTN1				
		(CANFA)RTN1-Aw		BK001794 (AY164733)	24
		(CANFA)RTN1-C		BK001793 (AY164732)	24
	(CANFA)RTN3				
		(CANFA)RTN3w		AY164706	24
		(CANFA)RTN3w (Part1)		BK003961	24
		(CANFA)RTN3w (Part2)		BK003962	24
		(CANFA)RTN3w (Part3)		BK003963	24
	(CANFA)RTN4				
		(CANFA)RTN4-Cw		AY164743	24
		(CANFA)RTN4-Cw (Part1)		BK003959	24
		(CANFA)RTN4-Cw (Part2)		BK003960	24
Capra hircus	(CAPHI)RTN3				
		(CAPHI)RTN3w (Part1)	BK003950		24
		(CAPHI)RTN3w (Part2)	BK003951		24
Ovis aries	(SHEEP)RTN3				
		(SHEEP)RTN3-A1w	BK003956		24
	(SHEEP)RTN4				
		(SHEEP)RTN4w	BK003958		24
Gallus gallus	(CHICK)RTN1				
		(CHICK)RTN1-A	AY164724	U17606, **AY164724**	18, 24
		(CHICK)RTN1-C	AY164723	U17605, **AY164723**	18, 24
	(CHICK)RTN3				
		(CHICK)RTN3w	BK044006	(AY164697	24
	(CHICK)RTN4				
		(CHICK)RTN4-Aw			22
		(CHICK)RTN4-B1	BK004061		24
		(CHICK)RTN4-B2	BK004062		24
		(CHICK)RTN4-C	AY164737	AY164737	22, 24
Columba livia	(COLLI)RTN1				
		(COLLI)RTN1w		BK004009 (AY164725)	24
Xenopus laevis	(XENLA)RTN1.1				
		(XENLA)RTN1.1-C		BK004007 (AY164721)	24
	(XENLA)RTN1.2				
		(XENLA)RTN1.2-C	BK004058		24
	(XENLA)RTN2				
		(XENLA)RTN2-A	BK004978		24
		(XENLA)RTN2-C	BK004977		24
	(XENLA)RTN3.1				
		(XENLA)RTN3.1		BK004012 (AY164749)	24
	(XENLA)RTN3.2				
		(XENLA)RTN3.2	BK004057		24
	(XENLA)RTN4-1				
		(XENLA)RTN4.1-A1		AY316197	23
		(XENLA)RTN4.1-A2		AY316196	23
		(XENLA)RTN4.1-A3		AY316195	23
		(XENLA)RTN4.1-B1		AY316194	23
		(XENLA)RTN4.1-B2		AY316193	23
		(XENLA)RTN4.1-C		AY316192	23
		(XENLA)RTN4.1-N		AY316191	23

	(XENLA)RTN4-2				
		(XENLA)RTN4.2-A1		AY316190	23
		(XENLA)RTN4.2-A2		AY316189	23
		(XENLA)RTN4.2-A3		AY316188	23
		(XENLA)RTN4.2-B1		AY316187	23
		(XENLA)RTN4.2-B2		AY316186	23
		(XENLA)RTN4.2-B3		AY316185	23
		(XENLA)RTN4.2-C		AY316184	23
		(XENLA)RTN4.2-N		AY316183	23
Silurana tropicalis	(XENTR)RTN1				
		(XENTR)RTN1-Aw		BK004008 (AY164722)	24
	(XENTR)RTN2				
		(XENTR)RTN2-A	BK005003		24
		(XENTR)RTN2-C	BK005002		24
	(XENTR)RTN3				
		(XENTR)RTN3		BK004013 (AY164750)	24
	(XENTR)RTN4				
		(XENTR)RTN4-A1w (Part1)	BK004063		24
		(XENTR)RTN4-A1w (Part2)	BK004064		24
		(XENTR)RTN4-B1		BK004011 (AY164736)	24
		(XENTR)RTN4-B2	BK004059		24
		(XENTR)RTN4-C	BK004060		24
		(XENTR)RTN4-N		BK004010 (AY164735)	24
Carassius auratus	(CARAU)RTN3				
		(CARAU)RTN3w		AY164748	24
	(CARAU)RTN4				
		(CARAU)RTN4-M		AY164754	22, 24
Danio rerio	(DANRE)*rtn1*				
		(DANRE)*rtn1-a1*	AY555034		
		(DANRE)*rtn1-a2*	AY555035		
		(DANRE)*rtn1-c*	AY555036	BC052753	25
	(DANRE)*rtn2*				
		(DANRE)*rtn2-c*	AY576807		
	(DANRE)*rtn3*			BC049315, BC062828	
		(DANRE)*rtn3-a1*	AY555037		
		(DANRE)*rtn3-a2*	AY555038		
	(DANRE)*rtn4*				
		(DANRE)*rtn4-l*	AY555039		
		(DANRE)rtn4-l(-10/195)	AY555040		
		(DANRE)rtn4-l(-63/188)	AY555041		
		(DANRE)*rtn4-m*	AY555042		
		(DANRE)*rtn4-n*	AY555043		
	(DANRE)*rtn5*				
		(DANRE)*rtn5-a1*	AY555044		
		(DANRE)*rtn5-a2*	AY555049		
		(DANRE)rtn5-a1(265-1584)	AY555046		
		(DANRE)rtn5-a1(297-2025)	AY555045		
		(DANRE)rtn5-a1(309-2025)	AY555047		
		(DANRE)rtn5-a1(558-1048)	AY555048		
		(DANRE)*rtn5-c*	AY555050	BC059623	25
	(DANRE)*rtn6*				
		(DANRE)*rtn6-a1*	AY555051		
		(DANRE)*rtn6-a2*	AY555062		
		(DANRE)*rtn6-a3*	AY555063		
		(DANRE)rtn6-a1(337/555)	AY555052		
		(DANRE)rtn6-a1(1576/1860)	AY555053		
		(DANRE)rtn6-a1(1761/2150)	AY555054		
		(DANRE)rtn6-a1(1773/2152)	AY555055		
		(DANRE)rtn6-a1(1774/2212)	AY555056		
		(DANRE)rtn6-a1(1775/2140)	AY555057		
		(DANRE)rtn6-a1(1775/2152)	AY555058		
		(DANRE)rtn6-a1(1775/2344)	AY555059		
		(DANRE)rtn6-a1(1777/1956)	AY555060		
		(DANRE)rtn6-a1(2023/2173)	AY555061		
	(DANRE)*rtn8*				
		(DANRE)*rtn8-c*	AY555064		
Takifugu rubripres	(FUGRU)RTN1			CAAB01001184	
		(FUGRU)rtn1-a1	AY555026		
	(FUGRU)RTN2				
		(FUGRU)rtn2c	AY555027		
	(FUGRU)RTN3			CAAB01002936	
		(FUGRU)rtn3-a1	AY555028	BK005087 (AY164745)	24
	(FUGRU)RTN4			CAAB01004137	
		(FUGRU)rtn4-l1	AY555029		
		(FUGRU)rtn4-l2	AY555030		
		(FUGRU)rtn4-l3	AY555031		
		(FUGRU)rtn4-n	AY555032	BK005090 (AY164753)	24
	(FUGRU)RTN7				
		(FUGRU)rtn7w	BK005143		
	(FUGRU)RTN8				
		(FUGRU)rtn8c	AY555033		
Ictalurus punctatus	(ICTPU)RTN1				
		(ICTPU)RTN1-C		BK005086 (AY164720)	24
	(ICTPU)RTN2				
		(ICTPU)RTN2w	BK004979		24
	(ICTPU)RTN5				
		(ICTPU)RTN5-Aw		BK005089 (AY164752)	24
		(ICTPU)RTN5-Bw		BK005102 (AY164751)	24

Paralichthys olivaceus	(PAROL)RTN3				
		(PAROL)RTN3	BK005088	(AY164746)	24
Oncorhynchus mykiss	(ONCMY)RTN1				
		(ONCMY)RTN1-C		BK005100 (AY262105)	24
	(ONCMY)RTN2*1				
		(ONCMY)RTN2*1	BK004983		24
	(ONCMY)RTN2*2				
		(ONCMY)RTN2*2	BK004982		24
	(ONCMY)RTN3				
		(ONCMY)RTN3-A1		BK004987 (AY262104)	24
		(ONCMY)RTN3-A2		BK005101 (AY262103)	24
	(ONCMY)RTN4				
		(ONCMY)RTN4-L	BK004986		24
		(ONCMY)RTN4-Mw		BK005093 AY262101	24
		(ONCMY)RTN4-N	BK004985		24
	(ONCMY)RTN7				
		(ONCMY)RTN7		BK005092 (AY262100)	24
	(ONCMY)RTN8				
		(ONCMY)RTN8w	BK004981		24
	(ONCMY)RTN9				
		(ONCMY)RTN9-A1	BK005094		24
		(ONCMY)RTN9-A2		BK005095 (AY262102)	24
	(ONCMY)RTN10				
		(ONCMY)RTN10-N	BK004984		24
	(ONCMY)RTN11				
		(ONCMY)RTN11	BK004980		24
Oncorhynchus tshawytscha	(ONCTS)RTN1				
		(ONCTS)RTN1w	BK004991		24
Salmo salar	(SALSA)RTN1				
		(SALSA)RTN1w (part1)	BK004997		24
		(SALSA)RTN1w (part2)	BK004996		24
	(SALSA)RTN3				
		(SALSA)RTN3w	BK004995		24
	(SALSA)RTN4				
		(SALSA)RTN4-M	BK004993		24
	(SALSA)RTN7				
		(SALSA)RTN7w	BK004994		24
	(SALSA)RTN10				
		(SALSA)RTN10W	BK004992		24
Coregonus clupeaformis	(CORCL)RTN1				
		(CORCL)RTN1w	BK005001		24
Cyprinus carpio	(CYPCA)RTN1				
		(CYPCA)RTN1-C		BK005091 (AY262099)	24
	(CYPCA)RTN3				
		(CYPCA)RTN3w	BK004976		24
	(CYPCA)RTN4				
		(CYPCA)RTN4-N		BK005098 (AY262098)	24
	(CYPCA)RTN5				
		(CYPCA)RTN5w	BK004975		24
	(CYPCA)RTN6				
		(CYPCA)RTN6		BK005097 (AY262097)	24
Gasterosteus aculeatus	(GASAC)RTN1				
		(GASAC)RTN1w	BK004990		24
	(GASAC)RTN3				
		(GASAC)RTN3-A1	BK004989		24
		(GASAC)RTN3-A2	BK004988		24
Oryzias latipes	(ORYLA)RTN1				
		(ORYLA)RTN1-C		BK005096 (AY262096)	24
	(ORYLA)RTN2				
		(ORYLA)RTN2	BK005000		24
	(ORYLA)RTN3				
		(ORYLA)RTN3w		BK005099 (AY164747)	24
	(ORYLA)RTN4				
		(ORYLA)RTN4w (part1)	BK004999		24
		(ORYLA)RTN4w (part2)	BK004998		24

Supplementary Tabel 1D: *Gene Bank accession numbers of vertebrate rtn genes*

[a] older accession numbers (in brackets) have been replaced by new third party annoation numbers (blue, bold)

(1) Roebroek et al., 1996
(2) Kools et al., 1994
(3) Roebroek et al., 1993
(4) Roebroek et al., 1998
(5) Moreira et al., 1999
(6) Oertle et al., 2003
(7) Yang et al., 2000
(8) Nagase et al., 1998
(9) GrandPré et al., 2000
(10) Prinjha et al., 2000
(11) Morris et al., 1999
(12) Zhang et al., 2002
(13) Barske et al., unpublished
(14) Geisler et al., 1992
(15) Stubbs et al., 1996
(16) Hamada et al., 2002
(17) Baka et al., 1996
(18) Ninkina et al., 1997
(19) Wieczorek and Hughes, 1992
(20) Chen et al., 2000
(21) Spillmann et al., 1998

(22) Simonen, M.; Lecoq, E.; Leiteritz, D., unpublished (23) Klinger et al., 2004
(24) Oertle et al., 2003 (25) Strausberg et al., direct submission

	(DANRE)rtn1 versus (DANRE)rtn5	(DANRE)rtn1 versus (HUMAN)RTN1	(DANRE)rtn5 versus (HUMAN)RTN1
mean d_N ± SE	13.39 ± 1.66	11.94 ± 1.58	14.14 ± 1.70
mean d_S ± SE	57.55 ± 4.18	68.48 ± 3.91	71.18 ± 3.81
d_N/d_S	0.23	0.17	0.20

	(DANRE)rtn2 versus (DANRE)rtn8	(DANRE)rtn2 versus (HUMAN)RTN2	(DANRE)rtn8 versus (HUMAN)RTN2
mean d_N ± SE	39.10 ± 2.31	37.49 ± 2.31	45.17 ± 2.36
mean d_S ± SE	63.82 ± 3.90	69.23 ± 3.67	68.99 ± 3.68
d_N/d_S	0.61	0.54	0.65

	(DANRE)rtn4 versus (DANRE)rtn6	(DANRE)rtn4 versus (HUMAN)RTN4	(DANRE)rtn6 versus (HUMAN)RTN4
mean d_N ± SE	27.81 ± 2.19	18.21 ± 1.87	32.79 ± 2.29
mean d_S ± SE	57.29± 4.09	70.66 ± 3.85	69.40 ± 3.83
d_N/d_S	0.49	0.26	0.47

	(FUGRU)RTN2 versus (FUGRU)RTN8	(FUGRU)RTN2 versus (HUMAN)RTN2	(FUGRU)RTN8 versus (HUMAN)RTN2
mean d_N ± SE	39.45 ± 2.32	38.81 ± 2.35	41.76 ± 2.35
mean d_S ± SE	65.68 ± 3.82	62.25 ± 3.91	67.16 ± 3.69
d_N/d_S	0.60	0.62	0.62

	(FUGRU)RTN3 versus (FUGRU)RTN7	(FUGRU)RTN3 versus (HUMAN)RTN3	(FUGRU)RTN7 versus (HUMAN)RTN3
mean d_N ± SE	29.80 ± 2.20	22.58 ± 2.02	32.75 ± 2.27
mean d_S ± SE	76.20 ± 3.59	71.31 ± 3.83	68.69 ± 3.92
d_N/d_S	0.39	0.31	0.48

Supplementary Table 1E: *Rates of nonsynonymous substitutions per nonsynonymous site (d_N) and rates of synonymous substitutions per synonymous site (d_S) calculated for the RHD*

Supplementary Table 2A: Mapping data for the analysis of conserved syntenies between rtn1 in zebrafish and RTN1in human

Accession 5'EST Accession 3'EST [1]	Zebrafish LN54 LG	Zebrafish LN54 Marker Symbol	Human Chromosom	Human Position	Human Accession	Description
AW127896 AW115873	20 20	fi04e05	6	6q15 / ???	BAA91551 no significant result	C6orf166 chromosome 6 open reading frame 166
AI437041 AI415949	20 20	fb37b08	14 14	14q24.3 / 78,190 K	NP_036377 NP_036377	SNW1 SKI-interacting protein SNW1 SKI-interacting protein
NM_131081	20	cdh2	18	18q11.2 / 25,530 K	AAB22854	CDH2 cadherin 2, type 1, N-cadherin (neuronal)
AI626515 AI601430	20 20	fc11b08	8	8p23.1 / ???	NP_689779 no significant result	TDH L-threonine dehydrogenase
AW174194 AW171259	20 20	fi40c10	14	14q / 103,700 K	NP_001510 no significant result	BRF1 BRF1 homolog, subunit of RNA polymerase III transcription initiation factor IIIB (S. cerevisiae)
NM_180966	20	esr2a	14	14q / 62,740 K	AAD32580	ESR2 estrogen receptor 2 (ER beta)
	20	rtn1 [2]	14	14q21-q22 / 58,180 K		RTN1 reticulon 1
AI584923 AI584393	20 20	fb93a10	15	15q14 / 38,826 K	NP_077016 no significant result	MGC4504 hypothetical protein MGC4504
AI584766 AI584258	20 20	fb83b05*	14	14q23.3-31 / 75,920 K	NP_036243 no significant result	AHSA1 AHA1, activator of heat shock 90kDa protein ATPase homolog 1 (yeast)
BF718073 AW019715	20 20	fd56a12	15	15q13 / 25,930 K	NP_004658 no significant result	HERC2 hect domain and RLD 2
AI959375 AI957952	20 20	fd08g07	14	14q32.13 / 91,760 K	BAA96049 no significant result	FLJ10648 function unknown protein 1
AI883033 AI667222	20 20	fd14e12	14	14q31-q32 / 92,410 K	no significant result NP_057234	ASB2 ankyrin repeat and SOCS box-containing 2
AI397003 AI384710	20 20	fb08c11	6	6q24.1 / ???	CAB66619 no significant result	C6orf55 chromosome 6 open reading frame 55
AI626529 AI601442	20 20	fc11c10	1	1q23.1 / 156,529 K	NP_060293 no significant result	FLJ20442 hypothetical protein FLJ20442
AI437173 AI444341	20 20	fb38e12	15	15q15.1 / 38,585 K	NP_002866 no significant result	RAD51 RAD51 homolog (RecA homolog, E. coli) (S. cerevisiae)
AI584886 AI584886	20 20	fb92f04	6	6q14.1 / ???	XP_029179 no significant result	FILIP1 filamin A interacting protein 1
AI396883 AI384463	20 20	fb14g10	2	2p23 / 26,450 K	NP_000174 no significant result	HADHB hydroxyacyl-Coenzyme A dehydrogenase/3-ketoacyl-Coenzyme A thiolase/enoyl-Coenzyme A hydratase (trifunctional protein), beta subunit
AF072456	20	bmp2b*	20	20p12 / 6,702 K	NP_001191	BMP2 bone morphogenetic protein 2
AI588714 AI588267	20 20	fb98e10	14	14q24.3 / 73,610 K	NP_006818 no significant result	TMP21 transmembrane trafficking protein
BE201200	20	fk87c02	14	14q24.3 / 73,900 K	NP_569736	JDP2 jun dimerization protein 2

BE200559	20		14		NP_569736	JDP2 jun dimerization protein 2

Accession 5'EST Accession 3'EST [1]	Zebrafish T51 LG	Zebrafish T51 Marker Symbol	Human Chromosom	Human Position	Human Accession	Description
AW077677	20	fj36b10	14	14q31.1 / 79,650 K	NP_056943	GTF2A1 general transcription factor IIA, 1,19/37kDa
AW077677	20		14	14q31.1 / 79,650 K	NP_056943	GTF2A1 general transcription factor IIA, 1, 19/37kDa
NM_131459	20	pdgfra*	4	4q11-q13 / 54,980 K	NP_006197	PDGFRA platelet-derived growth factor receptor, alpha polypeptide
AI722747	20	fc31a09	4	4q12 / 56,127 K	NP_060945	TPARL TPA regulated locus
AI721687	20				no significant result	
AI964923	20	fc83b10	14	14q23.1 / 57,730 K	NP_055807	DAAM1 dishevelled associated activator of morphogenesis 1
AI943021	20				no significant result	
AI584766	20	fb83b05*	14	14q23.3-31 / 75,920 K	NP_036243	AHSA1 AHA1, activator of heat shock 90kDa protein ATPase homolog 1 (yeast)
AI584258	20				no significant result	
AI558934	20	fb78b08	14	14q32.33 / 103,453 K	NP_060425	CDCA4 cell division cycle associated 4
AI558282	20				no significant result	
AW305563	20				no significant result	
AW281997	20	fj60e07	14	14q24.3-q31 / 79,960 K	NP_005056	SEL1L sel-1 suppressor of lin-12-like (C. elegans)
AW184521	20	fj15d08	14	14q31 / 91,480 K	AAH03622	ITPK1 inositol 1,3,4-triphosphate 5/6 kinase
AW232178	20				no significant result	
AI545336	20	fb74a06	14	14q32.13 / 91,675 K	NP_786924	C14orf130 chromosome 14 open reading frame 130
AI545120	20				no significant result	
AW174563	20	fj05f09	14	14q32 / 91,385 K	P10645	CHGA chromogranin A (parathyroid secretory protein 1)
AW203029	20				no significant result	
NM_131337	20	sox11b*	2	2p25 / 5,842 K	NM_003108	SOX11 SRY (sex determining region Y)-box 11
NM_131370	20	acat2*	6	6q25.3-q26 / 160,025 K	AAH00408	ACAT2 acetyl-Coenzyme A acetyltransferase 2 (acetoacetyl Coenzyme A thiolase)
AI584923	20	fb93a10	15	15q14 / 38,826 K	NP_077016	MGC4504 hypothetical protein MGC4504
AI584393	20				no significant result	
AI585238	20	fb95h11	14	14q23 / 63,540K	AAH25685	MAX MAX protein
AI584586	20				no significant result	
AI722866	20	fc32f10	2	2p25.2 / 9,590K	AAH11654	CPSF3 cleavage and polyadenylation specific factor 3, 73kDa
AI722326	20				no significant result	
AI931020	20	fc76b10	15	15q13.2 / 32,050K	NP_078989	FLJ22557 hypothetical protein FLJ22557
AI884253	20				no significant result	
AW077569	20	fj35h03	2	2p24 / 8,920K	T43458	KIDINS220 likely homolog of rat kinase D-interacting substance of 220 kDa
AW077331	20				no significant result	
NM_173245	20	vps18	15	15q14-q15 / 38,770K	NP_536672	VPS18 vacuolar protein sorting protein 18
NM_131450	20	rrm2	2	2p25-p24 / 10,283K	NP_001025	RRM2 ribonucleotide reductase M2 polypeptide
NM_131228	20	e(r)	14	14q24.1 / 67,846K	NP_004441	ERH enhancer of rudimentary homolog (Drosophila)
AI477869	20	fb57a02	2	2p24.1 / 16,089K	CAA68678	MYCN v-myc myelocytomatosis viral related oncogene, neuroblastoma derived (avian)
AI477486	20				no significant result	
BM736060	20	TDsubC_2E1	6	6q24.3 / ???	NP_056093	SASH1 SAM and SH3 domain containing 1
BM736061	20		6	6q24.3 / ???	NP_056093	SASH1 SAM and SH3 domain containing 1
	20	wz11823	2	2p24-p23 / 21,200K	CAA28420	APOB apolipoprotein B (including Ag(x) antigen)
AI497503	20	fb60h05	4	4q28 / 155,966K	P02679	FGG fibrinogen, gamma polypeptide
AI522694	20				no significant result	
AI877943	20	fc55e01	8	8q22-q23 / 108,910K	NP_001559.1|	EIF3S6 eukaryotic translation initiation factor 3, subunit 6 48kDa
AI793875	20				no significant result	
not available						
AW077587	20	fj65a12	6	6q21 / 108,840K	NP_001446	FOXO3A forkhead box O3A
AW077358	20	fj34b10	2	2p23.1 / 26,690K	AAG12992	OTOF otoferlin
AW077137	20				no significant result	
	20	wz12780	1	1q23.3 / 166,540K	AAN23123	PACE-1 ezrin-binding partner PACE-1
AI794465	20	fc44g01	1	1q23.3 / 166,490K	NP_060656	FLJ10706 hypothetical protein FLJ10706
AI883270	20				no significant result	
AF506208	20	mcm3	6	6p12 / 52,140K	NP_002379	MCM3 MCM3 minichromosome maintenance deficient 3 (S. cerevisiae)

[1] only one accession number for cloned genes
[2] RTN1 radiation hybrid PCR result: 00000010000000000001010001000010000101000002100000001001000000000001000000200001000120000001001
LOD score = 13.4
* Woods et. al., 2000

Supplementary Table 2B: Mapping data for the analysis of conserved syntenies between rtn2 in zebrafish and RTN2 in human

Accession 5'EST Accession 3'EST [1]	Zebrafish LN54 LG	Zebrafish LN54 Marker Symbol	Human Chromosom	Human Position	Human Accession	Description
BE016623	15	fk66c02	3	3q25.32 / 159,708K	AAF82807	LXN latexin protein
BE016156	15		3	3q25.32 / 159,708K	AAF82807	LXN latexin protein
AW827061	15	fk57h10	3	3q22.1 / 134,853 K	AAH63001	SRPRB signal recognition particle receptor, B subunit
AW826781	15		3		AAH63001	SRPRB signal recognition particle receptor, B subunit
NM_131670	15	atp1b3b (fb13c07)	3	3q22-q23 / 142,940 K	NP_001670	ATP1B3 ATPase, Na+/K+ transporting, beta 3 polypeptide
AI496976	15	fb53f10	19	19q13.2 / 44,025K	BAB18649	HNRPL heterogeneous nuclear ribonucleoprotein L
AI497448	15		19		no significant result	
AI477906	15	fb57d05	19	19q13 / 44,072 K	NP_036369	SIRT2 sirtuin (silent mating type information regulation 2 homolog) 2 (S. cerevisiae)
AI477520	15		19		no significant result	
AI522601	15	fb60b03	19	19q13.3 / 52,943 K	AAH07248	GLTSCR2 glioma tumor suppressor candidate region gene 2

AI497098	15		19	19q13.3 / 52,943 K	AAH07248	GLTSCR2 glioma tumor suppressor candidate region gene 2
		rtn 2 [2]	19	19q13.32 / 50,686 K		RTN2 reticulon 2
AI331148	15	fb05d08	17	17q23.2 / 60,300K	CAB66646	VMP1 likely ortholog of rat vacuole membrane protein 1
AI330892	15				no significant result	

Accession 5'EST Accession 3'EST [1]	Zebrafish T51 LG	Zebrafish T51 Marker Symbol	Human Chromosom	Human Position	Human Accession	Description
AI585206	15	fb95e09	17	17q23.2 / 57,800 K	NP_872375	FLJ37451 hypothetical protein FLJ37451
AI584556	15				no significant result	
AI545363	15	fb74d01	7	7q11.22 / 65,990 K	AAH15591	FLJ10900 hypothetical protein FLJ10900
AI545141	15				no significant result	
AW280776	15	fj45g03	17	17p13.3 / 659 K	NP_057164	CGI-150 CGI-150 protein
AW279847	15		17	17p13.3 / 659 K	NP_057164	CGI-150 CGI-150 protein
	15	tcf2	17	17cen-q21.3 / 36,270 K	NP_000449	TCF2 transcription factor 2, hepatic; LF-B3; variant hepatic nuclear factor
AW281708	15	fj53g11	17	17q11.2 / 27,103 K	XP_371036	KIAA0100 KIAA0100 gene product
AW281348	15				no significant result	
AI522601	15	fb60b03	19	19q13.3 / 52,943 K	AAH07248	GLTSCR2 glioma tumor suppressor candidate region gene 2
AI497098	15		19	19q13.3 / 52,943 K	AAH07248	GLTSCR2 glioma tumor suppressor candidate region gene 2
AI477906	15	fb57d05	19	19q13 / 44,072 K	NP_036369	SIRT2 sirtuin (silent mating type information regulation 2 homolog) 2 (S. cerevisiae)
AI477520	15				no significant result	
AI331661	15	fa99f01	19	19q13.3-q13.4 / 55,090 K	AAH64378	IL4I1 interleukin 4 induced 1
AI331619	15				no significant result	
AI444403	15	fb38a08	19	19q13.41 / 57,403 K	NP_055040	PPP2R1A protein phosphatase 2 (formerly 2A), regulatory subunit A (PR 65), alpha isoform
AI437123	15				no significant result	
AI546048	15	fb77e08	17	17p13.3 / 2,810 K	AAH63786	KIAA0664 KIAA0664 protein
AI544670	15				no significant result	
AW133613	15	fi09d09	17	17p13.3 / 2,570 K	AAH50603	MGC3329 hypothetical protein MGC3329
AW116121	15		17	17p13.3 / 2,570 K	AAH50603	MGC3329 hypothetical protein MGC3329
AI546041	15	fb77d11	17	17p13.3 / 500 K	AAK27973	FLJ10979 hypothetical protein FLJ10979
AI544668	15				no significant result	

[1] only one accession number for cloned genes
[2] RTN2 radiation hybrid PCR result: 10100100000000000000002120200010000000000100000011000000000000010110000102001000101001002101 1
LOD score = 13.4

Supplementary Table 2C: Mapping data for the analysis of conserved syntenies between rtn3 in zebrafish and RTN3 human

Accession 5'EST Accession 3'EST [1]	Zebrafish LN54 LG	Zebrafish LN54 Marker Symbol	Human Chromosom	Human Position	Human Accession	Description
AI496942	7	fb53c07	11	11q13.1 / 66,078 K	AAH00401	SF3B2 splicing factor 3b, subunit 2, 145kDa
AI497263	7		11	11q13.1 / 66,078 K	AAH00401	SF3B2 splicing factor 3b, subunit 2, 145kDa
AI558347	7	fb72a06	2	2p13.2-p13.3 / ???	NP_653183	TEX261 testis expressed gene 261
AI544537	7				no significant result	
AI722947	7	fc27g06	5	5q35.3 / ???	AAF67007	RNF130 ring finger protein 130
AI722468	7				no significant result	
AI657668	7	fc16a03	15	15q26.3 / 99,407 K	AAK15708	LOC55829 AD-015 protein
AI641466	7				no significant result	
AA497354	7	fa04g07	16	16p11.2 / 31,113 K	NP_005872	BCKDK branched chain alpha-ketoacid dehydrogenase kinase
AA497274	7				no significant result	
AI959182	7	fd07h02	15	15q21-q22 / 62,848 K	NP_057714	ACP33 acid cluster protein 33
AI957903	7				no significant result	
AI397205	7	fb06g09 [2]	11	11q13 / 61,964 K	NP_002023	FTH1 ferritin, heavy polypeptide 1
AI385072	7				NP_002023	FTH1 ferritin, heavy polypeptide 1
AF212919	7	men1**	11	11q13 / 64,825 K	NP_570711	MEN1 multiple endocrine neoplasia I
AW174010	7	fi38c09	11	11p13 / 31,700 K	NP_061913	ELP4 elongation protein 4 homolog (S. cerevisiae)
AW171173	7				no significant result	
AI882683	7	fb15b04	11	11p15.1 / 20,434 K	NP_006401	HTATIP2 HIV-1 Tat interactive protein 2, 30kDa
AI396618	7		11	11p15.1 / 20,434 K	NP_006401	HTATIP2 HIV-1 Tat interactive protein 2, 30kDa
	7	rtn3 [3]	11	11q13 / 63,740 K		RTN3 reticulon 3
AI657572	7	fc15c04	11	11p15.1 / 20,219 K	XP_061930	similar to Homeobox protein DBX1
AI641452	7		11	11p15.1 / 20,219 K	XP_061930	similar to Homeobox protein DBX1
AI722072	7	fd19a03	4	4p16.3 / 2,200 K	NP_078787	MGC4701 hypothetical protein MGC4701
AI722486	7		4	4p16.3 / 2,200 K	NP_078787	MGC4701 hypothetical protein MGC4701
AI332008	7	fa96d04	11	11q13.1 / 64,295 K	NP_004313	BAD BCL2-antagonist of cell death
AI330583	7				no significant result	
AI584984	7	fb93g04	X	Xq28 / 147,770 K	AAL86617	CD99L2 CD99 antigen-like 2
AI584442	7				no significant result	
AI657704	7	fc16d12	17	17p13.2 / ???	AAH32510	MGC49942 hypothetical protein MGC49942
AI641499	7		17	17p13.2 / ???	AAH32510	MGC49942 hypothetical protein MGC49942
AI721901	7	fc26h10	2	2p13.2 / 72,234 K	NP_063938	P450RAI-2 cytochrome P450 retinoid metabolizing protein
AI722415	7				no significant result	
AI657750	7	fc17a06 [4]	13	13q32 / 95,225 K	AAH33823	DNAJC3 DnaJ (Hsp40) homolog, subfamily C, member 3
AI641576	7				no significant result	

AW165381 AW165381	7 7	fe01c06	11	11q12.3 / 62,637 K	NP_036332 no significant result	B3GAT3 beta-1,3-glucuronyltransferase 3 (glucuronosyltransferase I)
AW174821 AW165225	7 7	fe06a10	14	14q11.2 / 21,536 K	AAD56725 no significant result	ACINUS apoptotic chromatin condensation inducer in the nucleus
AI626294 AI601857	7 7	fc12g04	1	1p36.13-q31.3 / 147,014 K	AAH08732 no significant result	APH-1A likely ortholog of C. elegans anterior pharynx defective 1A
AW128556 AW117040	7 7	fe17d05	16 16	16q22.1 / 70,020 K 16q22.1 / 70,020 K	NP_478126 NP_478126	MTR3 homolog of yeast mRNA transport regulator 3 MTR3 homolog of yeast mRNA transport regulator 3
BF717593 AW018955	7 7	fd47d02	11	11p15.3 / 9,016 K	NP_065695 no significant result	C11orf15 chromosome 11 open reading frame 15
no sequence available AI878766	7	fc66c05	11	11p15.2 / 14,530 K	AI878766	COPB coatomer protein complex, subunit beta
AI626516 AI601431	7 7	fc11b09	11 11	11p15 / 8,860 K 11p15 / 8,860 K	CAC35387 CAC35387	ST5 suppression of tumorigenicity 5 ST5 suppression of tumorigenicity 5

Accession 5'EST Accession 3'EST [1]	Zebrafish T51 LG	Zebrafish T51 Marker Symbol	Human Chromosom	Human Position	Human Accession	Description
AW175082 AW154742	7 7	fi32a10	1 1	1q42.13 / ??? 1q42.13 / ???	NP_775106 NP_775106	TGS TUDOR gene similar TGS TUDOR gene similar
	7	wz12563	4	4q32.3 / 171,510 K	BAA31601	KIAA0626 KIAA0626 gene product
AI558347 AI544537	7 7	fb72a06	2	2p13.2-p13.3 / ???	NP_653183 no significant result	TEX261 testis expressed gene 261
NM_131585	7	fth1** [2]	11	11q13 / 61,984 K	NM_002032	FTH1 ferritin, heavy polypeptide 1
AW233285 AW232790	7	fj30e04	11	11q12.3 / 61,456 K	NP_060311 no significant result	FLJ20487 hypothetical protein FLJ20487
AI584932 AI584400	7 7	fb93b07	15	15q22.2-q22.3 / 63,038 K	NP_006651 no significant result	CLPX ClpX caseinolytic protease X homolog (E. coli)
AI882683 AI396618	7 7	fb15b04	11 11	11p15.1 / 20,434 K 11p15.1 / 20,434 K	NP_006401 NP_006401	HTATIP2 HIV-1 Tat interactive protein 2, 30kDa HTATIP2 HIV-1 Tat interactive protein 2, 30kDa
AF212919	7	men1**	11	11q13 / 64,825 K	NP_570711	MEN1 multiple endocrine neoplasia I
AI722815 AI722283	7 7	fc32a02	17	17p11.2 / 17,110 K	NP_003644 no significant result	COPS3 COP9 constitutive photomorphogenic homolog subunit 3 (Arabidopsis)
AW154045 AW154581	7 7	fi29g02	11	11q12-q13.1 / 62,612 K	NP_004730 no significant result	MTA1L1 metastasis-associated 1-like 1
AI942769 AI884210	7 7	fc75e01	17	17p11-p13 / 7,068 K	NP_000009 no significant result	ACADVL acyl-Coenzyme A dehydrogenase, very long chain
NM_131630	7	prkri [4]	13	13q32 / 95,220 K	NP_006251	DNAJC3 DnaJ (Hsp40) homolog, subfamily C, member 3
AI878151 AI878428	7 7	fc58a11	12 12	12q14.3 / 69,704 K 12q14.3 / 69,704 K	NP_006422 NP_006422	CCT2 chaperonin containing TCP1, subunit 2 (beta) CCT2 chaperonin containing TCP1, subunit 2 (beta)
AW305645 AW282070	7 7	fj61g07	7 7	7q22 / 99,902 K 7q22 / 99,902 K	NP_005828 NP_005828	RPP20 POP7 (processing of precursor, S. cerevisiae) homolog RPP20 POP7 (processing of precursor, S. cerevisiae) homolog
AW419738 AW420537	7	fj82g07	14 14	14q11.1 / 19,963 K 14q11.1 / 19,963 K	AAB71850 AAB71850	METTL3 methyltransferase like 3 METTL3 methyltransferase like 3
AI626516 AI601431	7 7	fc11b09	11 11	11p15 / 8,860 K 11p15 / 8,860 K	CAC35387 CAC35387	ST5 suppression of tumorigenicity 5 ST5 suppression of tumorigenicity 5

[1] only one accession number for cloned genes
[2] fb06g09 (LN54) and fth1 (T51) represent the same gene
[3] RTN3 radiation hybrid PCR result: 00001000000000000000000000000000000000000000000000000000000010010000000000000100010100000000000
[4] fc17a06 (LN54) and prkri (T51) represent the same gene
LOD score = 15.9
** Yoder et. Litman, 2000

Supplementary Table 2D: Mapping data for the analysis of conserved syntenies between rtn4 in zebrafish and RTN4 human

Accession 5'EST Accession 3'EST [1]	Zebrafish LN54 LG	Zebrafish LN54 Marker Symbol	Human Chromosom	Human Position	Human Accession	Description
not available BE017380	6	fk75d08	22	22q13.1 / 33,990 K	Q9UGU5	HMG2L1 high-mobility group protein 2-like 1
AW174737 AW165160	6 6	fe02h09	20 20	20q11.21 / 32,969 K 20q11.21 / 32,969 K	NP_009169 NP_009169	PXMP4 peroxisomal membrane protein 4, 24kDa PXMP4 peroxisomal membrane protein 4, 24kDa
AI384762 AI397219	6 6	fb17a02*	2	2p13-p14 / 55,190 K	NP_008939 no significant result	RTN4 reticulon 4
AI588654 AI588215	6 6	fb97g10	14	14q11.1 / 19,540 K	BAB84883 no significant result	FLJ10357 hypothetical protein FLJ10357
AW019441 AW059314	6 6	fe11e12	2	2q31.1 / 172,890 K	BAA09486 no significant result	TLK1 tousled-like kinase 1
AI883574 AI878772	6 6	fc66d05	13	13q22.1 / 78,860 K	BAB55125 no significant result	C13orf10 chromosome 13 open reading frame 10
	6	rtn4 [2]	2	2p13-p14 / 55,190 K		RTN4 reticulon 4
AI416175 AI522470	6 6	fb19b11	12	12q13 / 56,220 K	NP_006182 no significant result	PA2G4 proliferation-associated 2G4, 38kDa
BF717955 AW019545	6 6	fd54d02	12	12q13.11 / 49,034 K	NP_057678 no significant result	FKBP11 FK506 binding protein 11, 19 kDa
NM_131286	6	sox21*	13	13q31-q32 / 94,210 K	NP_009015	SOX21 SRY (sex determining region Y)-box 21
AI416205 AI522481	6 6	fb19f01	19 19	19p13.2-p13.3 / 11,533K 19p13.2-p13.3 / 11,533K	P13686 P13686	ACP5 acid phosphatase 5, tartrate resistant ACP5 acid phosphatase 5, tartrate resistant
AW133793 AW128209	6 6	fi11h08	19	19p13.1 / 15,385 K	BAB55234 no significant result	WIZ widely-interspaced zinc finger motifs
AI437237 AI444529	6 6	fb39c08	2	2q32-q33 / 192,668 K	NP_004648 no significant result	SDPR serum deprivation response (phosphatidylserine binding protein)

AA494577	6				no significant result	
AA494670	6	fa10c06	2	2q33.3 / 204,100 K	AAG09681	CYP20A1 cytochrome P450, family 20, subfamily A, polypeptide 1
AI883564	6	fc66b09	2	2q31.1 / 174,990 K	NP_037473	PTD004 hypothetical protein PTD004
AI878763	6				NP_037473	
AW174122	6	fi39e04	2	2q33.2 / 203,650 K	NP_612477	LOC130026 hypothetical protein BC000993
AW171348	6				no significant result	
BF717616	6	fd47f07	13	13q33-q34 / 98,210 K	NP_005064	SLC15A1 solute carrier family 15 (oligopeptide transporter), member 1
AW018970	6				no significant result	
AI416096	6	fb33h05	2	2q33-q34 / 206,970 K	AAH22368	NDUFS1 NADH dehydrogenase (ubiquinone) Fe-S protein 1, 75kDa (NADH-coenzyme Q reductase)
AI437455	6		2		AAH22368	NDUFS1 NADH dehydrogenase (ubiquinone) Fe-S protein 1, 75kDa (NADH-coenzyme Q reductase)
AI722248	6	fd20h08	2	2q12 / 106,070 K	O43639	NCK2 NCK adaptor protein 2
AI721455	6				no significant result	

Accession 5'EST Accession 3'EST [1]	Zebrafish T 51 LG	Zebrafish T 51 Marker Symbol	Human Chromosom	Human Position	Human Accession	Description
AW595289	6	fk30b04	22	22q13.1 / 38,160 K	AAH16855	ATF4 activating transcription factor 4 (tax-responsive enhancer element B67)
AW566985	6		22	22q13.1 / 38,160 K	AAH16855	ATF4 activating transcription factor 4 (tax-responsive enhancer element B67)
AI558981	6	fb78g05	4	4q35.1 / 185,190 K	AAH22185	FLJ12716 hypothetical protein FLJ12716
AI558325	6		4	4q35.1 / 185,190 K	AAH22185	FLJ12716 hypothetical protein FLJ12716
AW174737	6	fe02h09	20	20q11.21 / 32,969 K	NP_009169	PXMP4 peroxisomal membrane protein 4, 24kDa
AW165160	6		20	20q11.21 / 32,969 K	NP_009169	PXMP4 peroxisomal membrane protein 4, 24kDa
AI384191	6	fb17f11*	2	2q31.1 / 170,626 K	I37989	SSB Sjogren syndrome antigen B (autoantigen La)
AI397239	6				no significant result	
AW171070	6	fi37a09	2	2q31.1 /170,430 K	NP_004783	PPIG peptidyl-prolyl isomerase G (cyclophilin G)
AW173843	6				no significant result	
AW019441	6	fe11e12	2	2q31.1 / 172,890 K	BAA09486	TLK1 tousled-like kinase 1
AW059314	6				no significant result	
AW202751	6	fj21g01	2	2q33 / 202,240 K	NP_055864	ALS2CR3 amyotrophic lateral sclerosis 2 (juvenile) chromosome region, candidate 3
AW232545	6		2	2q33 / 202,240 K	NP_055864	ALS2CR3 amyotrophic lateral sclerosis 2 (juvenile) chromosome region, candidate 3
AW567512	6	fk28d02	2	2q31.1 / 172,540 K	NP_001369	DNCI2 dynein, cytoplasmic, intermediate polypeptide 2
AW595038	6				no significant result	
AW153485	6	fi22c04	22	22q13.1 / 35,000 K	NP_002464	MYH9 myosin, heavy polypeptide 9, non-muscle
AW154082	6		22	22q13.1 / 35,000 K	NP_002464	MYH9 myosin, heavy polypeptide 9, non-muscle
NM_131286	6	sox21*	13	13q31-q32 / 94,210 K	NP_009015	SOX21 SRY (sex determining region Y)-box 21
AI497023	6	fb59c03	2	2p14-p16 / 55,438 K	NP_002444	MTIF2 mitochondrial translational initiation factor 2
AI522554	6		2	2p14-p16 / 55,438 K	NP_002444	MTIF2 mitochondrial translational initiation factor 2
AI384762	6	fb17a02*	2	2p13-p14 / 55,190 K	NP_008939	RTN4 reticulon 4
AI397219	6				no significant result	
BM735955	6	tdsubc_1f2	2	2p16 / 55,419 K	AAA36788	RPS27A ribosomal protein S27a
AA494577	6				no significant result	
AA494670	6	fa10c06	2	2q33.3 / 204,100 K	AAG09681	CYP20A1 cytochrome P450, family 20, subfamily A, polypeptide 1
AI416129	6	fb18c11	13	13q12.2-q13.3 / 47,360 K	NP_003841	SUCLA2 succinate-CoA ligase, ADP-forming, beta subunit
AI397474	6				no significant result	
NM_131445	6	chrna1	2	2q24-q32 / 175,585 K	NP_000070	CHRNA1 cholinergic receptor, nicotinic, alpha polypeptide 1 (muscle)
AW342883	6	fj80c12	2	2q31 / 176,790 K	BAB21806	KIAA1715 KIAA1715 protein
AW420343	6				no significant result	

[1] only one accession number for cloned genes
[2] RTN4 radiation hybrid PCR result: 00001100000000000000000011000011100000111110111001000000100200000000000100221000000111001000 0
LOD score = 11.6
* Woods et. al., 2000

Supplementary Table 2E: Mapping data for the analysis of conserved syntenies between rtn6 and rtn5 in zebrafish and RTN4 and RNT1 in human

Accession 5'EST Accession 3'EST [1]	Zebrafish LN54 LG	Zebrafish LN54 Marker Symbol	Human Chromosom	Human Position	Human Accession	Description
AW078165	13	fe25d09	11	11p13 / 34,140 K	NP_005889	M11S1 membrane component, chromosome 11, surface marker 1
AW059113	13		11	11p13 / 34,140 K	NP_005889	M11S1 membrane component, chromosome 11, surface marker 1
AI477555	13	fb58g07	10	10q21-q22 / 73,490 K	NP_002769	PSAP prosaposin (variant Gaucher disease and variant metachromatic leukodystrophy)
AI477669	13				no significant result	
AI601645	13	fc02e11	2	2p13-p14 / 66,680 K	NP_002389	MEIS1 Meis1, myeloid ecotropic viral integration site 1 homolog (mouse)
AI588472	13		2	2p13-p14 / 66,680 K	NP_002389	MEIS1 Meis1, myeloid ecotropic viral integration site 1 homolog (mouse)
AI601614	13	fc02b11	6	6p21.1 / 43,170 K	AAH02879	PARC p53-associated parkin-like cytoplasmic protein
AI588448	13				no significant result	
AI629244	13	fc10c06	6	6q27 / 167,189 K	NP_003721	RNASE6PL ribonuclease 6 precursor
AI601360	13				no significant result	
AI626149	13	fc06f04	3	3q23 / 143,190 K	NP_689989	MGC40579 hypothetical protein MGC40579
AI626469					no significant result	
AI626134	13	fc06e01	2	2p22.3 / 38,520 K	AAM97342	ARL6IP2 ADP-ribosylation-like factor 6 interacting protein 2
AI626460	13		2		no significant result	
AI584783	13	fb83c11	10	10q22 / 71,530 K	NP_542996	COL13A1 collagen, type XIII, alpha 1
AI584271	13				no significant result	
BG985848	13	ibd5135	2	2p21 / 47,190 K	XP_031626	TTC7 tetratricopeptide repeat domain 7
BG985849	13		2	2p21 / 47,190 K	XP_031626	TTC7 tetratricopeptide repeat domain 7

BF717669	13	fd50d08	2	2p21 / 47,094 K	NP_644808	SDNSF multiple coagulation factor deficiency protein 2
AW019194	13		2	2p21 / 47,094 K	NP_644808	SDNSF multiple coagulation factor deficiency protein 2
AW777712	13	fk49e09	10	10q25-q26 / 121,064 K	NP_006784	PRDX3 peroxiredoxin 3
AW778453	13		10	10q25-q26 / 121,064 K	NP_006784	PRDX3 peroxiredoxin 3
AI722119	13	fd19e06	X	Xq26.1 / 127,574 K	BAA90894	HT011 uncharacterized hypothalamus protein HT011
AI722533	13		X	Xq26.1 / 127,574 K	BAA90894	HT011 uncharacterized hypothalamus protein HT011
AW133840	13	fi12d12	1	1q44 / 241,040 K	AAH04485	PNAS-4 CGI-146 protein
AW116199	13				no significant result	
AI476830	13	fb50g11	10	10q22 / 76,873 K	P45880	VDAC2 voltage-dependent anion channel 2
AI477233	13		10	10q22 / 76,873 K	P45880	VDAC2 voltage-dependent anion channel 2
AI497423	13	fb62d04	14	14q32 / 101,980 K	NP_001814	CKB creatine kinase, brain
AI522785	13		14		no significant result	
AI584922	13	fb93a09	2	2q13 / 113,170 K	NP_714923	MGC46235 hypothetical protein MGC46235
AI584392	13				no significant result	
AW116409	13	fi15c03	10	10q26 / 120,950 K	NP_003741	EIF3S10 eukaryotic translation initiation factor 3, subunit 10 theta, 150/170kDa
AW134149	13		10	10q26 / 120,950 K	NP_003741	EIF3S10 eukaryotic translation initiation factor 3, subunit 10 theta, 150/170kDa
AW018508	13	fd58h04	10	10q25.1 / 106,152 K	NP_004823	GSTTLp28 glutathione-S-transferase like; glutathione transferase omega
AW019036	13				no significant result	
not available						
AW116140	13	fi09f10	2	2p16.1 / 60,690 K	NP_075044	BCL11A B-cell CLL/lymphoma 11A (zinc finger protein)
AI658312	13	fc21e02	10	10q22 / 70,990 K	NP_000179	HK1 hexokinase 1
AI641247					no significant result	
AW128798	13	fe37e06	10	10q22.1 / 70,847 K	NP_003162	SUPV3L1 suppressor of var1, 3-like 1 (S. cerevisiae)
AW128298	13				no significant result	
not available						
AW019477	13	fd52b02	10	10pter-q25.3 / 69,960 K	NP_071412	MAWBP MAWD binding protein
NM_131621	13	bmpr1a*	10	10q22.3 / 88,730 K	AAH28383	BMPR1A bone morphogenetic protein receptor, type IA
AI722246	13	fd20h06	6	6q27 / 170,548 K	NP_003185	TBP TATA box binding protein
AI721453	13				no significant result	
AI437278	13	fb39g06	10	10q11-q24 / 76,050 K	AAH03568	ADK adenosine kinase
AI444479	13				no significant result	
BE201264	13	fk89a06	10	10q24.3 / 105,950 K	NP_000485	COL17A1 collagen, type XVII, alpha 1
BE200663	13				no significant result	
AI629316	13	fc10e09 [3]	6	6q24 / 138,665 K	NP_055135	HEBP2 heme binding protein 2
AI601384	13				no significant result	
NM_131281	13	fgf8*	10	10q24 / 103,664 K	NP_006110	FGF8 fibroblast growth factor 8 (androgen-induced)
NM_131184	13	pax2a*	10	10q22.1-q24.3 / 102,860 K	NP_000269	PAX2 paired box gene 2
AI385024	13	fb14b12	10	10q22.2 / 71,795 K	AAH16840	MGC34695 hypothetical protein MGC34695
AI396797	13		10	10q22.2 / 71,795 K	AAH16840	MGC34695 hypothetical protein MGC34695
AW173999	13	fi38b10	10	10q22.2 / 73,997 K	NP_060096	DNAJB12 DnaJ (Hsp40) homolog, subfamily B, member 12
AW171164	13				no significant result	
AW174378	13	fi42e02	10	10q24.32 / 104,319 K	CAC08403	MGC2491 hypothetical protein MGC2491
AW171502	13				no significant result	
AI416105	13	fb18a04	14	14q / 33,172 K	NP_068733	CFL2 cofilin 2 (muscle)
AI397450	13		14	14q / 33,172 K	NP_068733	CFL2 cofilin 2 (muscle)
BF717718	13	fd50h11	14	14q32.12-q32.13 / 91,275 K	AAH23021	GOLGA5 golgi autoantigen, golgin subfamily a, 5
AW019226	13		14	14q32.12-q32.13 / 91,275 K	AAH23021	GOLGA5 golgi autoantigen, golgin subfamily a, 5
AI331561	13	fa94c12	14	14q23.1 / 59,490 K	NP_722518	SLC38A6 solute carrier family 38, member 6
AI332252	13				no significant result	
AW127891	13	fi04d12	2	2p23.2 / 32,130 K	NP_057039	CGI-27 C21orf19-like protein
AW115868	13		2		no significant result	
AW115968	13	fi05f05	1	1q32.3-q41 / 206,652 K	NP_055203	DJ434O14.5 novel putative protein similar to YIL091C yeast hypothetical 84 kD protein from SGA1-KTR7
AW127998	13		1	1q32.3-q41 / 206,652 K	NP_055203	DJ434O14.5 novel putative protein similar to YIL091C yeast hypothetical 84 kD protein from SGA1-KTR7
AI416084	13	fb33g03	15	15q14 / 39,320 K	NP_055953	KIAA0252 KIAA0252 protein
AI437443	13				no significant result	
AI658310	13	fc21d12	6	6q21 / 107,361 K	NP_057571	HSPC230 HSPC230 gene
AI641245	13				no significant result	
AI545712	13	fb75d02	20	20p11 / 14,259 K	NP_037413	FLRT3 fibronectin leucine rich transmembrane protein 3
AI544469	13				no significant result	
not available						
AI959634	13	fd12b09	13	13q12.2 / 26,947 K	NP_690876	MTIF3 mitochondrial translational initiation factor 3
AI331318	13	fa98g05	14	14q32.1 / 91,180 K	Q99538	LGMN legumain
AI331432	13				no significant result	
AI331273	13	fa97c03	14	14q22.2 / 52,939 K	NP_004115	GMFB glia maturation factor, beta
AI332203	13				no significant result	
AI558679	13	fb79b10 / btaf1	10	10q22-q23 / 93,870 K	NP_003963	BTAF1 BTAF1 RNA polymerase II, B-TFIID transcription factor-associated, 170kDa (Mot1 homolog, S. cerevisiae)
AI558448	13				no significant result	
AI721792	13	fd16d11	6	6p21 / ???	CAC01626	BTBD9 BTB (POZ) domain containing 9
AI666911	13				no significant result	
AI476860	13	fb51h12	1	1p34.3 / 32,272 K	BAB13825	FLJ10276 hypothetical protein FLJ10276
AI477319	13				no significant result	

Accession 5'EST Accession 3'EST [1]	Zebrafish T 51 LG	Zebrafish T 51 Marker Symbol	Human Chromosom	Human Position	Human Accession	Description
AW174924	13	fi30c07	10	10q21 / 70,622 K	NP_004719	DDX21 DEAD/H (Asp-Glu-Ala-Asp/His) box polypeptide 21
AW174924	13		10	10q21 / 70,622 K	NP_004719	DDX21 DEAD/H (Asp-Glu-Ala-Asp/His) box polypeptide 21
AI331027	13	fb04e08	1	1q42.1 / 220,500 K	NP_005417	TP53BP2 tumor protein p53 binding protein, 2
not abailable						

	13	rtn6 [2]	2	2p13-p14		RTN4 reticulon 4
BI896341	13	fc45e02	6	6q23.3 / 137,749 K	NP_786923	OLIG3 oligodendrocyte transcription factor 3
AI793378	13				no significant result	
AI877794	13	fc51f06	6	6q27 / 170,528 K	NP_002784	PSMB1 proteasome (prosome, macropain) subunit, beta type, 1
AI793686	13		6	6q27 / 170,528 K	NP_002784	PSMB1 proteasome (prosome, macropain) subunit, beta type, 1
not abailable						
AW466851	13	fk08d06	6	6p12.1 / 52,853 K	NP_001503	GSTA4 glutathione S-transferase A4
AI477555	13	fb58g07	10	10q21-q22 / 73,490 K	NP_002769	PSAP prosaposin (variant Gaucher disease and variant metachromatic leukodystrophy)
AI477669	13				no significant result	
AW165395	13	fe01e01	2	2p23.3 / 27,575 K	NP_002698	PPM1G protein phosphatase 1G (formerly 2C), magnesium-dependent, gamma isoform
AW165098	13				no significant result	
AW153634	13	fi24a01	10	10q22.2 / 74,440 K	NP_612366	LOC90550 hypothetical protein BC010682
AW154215	13				no significant result	
AW422923	13	fi49h02	10	10q24.32 / 104,049 K	NP_004732	NOLC1 nucleolar and coiled-body phosphoprotein 1
AW343783	13				no significant result	
NM_131261	13	ret1	10	10q11.2 / 43,370 K	NP_066124	RET ret proto-oncogene (multiple endocrine neoplasia and medullary thyroid carcinoma 1, Hirschsprung disease)
NM_131632	13	atoh7	10	10q22.1 / 69,883 K	NP_660161	ATOH7 atonal homolog 7 (Drosophila)
AW202834	13	fj22g12*	10	10pter-q26.12 / 105,340 K	NP_057000	LOC51063 hypothetical protein LOC51063
AW232659	13				no significant result	
not available						
AW116140	13	fi09f10	2	2p16.1 / 60,690 K	NP_075044	BCL11A B-cell CLL/lymphoma 11A (zinc finger protein)
AI883708	13	fc69a12 [3]	6	6q24 / 138,665 K	NP_055135	HEBP2 heme binding protein 2
AI942864	13				no significant result	
NM_131281	13	fgf8*	10	10q24 / 103,664 K	NP_006110	FGF8 fibroblast growth factor 8 (androgen-induced)
U10870	13	wnt8b*	10	10q24 / 102,365 K	BAB83924	WNT8B wingless-type MMTV integration site family, member 8B
NM_131184	13	pax2a*	10	10q22.1-q24.3 / 102,860 K	NP_000269	PAX2 paired box gene 2
AI385024	13	fb14b12	10	10q22.2 / 71,795 K	AAH16840	MGC34695 hypothetical protein MGC34695
AI396797	13		10	10q22.2 / 71,795 K	AAH16840	MGC34695 hypothetical protein MGC34695
AI626716	13	fc07e07	14	14q21-q22 / 58,180 K	NP_066959	RTN1 reticulon 1
AI601500	13				no significant result	
	13	rtn5 [4]	14	14q21-q22 / 58,180 K		RTN1 reticulon 1
not available						
AW154524	13	fi28b08	14	14q23.1 / 59,433 K	XP_050793	KIAA1393 KIAA1393 protein 14q23.1
AI877807	13	fc51g08	1	1q32.3-q41 / ???	NP_055203	DJ434O14.5 novel putative protein similar to YIL091C yeast hypothetical 84 kD protein from SGA1-KTR7
AI793697	13		1	1q32.3-q41 / ???	NP_055203	DJ434O14.5 novel putative protein similar to YIL091C yeast hypothetical 84 kD protein from SGA1-KTR7
	13	wz13526	6	6q21 / 107,361 K	NP_057571	HSPC230 HSPC230 gene
AI416084	13	fb33g03	15	15q14 / 39,320 K	NP_055953	KIAA0252 KIAA0252 protein
AI437443	13				no significant result	
AI545826	13	fb76a01	15	15q14 / 39,230 K	AAH24772	ANKT nucleolar protein ANKT
AI544503	13				no significant result	
AW175072	13	fi31h12	1	1p34.3 / 31,980 K	NP_060526	FLJ10315 hypothetical protein FLJ10315
AW154733	13		1	1p34.3 / 31,980 K	NP_060526	FLJ10315 hypothetical protein FLJ10315
not available						
AW343665	13	fi47f03	14	14q / 103,700 K	NP_001510	BRF1 BRF1 homolog, subunit of RNA polymerase III transcription initiation factor IIIB (S. cerevisiae)
AW595735	13	fk33c03	15	15q11.2-q21.3 / 39,266 K	Q9Y375	CIA30 CGI-65 protein
AW567099	13		15	15q11.2-q21.3 / 39,266 K	Q9Y375	CIA30 CGI-65 protein
AI558898	13	fb67g02	11	11q23 / 116,726 K	P06727	APOA4 apolipoprotein A-IV
AI544768					no significant results	
AW280593	13	fj43a10	14	14q24.1 / 66,143 K	AAH26274	RDH11 retinol dehydrogenase 11 (all-trans and 9-cis)
AW279672	13				no significant result	
	13	wz12332	14	14q24.1 / 66,220 K	BAA20779	ZFYVE26 zinc finger, FYVE domain containing 26
AI877953	13				no significant result	
AI793885	13	fc55f03	20	20p11.21 / 23,753 K	NP_001313	CST2 cystatin SA 20p11.21
AI331318	13	fa98g05	14	14q32.1 / 91,180 K	Q99538	LGMN legumain
AI331432	13				no significant result	

[1] only one accession number for cloned genes
[2] RTN6 radiation hybrid PCR result: 00000000000010000000020000001000010000000001100000111000000010010000100000000010000000000200001
[3] fc10e09 (LN54) and fc69a12 (T51) represent the same gene
[4] RTN5 radiation hybrid PCR result: 00000000000010010000000000000010000100000000000000000000011000000000001000000010001000000000000001
LOD score rtn5 = 8.3
LOD score rtn6 = 13.6
* Woods et. al., 2000

Supplementary Table 2F: Mapping data for the analysis of conserved syntenies between rtn8 in zebrafish and RTN2 in human

Accession 5'EST Accession 3'EST [1]	Zebrafish LN54 LG	Zebrafish LN54 Marker Symbol	Human Chromosom	Human Position	Human Accession	Description
AI416271	21	fb18g12	10	10q11.21 / ???	NP_055568	BMS1L BMS1-like, ribosome assembly protein (yeast)
AI522356	21				no significant result	
BE016964	21	fk71g05	4	4q21.22 / 78,441 K	NP_006826	CCNI cyclin I
BE016321	21			4q21.22 / 78,441 K	NP_006826	CCNI cyclin I
BE556775	21	fk95d02	9	9q34.13 / 125,023 K	BAA11486	KIAA0169
BE201579	21		9	9q34.13 / 125,023 K	BAA11486	KIAA0169
BE016557	21	fk65b10	9	9q34 / 133,834 K	NP_057118	MRPS2 mitochondrial ribosomal protein S2
BE016089	21		9	9q34 / 133,834 K	NP_057118	MRPS2 mitochondrial ribosomal protein S2
BE556816	21	fk91a03	4	4q21.22 / 78,541 K	AAH32518	CCNG2 cyclin G2
BE200769	21		4	4q21.22 / 78,541 K	AAH32518	CCNG2 cyclin G2
not available						
AA658637	21	fa55b05	4	4q21.22 / 78,276 K	XP_293687	hypothetical LOC345079
AF003943	21	celip	9	9q34.3 / 131,218 K	AAB35488	CEL carboxyl ester lipase (bile salt-stimulated lipase)

not available AA605859	21	fa20e05	9	9q33-q34 / 126,730 K	AAB41498	SPTAN1 spectrin, alpha, non-erythrocytic 1 (alpha-fodrin)
NM_131112	21	pou5f1/spg	6	6p21.31 / 31,239 K	NM_131112	POU5F1 POU domain, class 5, transcription factor 1
AI588748 AI588293	21 21	fb98h11	12 12	12q24.33 / 130,897 K 12q24.33 / 130,897 K	AAD21042 AAD21042	PUS1 pseudouridylate synthase 1 PUS1 pseudouridylate synthase 1
AI522462 AI397441	21 21	fb22d05	2	2q21.2 / 131,017 K	BAA92656 no significant result	FLJ20297 hypothetical protein FLJ20297
AI397201 AI385069	21 21	fb06g05	12 12	12q24 / 109,346 K 12q24 / 109,346 K	NP_057310 NP_057310	VPS29 vacuolar protein sorting 29 (yeast) VPS29 vacuolar protein sorting 29 (yeast)
NM_131758	21	epb72 *	9	9q34.1 / 119,493 K	NM_004099	STOM stomatin
AI794078 AI667139	21 21	fc38b04	9	9q34 / 131,070 K	NP_000359 no significant result	TSC1 tuberous sclerosis 1
AI657880 AI641410	21 21	fc14f10 [3]	11	11q23.1 / 111,453 K	NP_001922 no significant result	DLAT dihydrolipoamide S-acetyltransferase (E2 component of pyruvate dehydrogenase complex)
AW128712 AW117142	21 21	fe36e01	11	11q22.2 / 101,312 K 11q22.2 / 101,312 K	AAO38749 AAO38749	ANGPTL5 angiopoietin-like 5 ANGPTL5 angiopoietin-like 5
AI437383 AI416013	21 21	fb30h11	11	11q25 / 133,520 K	AAK27221 no significant result	JAM3 junctional adhesion molecule 3
		rtn 8 [2]	19	19q13.32 / 50,686 K		RTN2 reticulon 2
BE016985 BE016345	21 21	fk72d03	11 11	11q13.3 / 73,650 K	NP_057231 no significant result	PME-1 protein phosphatase methylesterase-1
BE556794 BE201598	21 21	fk95f07 [4] *	11 11	11p15.5 / 4,047 K 11p15.5 / 4,047 K	AAD37491 AAD37491	RRM1 ribonucleotide reductase M1 polypeptide RRM1 ribonucleotide reductase M1 polypeptide
AA495399 AA495322	21 21	fa01c01	11	11q13.1 / 65,546 K	NP_003851 no significant result	BANF1 barrier to autointegration factor 1
NM_131338	21	bf	6	6p21.3 / 32,021 K	AAH04143	BF B-factor, properdin
AI396667 AI384806	21 21	fb08e11	11 11	11q13 / 63,862 K	NP_857635 NP_857635	PRDX5 peroxiredoxin 5
AW059432 AW058939	21 21	fe14a07	11 11	11q13 / 62,415 K	P08195 P08195	SLC3A2 solute carrier family 3 (activators of dibasic and neutral amino acid transport), member 2 SLC3A2 solute carrier family 3 (activators of dibasic and neutral amino acid transport), member 2

Accession 5'EST Accession 3'EST [1]	Zebrafish T 51 LG	Zebrafish T 51 Marker Symbol	Human Chromosom	Human Position	Human Accession	Description
not available AA605745	21	fa18f04	22	22q11.23 / 23,284 K	NP_004166	SNRPD3 small nuclear ribonucleoprotein D3 polypeptide 18kDa
not available AA605859	21	fa20e05	9	9q33-q34 / 126,730 K	AAB41498	SPTAN1 spectrin, alpha, non-erythrocytic 1 (alpha-fodrin)
NM_131112	21	pou5f1/spg	6	6p21.31 / 31,239 K	NM_131112	POU5F1 POU domain, class 5, transcription factor 1
AW127732 AW115560	21 21	fj97b11	5 5	5p13 / 36,213 K 5p13 / 36,213 K	NP_005974 NP_005974	SKP2 S-phase kinase-associated protein 2 (p45) SKP2 S-phase kinase-associated protein 2 (p45)
AW174919 AW154617	21 21	fi30c01 *	19	19q13.1 / 45,926 K	BAA22524 no significant result	ITPKC inositol 1,4,5-trisphosphate 3-kinase C 19q13.1
AW128712 AW117142	21 21	fe36e01	11	11q22.2 / 101,312 K 11q22.2 / 101,312 K	AAO38749 AAO38749	ANGPTL5 angiopoietin-like 5 ANGPTL5 angiopoietin-like 5
not available AW343662	21 21	fi47e11	11	11q23.3 / 116,169 K	NP_116114	MGC13125 hypothetical protein MGC13125
AI965099 AI943209	21 21	fc86g11 [3]	11	11q23.1 / 111,453 K	NP_001922 no significant result	DLAT dihydrolipoamide S-acetyltransferase (E2 component of pyruvate dehydrogenase complex)
AW153341 AW116759	21 21	fi19e09	11 11	11pter-p15.5 / ??? 11pter-p15.5 / ???	CAA12176 CAA12176	ALG8 asparagine-linked glycosylation 8 homolog (yeast, alpha-1,3-glucosyltransferase) ALG8 asparagine-linked glycosylation 8 homolog (yeast, alpha-1,3-glucosyltransferase)
NM_131338	21	bf	6	6p21.3 / 32,021 K	AAH04143	BF B-factor, properdin
AI396667 AI384806	21 21	fb08e11	11 11	11q13 / 63,862 K	NP_857635 NP_857635	PRDX5 peroxiredoxin 5
AI497216 AI497552	21 21	fb63b04 *	15	15q22-qter / 72,761 K	AAA35738 no significant result	CYP1A2 cytochrome P450, family 1, subfamily A, polypeptide 2
AI584662 AI545474	21 21	fb81g12	11	11q12.3 / 62,362 K	NP_003155 no significant result	STX5A syntaxin 5A
AI626218 AI601826	21 21	fc12d06 *	11	11q12-q13 / 62,431 K	no significant result NP_006353	NXF1 nuclear RNA export factor 1
AI722645 AI721597	21 21	fc29g12	5	5q31.3 / 139,074 K	NP_057547 no significant result	HSPC195 hypothetical protein HSPC195
AI722697 AI721642	21 21	fc30d10	18	18 B2 / 36,914 K	NP_653324 no significant result	2610510D14Rik RIKEN cDNA 2610510D14 gene
AW059432 AW058939	21 21	fe14a07	11 11	11q13 / 62,415 K	P08195 P08195	SLC3A2 solute carrier family 3 (activators of dibasic and neutral amino acid transport), member 2 SLC3A2 solute carrier family 3 (activators of dibasic and neutral amino acid transport), member 2
NM_131455	21	rrm1 [4] *	11	11p15.5 / 4,047 K	AAD37491	RRM1 ribonucleotide reductase M1 polypeptide
	21	wz10483	5	5q33.3 / 156,294 K	NP_612388	LOC91937 hypothetical protein BC008988

[1] only one accession number for cloned genes
[2] RTN8 radiation hybrid PCR result: 00110000000000000010001110000010111101000000000000100100100100110000000000000000011010001010 1
[3] fc14f10 (LN54) and fc86g11 (T51) represent the same gene
[4] fk95f07 (LN54) and rrm1 (T51) represent the same gene
LOD score = 11.0
* Woods et. al., 2000

Supplementary Table 2G: Mapping data for the analysis of conserved syntenies between RTNs in fugu and mammals (FUGRU)RTN1

Fugu Scaffold	Fugu Position [a]	Ense. Peptide ID	Description	Human Chr	Human Position [a]	Mouse Chr	Mouse Position [a]	Rat Chr	Rat Position [a]
188	3	SINFRUP00000132119.1	AMBIGUOUS	14	58,564	12	67,183	6	94,852

188	16	SINFRUP00000132121.1	ADP RIBOSYLATION STRUCTURE CONTAINING	14	5,843	12	67,113	6	94,772
188	31	SINFRUP00000132124.1	RTN1	14	5,819	12	66,867	6	94,415
188	56	SINFRUP00000132133.1	KNSL7	3	44,809	9	123,275	n.d.r.	
188	63	SINFRUP00000132136.1	TACC3	4	1,696	5	31,927	14	82,754
188	69	SINFRUP00000132138.1	FGFRL1	4	1,002	n.d.r.		n.d.r.	
188	92	SINFRUP00000132142.1	Q9HCC9	4	2,307	5	32,517	14	82,244
188	103	SINFRUP00000132143.1	AMBIGUOUS	n.d.r.		5	32,587	n.d.r.	
188	104	SINFRUP00000132144.1	AMBIGUOUS	n.d.r.		5	32,587	n.d.r.	
188	113	SINFRUP00000132145.1	MRPL35	2	86,407	n.d.r.		4	105,352
188	117	SINFRUP00000132146.1	NM_022912	2	86,477	14	61,006	4	105,306
188	121	SINFRUP00000132147.1	NM_016079	2	86,735	18	6,539	4	105,079
188	126	SINFRUP00000132148.1	OS94_HUMAN	4	129,187	3	40,583	2	127,674
188	132	SINFRUP00000132152.1	STK18	4	129,269	3	40,624	2	127,719
188	144	SINFRUP00000132155.1	ITPK1	14	91,482	12	96,587	6	126,907
188	154	SINFRUP00000132157.1	C14orf130	14	91,674	12	96,782	6	127,044
188	162	SINFRUP00000132160.1	NM_018167	14	91,743	12	96,847	6	127,085
188	186	SINFRUP00000132162.1	AMBIGUOUS	n.d.r.		n.d.r.		6	127,367
188	192	SINFRUP00000132167.1	Q9P2D8	14	92,108	12	97,151	6	127,444
188	212	SINFRUP00000132173.1	NM_138344	14	92,383	12	97,331	6	127,609
188	214	SINFRUP00000132174.1	ASB2	14	92,402	12	97,345	6	127,626
188	225	SINFRUP00000132175.1	C14orf137	14	92,492	12	97,41	6	127,697
188	227	SINFRUP00000132176.1	DDX24	14	92,522	12	97,43	6	127,711
188	231	SINFRUP00000132179.1	SERPINA10	14	92,743	12	97,635	6	127,941
188	235	SINFRUP00000132183.1	MJD	14	90,541	12	95,953	6	126,216
188	244	SINFRUP00000132192.1	UBR1	15	41,033	2	122,547	3	107,609
188	259	SINFRUP00000132195.1	AMBIGUOUS	n.d.r.		n.d.r.		6	137,352

(FUGRU)RTN2

Fugu Scaffold	Fugu Position [a]	Ense. Peptide ID	Description	Human Chr	Human Position [a]	Mouse Chr	Mouse Position [a]	Rat Chr	Rat Position [a]
257	30	SINFRUP00000130858.1	GRLF1	19	52,155	n.d.r.		1	76,842
257	67	SINFRUP00000130860.1	AP2S1	19	52,039	7	11,399	1	77,153
257	106	SINFRUP00000130868.1	RTN2	19	50,686	7	0,013	1	78,731
257	114	SINFRUP00000130872.1	PPM1A	19	50,695	n.d.r.		1	78,721
257	128	SINFRUP00000130879.1	PTGIR	19	51,817	7	11,561	1	77,313
257	141	SINFRUP00000130883.1	AMBIGUOUS	19	51,801	7	11,573	6	124,486
257	141	SINFRUP00000130883.1	CALM2	19	51,801	7	11,573	1	77,325
257	141	SINFRUP00000130883.1	AMBIGUOUS	2	47,37	7	11,573	1	77,325
257	146	SINFRUP00000130886.1	KCNK12	2	47,747	n.d.r.		6	124,178
257	168	SINFRUP00000130889.1	GEMIN7	19	50,28	7	14,009	1	1,51
257	210	SINFRUP00000130898.1	Q8IWK3	19	50,315	7	13,98	1	1,527
257	225	SINFRUP00000130901.1	MRPL28	16	0,358	17	24,815	10	15,396
257	231	SINFRUP00000130904.1	RELB	19	50,214	7	14,06	1	78,998
257	237	SINFRUP00000130907.1	CLPTM1	19	50,169	7	14,092	1	79,033

(FUGRU)RTN3

Fugu Scaffold	Fugu Position [a]	Ense. Peptide ID	Description	Human Chr	Human Position [a]	Mouse Chr	Mouse Position [a]	Rat Chr	Rat Position [a]
346	11	SINFRUP00000140880.1	CD99L2	X	148,641	X	55,663	n.d.r.	
346	57	SINFRUP00000140896.1	Q8N8M0	7	100,378	n.d.r.		n.d.r.	
346	68	SINFRUP00000140901.1	NM_018978	11	124,063	9	37,593	n.d.r.	
346	99	SINFRUP00000140908.1	ING1L	4	185,125	n.d.r.		16	47,789
346	107	SINFRUP00000140913.1	AMBIGUOUS	n.d.r.		7	115,412	1	185,996
346	109	SINFRUP00000140914.1	Q9H3K6	16	29,503	7	115,414	1	185,999
346	124	SINFRUP00000140875.1	SF1 or PYGL	11	64,314	19	4,302	1	209,311
346	119	SINFRUP00000140917.1	PYGM	11	64,296	19	4,281	1	209,332
346	139	SINFRUP00000140921.1	RBM4	11	66,214	19	5,921	1	207,521
346	154	SINFRUP00000140925.1	MAP4K2	11	64,339	19	4,324	1	209,286
346	161	SINFRUP00000140929.1	MEN1	11	64,35	19	4,335	1	209,276
346	166	SINFRUP00000140930.1	RTN3	11	63,263	19	3,642	1	210,296
346	189	SINFRUP00000140937.1	NM_016581	19	11,489	n.d.r.		8	21,184
346	196	SINFRUP00000140938.1	MTA1L1	11	62,14	19	8,09	1	211,781

(FUGRU)RTN4

Fugu Scaffold	Fugu Position [a]	Ense. Peptide ID	Description	Human Chr	Human Position [a]	Mouse Chr	Mouse Position [a]	Rat Chr	Rat Position [a]
2616	3	SINFRUP00000127275.1	RTN4	2	55,213	11	29,875	14	110,775

(FUGRU)RTN7

Fugu Scaffold	Fugu Position [a]	Ense. Peptide ID	Description	Human Chr	Human Position [a]	Mouse Chr	Mouse Position [a]	Rat Chr	Rat Position [a]
3887	1	SINFRUP00000142114.1	RTN7	(11) [b]	63,263	n.d.r.		n.d.r.	
3887	3	SINFRUP00000142116.1	GEMIN6	2	38,981	17	78,861	6	3,128

(FUGRU)RTN8

Fugu Scaffold	Fugu Position [a]	Ense. Peptide ID	Description	Human Chr	Human Position [a]	Mouse Chr	Mouse Position [a]	Rat Chr	Rat Position [a]
2117	12	SINFRUP00000163874.1	CENTD2	11	72,136	n.d.r.		1	158,977
2117	24		RTN8 [c]	(19) [d]	50,686	n.d.r.		n.d.r.	

[a] positions are given in kilobasepairs
[b] position of RTN3 on human chromosom 11 was not retrieved from ensembl Martview, but from NCBI locuslink
[c] RTN8 was not annoated autamically by ensemble peptide prediction and therefore did not recieve an Ense. Peptide ID
[d] position of RTN2 on human chromosom 19 was not retrieved from ensembl Martview, but from NCBI locuslink
n.d.r. = no data retrieved with ensembl MartView

Supplementary Table 2 A-G: *Mapping data for the analyses of conserved syntenies between zebrafish and human and between fugu and human, with respect to rtns.*

(DANRE)rtn1

Exon Nr	3' splice site	5' splice site	aa at the exon border Zebrafish rtn1	exon size (bp) Zebrafish rtn1	intron size (bp) Zebrafish rtn1 [d]	aa at the exon border Human RTN1	exon size (bp) Human RTN1	intron size (bp) Human RTN1
I(a)		GCT TCC ACA G gtaatgcgat Ala Ser Thr	G/AT Asp	>391 [a] (223)	>20,000 [e]	G/GT Gly	450 (241)	125,244
II	tctcatgcag AT AAA TCA AC Lys Ser Thr	CCC CCT ACA G gtgagcatca Pro Pro Thr	G/AA Glu	720	3,216	G/AA Glu	774	18,039
III	ttcttaatag AA GAC TCT GAA Asp Ser Glu	AGG GAG AAA G gtaaatgcat Arg Glu Lys	G/CA Ala	795	>61,000 [e]	G/CT Ala	750	119,422
I (c)		AAG TGC CAG G gtaatgtgag Lys Cys Gln	G/CA Ala	>211 [f] (73)	>48,000 [e]	G/CT Ala	359 (61)	22,946
IV (4) [c]	ctgtatccag CA ATG GAG CTG Met Glu Leu	CAT CCC TTC AA gtatgacttc His Pro Phe	AA/A Lys	208	85	AA/G Lys	208	1,778
V (5) [c]	ctggatacag A GTG TAT CTG Val Tyr Leu	TCG CTA AAG gttgaagcct Ser Leu Lys	AAG/TTT Lys/Phe	139	2,126	AAA/TTT Lys/Phe	139	1,446
VI (6) [c]	ttcactctag TTT GCA GTC Phe Ala Val	CTT ATT ATG G gtgagaagca Leu Ile Met	G/TG Val	70	95	G/CT Ala	70	593
VII (7) [c]	ctttcttcag TG GTG GTG TGC Val Val Cys	AAA TAC CAG gtcagagtgg Lys Tyr Gln	CAG/GCA Gln/Ala	47	100	CAG/GCA Gln/Ala	47	88
VIII (8) [c]	ttgtctccag GCA CAG ATC Ala Gln Ile	GTG GTA GCA AA gtaagcagtc Val Val Ala	AA/G Lys	59	1,220	AA/G Lys	59	6,277
IX (9) [c]	agctctcgag G ATC CAG GAG Ile Gln Glu			>1,098 [b] (43)			792 (43)	

Lower case letters are the intron sequence, upper case letters are the exon sequence at the intron-exon boundary. The 3' splice site (acceptor) is the boundary from the intron to the exon, the 5' splice site (donor) from the exon to the intron.
a = 223bp coding region and in addition at least 168 bp 5'UTR in the same exon
b = 43 bp coding region (including the stop codon) and addition 1055 bp of the 3'UTR in the same exon.
c = Number in brackets is the exon number of the corresponding human RTN1 gene.
d = Intron sizes were measured using long genomic clones (Ensembl sequence assembly).
e = This intron harbours NNN stretches. Therefore the real size may differ slightly.
f = 73 bp coding + 138 bp 5'UTR (upstream stop codon)

(DANRE)rtn2

Exon Nr	3' splice site	5' splice site	aa at the exon border Zebrafish rtn2	exon size (bp) Zebrafish rtn2	intron size (bp) Zebrafish rtn2 [d]	aa at the exon border Human RTN2	exon size (bp) Human RTN2	intron size (bp) Human RTN2
I(c)		AGC AGT AAA G gtgagggtaa Ser Ser Lys	G/TA Val	>78 [a] (13)	> 11,950 [e]	G/TG Val	>54 (13)	3,605
II (6) [c]	ctccctacag TA ATG GAC CTG Met Asp Leu	CAT CCC TTC CA gtgagtgtct His Pro Phe	CA/G Gln	208	1,902	CA/G Gln	208	359
III (7) [c]	tgtgctgcag G TCA TAT CTA Ser Tyr Leu	TCA CTC AAG gtgaggcctg Ser Leu Lys	AAG/TTC Lys/Phe	139	6,030	AAG/CTG Lys/Leu	139	141
IV (8) [c]	ttttccacag TTC TGG CTG Phe Trp Leu	ATC ATC ATC G gtaggatgca Ile Ile Ile	G/GT Gly	70	> 3, 840 [e]	G/GA Gly	70	119
V (9) [c]	ttattttcag GT GTG ATT GCA Val Ile Val	CGT CAC CAG gtaatatatc Arg His Gln	CAG/GAT Gln/Asp	47	455	CAG/GCT Gln/Ala	47	2,357
VI (10) [c]	tcatttacag GAT AAA GTG Asp Lys Val	ATC AAG GAC TT gtgagtacag Ile Lys Asp	TT/C Phe	59	189	AA/G Lys	59	265
VII (11) [c]	tgtcaaacag CTTT TAT CGC Phe Tyr Arg			>117 [b] (76)			496 (82)	

Lower case letters are the intron sequence, upper case letters are the exon sequence at the intron-exon boundary. The 3' splice site (acceptor) is the boundary from the intron to the exon, the 5' splice site (donor) from the exon to the intron.

a = 13 bp coding region and in addition at least 65 bp 5'UTR in the same exon
b = 76 bp coding region (including the stop codon) and in addition at least 117 bp 3'UTR in the same exon. The 3' UTR is not fully cloned.
c = Number in brackets is the exon number of the corresponding human RTN2 gene.
d = Intron sizes were measured using long genomic clones (Ensembl sequences assembly).
e = This intron harbours NNN stretches. Therefore the real size may differ slightly.

(DANRE)rtn3

Exon Nr	3' splice site	5' splice site	aa at the exon border Zebrafish rtn3	exon size (bp) Zebrafish rtn3	intron size (bp) Zebrafish rtn3 [d]	aa at the exon border Human RTN3	exon size (bp) Human RTN3	intron size (bp) Human RTN3
I(a)		AAG TTT TCC G gtaagacaac Lys Phe Ser	G/AT Asp	>250 [a] (94)	8,096	G/AT Asp	334 (142)	23,065
II	attttttccag AT Ser	TCC TTTTTT Phe Phe	TCT CCT CAA G gcaagtgtat Ser Leu Gln	G/TG Val	45	22,584	G/TG Val	57	45,081
III (5) [c]	tgtcatgcag TG CTG Asn	AAT GAC Asp Leu	CAC CCC TTC AA gtaagagtct His Pro Phe	AA/G Lys	208	3,577	AA/A Lys	208	2,305
IV (6) [c]	cctgtaacag G ATG Ala	GCT CTG Leu Met	TCC CTC AAG gtcagattta Ser Leu Lys	AAG/CTG Lys/Leu	139	125	AAG/CTG Lys/Leu	139	423
V (7) [c]	ctgctttcag Leu	CTG GCA GTT Ala Val	CTC ATC CTC G gtaggctttc Leu Ile Leu	G/CC Ala	70	102	G/CT Ala	70	523
VI (8) [c]	tgtttttcag CC CTG Asp	GAC ATC Ile Leu	AAA AAC AAG gtcagatata Lys Asn Lys	AAG/ACC Lys/Thr	47	3,333	AAG/ACC Lys/Thr	47	2,403
VII (9) [c]	tcttccacag Thr	ACC CAG ATT Gln Ile	ACA GTC GCG AA gtaagtctgc Thr Val Ala	AA/G Lys	59	3,772	AA/G Lys	59	1,985
VIII (10)[c]	ctccctcag G Leu	CTA CAA GAG Gln Glu			522 [b] (49)			1,735 (46)	

Lower case letters are the intron sequence, upper case letters are the exon sequence at the intron-exon boundary. The 3' splice site (acceptor) is the boundary from the intron to the exon, the 5' splice site (donor) from the exon to the intron.

a = 94 bp coding region and in addition at least 156 bp 5'UTR in the same exon
b = 49 bp coding region (including the stop codon) and addition 473 bp of the 3'UTR in the same exon. The 3' UTR is not fully cloned.
c = Number in brackets is the exon number of the corresponding human RTN3 gene.
d = Intron sizes were measured using long genomic clones (Ensembl sequence assembly).

(DANRE)rtn4

Exon Nr	3' splice site	5' splice site	aa at the exon border Zebrafish rtn4	exon size (bp) Zebrafish rtn4	intron size (bp) Zebrafish rtn4 [d]	aa at the exon border Human RTN4	exon size (bp) Human RTN4	intron size (bp) Human RTN4
I(l)		TCG TGC TCA T gtaagtaatt Ser Cys Ser	T/TG Leu	>609 [a] (403)	>14,620 [e]			
I(m)		AAA GAA CAG G gtatatgctt Lys Glu Gln	G/TG Val	>162 [f] (73)	>10,324 [e]			
I(n)		TCC AAA CAA G gttagttagt Ser Lys Gln	G/TG Val	>64 [g] (16)	4,703			
II (4) [c]	ttgtctccag TG CTG Val	GTG GAG Glu Leu	CAC CCT TTC AA gtgagagact His Pro Phe	AA/G Lys	208	2,803	AG/G Arg	208	4,838
III (5) [c]	cttctttcag G CTG Met	ATG TAC Tyr Leu	TCG CTC AAG gtttgtttgt Ser Leu Lys	AAG/TTT Lys/Phe	139	>8,000 [e]	AAG/TTT Lys/Phe	139	7,776
IV (6) [c]	TTT Phe	GCT GTT Ala Val	ATT ATT TTG G gtatgtctgt Ile Ile Leu	G/GT Gly	70	838	G/CT Ala	70	827
V (7) [c]	cttcctacag GT GGT Phe	TTC ATT Ile Gly	AAG CAT CAG gtaggtttgc Lys His Gln	CAG/GCA Gln/Ala	47	157	CAG/GCA Gln/Ala	47	199
VI (8) [c]	cctgatacag Ala	GCA CAA ATT Gln Ile	GTT GTG GGA AA gtaagtctgt Val Val Gly	AA/G Lys	59	3,675	AA/A Lys	59	364
VII (9) [c]	tcattaacag G GCC Ile	ATC CAG Gln Aln			1,013 [b] (43)			1,009 (43)	

Lower case letters are the intron sequence, upper case latters are the exon sequence at the intron-exon boundary. The 3' splice site (acceptor) is the boundary from the intron to the exon, the 5' splice site (donor) from the exon to the intron.
a = 403 bp coding region and in addition at least 206 bp 5'UTR in the same exon
b = 43 bp coding region and in addition 970 bp 3'UTR in the same exon
c = Number in brackets is the exon number of the corrsponding human nogo/RTN4 gene.
d = Intron sizes were measured using long genomic clones (Ensembl sequence assembly).
e = This intron harbours NNN stretches. Therefore the real size may differ slightly.
f = 73 bp coding + 89 bp 5'UTR
g = 16 bp coding region and in addition at least 48 bp 5'UTR in the same exon

(DANRE)rtn5

Exon Nr	3' splice site	5' splice site	aa at the exon border Zebrafish rtn5	exon size (bp) Zebrafish rtn5	intron size (bp) Zebrafish rtn5 [d]	aa at the exon border Human RTN1	exon size (bp) Human RTN1	intron size (bp) Human RTN1
I(a)		GCA TCT ACA G gtaaatttgg Ala Ser Thr	G/GT Gly	>305 [a] (187)	>18,000 [e]	G/GT Gly	450 (241)	125,244
II	gtctctctag GT GAC TCT CTA Asp Ser Leu	TCC CCT ACA G gtagatcctg Ser Pro Thr	G/GT Gly	807	2,596	G/AA Glu	774	18,039
III	ttttttccag GT CGA GAG TCT Arg Glu Ser	AGA CAG AAA G gtaagagact	G/TG Val	900	>20,200 [e]	G/CT Ala	750	119,422
I(c)		AGA GGG CAG G gtacatattt Arg Gly Gln	G/TG Val	>224 [f] (49)	> 11,000 [e]	G/CT Ala	359 (61)	22,946
IV (4) [c]	ttctcctcag TG GTA GAT CTA Val Asp Leu	CAT CCA TTC AA gttagtccag His Pro Phe	AA/G Lys	208	76	AA/G Lys	208	1,778
V (5) [c]	ctcttatcag G TCC TAT CTG Ser Tyr Leu	TCC ATT AAG gtgaaaaatg Ser Ile Lys	AAG/TTT Lys/Phe	139	1,429	AAA/TTT Lys/Phe	139	1,446
VI (6) [c]	gtgtgtttag TTT GCA GTG Phe Ala Val	TTA ATT CTG G gtaagaatac Leu Ile Leu	G/CT Ala	70	627	G/CT Ala	70	593
VII (7) [c]	ttttttttag CT GTG ATT TCC Val Ile Ser	AAG TAC CAG gtaatgtttc Lys Tyr Gln	CAG/ACA Gln/Thr	47	1,277	CAG/GCA Gln/Ala	47	88
VIII (8) [c]	tctctttcag ACA CAG ATT Thr Gln Ile	GTA ATG GGA AA gtaagttttg Val Met Gly	AA/G Lys	59	111	AA/G Lys	59	6,277
IX (9) [c]	tattttacag G ATT AGA GAA Ile Arg Glu			>172 [b] (40)			792 (43)	

Lower case letters are the intron sequence, upper case letters are the exon sequence at the intron-exon boundary. The 3' splice site (acceptor) is the boundary from the intron to the exon, the 5' splice site (donor) from the exon to the intron.
a = 187 bp coding region and in addition at least 118 bp 5'UTR in the same exon
b = 40 bp coding region (including the stop codon) and in addition at least 132 bp of the 3'UTR in the same exon. The 3' UTR is not fully cloned.
c = Number in brackets is the exon number of the corresponding human RTN1 gene.
d = Intron sizes were measured using long genomic clones (Ensembl sequence assembly).
e = This intron harbours NNN stretches. Therefore the real size may differ slightly.
f = 49 bp coding region and in addition 224 bp 5'UTR in the same exon

(DANRE)rtn6

Exon Nr	3' splice site	5' splice site	aa at the exon border Zebrafish rtn6	exon size (bp) Zebrafish rtn6	intron size (bp) Zebrafish rtn6 [d]	aa at the exon border Human RTN4	exon size (bp) Human RTN4	intron size (bp) Human RTN4
I(a)		CCG CCG GCC G gtgagtaacc Pro Pro Ala	G/GA Gly	>1,242 [a] (958)	> 2,000 [e]			
II	tgtttttcag GA GAG CCT GAA Glu Pro Glu	CTT CCG TCA G gtacgcttct Leu Pro Ser	G/AA Glu	45	1,132			
III	tgatccgcag AA CGC TGC CGT Arg Cys Arg	CCC ACA GCA G gtacaccagc Pro Thr Ala	G/TG Val	1,059	>960 [e]			
II (4) [c]	gtgtgcacag TG CTG CAG CTG Leu Gln Leu	CAT CCC TTC AG His Pro Phe	AG/G Arg	208	>330 [e]	AG/G Arg	208	4,838
III (5) [c]	gtgtgtgcag G CAG TAT CTG Gln Tyr Leu	TCG CTG AAG Ser Leu Lys	AAG/TTG Lys/Leu	139	>150 [e]	AAG/TTT Lys/Phe	139	7,776
IV (6) [c]	tctcctgcag TTG GCA GTG Leu Ala Val	CTC ATT ATC G gtgagtgtgt Leu Ile Ile	G/CT Ala	70	>22 [e]	G/CT Ala	70	827
V (7) [c]	CT TTG ATT GGA Leu Ile Gly	AGA CAT CAG Arg His Gln	CAG/TCA Gln/Ser	47	>670 [e]	CAG/GCA Gln/Ala	47	199
VI (8) [c]	tgtcttccag TCA GAG ATC Ser Glu Ile	GCT TTG GGG AA gtaagtcact Ala Leu Gly	AA/G Lys	59	128	AA/A Lys	59	364
VII (9) [c]	ctgttctcag G GTT CTG GCG Val Leu Ala			>364 [b] (43)			1,009 (43)	

Lower case letters are the intron sequence, upper case letters are the exon sequence at the intron-exon boundary. The 3' splice site (acceptor) is the boundary from the intron to the exon, the 5' splice site (donor) from the exon to the intron.

a = 958 bp coding region and in addition at least 284 bp 5'UTR in the same exon
b = 43 bp coding region (including the stop codon) and in addition 321 bp 3'UTR i n the same exon.
c = Number in brackets is the exon number of the corresponding human RTN4 gene.
d = Intron sizes were measured using long genomic clones (Ensembl sequence assembly).
e = This intron harbours NNN stretches. Therefore the real size may differ slightly.

(DANRE)rtn8

Exon Nr	3' splice site	5' splice site	aa at the exon border Zebrafish rtn8	exon size (bp) Zebrafish rtn8	intron size (bp) Zebrafish rtn8 [d]	aa at the exon border Human RTN2	exon size (bp) Human RTN2	intron size (bp) Human RTN2
I(c)		GCC AGC AAA G gtgagagtct Ala Ser Lys	G/TG Val	>66 [a] (13)	> 6,650 [e]	G/TG Val	>54 (13)	3,605
II (6) [c]	ccctctctag TG TTG GAT CTG Leu Asp Leu	CAT CCC TTC CA gtgagtatgc His Pro Phe	CA/G Gln	208	>750 [e]	CA/G Gln	208	359
III (7) [c]	G TCA TAT TTG Ser Tyr Leu	TCA GTG AAG Ser Val Lys	AAG/TTT Lys/Phe	139	>4,020 [e]	AAG/CTG Lys/Leu	139	141
IV (8) [c]	gtttgtgtag TTT ATT GTA Phe Ile Val	GTG ATG TCT G gtaagaatat Val Met Ser	G/GT Gly	70	148	G/GA Gly	70	119
V (9) [c]	ctgttgacag GT GTG ATA TGC Val Ile Cys	CTC CAG CAG gtaagtgccc Leu Gln Gln	CAG/GAG Gln/Glu	47	231	CAG/GCT Gln/Ala	47	2,357
VI (10) [c]	ttttttacag GAG AGG ATC Glu Arg Ile	ATC ACT GAA AT gtaagtattt Ile Thr Glu	AT/G Met	59	>1,870 [e]	AA/G Lys	59	265
VII (11) [c]	G GTT GAT CTT Val Asp Leu			>304 [b] (91)			496 (82)	

Lower case letters are the intron sequence, upper case letters are the exon sequence at the intron-exon boundary. The 3' splice site (acceptor) is the boundary from the intron to the exon, the 5' splice site (donor) from the exon to the intron.

a = 13 bp coding region and in addition at least 53 bp 5'UTR in the same exon
b = 91 bp coding region (including the stop codon) and in addition at least 213 bp 3'UTR in the same exon. The 3' UTR is not fully cloned.
c = Number in brackets is the exon number of the corresponding human RTN2 gene.
d = Intron sizes were measured using long genomic clones (Ensembl sequences assembly).
e = This intron harbours NNN stretches. Therefore the real size may differ slightly.

(FUGRU)rtn1

Exon Nr	3' splice site	5' splice site	aa at the exon border Fugu rtn1	exon size (bp) Fugu rtn1	intron size (bp) Fugu rtn1 [d]	aa at the exon border Human RTN1	exon size (bp) Human RTN1	intron size (bp) Human RTN1
I(a)		GCA TCT ACA G gtaaaccgga Ala Ser Thr	G/AT Asp	>230 [a] (214)	>5,560 [e]	G/GT Gly	450 (241)	125,244
II	tcttccacag AT GAC TCC ATG Asp Ser Met	TCC CCC ACG C gtaagtacag Ser Pro Thr	C/AA Gln	726	354	G/AA Glu	774	18,039
III	ttgagagcag AA AAG GAA TTC Lys Glu Phe	AAA CAG AAA G gtcagctcct Lys Gln Lys	G/CG Ala	684	>5,420 [e]	G/CT Ala	750	119,422
IV (4) [c]	ctcctcacag CG ATC GAC CTT Ile Asp Leu	CAT CCT TTC AA gtgagccgac His Pro Phe	AA/A Lys	208	70	AA/G Lys	208	1,778
V (5) [c]	ttgcttccag A TCC TAC TTG Ser Tyr Leu	TCC CTG AAG gtgtgcctca Ser Leu Lys	AAG/TTT Lys/Phe	139	161	AAA/TTT Lys/Phe	139	1,446
VI (6) [c]	tgtgttccag TTT GCT GTT Phe Ala Val	CTC ATT CTT G gtgagatcat Leu Ile Leu	G/CT Ala	70	177	G/CT Ala	70	593
VII (7) [c]	gtctctacag CT GTG GTC TCC Val Val Ser	AAG CAT CAG gtcggtggct Lys His Gln	CAG/GCG Gln/Ala	47	74	CAG/GCA Gln/Ala	47	88
VIII (8) [c]	ctcttttcag GCG CAA ATC Ala Gln Ile	GTG GTG GGG AA gtgagttgccg Val Val Gly	AA/G Lys	59	422	AA/G Lys	59	6,277
IX (9) [c]	ctctgtacag G ATC CAA GCC Ile Gln Ala			>75 [b] (43)			792 (43)	

Lower case letters are the intron sequence, upper case letters are the exon sequence at the intron-exon boundary. The 3' splice site (acceptor) is the boundary from the intron to the exon, the 5' splice site (donor) from the exon to the intron.

a = 214 bp coding region and in addition at least 16 bp 5'UTR in the same exon
b = 43 bp coding region (including the stop codon) and in addition at least 32 bp 3'UTR in the same exon.
c = Number in brackets is the exon number of the corresponding human RTN1 gene.
d = Intron sizes were measured using long genomic clones (Ensembl sequence assembly).
e = This intron harbours NNN stretches. Therefore the real size may differ slightly.

(FUGRU)rtn2

Exon Nr	3' splice site	5' splice site	aa at the exon border Fugu rtn2	exon size (bp) Fugu rtn2	intron size (bp) Fugu rtn2 [d]	aa at the exon border Human RTN2	exon size (bp) Human RTN2	intron size (bp) Human RTN2
I(c)		GCC AGT AAA G gtgagagttt Ala Ser Lys	G/TG Val	>25 (13) [a, f]	1,770	G/TG Val	>54 (13)	3,605
II (6) [c]	tcttctccag TG CTG Val Asp Leu	GTG GAC CAC CCT TTT AA gtaagtagta His Pro Phe	AA/G Lys	208 [f]	210	CA/G Gln	208	359
III (7) [c]	tggcccccag G TTG Thr Tyr Leu	ACG TAC TCG CTC AAG gtgagtcact Ser Leu Lys	AAG/TTT Lys/Phe	139	878	AAG/CTG Lys/Leu	139	141
IV (8) [c]	ctgctctcag Phe Leu Val	TTT CTG GTT CTC ATC ATT G gtaagacaga Leu Ile Ile	G/GT Gly	70	69	G/GA Gly	70	119
V (9) [c]	tctgctccag GT GCT Val Ile Ala	GTG ATC CGC CAT CAG gtaacggccc Arg His Gln	CAG/GAG Gln/Glu	47	78	CAG/GCT Gln/Ala	47	2,357
VI (10) [c]	gatttcacag Glu Lys Val	GAG AAG GTG ATT AAG GAC AT gtaagtgtgg Ile Lys Asp	AT/C Ile	59	221	AA/G Lys	59	265
VII (11) [c]	tcattcgcag C Phe Gln Arg	TTT CAG AGA		>353 [b] (76)			496 (82)	

Lower case letters are the intron sequence, upper case letters are the exon sequence at the intron-exon boundary. The 3' splice site (acceptor) is the boundary from the intron to the exon, the 5' splice site (donor) from the exon to the intron.

a = 13 bp coding region and in addition at least 12 bp 5'UTR in the same exon
b = 76 bp coding region (including the stop codon) and in addition at least 277 bp 3'UTR in the same exon.
c = Number in brackets is the exon number of the corresponding human RTN2 gene.
d = Intron sizes were measured using long genomic clones (Ensembl sequence assembly).
e = This intron harbours NNN stretches. Therefore the real size may differ slightly.
f = Size was derived from genomic sequence.

(FUGRU)rtn3

Exon Nr	3' splice site	5' splice site	aa at the exon border Fugu rtn3	exon size (bp) Fugu rtn3	intron size (bp) Fugu rtn3 [d]	aa at the exon border Human RTN3	exon size (bp) Human RTN3	intron size (bp) Human RTN3
I(a)		AAA CTG TCC G gtaaggaaat Lys Leu Ser	G/TT Val	>163 [a] (91)	835	G/TG Val	334 (142)	23,065
II (5) [c]	ttctgcacag TT CTC Lys Asp Leu	AAG GAT CAT CCC TTC AA gtacgtgcga His Pro Phe	AA/A Lys	208	865	AA/A Lys	208	2,305
III (6) [c]	ctctctgcag A ATA Ser Leu Ile	TCA CTG TCT CTT AAG gtgaaaactt Ser Leu Lys	AAG/CTG Lys/Leu	139	339	AAG/CTG Lys/Leu	139	423
IV (7) [c]	ctgccgacag CTG GCT GTG Leu Ala Val	CTC ATT CTG G gtgagcaatg Leu Ile Leu	G/CC Ala	70	558	G/CT Ala	70	523
V (8) [c]	tgttctccag CC AAC ATT CTT Asn Ile Leu	AAA AAC AAG gtaagcccga Lys Asn Lys	AAG/ACC Lys/Thr	47	659	AAG/ACC Lys/Thr	47	2,403
VI (9) [c]	tttcttccag ACC CAG ATT Thr Gln Ile	ACG ATG GCC AA gtaagtaagc Thr Met Ala	AA/G Lys	59	95	AA/G Lys	59	1,985
VII (10) [c]	cttccttcag G TTG CAA GAG Leu Gln Glu			>67 [b] (49)			1,735 (46)	

Lower case letters are the intron sequence, upper case letters are the exon sequence at the intron-exon boundary. The 3' splice site (acceptor) is the boundary from the intron to the exon, the 5' splice site (donor) from the exon to the intron.

a = 91 bp coding region and in addition at least 72 bp 5'UTR in the same exon
b = 49 bp coding region (including the stop codon) and in addition at least 18 bp 3'UTR in the same exon.
c = Numbers in brackets is the exon number of the corresponding human RTN3 gene.
d = Intron sizes were measured using long genomic clones (Ensembl sequence assembly).

(FUGRU)rtn4

Exon Nr	3' splice site	5' splice site	aa at the exon border Fugu rtn4	exon size (bp) Fugu rtn4	intron size (bp) Fugu rtn4 [d]	aa at the exon border Human RTN4	exon size (bp) Human RTN4	intron size (bp) Human RTN4
I(l)		CCT TCA TCT T gtaagtttct Pro Ser Ser	T/GT Cys	>673 [a] (463)	2,289			
II	aatcctgcag GT ATT Ala Leu Ile	AAC AGC AGA G gtaacctgat Asn Ser Arg	G/AT Asp	39	809			
III	tcctccacag AT TCT Val Thr Ser	TTC CCT ACA G gcaagttttc Phe Pro Thr	G/TG Val	54	8,787			
I(n)		GCC AAA CGG G gttagttgtt Ala Lys Arg	G/TG Val	>33 [f] (16)	1,859			
IV (4) [c]	tcacttgcag TG CTT Val Asp Leu	CAC CCG TTC AA gtgagtctcc His Pro Phe	AA/G Lys	208	116	AG/G Arg	208	4,838
V (5) [c]	tgtcttttag G CAG TAC CTC Gln Tyr Leu	TCC ATC AAG gtgagcagga Ser Ile Lys	AAG/TTT Lys/Phe	139	448	AAG/TTT Lys/Phe	139	7,776
VI (6) [c]	ccttccctag TTT GCA GTG Phe Ala Val	CTC ATT CTG G gtaagtcccc Leu Ile Leu	G/GT Gly	70	109	G/CT Ala	70	827
VII (7) [c]	tgttgtttag GT GCA Leu Ile Ala	AAA CAC CAG gtgagttttt Lys His Gln	CAG/GCT Gln/Ala	47	83	CAG/GCA Gln/Ala	47	199
VIII (8) [c]	gtatttttag GCT CAG ATT Ala Gln Ile	ATC GTT GGA AA gtaagttaga Ile Val Gly	AA/G Lys	59	87	AA/A Lys	59	364
IX (9) [c]	cttcctgcag G ATC CAG GCA Ile Gln Ala			>87 [b] (43)			1,009 (43)	

Lower case letters are the intron sequence, upper case letters are the exon sequence at the intron-exon boundary. The 3' splice site (acceptor) is the boundary from the intron to the exon, the 5' splice site (donor) from the exon to the intron.
a = 463 bp coding region and in addition at least 210 bp 5'UTR in the same exon.
b = 43 bp coding region (including the stop codon) and in addition at least 44 bp 3'UTR in the same exon.
c = Number in brackets is the exon number of the corresponding human RTN4 gene.
d = Intron sizes were measured using long genomic clones (Ensembl sequence assembly).
e = This intron harbours NNN stretches. Therefore the real size may differ slightly.
f = 16 bp coding region and in addition at least 17 bp 5'UTR in the same exon.

(FUGRU)rtn7

Exon Nr	3' splice site	5' splice site	aa at the exon border Fugu rtn7	exon size (bp) Fugu rtn7	intron size (bp) Fugu rtn7 [d]	aa at the exon border Human RTN3	exon size (bp) Human RTN3	intron size (bp) Human RTN3
I(a)			/TC			G/TG Val	334 (142)	23,065
IIa (5) [c]	cccaaacag TC CTT Leu Gln Leu	ATC ACC TTT AG gtgaggggat Ser Pro Leu	AG/A Arg	151 [f]	175	AA/A Lys	208	2,305
IIb (5) [c]	ctatttttag A GTT TAT AAA Val Tyr Lys	CAT CCA TTT AG gtaagacaca His Pro Phe	AG/G Arg	57 [f]	94			
III (6) [c]	cctcctacag G CTG Ser Leu Leu	TCT ATG AAG gtcaggttaa Ser Met Lys	AAG/GTG Lys/Val	139 [f]	>2010 [e]	AAG/CTG Lys/Leu	139	423
IV (7) [c]	ttgtccacag GTG ACT GCT Val Thr Ala	CTC ATT ATT G gtgggtcttt Leu Ile Ile	G/CT Ala	70 [f]	77	G/CT Ala	70	523
V (8) [c]	ttttttgtag CT GAC ATC TTA Asp Ile Leu	AGG AAA AAG gtactaatgt Arg Lys Lys	AAG/ACA Lys/Thr	47 [f]	275	AAG/ACC Lys/Thr	47	2,403
VI (9) [c]	ttgtcttcag ACA CAG ATT Thr Gln Ile	ACA AAA TAC CA gtgagttttc Thr Lys Tyr	CA/G Gln	59 [f]	569	AA/G Lys	59	1,985
VII (10) [c]	gtgttttcag G CTG CAG GAC Leu Gln Asp			(49) [b, f]			1,735 (46)	

Lower case letters are the intron sequence, upper case letters are the exon sequence at the intron-exon boundary. The 3' splice site (acceptor) is the boundary from the intron to the exon, the 5' splice site (donor) from the exon to the intron.

b = 49 bp coding region (including the stop codon)
c = Number in brackets is the exon number of the corresponding human RTN3 gene.
d = Intron sizes were measured using long genomic clones (Ensembl sequence assembly).
e = This intron harbours NNN stretches. Therefore the real size may differ slightly.
f = Size was derived from genomic sequence.

(FUGRU)rtn8

Exon Nr	3' splice site	5' splice site	aa at the exon border Fugu rtn8	exon size (bp) Fugu rtn8	intron size (bp) Fugu rtn8 [d]	aa at the exon border Human RTN2	exon size (bp) Human RTN2	intron size (bp) Human RTN2
I(c)		GCC AGC AAA C gtaaggaaat Ala Ser Lys	C/TC Leu	>89 [a] (13)	820	G/TG Val	>54 (13)	3,605
II (6) [c]	atgtgtccag TC ATG GAT CTG Met Asp Leu	CAC CCC TAC CA gtgagtgtgt His Pro Tyr	CA/G Gln	208	146	CA/G Gln	208	359
III (7) [c]	ctgtccccag G TCA TAT CTG Ser Tyr Leu	TCA ATT AAG gtaggtgtgt Ser Ile Lys	AAG/TTT Lys/Phe	139	295	AAG/CTG Lys/Leu	139	141
IV (8) [c]	atcctctcag TTT GTT GTG Phe Val Val	GTG ATA AGT G gtgagtttac Val Ile Ser	G/CG Ala	70	136	G/GA Gly	70	119
V (9) [c]	tgctgaacag CG GTC ATC GGC Val Ile Gly	AAG CAG CAA gtgagtttct Lys Gln Gln	CAA/GTG Gln/Val	47	96	CAG/GCT Gln/Ala	47	2,357
VI (10) [c]	ggctttcaag GTG CGC CTA Val Arg Leu	ATA AGA AAC CT gtgagtaaat Ile Arg Asn	CT/G Leu	59	76	AA/G Lys	59	265
VII (11) [c]	ctttttttag G TGC CTC AGC Cys Leu Ser			>141 [b] (109)			496 (82)	

Lower case letters are the intron sequence, upper case letters are the exon sequence at the intron-exon boundary. The 3' splice site (acceptor) is the boundary from the intron to the exon, the 5' splice site (donor) from the exon to the intron.

a = 13 bp coding region and in addition at least 76 bp 5'UTR in the same exon
b = 109 bp coding region (including the stop codon) and in addition at least 32 bp 3'UTR in the same exon.
c = Number in brackets is the exon number of the corresponding human RTN2 gene.
d = Intron sizes were measured using long genomic clones (Ensemble sequence assembly).

Supplementary Tabel 3: *Exon and intron sizes of zebrafish and fugu rtns*

4 Identification of two *nogo/rtn4* genes and analysis of Nogo-A expression in *Xenopus laevis*

4.1 Abstract

Myelin-associated axon growth inhibitors such as Nogo-A/RTN4-A impair axon regeneration in the adult mammalian CNS. Here, the cloning and expression of two independent *Xenopus laevis rtn4* orthologs is described. As in mammals, alternative transcripts are generated both through differential splicing and promoter usage, giving rise to *Xenopus* nogo-A, -B, -C and to a new isoforms, nogo-N/rtn4-N. *Xenopus* is therefore the 'lowest' vertebrate where Nogo-A was identified.

Xenopus Nogo-A/RTN4-A is predominantly expressed in the nervous system, whereas the other isoforms mainly occur in non-neuronal tissues. Nogo-A/RTN4-A specific antisera detect the protein in myelinated fiber tracts of the spinal cord, hindbrain, optic nerve, tectum opticum and in isolated oligodendrocytes. In addition, subpopulations of CNS neurons are Nogo-A/RTN4-A positiv. This expression pattern is consistent with that observed for rat Nogo-A and suggests similar functions. Nogo-A in *Xenopus* myelin might therefore contribute to the failure of spinal cord regeneration in frogs - a feature that may have evolved during the transition from fish to land vertebrates.

4.2 Introduction

In the adult mammalian and avian CNS, regeneration of lesioned nerve fibers is prevented by inhibitory proteins that are particularly enriched in myelin and oligodendrocytes (Caroni and Schwab, 1988b), such as MAG (McKerracher et al., 1994), OMgp (Wang et al., 2002b) and Nogo/RTN4 (Chen et al., 2000; GrandPré et al., 2000; Prinjha et al., 2000). Earlier functional studies indicated the presence of related neurite growth inhibitors, in particular the IN-1 antigen, in oligodendrocytes/CNS myelin of *Xenopus* (Lang et al., 1995). The IN-1 antibody has originally been raised against a 250 kD myelin fraction (Caroni and Schwab, 1988a), and based on its neutralizing activity the bovine Nogo-A ortholog (bNI220) has been purified (Spillmann et al., 1998).

Nogo/RTN4 is a member of the RTN family of proteins (Chen et al., 2000; GrandPré et al., 2000; Prinjha et al., 2000). These proteins share a conserved 188 amino acids (aa) long C-terminal RHD (Oertle et al., 2003b). The two hydrophobic stretches within the RHD could serve as transmembrane domains for their insertion in ER and plasma membranes (Oertle et al., 2003c; van

de Velde et al., 1994). Outside the RHD domain, Nogo/RTN4 and the other three RTN proteins (RTN1-3) have no obvious sequence similarities.

In mammals, the *nogo/rtn4* gene gives rise to different isoforms both through alternative splicing and alternative promoter usage with the three major transcripts known as *nogo-A*, *nogo-B* and *nogo-C* (Oertle et al., 2003a). The largest isoform, Nogo-A/RTN4-A has been described as a potent neurite growth inhibitor of CNS myelin with two inhibitory sites. A stretch in the Nogo-A-specific region (NiG-Δ20) is strongly inhibitory for neurite outgrowth and cell spreading *in vitro* (Oertle et al., 2003d). In addition, the loop region between the two C-terminal hydrophobic domains of the RHD (called Nogo-66) has been shown to induce collapse of neuronal growth cones *in vitro* (GrandPré et al., 2000).

The RTN proteins are evolutionary conserved in eukaryotes (Oertle et al., 2003b), and therefore Nogo-A homologs may exist and impair CNS axon regeneration in amphibians. In frogs, CNS axons fail to regenerate in the spinal cord after metamorphosis (Beattie et al., 1990; Forehand and Farel, 1982). The inability of regeneration correlates with non-permissive properties of spinal cord myelin and oligodendrocytes in cocultures with axons, indicating the expression of inhibitory proteins in this region (Lang et al., 1995; Lang and Stuermer, 1996). CNS myelin and oligodendrocytes from the optic nerve and tectum, where amphibian axons do regenerate, were not inhibitory to growing axons *in vitro* (Lang et al., 1995). Reasons may lie in regional differences concerning the expression of myelin inhibitors or their subcellular localization, e.g. surface exposure in myelin membranes or retention in the ER.

Conserved sequence motifs of mammalian *nogo*-A were used to search for *Xenopus nogo/rtn4* homologs. Various transcripts corresponding to the three major isoforms rtn4-A, -B and -C were identified. In contrast to mammals, an additional short, so far unknown isoform, termed rtn4-N was found. The *nogo*/*rtn*4 gene underwent a *Xenopus* specific duplication, which would allow independent transcriptional regulation of the two *nogo* gene copies. Tissue specific transcription of the different nogo/rtn4 cDNAs was analysed by RT-PCR. Nogo-A/RTN4-A protein expression was detected with *Xenopus* Nogo-A/RTN4-A specific antibodies in oligodendrocytes and major myelinated fiber tracts. Its distribution compares to the Nogo-A expression in mammals and – since Nogo-A forms are not found in zebrafish (Klinger et al., 2002) – indicates that the evolution of this neurite growth inhibitor has occurred in land vertebrates.

4.3 Materials and methods

4.3.1 Animals

All animals were kept at the animal research facility of the University of Konstanz in compliance with animal welfare legislation. *Xenopus laevis* were anesthetized and killed in a 0.03% solution of MS222 (Sigma-Aldrich, Seelze, Germany) for tissue preparation. Chinchilla bastard rabbits were used for immunization and RTN4 antibody generation.

4.3.2 Nomenclature of Xenopus nogo/rtn4 transcripts

Xenopus nogo transcripts were named according to the nomenclature guidelines for reticulon genes (Oertle et al., 2003b). In brief, rtn serves as a gene symbol for chordate reticulons. Paralogous rtn sequences are arbitrarily numbered with nogo being rtn4. Reticulon genes that have been duplicated within the same species share the same symbol and differ by an additional number (e.g. rtn4.1 and rtn4.2). To distinguish rtn genes of various species, a prefix according to the identification code proposed by SWISS-PROT is used (e.g. (XENLA)rtn4.1). Alternative transcripts from different promoters receive a new letter (e.g. (XENLA)rtn4.1-A, (XENLA)rtn4.1-C), while alternatively spliced transcripts derived from the same promoter have the same letter but are distinguished by the consecutive numbering (e.g. (XENLA)rtn4.1-A1, (XENLA)rtn4.1-A2). For historical reasons, rtn4-A and rtn4-B do not comply with this rule (Chen et al., 2000; GrandPré et al., 2000; Prinjha et al., 2000).

4.3.3 Cloning with degenerate primers

Total RNA was isolated from *Xenopus laevis* embryos older than stage 50 (Trizol; Wak Chemie, Bad Homburg, Germany) and reverse-transcribed following the manufacturer' s instructions (Ready to Go T-primed first strand kit, Amersham Biosciences, Freiburg, Germany). Conserved sequence motifs of the nogo-A cDNA of rat, human and chicken were used to design degenerate primers (Nogo-A-RN/se1: 5'-CA[AG] GA[AG] AC[AGCT] GA[AG] GC[AGCT] CC[AGCT] TA[CT] AT-3', Nogo-A-RN/as2: AC[AG] TA[AGCT] GT[AG] AA[AGCT] ACC CAC AT). Using standard PCR, two different partial cDNA clones (1.2 kb) coding for two *Xenopus* rtn4 genes were amplified. Both clones contain nogo-A specific sequence (837 bp for (XENLA)rtn4.1 and 849 bp for (XENLA)rtn4.2) and parts of the reticulon homology domain (381 bp and 384 bp, respectively).

4.3.4 5'- and 3'-Rapid amplification of cDNA ends (RACE) and full-length cloning

The SMART RACE cDNA Amplification Kit (BD Clontech, Heidelberg, Germany) was used to determine the 5'- and 3'-sequences including the putative start methionines and 3'-noncoding regions for both, the (XENLA)rtn4.1 and (XENLA)rtn4.2, transcripts. Total RNA (1.3 µg/reaction) served as template for the synthesis of first-strand 5'-Ready cDNA using 5'-CDS and SMART II oligonucleotides and 3'-Ready cDNA using 3'-CDS primer, according to the manufacturer' s protocol.
The rtn4-A specific primer 5'-RACE GSP XL (5'-AGA ATC TGG TGA GCT TTC ATC GGA GGG C-3'; bp 1797-1824 of (XENLA)rtn4.1-A3 and bp 1764-1791 of (XENLA)rtn4.2-A3, respectively) was used to amplify 5'-cDNA ends of both rtn4-A transcripts. To clone additional rtn4 isoforms (B, C and N), a 5'-RACE primer located in the RHD was used (5'-RACE GSP XL 3: 5'-CTG GCA CCG CCA GGT TGG ACT CCA AGA TGG-3'; bp 2720-2749 of (XENLA)rtn4.1-A3 and bp 2687-2716 of (XENLA)rtn4.2-A3, respectively).
The 3' ends including UTRs were completed using primer 3'RACE GSP XL (5'- CCC CCT TCG AAG GAA GAT GAT GGT TCC-3'; bp 2422-2448 of (XENLA)rtn4.1-A3) and 3'RACE GSP XL2 (5'- AAC CCG AAC CCC CTT CAA AGA AAG ATG AGG-3'; bp 2375-2404 of (XENLA)rtn4.2-A3), respectively. All RACE reactions were performed as described in the manufacturer's protocol and PCR products were directly cloned into pCRII-TOPO vector (Invitrogen, Karlsruhe, Germany).
Full-length clones of the alternative nogo transcripts (rtn4-A, -B, -C and -N) were obtained for both *Xenopus laevis* nogo genes using primers located at the 5'-and 3'-ends of the various transcripts. (XENLA)rtn4.1 and (XENLA)rtn4.2 specific dbESTs were identified as described elsewhere (Oertle et al., 2003b). Sequences were deposited in GenBank (GenBank accession numbers AY316183-AY316197).

4.3.5 DNA sequencing and sequence analysis

Plasmid DNA of RACE and full-length clones was prepared using the QIAprep® 8 Miniprep Kit (Qiagen, Hilden, Germany). Both DNA strands were sequenced using the Abi Prism® BigDye™ Terminator Cycle Sequencing Kit (Applied Biosystems, Darmstadt, Germany). Sequencing products were analyzed on an AbiPrism 3100 Genetic Analyzer (Applied Biosystems, Darmstadt, Germany). Single sequences were assembled using the Lasergene software package (GATC Biotech, Konstanz, Germany). Molecular evolutionary analyses were conducted using

MEGA version 2.1 (Kumar et al., 2001). In brief, sequences were aligned at the amino acid level by the CLUSTALW program and gaps were pair-wise deleted. Numbers of synonymous nucleotide substitutions per synonymous site (d_S) and nonsynonymous substitutions per nonsynonymous site (d_N) were estimated (Nei and Gojobori, 1986) for both (XENLA)rtn4 sequences and the human ortholog.

4.3.6 RT-PCR

Various tissues (spinal cord, tectum opticum, forebrain, retina, sciatic nerve, heart, muscle, lung, kidney, liver) were dissected from adult *Xenopus laevis* and used for preparation of total RNA with QIAshredders and the RNeasy Mini Prep Kit (Qiagen, Hilden, Germany) following manufacturer's instructions (<30 mg tissue/column). Muscle tissue was additionally subjected to proteinase K digestion (200 µg/30 mg tissue).
First-strand cDNA was synthesized with the Superscript First-Strand Synthesis System for RT-PCR (Invitrogen, Karlsruhe, Germany). Up to 5 µg of total RNA were reverse-transcribed under standard conditions with 0.5 µg oligo$(dT)_{12\text{-}18}$ primer. Zero-transcriptions (without Superscript II in the reaction) were performed in parallel, to control for genomic DNA contaminations in subsequent PCRs. Amount and quality of the different cDNA samples were evaluated comparing the expression level of the housekeeping gene clathrin (primers: 5'-GAC AGT GCC ATC ATG AAT CC-3' and 5'-TTT GTG CTT CTG GAG GAA AGA A-3'; 28 cycles, annealing 50°C, elongation 60 sec). Using this PCR as an internal reverence, concentration of the cDNAs was adjusted to comparable levels.
A standard 25 µl PCR reaction contained 2.5 µl of 10 x reaction buffer (500 mM NaCl/ 15 mM $MgCl_2$/ 100mM Tris-Cl, pH = 9.0; Amersham Biosciences, Freiburg, Germany), 0.3 µl dNTP mix (10 mM each), 1 µl of first strand cDNA, 0.75 U Taq DNA polymerase (Amersham Biosciences, Freiburg, Germany) and 50 pmol of the appropriate sense and antisense primers (see **Supplementary Table 1A** for sequence information and arrows in **Fig. 1** for primer positions). PCR conditions for rtn4.1-A and rtn4.2-A (primers III + IV and VIII + IX, respectively) were 94°C for 30 sec, 76°C for 30 sec and 72 °C for 75 sec (30 cycles). Different splice variants of rtn4.1-A and rtn4.2-A (1, 2 and 3) were amplified using the Expand Long Template PCR System (Roche Diagnostics, Mannheim, Germany), since PCR with Taq polymerase failed in this GC rich sequence. This 'sensitive' PCR was performed with primers I+II and VI+VII, respectively, twice the amount of cDNA (2 µl) and the following cycling parameters: 92°C for 10 sec, 66°C for 10 sec, 68°C for 40 sec (24 cycles), 92°C for 10 sec, 66°C for 10 sec, 68°C for 40 sec +1 sec/cycle (15 cycles).
Rtn4.1-B and rtn4.2-B splice variants were amplified using primer combinations I + V and VI + X, respectively (92°C for 10 sec, 63°C for 10 sec, 68°C for 23 sec (20 cycles), 92°C for 10 sec, 63°C for 10 sec, 68°C for 23 sec +1 sec/cycle (15 cycles)). The short elongation time excluded amplification of A-splice variants in the same PCR reaction. All alternative splice products were subcloned into pCRII-TOPO vector and confirmed by sequencing.
Conditions for rtn4.1-C and rtn4.2-C (standard PCR; primers XI + XII and XI + XV, respectively) were 94°C for 20 sec, 63°C for 15 sec and 72°C for 40 sec (35 cycles). Rtn4.1-N was amplified using primer combination XIII + XII and standard PCR (94°C for 20 sec, 65°C for 15 sec and 72°C for 45 sec; 35 cycles). For rtn4.2-N detection, the AccuPrime System together with primers XIV + XV was applied (94°C for 20 sec, 63°C for 15 sec and 68°C for 45 sec; 35 cycles).
For each primer combination, positive and negative control PCRs on rtn4.1 and -2 plasmid DNA were included, to prove specificity for one of the two genes. All PCRs were performed at least in duplicate, analysed on 1.5% (w/v) agarose gels and documented with a Molecular Imager FX (Bio-Rad, München, Germany).

4.3.7 Oligodendrocyte cultures

Tectum opticum and spinal cord of anesthetized postmetamorphotic froglets were dissected in L-15 medium (Invitrogen, Karlsruhe, Germany) and the meninges and peripheral nerve roots were removed. The tissue was chopped with a McIlwain tissue chopper (Vibratome, St. Louis MO, USA) and the fragments were rinsed twice in L-15 containing 10% (v/v) fetal calf serum (FCS, Invitrogen, Karlsruhe, Germany). After centrifugation, the tissue was resuspended in 80% (v/v) DMEM/Ham`s F-12 1:1, containing 10% (v/v) FCS, 0.4% (w/v) methyl-cellulose, 15 mM HEPES, 3.5 mg/ml glucose, 0.1 mg/ml glutamine, 5 x 10^{-3} mg/ml insuline, 0.1 mM putrescine, 2 x 10^{-5} mM progesterone, 3 x 10^{-5} mM sodium-selenite (all Sigma-Aldrich, Seelze, Germany) and 0.05 mg/ml gentamicine (Invitrogen, Karlsruhe, Germany) and plated on polylysine/laminin-coated coverslips (Bastmeyer et al., 1989). Cultures were further treated as described in (Lang et al., 1995). Differentiated oligodendrocytes were obtained by adding 10 µM Forskolin (Biomol GmbH, Hamburg, Germany) to the culture medium.

4.3.8 Antibodies

For generation of antisera AS702 and AS706, two different regions of the (XENLA)rtn4.1-A sequence (for details see **Fig. 1**) were cloned into pTrcHis expression vector (Invitrogen, Karlsruhe, Germany) and recombinantly expressed in Top 10F' E. coli after IPTG induction. His-tagged proteins were purified under denaturing conditions on Ni^+-NTA spin columns (Qiagen, Hilden, Germany) according to the manufacturer. 500 µl of eluted protein were mixed with adjuvant (500 µl MPL+TDM+CWS, No. M6661, Sigma-Aldrich, Seelze, Germany,) and injected into rabbits every

second week for 5 times. IgG fractions were isolated via a Protein A affinity chromatography (Amersham Biosciences, Freiburg, Germany) according to standard protocols. Specificity of AS702 and AS706 was increased by pre-absorption against general E. coli and unrelated His-tagged proteins. Proteins 833 (RTN4.1) and 834 (RTN4.2) were similarly expressed and purified to test specificity of AS702 and AS706.
Antibodies were used as follows: AS702 and AS706 against *Xenopus* Nogo-A/RTN4-A at 1:1,000 for immunohistochemistry on tissue sections and at 1:10,000 for western blotting; AS472 against rat Nogo-A (aa 623-640, affinity purified) at 1:10,000; monoclonal antibody (mAb) Olig hybridoma supernatant against oligodendrocytes/myelin (Steen et al., 1989) at 1:2 and mAb IN-1 hybridoma supernatant (Caroni and Schwab, 1988a) undiluted. Secondary antibodies were Cy3-conjugated donkey anti-rabbit IgG; HRP-conjugated goat anti-rabbit IgG (Jackson ImmunoResearch West Grove PA, USA), Alexa 488-conjugated goat anti-mouse IgG (Molecular Probes, Eugene OR, USA), and biotin-conjugated goat anti-mouse IgM (μ-chain specific; Vector Laboratories, Burlingame CA, USA).

4.3.9 Immunohistochemistry

For AS702, AS706 and IN-1 staining, isolated brains and spinal cords and retina with optic nerves of stage 66 *Xenopus laevis* were embedded in TissueTek (Sakura Finetek, Zoeterwoude, The Netherlands) and frozen in liquid nitrogen. 12 μm thick sections were cut on a cryostat (Leica, Bensheim Germany), collected on SuperFrost Plus glass slides (Menzel-Glaser, Freiburg, Germany), fixed in Clark's solution (95% (v/v) ethanol / 5% (v/v) acetic acid; 25 min at 4°C), rehydrated in 70% (v/v) ethanol (10 min at 4°C) and rinsed in PBS. Alternatively, tissues were fixed in 2% (w/v) PFA (overnight at 4°C), washed in PBS, transferred into a 20% (w/v) sucrose solution (overnight at 4°C) and embedded in TissueTek prior to sectioning. PFA fixed sections were stained with AS702, AS706 or the myelin marker Olig. For Olig staining 0.1% (v/v) TritonX 100 (Sigma-Aldrich, Seelze, Germany) was added to the antibody solution.
Sections were incubated with primary antibodies (overnight at 4°C), rinsed in PBS, incubated with appropriate secondary antibodies (either Cy3-conjugated or biotinylated antibodies together with ABC and DAB kits (Vector Laboratories, Burlingame CA, USA); 1 h at RT), rinsed and coverslipped with Mowiol (Merck Biosciences, Schwalbach, Germany) containing n-propyl gallate (Sigma-Aldrich, Seelze, Germany).
Cultured oligodendrocytes were fixed in methanol (-20°C, 5 min), rinsed in PBS, incubated with AS706 overnight at 4°C, rinsed in PBS, incubated with Cy3-conjugated secondary antibody plus 50 ng/ml DAPI (4',6'-Diamidino-2-Phenylindole; Sigma-Aldrich, Seelze, Germany) for 1 h at RT, rinsed, and coverslipped with Mowiol (Merck Biosciences, Schwalbach, Germany). For blocking experiments, AS706 was preincubated with 0.45 mg/ml recombinant protein 706 for 1 h at 4°C prior to staining.

4.3.10 Gel Electrophoresis and immunoblotting

Xenopus laevis tissues were homogenized, separated on NewPAGE® Novex® 3-8% high resolution gradient tris-acetate gels (Invitrogen, Karlsruhe, Germany) and transferred to Hybond C Super nitrocellulose membranes (Amersham Biosciences, Freiburg, Germany) in a tank blot apparatus. For immunodetection, the membranes were incubated in blocking solution (3% (w/v) milk powder/ 0.05% (v/v) Tween20/ 350 mM NaCl in PBS) at RT for at least 30 min. Primary antibody was added overnight at 4°C. After 3 washes for 15 min each with washing buffer (350 mM NaCl/ 0.05% (v/v) Tween20 in PBS) the membranes were incubated with HRP-coupled secondary antibody for 1-2 h at RT. After 3 washes (10 min each), the blots were developed using the ECL Detection Kit (Amersham Biosciences, Freiburg, Germany) or SuperSignal West Pico (Pierce, Bonn, Germany) and exposed to X-ray films (Hyperfilm-ECL; Amersham Biosciences, Freiburg, Germany).

4.4 Results

4.4.1 Identification and characterization of Xenopus laevis rtn4

Full-length cDNAs of altogether 15 different *Xenopus laevis* (XENLA) nogo/rtn4 transcripts were cloned by degenerate PCR, RACE and RT-PCR. **Figure 1** gives a schematic overview of these transcripts and illustrates the relationship between *Xenopus* and rat rtn4 isoforms. Based on the RHDs, which form the C-terminal part of all RTN4 proteins, the sequences were asigned to two groups (rtn4.1, rtn4.2), indicating a *Xenopus laevis* specific gene duplication (see below section 4.4.2). As in human, rat and mouse (Chen et al., 2000; GrandPré et al., 2000; Prinjha et al., 2000),

the three major transcripts rtn4-A, -B and -C also exist for both *Xenopus* genes. Small, alternatively spliced exons lead to multiple mRNA variants of the -A and -B isoforms (**Fig. 1**, **3**). Unexpectedly, an additional, so far unknown rtn-4 isoform with a short N-terminus of 5 aa, which was named (XENLA)rtn4-N, was identified.

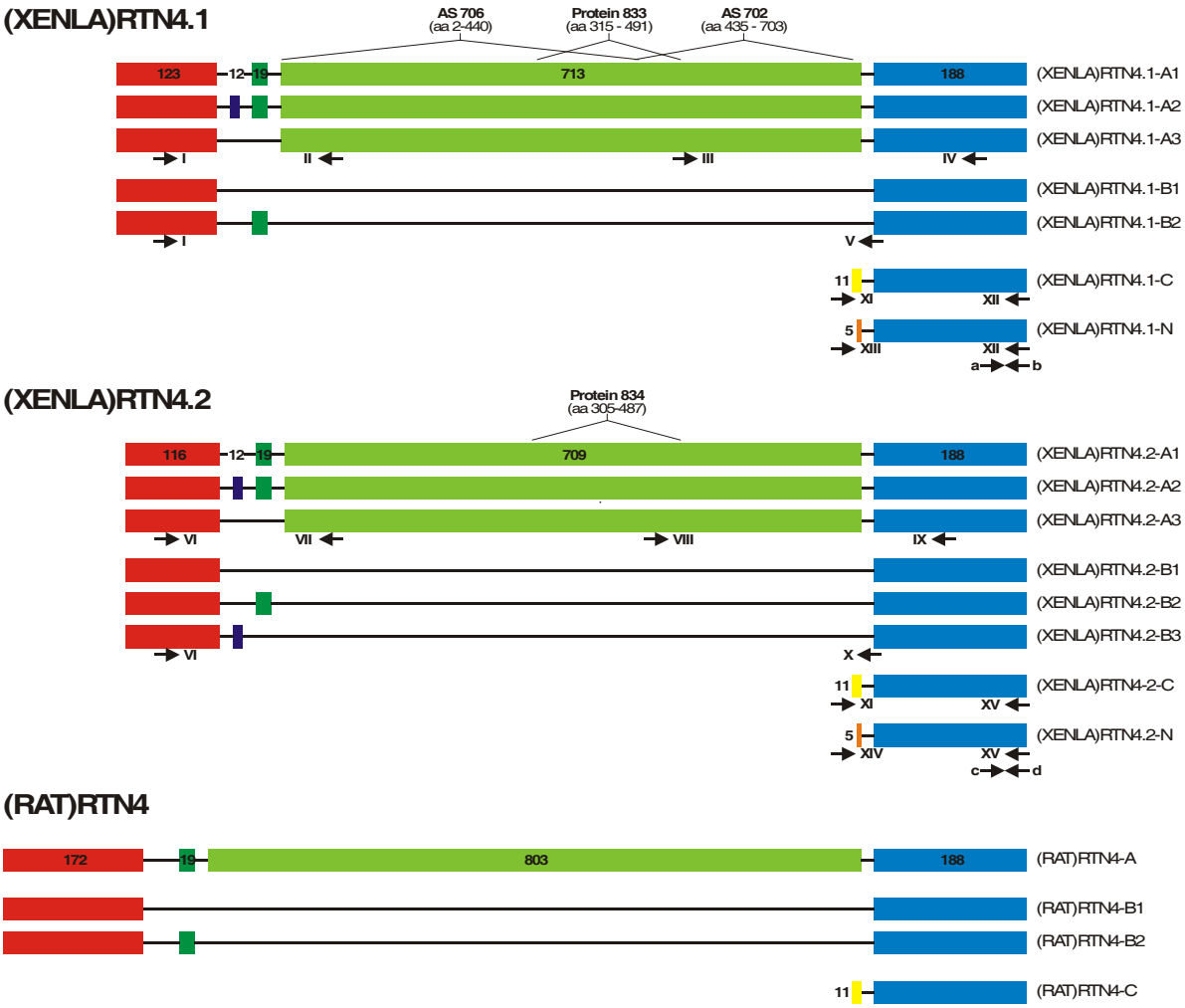

Fig. 1: *Schematic representation of Xenopus nogo/rtn4 in comparison to rat nogo/rtn4 transcripts*
Two *nogo*/*rtn4* genes were identified in *Xenopus laevis* and the different transcripts were named according to the nomenclature guidelines for reticulon genes ((XENLA)rtn4.1, (XENLA)rtn4.2; see Materials and Methods section 4.3). Their overall structures correspond to mammalian rtn4. Nogo-A/rtn4-A consists of an N-terminal A/B-specific region (red), a central A-specific region (light green) and the RHD (blue). In the B-isoforms, the A-specific region is missing. For both the A- and B-isoforms, multiple minor splice variants exist due to the alternative usage of two (*Xenopus*) or one (mammals) small exons (dark blue and dark green). RTN4-C (yellow) and RTN4-N (orange) are transcribed from alternative promoters, but the RHD is the same as for the -A and -B isoforms. The amino acid length of the respective regions is depicted by arabic numbers. Localizations of primers are indicated by arrows and roman numbers (RT-PCR) or lower case letters (genomic PCR). The range of recombinant proteins used for generation of polyclonal antisera against Nogo-A is outlined with brackets.
AS, polyclonal antiserum

The full-length (XENLA)rtn4.1-A1/4.2-A1 sequences consist of 4024/3898 base pairs (bp), with open reading frames (ORFs) coding for 1043/1032 aa, respectively. Compared to rat Nogo-A, the

coding regions are 120/131 aa shorter based on length differences both in the Nogo-A/B specific regions (49/56 aa shorter) and the Nogo-A specific regions (71/75 aa shorter). The RHDs are exactly as long as in the rat (188 aa; **Fig. 1**). At their C-termini, a dilysine ER retention motif (KRKAE) is present. *Xenopus* rtn4.1-A and rtn4.2-A each have one major (rtn4-A1) and two minor splice variants arising from the alternative usage of two small exons of 36 bp (12 aa) and 57 bp (19 aa; **Fig. 1**). These exons are either both present (rtn4-A2), both absent (rtn4-A3) or individually used (rtn4-A1). The 36 bp exon is unique for the *Xenopus rtn4* genes and was not identified in mammals (Oertle et al., 2003a). The full-length Nogo-A1/RTN4-A1 proteins and the respective rat ortholog share an overall identity of 34%, with the highest sequence conservation in the RHD. *Xenopus* RTN4.1-A1 and RTN4.2-A1 are 78.3% identical and are therefore more closely related to each other than to any other mammalian Nogo-A/RTN4-A. Rtn4.1-B and rtn4.2-B are alternative splice forms of rtn4.1-A and rtn4.2-A, respectively, sharing the respective N-terminal A/B-specific regions with the start codons, the RHDs and the untranslated regions (UTRs), but lacking the A-specific central exons (**Fig. 1**). The sequences surrounding the putative start methionines of rtn4.1-A/B and rtn4.2-A/B (cccGcc**ATG**G/gccGca**ATG**G) comply with the consensus motif for initiation of translation (gccAcc**ATG**G) that particularly requires a G residue following the ATG and a purine at position –3 (Kozak, 1996).

Although there are no upstream stop codons in the cloned 5' UTRs (110/118 bp), the consensus motifs and the absence of alternative start codons suggest that the identified methionines are the N-termini of the respective (XENLA)RTN4-A and -B proteins. In the 3' UTRs (782/681 bp), polyadenylation signals (AATAAA) were identified 20/27 bp upstream of the poly-A tails, proving that the entire 3'-UTRs were cloned for both *rtn4* genes.

As in mammals (Oertle et al., 2003a), (XENLA)rtn4.1-C and (XENLA)rtn4.2-C are driven by alternative promoters. The C-specific exons each code for 11 aa that are 91% identical to each other and share 36% sequence identity with rat exon 1C (Oertle et al., 2003a). The sequences surrounding the putative start methionines are tcaGaa**ATG**G and tcaGag**ATG**G.

Interestingly, a further isoform, rtn4-N, for both *Xenopus* genes that has not been found in any mammalian species, was identified. The transcription of (XENLA)rtn4-N is probably driven from an alternative promoter. The lengths of the N-specific exons are 16 bp (5 aa) and the encoded aa are 100% identical. An orthologous isoform with 80% sequence identity has also been identified in zebrafish (Klinger et al., 2002).

All sequences were deposited in GenBank (GenBank accession numbers AY316183 to AY316197).

4.4.2 Existence of two Xenopus rtn4 genes

Two *Xenopus* rtn4-A clones with a sequence divergence of 13% at the cDNA level were initially identified by PCR with degenerate primers (for details see Materials and Methods). To test whether these two forms are alleles or independent *Xenopus rtn4* genes, length and sequence identity of RHD introns were analysed (**Fig. 2**). Since rtn4-A, -B, -C and -N are isoforms transcribed from the same gene and share the RHD, evidence for two RHDs is sufficient to prove the existence of two independent *rtn4* genes.

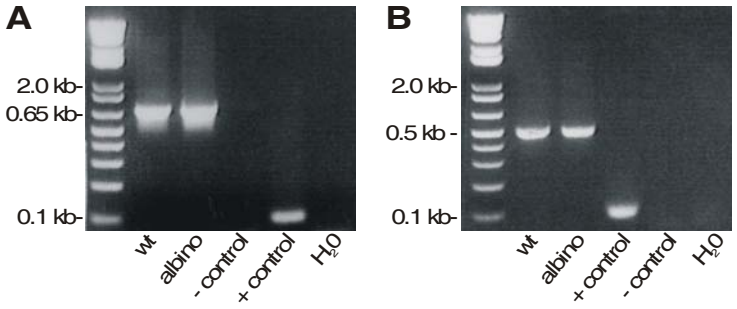

Fig. 2: *PCR analysis of Xenopus rtn4 introns*

The existence of two independent *nogo*/*rtn4* genes was proven by PCR analysis of intron sizes. Specificity of the used primer pairs for one of the two *rtn4* genes (primers a + b for rtn4.1 and primers c + d for rtn4.2; see **Fig. 1**) was verified by PCR on cloned plasmid DNA (+ control; - control).

A) Primers a + b amplified the expected PCR product of 110 bp only on rtn4.1 (lane 4) but not on rtn4.2 (lane 3) plasmid DNA. On two different genomic DNA templates (prepared from either wildtype or albino *Xenopus laevis*), the amplicon was 678 bp (lanes 1 and 2).

B) Primers c + d were specific for rtn4.2 (lane 3) and no amplification was achieved on rtn4.1 negative control plasmid (lane 4). The PCR product on genomic DNA templates was 490 bp (lanes 1 and 2).

wt, wildtype

Based on the known intron/exon structure of the human and mouse orthologs (Oertle et al., 2003a), PCR was performed on genomic DNA to amplify intron IV sequences (between the 4th and 5th exon of the RHD; for primer sequences and positions, see **Supplementary table 1B** and **Fig. 1**). Rtn4.l specific primers amplified the expected product of 110 bp on rtn4.l positive control plasmid DNA but not on rtn4.2 (negative control). PCR on two different genomic DNA templates (wildtype (wt) and albino) resulted in an amplicon of 678 bp (**Fig. 2A**). In contrast, rtn4.2 specific primers amplified the expected product on rtn4.2 positive control plasmid DNA, but not on an rtn4.1 negative control. On genomic DNA, the amplicon was 490 bp (**Fig. 2B**). Thus, this intron of *rtn4.1* is 188 bp longer. Its sequence differs by 36% from its *rtn4.2* counterpart. Similar results were obtained by the analysis of other introns and of the 3' UTRs (data not shown), proving the existence of two independent *rtn4* genes in *Xenopus laevis*.

Whether the two *rtn4* genes result from the *Xenopus laevis* specific tetraploidization was evaluated computing the rates of synonymous (silent) and nonsynonymous (aa altering) nucleotide substitutions (d_S and d_N; **Supplementary Table 2**). Assuming that silent mutations accumulate at approximately constant rates, elapsed time since the duplication is proportional to

d_S of the two *Xenopus* rtn4-A transcripts and can be calculated by comparison to the corresponding rates of the human and rat cDNAs (Hughes and Hughes, 1993). Consistent with an *rtn4* gene duplication more recent than the divergence of rodents and primates ~80-100 MYA (Li et al., 1990), d_S of the two *Xenopus* rtn4-A transcripts (26.6 ± 2.2 substitutions/100 sites) was lower than the mammalian d_S (44.3 ± 3 substitutions/100 sites). This rate is comparable to d_S of other duplicated *Xenopus* genes (Hughes and Hughes, 1993), suggesting that the *rtn4* gene duplication occurred during the tetraploidization event ~30 MYA. Unexpectedly, the rate of aa altering mutations (d_N) of the rtn4-A transcripts (10.3 ± 0.7 substitutions/100 sites) was explicitly higher than for other duplicated *Xenopus* genes, almost reaching the d_N of the rat and human rtn4 orthologs (11.9 ± 0.7 substitutions/100 sites). However, neither of the two copies evolved significantly faster than the other at nonsynonymous sites (59.6 ± 2.5 compared to 58.4 ± 2.6), as was shown by separate comparison of each *Xenopus* gene to the human rtn4 ortholog.
This result indicates that both *Xenopus rtn4* genes evolved equally fast and that neither gene copy is redundant and therefore free to accumulate mutations without constraint.

4.4.3 RT-PCR analysis of Xenopus rtn4 mRNA expression

Transcription of *rtn4* in different tissues of adult *Xenopus laevis* was analysed by RT-PCR (for an overview see **Table 1**). Using primers that do not discriminate between the three different rtn4.1-A splice variants (primers III + IV, see **Fig. 1**), expression was predominantly observed in CNS tissues, i.e. spinal cord, tectum opticum, forebrain and eye, but also in sciatic nerve and heart (**Fig. 3A**). Faint bands indicating low expression levels were visible in muscle, lung and kidney. Rtn4.2-A transcripts, in comparison, were expressed in a similar pattern at an overall lower level, especially in sciatic nerve, and with these PCR conditions not detectable in lung, kidney and liver (**Fig. 3C**, primers VIII + IX). To distinguish between the three splice products of rtn4-A (-A1, -A2 and -A3), sensitive RT-PCR was applied (see Materials and Methods). Amplification of the region that could vary in length due to the alternative usage of the two 36 bp and 57 bp exons (primer I + II for rtn4.1-A and VI + VII for rtn4.2-A; **Fig.1**) detected only the major splice variant (-A1; with the 57 bp exon and without the 36 bp exon) in all neuronal tissues and heart (data not shown). In non-neuronal tissues, additional, so far undetected expression and alternative splice products were revealed. For rtn4.1, the major transcript (-A1) was expressed in muscle, lung and kidney, whereas rtn4.1-A2 (containing both exons) was present only in muscle and rtn4.1-A3 (both exons missing) only in kidney (**Fig. 3B**). Using this more sensitive PCR for rtn4.2, -A1 mRNA transcripts were unexpectedly found in all non-neuronal tissues (**Fig. 3D**). Rtn4.2-A2 was detectable in kidney and liver whilst rtn4.2-A3 expression was restricted to kidney.

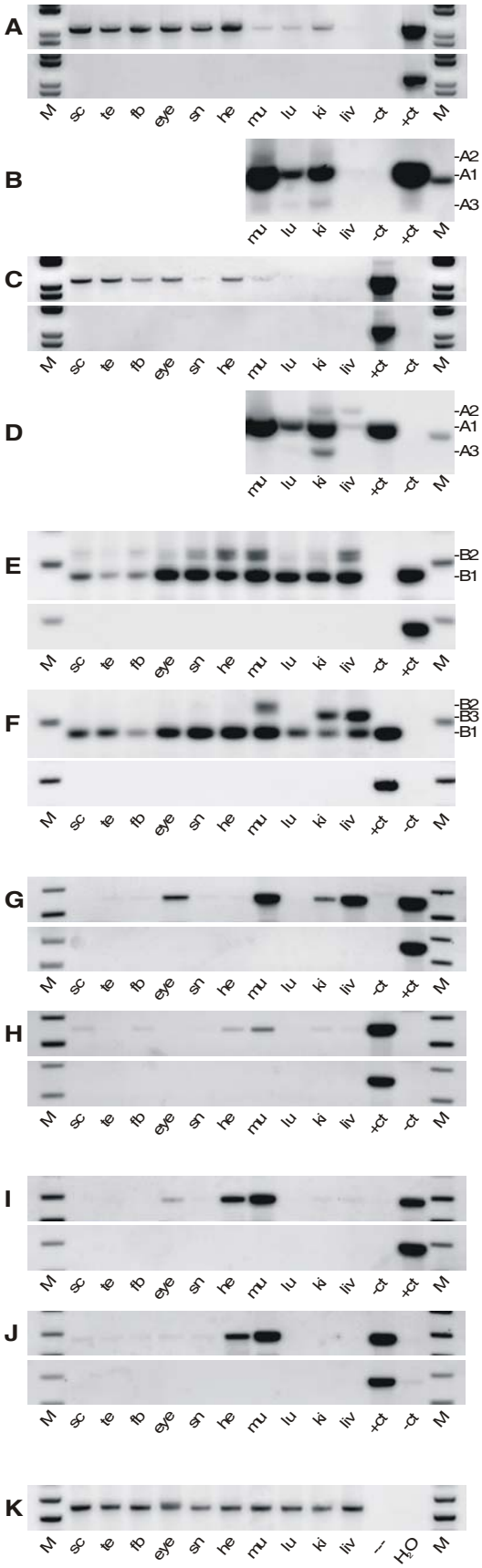

Fig. 3: *RT-PCR analysis of Xenopus rtn4 mRNA expression*

Transcripts of rtn4-A, -B, -C and -N were detected in various *Xenopus* tissues (upper row of panels A-J). Lanes +ct and -ct are control PCRs on plasmid DNAs to prove specificity of the primers for rtn4.1 and rtn4.2, respectively. A 'zero reverse transcriptase' negative control was conducted with each primer pair to show that no bands were amplified due to genomic DNA contamination of the templates (lower row of panels A-J).

A) Amplification of rtn4.1-A.

B) Detection of rtn4.1-A splice variants in non-neuronal tissues.

C) Amplification of rtn4.2-A.

D) Detection of rtn4.2-A splice variants in non-neuronal tissues.

E) Analysis of rtn4.1-B splice variants.

F) Analysis of rtn4.2-B splice variants.

G) Amplification of rtn4.1-C.

H) Amplification of rtn4.2-C.

I) Expression of rtn4.1-N.

J) Expression of rtn4.2-N.

K) RT-PCR with clathrin-specific primers served as positive control to ensure that equal amounts of cDNA template were used in each reaction. H_2O was a 'no template' control.

sc, spinal cord; te, tectum opticum; fb, forebrain; sn, sciatic nerve; he, heart; mu, muscle; lu, lung; ki, kidney; liv, liver; +ct, positive control; -ct, negative control

Transcripts for both rtn4-B1 forms (the main -B splice variant) were verified in all tissues analysed (**Fig. 3E**, **F**), although expression levels were low in spinal cord, tectum opticum, forebrain (rtn4.1 and -2) and lung (rtn4.2). Hence, transcription of the rtn4-B forms predominantly in non-neuronal tissues is almost complementary to the rtn4-A expression. For rtn4.1-B, one additional splice form appeared in all tissues (rtn4.1-B2; **Fig. 3E**). In contrast, tissue-specific alternative splicing was observed for rtn4.2, with rtn4.2-B2 occurring only in muscle and rtn4.2-B3 in kidney and liver (**Fig. 3F**).

Rtn4.1-C mRNA was detectable in eye, muscle, kidney and liver (**Fig. 3G**). In comparison, rtn4.2-C transcription occurred at a much lower level with clearly detectable expression only in heart and muscle (**Fig. 3H**). Similarly, the rtn4.1-N and rtn4.2-N isoforms were both mainly expressed in heart and muscle (**Fig. 3I**, **J**). Taken together, these RT-PCR results indicate that the various transcripts of each *Xenopus rtn4* gene are differentially expressed. While the major -A, -B and -N isoforms have a comparable expression pattern for both *Xenopus rtn4* genes, the distribution of the -C form as well as of minor -A and -B splice variants differ between the two genes.

4.4.4 Distribution of Xenopus *Nogo-A/RTN4-A protein*

Selected A-specific regions of RTN4.1 were recombinantly expressed (see Materials and Methods) and used for the generation of polyclonal antisera AS702 and AS706 (**Fig. 1**). To show whether the obtained antisera are specific for RTN4.1 or recognize both *Xenopus* RTN4-A proteins, a part of RTN4.1-A (protein 833, **see Fig. 1**), of RTN4.2-A (protein 834) and an unrelated control protein were recombinantly expressed (**Fig. 4C**, left panel) and Western blots were probed with AS702 (**Fig. 4C**, middle panel) and AS706 (**Fig. 4C**, right panel). Both antisera recognized RTN4.1-A as well as RTN4.2-A proteins (**Fig. 4C**) and did not discriminate between the RTN4-A-proteins of the two genes.

In *Xenopus* spinal cord homogenate, AS702 (**Fig. 4A**) and AS706 (data not shown) recognized two bands of approximately 200 kD. Since the calculated molecular weights (113.99 kD/113.59 kD) and pIs (4.4/4.5) of the two Nogo-A1/RTN4-A1 proteins are almost identical, the second band most probably represents a different posttranslational modification of one or both proteins. In comparison to rat Nogo-A (about 220 kD; **Fig. 4A**), the *Xenopus* proteins migrated faster in SDS-PAGE, which is consistent with the 13 kD difference in the calculated molecular weights. Western blot studies on *Xenopus* tissues revealed that Nogo-A/RTN4-A expression was mainly restricted to the nervous system, which is in accordance with the RT-PCR analysis. In addition to spinal cord, two protein forms were detected in tectum opticum, forebrain, sciatic and optic

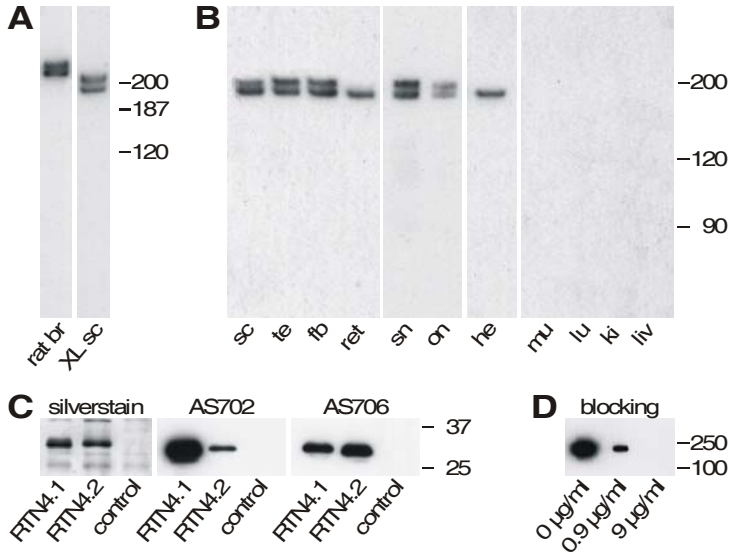

Fig. 4: *Western blot analysis of Xenopus Nogo-A/RTN4-A protein expression*

A) *Xenopus* Nogo-A/RTN4-A proteins detected with AS702 in spinal cord homogenate (XL sc) exhibit a lower molecular weight than the homologous rat protein detected with AS472 (Chen et al., 2000) in brain homogenate (rat br). Rat and *Xenopus* Nogo-A proteins migrate aberrantly slow in SDS-PAGE due to their acidic nature.

B) Expression of Nogo-A/RTN4-A proteins in different *Xenopus* tissues was analyzed with the Nogo-A specific AS702.

sc, spinal cord; te, tectum opticum; fb, forebrain; ret, retina; sn, sciatic nerve; on, optic nerve; he, heart; mu, muscle; lu, lung; ki, kidney; liv, liver.

C) A part of RTN4.1-A (protein 833, see **Fig. 1**), of RTN4.2-A (protein 834) and an unrelated control protein were recombinantly expressed (left panel, silver staining) and Western blots were probed with AS702 (middle panel) and AS706 (right panel). AS702 and AS706 recognized both RTN4.1-A and RTN4.2-A.

D) Tectum opticum homogenate was probed with AS706 and a concentration-dependent signal reduction was achieved by blocking the antiserum with increasing amounts of recombinantly expressed 706 protein (0 µg/ml; 0.9 µg/ml; 9 µg/ml). AS, polyclonal antiserum.

nerves, but only one was found in retina and heart (**Fig. 4B**). No Nogo-A/RTN4-A protein was observed in non-neuronal tissues (i.e. muscle, lung, kidney or liver). Specificity of polyclonal AS706 for *Xenopus* RNT4-A was shown on Western blots of tectum opticum homogenate. Concentration-dependent signal reduction was achieved by blocking the antiserum with increasing amounts of recombinantly expressed 706 protein (**Fig. 4D**). Adding 0.9 µg/ml 706 protein to the antibody solution significantly reduced the signal whereas a concentration of 9 µg/ml led to a complete loss.

Immunostaining on cross sections of adult *Xenopus* spinal cord revealed Nogo-A/RTN4-A expression in myelinated tracts of the white matter (**Fig. 5C**), as was observed for the rat Nogo-A protein (Chen et al., 2000). The staining pattern was comparable to the distribution of the oligodendrocyte markers Olig (**Fig. 5A**), O4 (data not shown) and of the IN-1 antibody (**Fig. 5B**). On sagittal sections of *Xenopus* brain, Olig labeled myelinated longitudinal and transverse fiber tracts in the ventral part of the brainstem (**Fig. 5D**). Corresponding fiber tracts were also detected, though weaker, with the IN-1 antibody (**Fig. 5E**). In addition, Olig brightly stained a single layer in the optic tectum that was not revealed with IN-1. Nogo-A/RTN4-A expression detected after Clark's fixation with AS706 (**Fig. 5F**) and AS702 (data not shown) encompassed myelinated as well as cellular regions of the *Xenopus* brain. Myelinated fiber tracts in the brainstem and in the

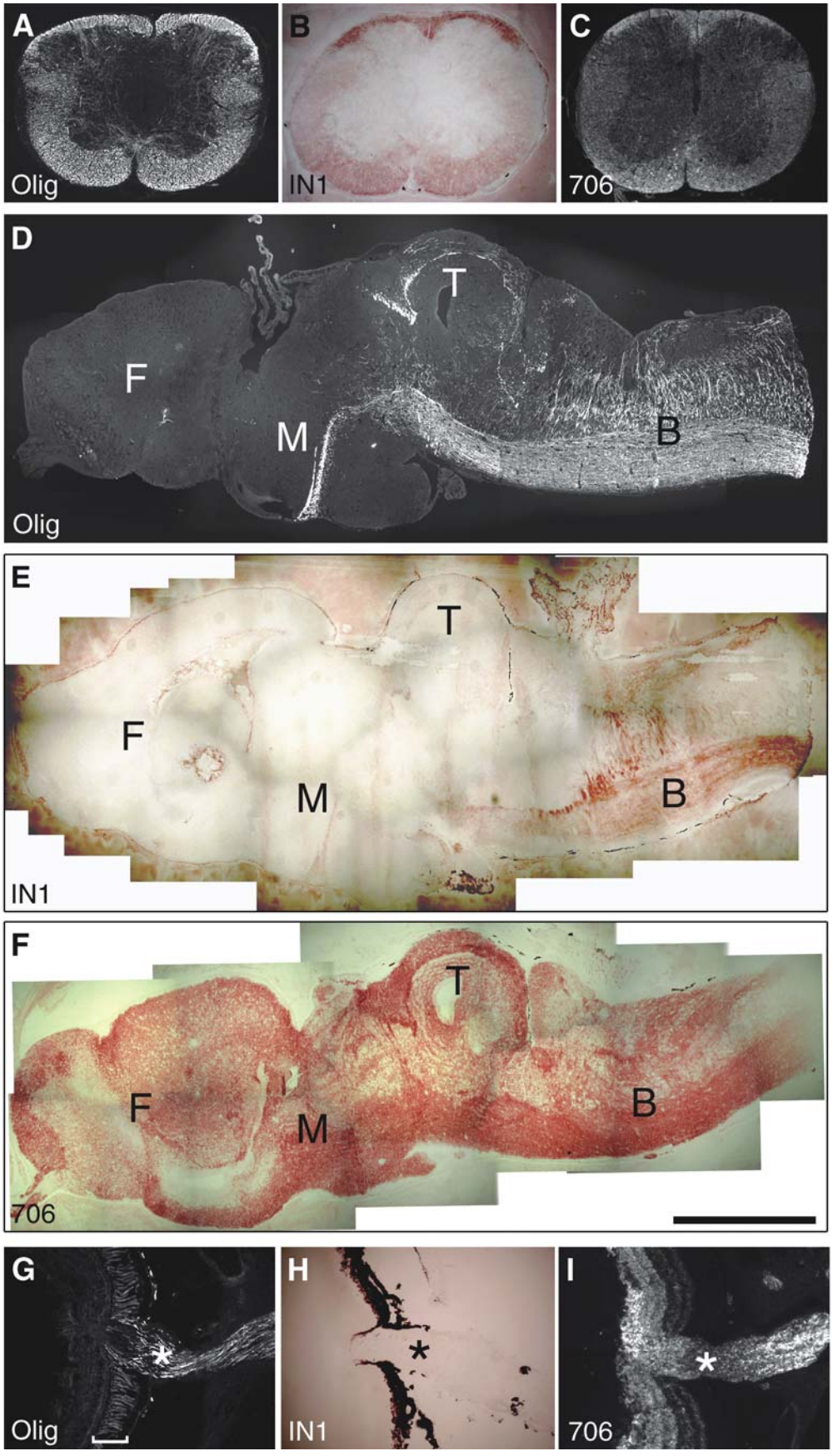

Fig. 5: *Immunolocalization of Nogo-A/RTN4-A protein in the Xenopus CNS*

Sections of *Xenopus* spinal cord (**A**-**C**; cross), brain (**D**-**F**, sagittal) and optic nerve (**G**-**I**, longitudinal) were immunostained with AS706 (**C**, **F**, **I**). The expression of Nogo-A/RTN4-A protein was compared to the distribution of the oligodendrocyte-specific marker Olig (**A**, **D**, **G**) and the mAb IN-1 staining (**B**, **E**, **H**). Nogo-A is detected in myelinated fiber tracts of the spinal cord (**C**), brain (**F**) and optic nerve (**I**). AS706 also labels unmyelinated regions in the forebrain/midbrain (**F**).
B, brainstem; F, forebrain; M, midbrain; T, tectum opticum; *, optic nerve; [, unspecific staining of photoreceptors. Scale bar is 500 µm in **A**-**C**, 1000 µm in D-F and 200 µm in **G**-**I.**

optic tectum were stained. In addition, extensive labeling of non-myelinated areas that has also been demonstrated for rat Nogo-A (Huber et al., 2002) was observed especially in the forebrain region (**Fig. 5F**). Myelin in the adult optic nerve was detected with the Olig marker (**Fig. 5G**) and corresponded to staining pattern of AS706 (**Fig. 5I**) and AS702 (data not shown), indicating Nogo-A/RTN4-A expression in the optic nerve and tract. The IN-1 antibody, however, failed to label the *Xenopus* optic nerve (**Fig. 5H**), which is consistent with our earlier results (Lang et al., 1995). Localization of Nogo-A/RTN4-A protein in *Xenopus* CNS myelin was consolidated by immunostaining of cultured oligodendrocytes isolated from spinal cord (**Fig. 6A**) and optic tectum (**Fig. 6C**), respectively. After permeabilisation, oligodendrocytes from both tissues were strongly positive for Nogo-A/RTN4-A - in particular the radially organised cytoplasm (**Fig. 6A, C**). Antibody specificity for *Xenopus* Nogo-A/RTN4-A was verified in control experiments. AS706 no longer stained the oligodendrocytes from spinal cord (**Fig. 6B**) and tectum opticum (**Fig. 6D**) after preincubation with the recombinant protein used for its generation.

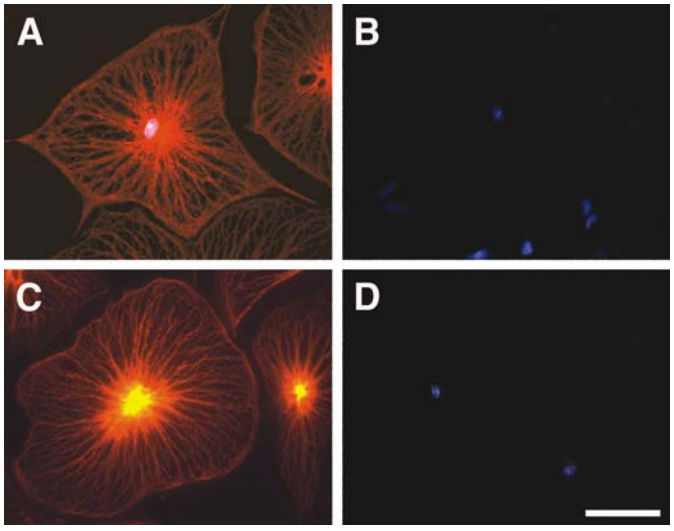

Fig. 6: *Detection of Nogo-A/RTN4-A protein in Xenopus oligodendrocytes*

Cultured oligodendrocytes isolated from *Xenopus* spinal cord (**A**, **B**) or optic tectum (**C**, **D**) were stained with the Nogo-A/RTN4-A specific AS706 (red) and the nuclear stain DAPI (blue). Nogo-A/RTN4-A is predominantly detected in intracellular compartments after permeabilization (**A**, **C**).

This staining is blocked by preincubation of AS706 with the protein used for antibody generation (**B**, **D**).

Scale bar is 50 µm.

The staining pattern with *Xenopus* Nogo-A/RTN4-A antisera was strongly dependent on the fixation method. After formaldehyde fixation, Nogo-A/RTN4-A was detected in specific cells and their processes in spinal cord (**Fig. 7A**) and brain sections (**Fig. 7D**). These cells were not recognized by the oligodendrocyte marker Olig (**Fig. 7B**, **E** and superpositions in **Fig. 7C**, **F**) and probably represent neurons, as shown in rat (Huber et al., 2002). Under these conditions, Nogo-

A/RTN4-A staining of white matter and oligodendrocyte cell bodies (identified by Olig, **Fig. 7H**) was lost (**Fig. 7G**).

These results demonstrate that *Xenopus* Nogo-A/RTN4-A proteins are expressed in oligodendrocytes, CNS myelin and subpopulations of neurons. This pattern is comparable to that of the rat ortholog, which may indicate related functions.

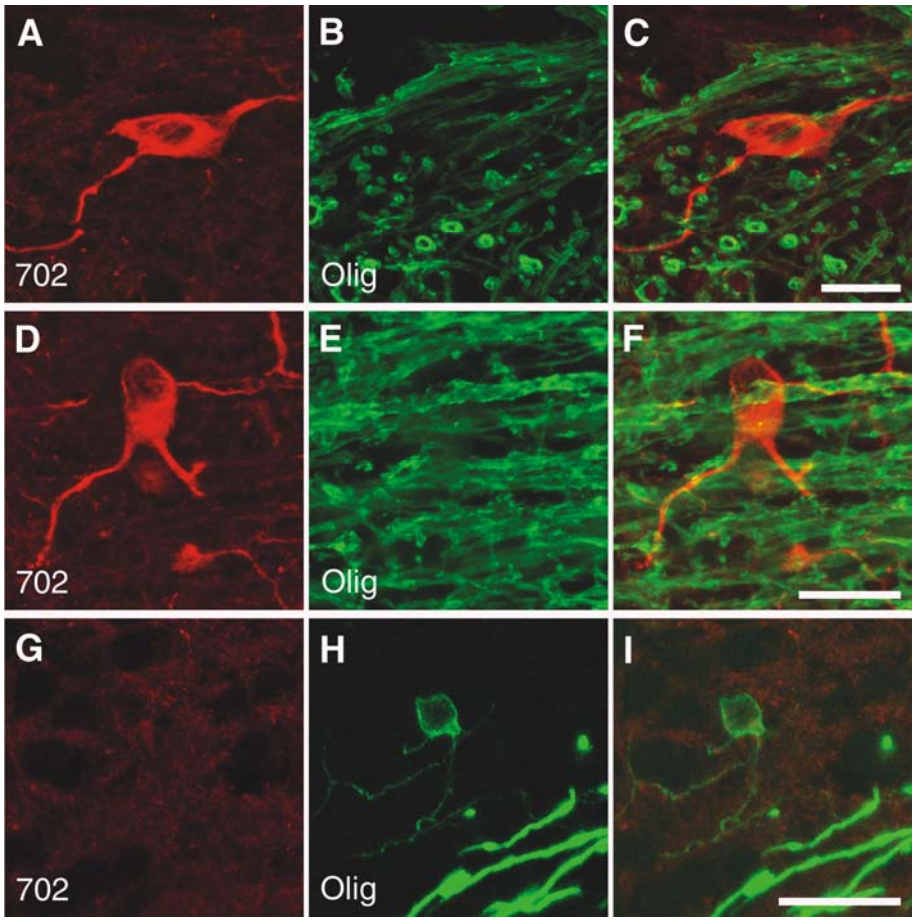

Fig. 7: *Detection of Nogo-A/RTN4-A protein in neurons*

Confocal microscopic analysis was performed on PFA-fixed sections of *Xenopus* spinal cord (**A**-**C**) and brain (**D**-**I**). The cellular staining observed with AS702 (**A**, **D**) does not colocalize with the myelin marker Olig (**B**, **E**), indicating neuronal expression of Nogo-A/RTN4-A. With this fixation protocol, no staining of oligodendrocyte cell bodies (identified by Olig; **H**) was observed with AS702 (**G**).

Superpositions of the two stainings are shown in C, F and I, respectively. Scale bar is 20 µm.

4.5 Discussion

Here, I report the identification of *nogo*/*rtn4* genes in *Xenopus laevis* and provide evidence for the expression of Nogo-A homologous proteins. Inhibitory proteins like Nogo-A, MAG and OMgp (Chen et al., 2000; McKerracher et al., 1994; Wang et al., 2002b) are suggested to impair axonal regeneration in the adult mammalian CNS. Since *Xenopus* spinal cord oligodendrocytes and CNS

myelin also exert inhibitory functions *in vitro* (Lang et al., 1995), similar proteins are expected in this species. In contrast, CNS axons readily regenerate in the optic nerve and spinal cord of fish and urodeles (Clarke et al., 1988; Gaze, 1970). Anura, like *Xenopus laevis*, take an intermediate position: retinal ganglion cell axons are capable of lifelong regeneration (Gaze, 1970) but spinal cord fiber tracts fail to regenerate after metamorphosis and myelination of axons (Beattie et al., 1990). Our present results show that Nogo-A orthologs as candidate growth inhibitory factors exist in frogs.

Two independent *rtn4* genes (*rtn4.1* and *rtn4.2*) that result from the tetraploidization of the *Xenopus* genome were identified. As in mammals, several mRNA transcripts are generated from *rtn4.1* and *rtn4.2* either through alternative splicing (rtn4-A; rtn4-B) or probably alternative promoter usage (rtn4-C; rtn4-N). The sequences of *Xenopus* rtn4-A, -B and -C are related to the three major transcripts of the mammalian *nogo/rtn4* gene whereas *Xenopus* rtn4-N is a newly identified short form that has not been identified in mammals (Oertle et al., 2003a).

The expression of the main *Xenopus* Nogo-A/RTN4-A isoforms (RTN4-A1) of both *rtn4.1* and *rtn4.2* genes is mostly restricted to CNS regions and to heart as shown by RT-PCR and Western blotting. This pattern is comparable to Nogo-A expression in mammals as summarised in **Table 1**. Immunostainings with antisera raised against *Xenopus* Nogo-A/RTN4-A on tissue sections are also consistent with the Nogo-A distribution in rodents (Huber et al., 2002; Josephson et al., 2001; Wang et al., 2002c). *Xenopus* Nogo-A/RTN4-A is expressed in myelinated tracts of the spinal cord and hindbrain, i.e. regions labeled by the myelin marker Olig (Steen et al., 1989). This distribution corresponds to the outcome of earlier functional assays demonstrating the presence of axon growth inhibitory activity in myelin and oligodendrocytes of the *Xenopus* spinal cord (Lang et al., 1995). *Xenopus* Nogo-A/RTN4-A specific antisera also labeled isolated oligodendrocytes in culture. Thus, the distribution of *Xenopus* Nogo-A/RTN4-A in oligodendrocytes and CNS myelin is consistent with its postulated role as an inhibitor for axon regeneration.

	RTN4-A1		RTN4-B1		RTN-C		RTN4-N
	Xenopus	Human/Rat	Xenopus	Human/Rat	Xenopus	Human/Rat	Xenopus
Spinal cord	++	++	+	+	-	±	-
Tectum*	++	++	+	+	-	±	-
Forebrain	++	++	+	+	-	±	-
Eye	++	++	++	+	+ (4.1) - (4.2)	+	+ (4.1) - (4.2)
Sciatic Nerve	++ (4.1) + (4.2)	±	++	++	-	-	-
Heart	++	+	++	+	- (4.1) + (4.2)	-, + ($)	++
Muscle	±	+, - (#)	++	+	++ (4.1) + (4.2)	++	++
Lung	±	-	++ (4.1) + (4.2)	++	-	-	-
Kidney	±	-	++ (4.1) + (4.2)	+	+ (4.1) - (4.2)	+	-
Liver	-	-	++ (4.1) + (4.2)	-	++ (4.1) - (4.2)	+, - ($)	-

Table 1: *Comparison of semiquantitative expression levels of the major RTN4 isoforms in Xenopus and mammals (human, rat)*

Data for *Xenopus* are based on RT-PCRs shown in **Fig. 3** and Western blots (**Fig. 4B**) and apply to both genes if not indicated in parentheses. Data for human and rat are taken from tables in (Hunt et al., 2002a; Oertle and Schwab, 2003).
++, strong expression; + clear expression; ± weak expression; - no detectable expression
*, tectum opticum in *Xenopus*; midbrain structures (thalamus, amygdala, habenular nuclei) in mammals; $, conflicting data; # positiv in immature skeletal muscle, negativ in adult muscle

However, Nogo-A/RTN4-A1 is also detected in myelin and oligodendrocytes of the optic nerve and the forebrain. Moreover, RTN4-A1 proteins are already expressed early in development (data not shown) when oligodendrocytes or neurons are not yet present. An early presence of Nogo-A has also been described in a variety of foetal rat tissues (Huber et al., 2002; Josephson et al., 2001). This early appearance and the intracellular localization of Nogo-A/RTN4-A suggest further, yet unidentified functions that are not related to axonal growth inhibition.

The expression pattern revealed by RTN4-A specific antisera differ from the weak and more restricted staining observed with mAb IN-1. One speculation is that IN-1 recognizes a Nogo-A modification or conformational epitope relevant for surface exposure and function. This would explain why only mAb IN-1 is able to discriminate between spinal cord and forebrain oligodendrocytes and to partially neutralize the inhibitory activity of *Xenopus* spinal cord and hindbrain myelin (Lang et al., 1995). This implies that changes in subcellular distribution (intracellular vs. surface) or posttranslational modifications are essential for the acquisition of the suggested inhibitory activity of Nogo-A in the adult CNS *in vivo*. Future analyses of the inhibition process and the elucidation of the respective roles of *Xenopus* RTN4.1-A and RTN4.2-A will be required to address those unresolved problems. Moreover, relevant axonal receptors remain to be identified. The contribution of other inhibitory myelin components such as MAG, OMgp and proteoglycans (Morgenstern et al., 2002) needs to be considered and the potential role of Nogo-66 in the regeneration/inhibition scenario (GrandPré et al., 2000) has to be clarified in frogs.

Apart from myelinated regions, *Xenopus* Nogo-A/RTN4-A antisera stain forebrain and midbrain regions that are not detected by myelin markers. These are seemingly neurons and neuropil, which is consistent with the detection of mammalian Nogo-A in neurons and neuronal processes (Huber et al., 2002; Josephson et al., 2001; Wang et al., 2002c). The putative neuron-specific functions of Nogo-A, which probably differ from the oligodendrocyte-related inhibitory activity, remain to be explored.

Compared to the preferential expression of Nogo-A/RTN4-A in the nervous system, the -B isoforms are ubiquitously expressed with highest levels in non-neuronal tissues (**Table 1**). High-level expression of the Nogo-A splice form in a specific tissue seems to be paralleled by low levels of the -B isoforms, as is observed in mammals (Oertle et al., 2003a). Besides the many

similarities between *Xenopus* and mammalian Nogo-A expression, differences exist. The -A isoform is not detected in mammalian lung and kidney, but present in these organs in *Xenopus*, and Nogo-B in liver is only found in *Xenopus*. (**Table 1**; Hunt et al., 2002b; Oertle and Schwab, 2003). In addition, more minor splice variants of Nogo-A and -B exist in *Xenopus* than in mammals, resulting from the alternative usage of two small exons located between the A/B-specific exon and the large A-specific exon (**Fig. 1**). The weak expression of these minor splice variants is comparable to the expression levels of the mammalian minor splice variants (RTN4-B2, -D, -E, -F, -G, -Aa, -Ab; Oertle et al., 2003a) and could indicate a modulatory or developmentally regulated role as suggested for the human testis-specific RTN4-E splice variant (Zhou et al., 2002).

As in mammals, *Xenopus* RTN4-C is enriched in the adult skeletal muscle (**Table 1**). The *Xenopus* rtn4.1-C isoform is also expressed in liver, eye and kidney. In contrast, the rtn4.2-C paralog is hardly detectable except for muscle. This could indicate that the putative *Xenopus rtn*4.2-C promoter is undergoing transcriptional silencing.

The rtn4-N mRNAs have a similarly restricted expression pattern, both being enriched in heart and muscle (**Fig. 3**, **Table 1**). An N-specific exon has not been identified in mammals. In zebrafish, however, a homologous rtn4-N is present, but no rtn4-A, -B and -C transcripts (Klinger et al., 2002). It can therefore be hypothesized that the N-terminal sequences specific for rtn4-A/-B and rtn4-C were newly acquired during the evolution of land vertebrates (Oertle et al., 2003b). Accordingly, amphibians (e.g. *Xenopus laevis*) express the 'ancestral' rtn4-N (that is also found in fish) and the ‘modern’ rtn4-A, -B and -C forms present in 'higher' vertebrates. *Xenopus* is, so far, the evolutionary 'lowest' organism that has the exceptionally large Nogo-A-specific exon, which codes for the potent inhibitory region NiG-Δ20 contained only in Nogo-A (Oertle et al., 2003d). Hence, the *Xenopus rtn4* genes might help to elucidate how Nogo-A acquired its inhibitory function. Conversely, *Xenopus* expresses the 'ancient' isoform rtn4-N, allowing the exploration of 'old' rtn4 features that are relevant in fish and frogs.

The duplication of *Xenopus nogo/rtn*4 was dated to ~30 MYA using the rate of silent nucleotide substitutions as a "molecular clock" (Hughes and Hughes, 1993). In general, genome duplication events increase the amount of genetic material, which is considered as prerequisite for the development of new genes with new functions. Duplicated genes can adopt different fates: both are expressed and have similar function, one copy accumulates mutations and eventually turns into a non-functional pseudogene, or a series of non-deleterious aa-altering mutations transforms one copy into a gene with a new function, as can be determined by a significantly faster evolutionary rate (Van de Peer et al., 2001). On the other hand, mutations in regulatory elements

together with the conservation of coding regions can alter the spatiotemporal expression of two genes with comparable function. The respective *Xenopus* rtn-4 transcripts of both genes display similar expression patterns, suggesting that the promoter regions responsible for the transcriptional regulation of these isoforms did not undergo major functional changes after the duplication event. Thus, these genes appear to be redundant rather than complementary, which is also supported by our observation that neither of the two copies in comparison to the human ortholog evolved faster. However, both *rtn4* genes accumulated more aa altering mutations than one might expect for an evolutionary time of ~30 MYA (Hughes and Hughes, 1993), which suggests the commencement of a potential diversification and of functional changes of both copies.

The present identification of nogo/rtn4 in *Xenopus laevis* and the analysis of the expression pattern of Nogo-A/RTN4 provide a first step towards understanding the evolution of myelin associated proteins with axon growth inhibiting effects. Future experiments will determine the contribution of Nogo-66 and the Nogo-A specific region to the growth inhibitory properties of *Xenopus* spinal cord myelin. A possible approach to tackle this issue is the generation of function-blocking antibodies binding to the oligodendrocyte surface. In addition, this study is a first entry point for functional analysis of Nogo-A during development and axonal growth.

The synthesis of ancient and modern features within the *nogo/rtn4* gene locus of *Xenopus* as well as the indications for a beginning diversification of the duplicated paralogs are relevant for the comprehension of gene evolutionary processes, particularly in the transition to land vertebrates.

4.6 Acknowledgements

C.A.O.S. was supported by the Deutsche Forschungsgemeinschaft (DFG), M.K. by the "Stiftung der Deutschen Wirtschaft für Qualifizierung und Kooperation e.V. (sdw)" T.O. and M.E.S. by the Swiss National Science Foundation (Grant No. 31-63633) and by the NCCR on Neural Plasticity and Repair. The hybridoma supernatant of the monoclonal antibody Olig (developed by M. Constantine-Paton) was obtained from the Developmental Studies Hybridoma Bank developed under auspices of the NICHD and maintained by the University of Iowa, Department of Biological Science. Iowa City, IA 52242. We thank U. Binkle for technical assistance and J. Taylor for critical reading of the manuscript.

Published as:

Klinger, M., Diekmann, H., Heinz, D., Hirsch, C., Hannbeck von Hanwehr, S., Petrausch, B., Oertle, T., Schwab, M. E. and Stuermer, C. A. O. (2004). Identification of two nogo/rtn4 genes and analysis of Nogo-A expression in Xenopus laevis. *Mol Cell Neurosci* **25**, 205-16.

4.7 Supplementary data

Nr	Sequence	Position (bp)	
I	CTCTCAGCCGTTCTCTGGATCCC	135-157	of (XENLA)RTN4.1-A3
II	GGT AAA TGA CTG GTG ATC CTC GAT ACG	570-596	of (XENLA)RTN4.1-A3
III	GTG ACT TGA TAA AGG GAA CCG AAT CTG T	1816-1843	of (XENLA)RTN4.1-A3
IV	GCT CCT TGA CTG TGC AGT TGA CAT GG	2897-2922	of (XENLA)RTN4.1-A3
V	TTA ATG TCC CGC CAG TAA ATA AGG TCG	2514-2540	of (XENLA)RTN4.1-A3
VI	CTC TCA CAC GTT CCC TGT CTC CT	108-130	of (XENLA)RTN4.2-A3
VII	CTA AAG TGT CTA TTA ATG ACC TGG ACG CG	540-568	of (XENLA)RTN4.2-A3
VIII	GCG ACT TAA TAA AGG GAA CTC AAT CTG C	1673-1700	of (XENLA)RTN4.2-A3
IX	CTC AGC GAC TGT GCGATT GAC CTG A	2754-2778	of (XENLA)RTN4.2-A3
X	TTA ATG TCC CGC CAG TAA ATC AGA TCC	2481-2507	of (XENLA)RTN4.2-A3
XI	ACC AAC CTT GGA TTG CCC GTC AG	-25 - -3	of (XENLA)RTN4-1-C
XII	GTC TGA TGT GCT CTT GAG A	3012-3030	of (XENLA)RTN4-1-A3
XIII	ACC TCC CGA GTG CAC C	-40 - -25	of (XENLA)RTN4-1-N
XIV	GTG AGT GTC GGT GTG TG	-73 - -57	of (XENLA)RTN4-2-N
XV	GGT CTG AAG TAT TTT TCA GG	2979-2998	of (XENLA)RTN4-2-A3

Supplementary Table 1A: *Primers for RT-PCR*

Nr	Sequence	Position (bp)	
a	TGA TTT CCC TGT TCA GTA TTC CTG TC	2930-2955	of (XENLA)RTN4.1-A3
b	TCT CAA GAG CAC ATC AGA CCT GAT TCTc	3012-3039	of (XENLA)RTN4.1-A3
c	TCA TTT CCC TGT TCA GTA TTC CTG TT	2897-2922	of (XENLA)RTN4.2-A3
d	CCT GAA AAA TAC TTC AGA CCT GAT TTT G	2979-3006	of (XENLA)RTN4.2-A3

Supplementary Table 1B: *Primers for intron amplification*

±	(HUMAN)rtn4-A versus (RAT)rtn4-A		(XENLA)rtn4.1-A1 versus (XENLA)rtn4.2-A1		(XENLA)rtn4.1-A1 versus (HUMAN)rtn4-A	(XENLA)rtn4.2-A1 versus (HUMAN)rtn4-A
	mean d_S ± SE	mean d_N ±SE	mean d_S ± SE	mean d_N ±SE	mean d_N ±SE	mean d_N ±SE
full length rtn4-A1	44.3 ±3.0	11.9 ±0.7	26.6 ±2.2	10.3 ±0.7	59.6 ±2.5	58.4 ±2.6
A/B specific region	49.1 ±7.9	7.6 ±1.5	39.9 ±8.9	19.0 ±3.0	84.0 ±11.1	76.0 ±10.4
A specific region	46.5 ±3.8	15.5 ±1.0	21.5 ±2.4	10.6 ±0.9	79.6 ±3.9	75.6 ±3.5
RHD	33.1 ±5.9	1.2 ±0.5	38.7 ±6.4	4.0 ±1.0	13.2 ±2.2	14.1 ±2.2

Supplementary Table 2: *Rate of synonymous (d_S) and nonsynonymous (d_N) substitions*

5 Identification of Nogo-66 receptor (NgR) and homologous genes in fish

5.1 Abstract

The Nogo-66 receptor NgR has been implicated in the mediation of inhibitory effects of CNS myelin on axon growth in the adult mammalian CNS. NgR binds to several myelin-associated ligands (Nogo-66, myelin associated glycoprotein, oligodendrocyte-myelin glycoprotein) which - among other inhibitory proteins - impair axonal regeneration in the CNS of adult mammals. In contrast to mammals, severed axons readily regenerate in the fish CNS. Nevertheless, fish axons are repelled by mammalian oligodendrocytes *in vitro*. Therefore, the identification of fish NgR homologs is a crucial step towards understanding NgR functions in vertebrate systems competent of CNS regeneration. Here, the discovery of four zebrafish (*Danio rerio*) and five fugu (*Takifugu rubripes*) NgR homologs is reported. Synteny between fish and human, comparable intron-exon structures and phylogenetic analyses provide convincing evidence that the true fish orthologs were identified. The topology of the phylogenetic trees shows that the extra fish genes were produced by duplication events that occurred in ray-finned fishes prior to the divergence of the zebrafish and pufferfish lineages. Expression of zebrafish NgR homologs was detected relatively early in development and prominently in the adult brain suggesting functions in axon growth, guidance or plasticity.

5.2 Introduction

In contrast to mammals, lesioned axons readily regenerate in the fish CNS and re-establish appropriate connections with their targets (Gaze, 1970). This success of axonal regeneration depends on intrinsic properties of fish neurons and on a growth-promoting environment for regenerating axons (Stuermer et al., 1992). Fish CNS myelin as well as oligodendrocytes are permissive substrates for axonal growth and do not induce growth cone collapse (Ankerhold et al., 1998; Bastmeyer et al., 1991). Therefore, homologs of mammalian inhibitory proteins such as the IN-1 antigen (Caroni and Schwab, 1988a), MAG (Mukhopadhyay et al., 1994) and oligodendrocyte-myelin glycoprotein (OMgp) (Kottis et al., 2002) are most probably not present in fish (Bastmeyer et al., 1991; Wanner et al., 1995). On the other hand, rat and bovine CNS myelin as well as rat oligodendrocytes are inhibitory substrates for regenerating goldfish retinal axons *in vitro*, indicating that fish axons are sensitive to mammalian neurite growth inhibitors (Bastmeyer et al., 1991; Wanner et al., 1995).

In mammals, the Nogo-66 receptor (NgR) has been proposed to play an important role in the mediation of axonal growth inhibition (Domeniconi et al., 2002; Fournier et al., 2001; Liu et al., 2002; Wang et al., 2002b). NgR is a GPI-linked, leucine-rich repeat (LRR) protein that binds to the 66 amino acid (aa) loop between the two C-terminal hydrophobic domains of Nogo (termed Nogo-66; GrandPré et al., 2000) and transduces Nogo-66 mediated axonal inhibition (Fournier et al., 2001). The recent discovery that MAG and OMgp also require the interaction with NgR for their inhibitory effects (Domeniconi et al., 2002; Liu et al., 2002; Wang et al., 2002b) is suggestive of a common signaling pathway for these myelin inhibitors.

It is an intriguing question whether fish posses an NgR ortholog and what its function might be in this class of organisms. Because CNS axons regenerate successfully in fish, the functions of fish NgR proteins are likely to differ from the mammalian function as transducer of growth inhibition. However, NgR might be involved in the mediation of the inhibitory effect of mammalian CNS myelin on fish axons *in vitro*. In this context, I set out to identify NgR homologs in fish. Four different NgR-related genes were cloned and sequenced from zebrafish and five genes were uncovered in the fugu genome. While the study was in progress, two additional NgR homologs were identified in human and rodents (Pignot et al., 2003) and the five fugu NgR genes were discovered (He et al., 2003). Phylogenetic relationships among all available NgRs demonstrate that this family of genes was produced by separate duplication events in the ancestors of vertebrates and early in actinopterygian evolution. In zebrafish, the mRNA distribution during development and in different adult tissues is consistent with a potential role for these proteins in the regulation of axon growth and plasticity.

5.3 Materials and methods

5.3.1 Cloning of zfNgR, zfNgRH1a, zfNgRH1b and zfNgRH2a

By searching the NCBI database, zebrafish genomic sequences homologous to human NgR were identified and amplified from cDNA with specific primers (**Supplementary Table 1**). Sequences were completed performing 5'- and 3'-RACE, respectively. In brief, mRNA was extracted from a pool of 48 hours post fertilization (hpf) zebrafish embryos (FastTrack™ 2.0 kit Invitrogen) and used 0.9 µg/reaction as template for the synthesis of either first-strand 5'-Ready cDNA using 5'-CDS and SMART II oligonucleodides or of 3'-Ready cDNA using 3'-CDS primer, according to the manufacturer's instructions (SMART RACE cDNA Amplification Kit BD Clontech). PCR fragments were directly subcloned into the pCRII cloning vector (Invitrogen) and plasmid DNA was prepared using the QIAprep® 8 Miniprep Kit (Qiagen). Both DNA strands were sequenced using the Abi Prism® BigDye™ Terminator Cycle Sequencing Kit (Applied Biosystems) and analyzed on an AbiPrism 3100 Genetic Analyzer. Single sequences were assembled using SeqMan™II of the DnaStar software package (GATC Biotech).

5.3.2 Sequence alignments, phylogenetic analysis

Zebrafish and fugu genomic sequences were obtained using blast algorithms (Altschul et al., 1997) at NCBI (www.ncbi.nlm.nih.gov/BLAST/),Ensembl(www.ensembl.org/Danio_rerio/blastview;www.ensembl.org/Fugu_rubripes/blastview) and the Doe Joint Genome Institute (www.aluminum.jgi-psf.org/prod/bin/runBlast.pl?db=fugu6) web pages. The fugu cDNAs were deduced from the respective genomic sequences by comparison with the zebrafish

cDNAs. The human, macaque, rat and mouse sequences were already available in GenBank (gi20127617, gi9280024, gi21311542, gi28496903, gi27701808, gi25056697, gi27500320 and gi29244159). Exon-intron structures were examined by comparison of cDNA against genomic sequences, considering the GT-AG rule of splice donor and acceptor sites.
Nucleotide sequences were translated using BioEdit (Hall, 1999) and aligned as amino acids using ClustalW (Thompson et al., 1994). The alignment was edited by hand and then converted back into nucleotides to produce a codon alignment. The multi-species NgR amino acid alignment was also used in a model-based HMMER 2.3 (Sean Eddy) search of the NCBI non-redundant (protein), ENSEMBL and Doe Joint Genome Institute databases for invertebrate (*Drosophila melanogaster, Anopheles gambiae*) and ascidian (*Ciona intestinalis*) orthologs. Phylogenies of NgR-related sequences were reconstructed using maximum parsimony (MP) and genetic distance-based methods with PAUP*4.0 (Swofford, 2002) and using a maximum likelihood (ML) approach with MrBayes (Huelsenbeck and Ronquist, 2001). The transition transversion ratio (1:1.41) was estimated using PAUP and included in the MP analyses. One MP analysis considered characters from the complete alignment and the second excluded 3rd codon positions. Two methods for estimating genetic distance were used, HKY85 (Hasegawa et al., 1985) and LogDet (Lockhart et al., 1994). Neighbor-joining (Saitou and Nei, 1987) trees were reconstructed from genetic distances. Support for nodes in the MP and NJ trees was assessed using 1000 bootstrap reiterations (Felsenstein, 1985). ML trees were reconstructed from the nucleotide alignment with nst=6 (Tavare, 1986) and rates=invgamma (Yang, 1993) and from the amino acid alignment using the blossum model (Henikoff and Henikoff, 1992). In the amino acid-based analysis rate variation among positions was assumed to follow a continuous gamma distribution approximated from eight discrete rate categories. The parallel version of MrBayes (Huelsenbeck and Ronquist, 2001) was used on four processors, one of each of four Markov Chains.
Mega (Kumar et al., 1994) was used to identify aa residues unique to one subfamily of NgR genes. Evolutionary rates between the human NgR genes were compared using a test developed by Tajima (Tajima, 1993) as implemented in Mega (Kumar et al., 1994). Signal peptides were predicted using SignalP V1.1 at http://www.cbs.dtu.dk/services/SignalP/ (Nielsen et al., 1997) and GPI-anchor sites using big-PI Predictor at http://mendel.imp.univie.ac.at/sat/gpi/gpi_server.html (Eisenhaber et al., 1999).

5.3.3 Radiation hybrid mapping and synteny analysis

Zebrafish NgRH1a, NgRH1b and NgRH2a were mapped on the LN54 radiation hybrid panel using standard conditions (Hukriede et al., 1999) and the respective web interface (http://mgchd1.nichd.nih.gov:8000/zfrh/beta.cgi). Since no unequivocal result was obtained for NgR on this panel, this receptor was mapped on the Goodfellow T51 radiation hybrid panel (Research Genetics, Inc.) by instant mapping at http://134.174.23.167/zonrhmapper/instantMapping.htm.
For synteny analysis (Woods et al., 2000), other zebrafish genes and ESTs already mapped on the LN54 and T51 radiation hybrid and HS maps (http://zfin.org/cgi-bin/mapper_select.cgi) were assigned to putative human orthologs by BLASTX searches (Altschul et al., 1997) against the NCBI human non-redundant (nr) protein sequence database (http://www.ncbi.nlm.nih.gov/blast/blast.cgi). For EST clones that have been sequenced at the 5' and 3' ends, both sequences were used for BLASTX searches. If the results of these searches had expect scores (*E* values) of ≤-5, the putative orthologs were further tested with reciprocal searches against the zebrafish subset of nr sequences and dbEST databases. A human ortholog was confirmed if the original zebrafish gene or EST (or a gene or EST that showed highly significant overlap with the original sequence) was in the top 15 matches of the reciprocal search by TBLASTN. Fugu synteny data were retrieved with MartView (http://www.ensembl.org/Fugu_rubripes/martview).

5.3.4 Southern blotting

Genomic DNA was prepared from one individual *honkong* inbread adult zebrafish and digested with *Bcl I*, *Bgl II*, *Hind III* and *Pst I*, respectively. After electrophoretic separation, genomic DNA fragments were transferred to a Hybond N^+ nitrocellulose membrane (Amersham Biosciences) under alkaline conditions (Chomczynski and Qasba, 1984). The DNA probe was labeled using the 'AlkPhos Direct' labeling kit (Amersham Biosciences) and applied according to the manufacturer's protocol, with longer prehybridization and washing times and increased washing volumes. Blots were developed with CDP-Star detection reagent (Amersham Biosciences).
To determine the expected number and sizes of bands to be detected, restriction maps of the subcloned and sequenced southern probe and of the relevant genomic region were established using MapDraw™ of the DnaStar software package (GATC Biotech). Due to polymorphisms in the genomic sequences, the size of the expected fragments remains an estimation.

5.3.5 RT-PCR

100 zebrafish embryos (appr. 100 mg) for each stage or 50 mg of various adult tissues were used for preparation of total RNA with the RNeasy Mini Prep Kit (Qiagen) following manufacturer's instructions. Muscle tissue was

additionally subjected to proteinase K digestion (200 µg/30 mg tissue). First-strand cDNA was synthesized under standard conditions with the Superscript First-Strand Synthesis System (Invitrogen) using oligo$(dT)_{12-18}$ primer. Zero-transcriptions (without Superscript II in the reaction) were performed in parallel, to control for genomic DNA contaminations in subsequent PCRs. Amount and quality of the different cDNA samples were evaluated comparing the expression level of the housekeeping gene actin. Primer informations are listed in **Supplementary Table 1**.

5.3.6 GenBank accession numbers.

zfNgR cDNA sequence, AY257178; zfNgRH1a cDNA, AY263332; zfNgRH1b cDNA, AY263334; zfNgRH2a, AY263333

5.4 Results

5.4.1 Identification and phylogenetic analyses of fish NgRs

Database searches uncovered four different zebrafish (*Danio rerio*) genomic sequences with significant homology to human NgR. Full-length cDNAs were identified by RT-PCR, 5'- and 3'-RACE. Analysis of fugu (*Fugu rubripes*) genomic sequences revealed the presence of five NgR-related genes. The zebrafish (zf) genes were named zfNgR, zfNgRH1a, zfNgRH1b and zfNgRH2a and the fugu genes received analogous names, reflecting the results of the phylogenetic analyses (see below).

Using ClustalW and BioEdit an unambiguous alignment of 17 NgR-related sequences that was 819 nucleotides long was produced (see **Supplementary Figure 1**). The Drosophila Slit gene was the invertebrate sequence with the best match to the HMMER model, which was based upon an alignment of vertebrate NgR proteins. However, there are vertebrate Slit proteins that are more closely related to Drosophila Slit than NgR. There are no matches to the HMMER model based upon all vertebrate NgRs in the peptides annotated in the mosquito *Anopheles gambiae*) and ciona (*Ciona intestinalis*) genome databases. Therefore, it appears that no true orthologs of NgR are present in invertebrates and ascidians. Phylogenetic trees reconstructed using MP, ML and genetic distance-based methods had the same topology and produced trees comprised of distinct NgR, NgRH1 and NgRH2 clades (**Fig. 1**). This pattern was observed when all nucleotide positions were included in the analyses and also in the MP analysis excluding 3rd codon positions. The three NgR clades were well-supported (**Fig. 1**). Each clade included a human, mouse, zebrafish and at least one fugu sequence, indicating that the gene duplication events producing NgR, NgRH1 and NgRH2 occurred before the divergence of ray-finned fish (actinopterygians) and tetrapods (sarcopterygians). The NgR clade also included orthologs for macaque and rat. The NgRH1 clade contained two fugu and two zebrafish genes and the NgRH2 clade included two fugu genes and only one zebrafish gene (**Fig. 1**). In all phylogenetic analyses the relationships among the fish sequences were consistent with the hypothesis that the NgRH1 and NgRH2 duplicates were produced before the ancestors of zebrafish and fugu diverged.

The zebrafish transcripts encode proteins of 479 aa (NgR), 458 aa (NgRH1a), 457 aa (NgRH1b) and 478 aa (NgRH2a) (**Fig. 3A, Supplementary Fig. 3**). The sequences of the fugu proteins were deduced from genomic data by comparison with the zebrafish sequences, but their expression was not validated. They are 467 aa (NgR), 454 aa (NgRH1a) and 451 aa (NgRH2a) long (**Fig. 3A, Supplementary Fig. 4**). For fugu NgRH1b and NgRH2b, the first exon could not be identified

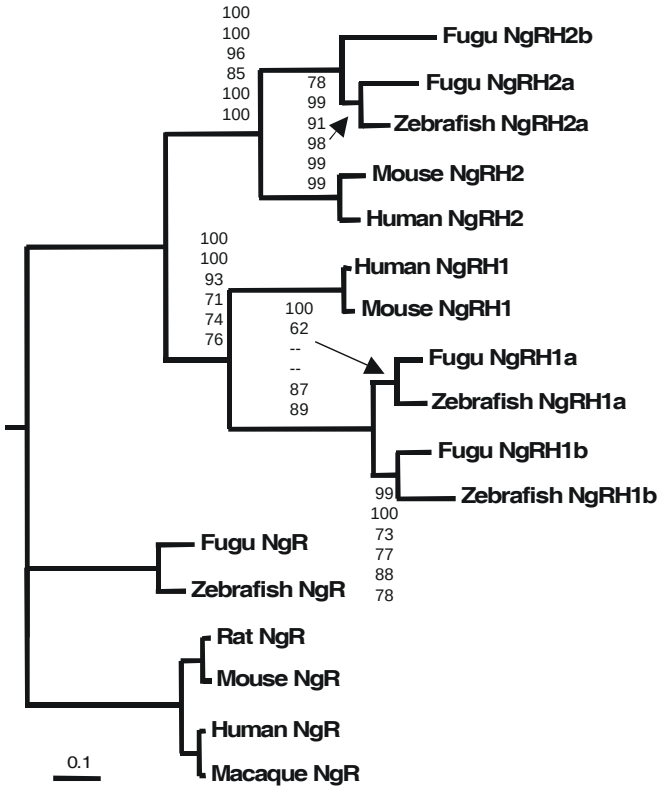

Fig. 1: *Evolutionary relationships among vertebrate NgR and NgR-related genes*

Topology shown is a consensus tree based upon maximum likelihood (ML) analysis of an amino acid (aa) alignment (273 positions, **Supplementary Fig. 1**). Placement of root reflects the results of an analysis that included the *Drosophila* Slit gene (252 aa positions, **Supplementary Fig. 2**). The same topology was reconstructed from a nucleotide alignment using MP, genetic distance estimates and ML. Support for nodes is 100% (all ML trees or all boostrap trees) except where indicated. Percent bootstrap support (1000 reiterations) is shown from top to bottom: ML analysis of aa alignment, ML analysis of nucleotides, MP analysis of 1st and 2nd codon positions, MP analysis of all positions, HKY genetic distance and LogDet genetic distance. Scale represents 10% protein sequence divergence.

Fugu, Fugu rubripes; Human, Homo sapiens; Macaque, Macaca fascicularis; Mouse, Mus musculus; Rat, Rattus norvegicus; Zebrafish, Danio rerio.

and the size of the respective proteins can therefore not be calculated. As in human, all proteins contain predicted signal sequences followed by eight leucine-rich repeat (LRR) domains that are framed by LRR amino- and carboxy-terminal (LRRNT, LRRCT) domains. At the C-terminus a region with only weak similarity among these related proteins is followed by a GPI anchorage site.

Mega (Kumar et al., 1994) was used to identify aa residues unique to one subfamily of NgR genes. The alignment used for this survey included Drosophila Slit in order to distinguish ancestral and derived subfamily-specific residues. This alignment was shorter (252 aa, **Supplementary Fig. 2**) than the NgR-only alignment (273 aa, **Supplementary Fig.1**) Eighty-three aa were conserved (monomorphic) in all NgRs and 57 of these were shared between the vertebrate NgRs and Drosophila Slit, meaning that the three NgR subfamilies differ from Drosophila Slit at 26 shared and monomorphic residues. The NgR subfamily is defined by six unique aa substitutions, four of which are derived. NgRH1 proteins have seven diagnostic and

derived residues, whereas NgRH2 proteins share eight diagnostic residues and of these seven are derived. Residues at position 134 (with respect to human NgR, **Supplementary Fig. 2**) are diagnostic for each of the three subfamilies. Note that all of these observations must be considered in light of limited species sampling (ingroup and outgroup) meaning that the number of diagnostic residues might decrease, when NgR sequences of more species are available. Most of the identified diagnostic residues have either polar or charged side chains. Mapping on the published NgR structure (Barton et al., 2003; He et al., 2003) revealed that 18 out of the 21 diagnostic aa are surface exposed and locate to the top and bottom part of the NgR ectodomain and not to the central, concave face of the curved ß-sheet (data not shown). This specificity for one subclass and their predominant surface exposure probably renders these aa essential for the discrimination between different ligands for NgR, NgRH1 and NgRH2.

Evolutionary rates between the human NgR genes were compared using a test developed by Tajima (Tajima, 1993) as implemented in Mega (Kumar et al., 1994). This rate test counts the number of unique substitutions in pairs of sequences relative to an outgroup (here Drosophila slit). NgRH1 and NgRH2 are more similar to one another than either is to NgR (mean number of aa substitutions: NgR to NgRH1: 114.9; NgR to NgRH2: 111.8; NgRH1 to NgRH2: 105.2). The respective value between the whole NgR family and Drosophila Slit (159.9) is significantly higher. This test was also used to compare substitution rates between pairs of duplicated fish genes (fugu NgRH1a and fugu NgRH1b, zebrafish NgRH1a and zebrafish NgRH1b, fugu NgRH2a and fugu NgRH2b) using the single copy human ortholog as the outgroup. In none of the comparisons a significant difference ($p < 0.05$) in substitution rates between pairs of NgR genes relative to the outgroup was discover. Of note was the large, but not significant, difference in unique substitutions between fugu NgRH1a (9) and fugu NgRH1b (18) relative to the outgroup (human NgRH1).

Taken together, these results show that NgR homologs with similar structural motifs as human NgR exist in actinopterygians and that this gene family has arisen through several separate duplication events. The presence of three distinct subclasses was supported by phylogenetic analyses as well as by the identification of diagnostic residues.

5.4.2 Conserved syntenies of fish and human NgR, NgRH1 and NgRH2

The zebrafish genes zfNgR, zfNgRH1a, zfNgRH1b and zfNgRH2a were mapped on LG5, LG1, LG14 and LG15 (LOD scores of 12.0, 15.7, 20.5 and 17.2), respectively, and compared to the location of the human orthologs (**Fig. 2**, **Supplementary Tables 2A-D**).

Conservation of synteny is found between zebrafish LG5 and human chromosome 22, establishing a new syntenic group containing NgR, the previously mapped gene *pes* (Woods et al., 2000) and four ESTs (**Fig. 2A**). An additional, so far unrecognized synteny is formed by eight other zebrafish ESTs on LG5 and their orthologs on human chromosome 12. ZfNgRH1a together with three neighboring ESTs on LG1 and zfNgRH1b with four ESTs on LG14 both define new

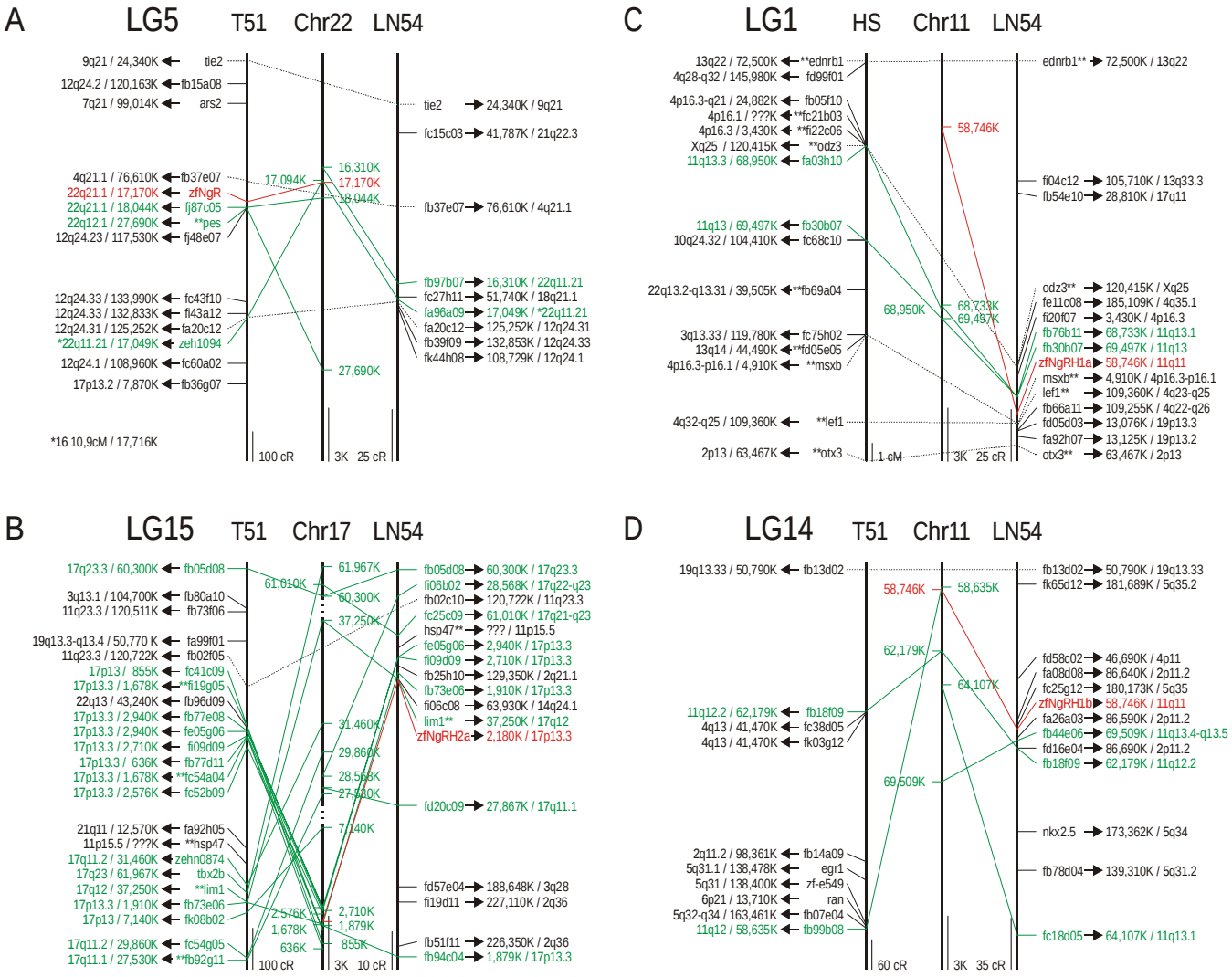

Fig. 2: *Analysis of zebrafish and human syntenic relationships*

Map locations of ESTs and genes in the radiation hybrid panels (T51 and LN54) and the heatshock (HS) panel were obtained from ZFIN. The relative chromosomal locations of the human orthologs were deduced from data in LocusLink. Markers that are syntenic to NgR, NgRH1 and NgRH2 (red), respectively, are shown in green. Markers present on more than one zebrafish panel are connected by dotted lines.

A) Conserved synteny of zebrafish linkage group (LG) 5 and human chromosome (Chr) 22 defined by zfNgR (red). * chromosomal position of the human ortholog of EST fa96a09 could not be identified unambiguously.

B) Conserved synteny of zebrafish LG15 and human Chr 17 defined by zfNgRH2a (red).

C) Conserved synteny of zebrafish LG1 and human Chr 11 defined by zfNgRH1a (red).

D) Conserved synteny of zebrafish LG14 and human Chr 11 defined by zfNgRH1b (red).

cR, centiray; cM, centimorgan; K, kilobasepairs, ** these EST have been published by Woods et al., 2000.

syntenies with the same region (11q12-11q13) of human chromosome 11 (**Fig. 2C, D**), indicating that at least this part of the human genome underwent a fish-specific duplication. Mapping of zfNgRH2a and 14 additional ESTs extends the existing large syntenic region between LG15 in zebrafish and chromosome 17 in human (**Fig. 2B**), including *crk* (ESTs fi19g05, fc54a04), DKFZP564A122 (EST fb92g11) and *lim1* (Woods et al., 2000).

The five NgR-related fugu genes were identified within the genomic sequences of scaffolds 67, 1244, 1581, 154 and 1111 (Ensembl release 11.2.1). Comparison of other predicted fugu genes in the vicinity of the NgRs with the chromosomal localization of the respective mammalian ortholog again revealed conserved syntenies (**Supplementary Table 3**). Orthologs of genes from scaffolds 1244 and 1581 (fugu NgRH1a and fugu NgRH1b, respectively) mapped to human chromosome 11, whereas genes of scaffolds 154 and 1111 (fugu NgRH2a and fugu NgRH2b, respectively) have orthologs on human chromosome 17, indicating a fish specific duplication of these chromosomal segments.

These comparative mapping results support the phylogenetic analysis with the assignment of orthologous groups in the NgR receptor family and with fish specific duplications of NgRH1 and NgRH2.

5.4.3 Genomic analysis of NgR, NgRH1 and NgRH2

Exon-intron structures and intron phasing of NgR, NgRH1 and NgRH2 were examined for the respective human, fugu and zebrafish genes by comparison of cDNA against genomic sequences (**Fig. 3A, Supplementary Table 4**). NgR genes from human, fugu and zebrafish are comprised of two coding exons (separated by a phase 1 intron), indicating that the true fish orthologs of human NgR have been identified. Human NgRH2 is also composed of two coding exons whereas the orthologous fish genes each have an additional phase 3 intron at the same position, indicating an intron insertion in the gene of the common ancestor of zebrafish and fugu. The coding part of the first exon is identical in length for the homologous NgRH2 (13 bp) and NgR (22 bp) genes. For NgRH1, the exon-intron structure is less conserved (**Fig. 3A**). The human NgRH1 gene consists of three coding exons. The respective fugu genes have an additional phase 3 intron dividing exon II. At exactly the same position, an intron is also located in the zebrafish NgRH1a and NgRH1b genes (**Supplementary Table 4**). However, the second phase 3 intron is missing in zebrafish. Compared to the orthologous human gene, the second exon in zebrafish NgRH1a and NgRH1b (IIa) is less than half in size and the third zebrafish exon is consequently longer. Intron phasing is strictly conserved for all NgR related genes, with a phase 1 intron followed by one or two consecutive phase 3 introns (**Fig. 3A, Supplementary Table 4**).

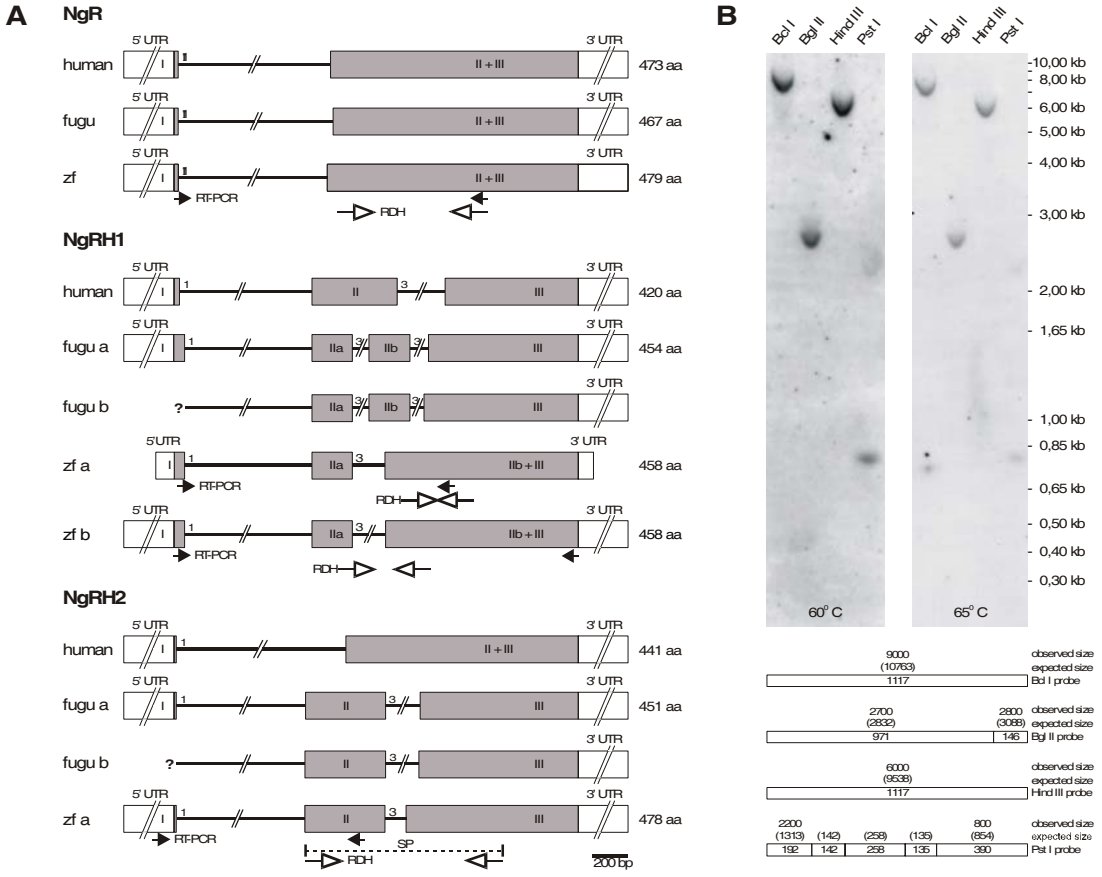

Fig. 3: *Analysis of NgR, NgRH1 and NgRH2 genes*

A) Exon-intron arrangements of NgR, NgRH1 and NgRH2 genes are schematically shown for human, fugu and zebrafish (zf). Exons are drawn as Roman numbered boxes with the coding regions shaded in grey. Intron phases are specified with Arabic numbers. For fugu NgRH1b and fugu NgRH2b, the short N-terminal exons could not be identified within the genomic sequences (marked with **?**). Localizations of primers for the analysis of the zebrafish genes/transcripts are indicated by closed (RT-PCR) and open (radiation hybrid mapping (RDH)) arrows, respectively. The range of the zfNgRH2a southern probe (SP) is outlined with a dotted line.

B) Southern blot analysis of zfNgRH2a. Genomic DNA was digested with *Bcl I*, *Bgl II*, *Hind III* and *Pst I*, respectively (top of each lane). The same DNA was used as PCR template for the generation of the NgRH2a specific probe to avoid sequence polymorphisms. Blots were hybridized and washed at either 60 °C (left) or 65 °C (right). Molecular weights in kilobases (kb) are indicated on the right. The schematic drawing depicts the size of the DNA bands observed on the southern blots, the sizes of DNA bands predicted from virtual digestion of the relevant genomic region (in brackets) and a restriction map of the southern probe for each restriction enzyme (boxes).

To determine whether a second NgRH2 gene exists in zebrafish (as in fugu), Southern blots were hybridized with a zfNgRH2a specific probe. From virtual digestion of genomic sequences, a single band of 10.7 kb (*Bcl I*) and 9.5 kb (*Hind III*), respectively, or multiple bands (3.1 kb and 2.8 kb for *Bgl II* and 1.3 kb, 0.85 kb, 0.26 kb, 0.14 kb and 0.13 kb for *Pst I*) were expected for a single copy gene (**Fig. 3B**). As predicted, one (*Bcl I* and *Hind III* digest) or two bands (*Bgl II*) were detected on Southern blots under high (65°C) as well as low (60°C) stringency conditions (**Fig. 3B**). The 3.1 kb band of the *Bgl II* digest is weakly labeled, since only a minor part of the

probe (146 bp) overlaps with it. For *Pst I*, two bands (0.85 kb and weakly ~2.2 kb) were observed. The other predicted bands (0.13 kb, 0.14 kb, and 0.26 kb) were too small for detection. Differences between predicted and observed band sizes in all four digests can be explained by restriction length polymorphisms of the blotted genomic DNA compared to the database sequences used for fragment prediction. Since no additional bands appeared in the Southern blot hybridization, no indication for the presence of a second NgRH2 gene (zfNgRH2b) in zebrafish was found.

5.4.4 RT-PCR analyses of zfNgR, zfNgRH1a and zfNgRH2a mRNA expression

Transcription of NgR, NgRH1a, NgRH1b and NgRH2a during zebrafish development and in different adult tissues was analysed by RT-PCR (**Fig. 4A**-**D** and **F**-**I**; upper rows). In zebrafish embryos, NgR mRNA expression started at about 10 hours post fertilization (hpf) and increased thereafter (**Fig. 4A**). The absence of an NgR PCR product at 3 hpf and 6 hpf is not due to degraded RNA or bad template cDNA, since a strong signal was detectable in the actin positive control in these early stages (**Fig. 4E**). Considerable NgR mRNA levels were only detected after 20 hpf, paralleling the development of the nervous system. Onset of transcription of the homologous receptors NgRH1a and NgRH2a was time-delayed with respect to NgR. Low mRNA levels were revealed for NgRH2a at 20 hpf (**Fig. 4D**) and even later for NgRH1a at 48 hpf (**Fig. 4B**), whereas significant expression was detectable only at 48 hpf (NgRH2a) and 96 hpf (NgRH1a). NgRH1b had the broadest expression pattern of the zebrafish NgR paralogs. Transcription was observed at all stages after 3 hpf, with higher mRNA levels at older stages of development (**Fig. 4C**).

In adult zebrafish, expression of NgR was predominantly observed in brain, but also in eye and heart (**Fig. 4F**). Faint bands indicating very low expression levels were visible in spinal cord and gill. NgRH2a transcripts were detected in a comparable pattern, except for a lower level in brain (**Fig. 4I**). Neither NgR nor NgRH2a were found in muscle. NgRH1a was almost exclusively expressed in brain, with marginal levels detectable in eye, heart and muscle (**Fig. 4G**). Expression of NgRH1b mRNA was highest in brain and heart and low levels were observed in eye, gill and muscle (**Fig. 4H**).

These result show that the expression of zebrafish NgR family members is developmentally regulated and occurs most prominently in brain.

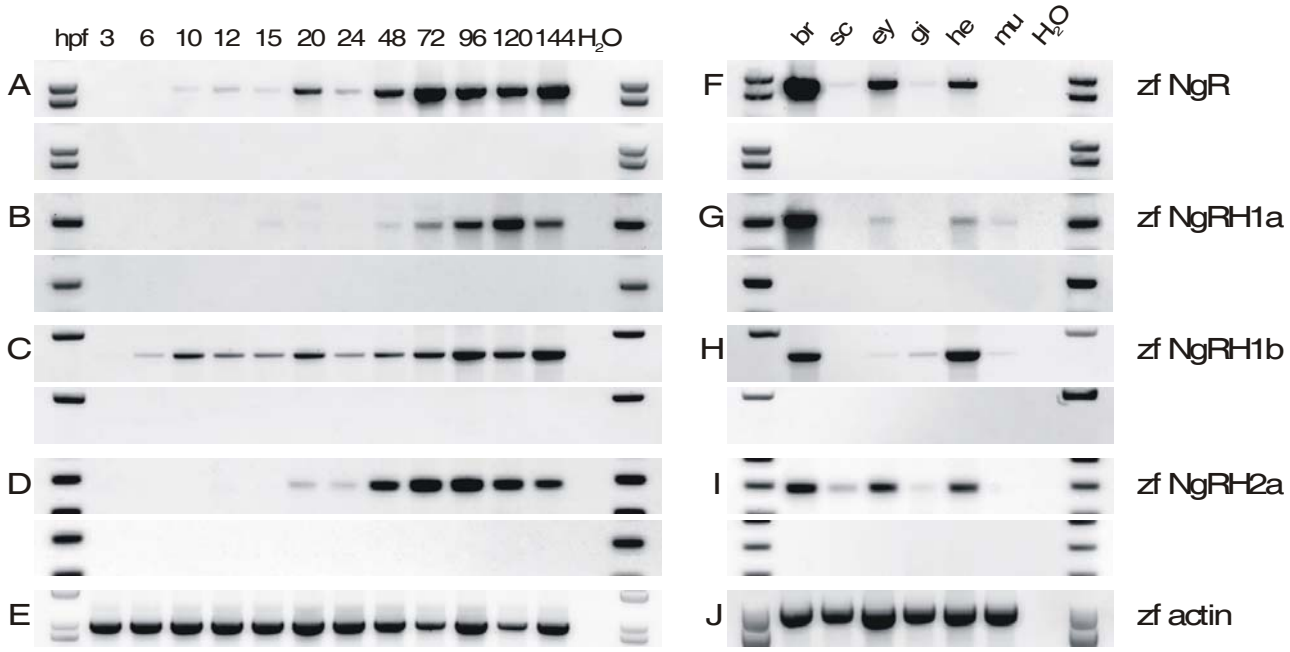

Fig. 4: *RT-PCR analysis of zfNgR, zfNgRH1a, zfNgRH1b and zfNgRH2a mRNA expression*

Expression of zfNgR and its homologs was examined during development (**A**-**D**, upper rows) and in various adult tissues (**F**-**I**, upper rows). A zero reverse transcriptase negative control (without SuperscriptII enzyme) was conducted with each primer pair to show that no bands are amplified due to genomic DNA contamination of the templates (lower row of **A**-**D** and **F**-**I**). RT-PCR with actin-specific primers was used as positive control to ensure that equal amounts of cDNA template were put into each reaction (**E**, **J**).

hpf, hours post fertilization; br, brain; sc, spinal cord; ey, eye; gi, gill; he, heart; mu, muscle; H_2O, no template control.

5.5 Discussion

Here, the discovery of NgR in zebrafish and fugu is reported. In addition fish genes that are orthologs of two recently described human NgR-related genes, NgRH1 and NgRH2 (Barton et al., 2003; Pignot et al., 2003) were uncovered. The fugu genes were recently identified independently by another group (He et al., 2003). The phylogenetic analyses show that duplication events before the divergence of tetrapods (sarcopterygians) and ray-finned fish (actinopterygians) and in actinopterygia before the divergence of the zebrafish and fugu ancestors have lead to the current diversity of NgR in vertebrates. NgR is considered to be an important receptor for the restrictive effects of CNS myelin on axon growth in the adult mammalian CNS, since it interacts with several myelin inhibitors. It binds with high affinity to an extracellular segment of Nogo (Nogo-66) as well as to MAG and OMgp (Domeniconi et al., 2002; Fournier et al., 2001; Liu et al., 2002; Wang et al., 2002b), suggesting a convergence of signaling pathways. The identity of the NgRH1 and NgRH2 ligands is yet unknown, since they do not bind to either Nogo-66, MAG or OMgp (Barton et al., 2003; Pignot et al., 2003).

Although fish axons are capable of regeneration, they are nevertheless repelled by mammalian CNS myelin and oligodendrocytes (Bastmeyer et al., 1991). In the case that Nogo-66, MAG and/or OMgp, which are expressed in mammalian oligodendrocytes, induce this repulsion, an interaction with an akin NgR receptor might be involved in the mediation of the cross species inhibitory effect. Moreover, the question arises which functions homologous NgRs and ligands might have in fish. With the identification of fish NgR genes, these issues can now be addressed. Four members of the zebrafish NgR receptor family and five NgR related fugu genes were discovered. Syntenic chromosomal positions and phylogenetic relationships provide convincing evidence that the true zebrafish and fugu orthologs of human NgR, NgRH1 and NgRH2, respectively have been identified. Analysis of the genomic structures and the determination of diagnostic aa residues also confirmed the assignment of orthologous groups within the NgR receptor family.

Their phylogeny demonstrates clearly that the duplication events that produced three clades of vertebrate NgR genes occurred prior to the divergence of ray-finned fishes (actinopterygians) and tetrapods (sarcopterygians). However, no invertebrate or ascidian NgR gene could be identified.

The duplication of fugu NgRH2 and of fugu and zebrafish NgRH1 and the tree topology shown in **Fig. 1** are consistent with the predictions of the ancient fish-specific genome duplication hypothesis (Amores et al., 1998). In this case, the zebrafish NgRH2b gene has yet to be discovered or a specific loss has to be assumed.

Fish NgR proteins show the same overall structure as human NgR and the LRRNT, LRR and LRRCT domains are strikingly similar (>60%) at the amino acid sequence level (**Supplementary Fig. 2 and 3**). In mammals, this region has been shown to be responsible for ligand binding (Domeniconi et al., 2002; Fournier et al., 2001; Wang et al., 2002b). Its three-dimensional crystal structure has a curved topology of prominantly repeating ß-strands (Barton et al., 2003; He et al., 2003). He et al. proposed that a functional, ligand-binding site of NgR is located on the concave face of this ß-sheet, since it contains predominently aa resiues conserved between all three NgR subclasses (He et al., 2003). However, the present analyses, which included more NgR-related genes and Drosophila Slit as a reference for an ancestral, LRR containing protein revealed that most of these residues are also conserved in Slit and are most probably structure-determining. Residues responsible for defining ligand specificity are expected to be conserved in only one of the three NgR subclasses. Due to the inclusion of fish sequences I was able to substantiate the analysis of Barton (Barton et al., 2003) and to identify distinct residues that are diagnostic for each of the NgR subclass in fish and mammals. Most of these aa are surface-exposed, polar or

charged residues and might well be involved in specific receptor-ligand interactions. These predictions have to be confirmed by future biochemical or mutagenic data.

The high sequence conservation of the LRRNT/LRR/LRRCT domain between fish and mammals combined with the presence of diagnostic aa suggests that zebrafish NgR may be able to bind to and mediate the repellent signal of these mammalian CNS myelin inhibitors in cross species in vitro assays. Future studies will have to show if molecular interactions between fish NgR and mammalian Nogo-66, MAG or OMgp are indeed possible. Another attractive hypothesis would be a function of the NgR family members in axonal growth and guidance, particularly since they exhibit a striking sequence similarity to the slit proteins that have already been shown to confer a similar task (Brose et al., 1999).

An important unanswered question is the identity of the natural ligand(s) of zebrafish NgR and its function. Fish oligodendrocytes probably lack growth inhibiting molecules, since they support axonal elongation *in vitro* (Bastmeyer et al., 1991; Stuermer et al., 1992). At present, neither MAG nor OMgp have been identified in fish. Although an orthologous Nogo-66 is present in actinopterygians (Oertle et al., 2003b), it is not clear whether it is expressed in fish myelin, displays binding properties to NgR and mediates any inhibitory activity. Additional ligands conferring a yet unidentified function that is not related to axonal growth inhibition are expected. It is now possible to determine whether zebrafish NgR or additional receptors recognizing other myelin inhibitors (such as the Nogo-A specific region or semaphorins) mediate growth cone collapse upon contact with mammalian CNS myelin *in vitro*. In addition, it has to be clarified whether zebrafish also possess a homologous $p75^{NTR}$ receptor. In mammals, $p75^{NTR}$ has been described as a co-receptor of the GPI-linked NgR receptor that transduces the inhibitory activity of myelin-associated inhibitors to the neuron (Wang et al., 2002a). Two zebrafish EST clones with adequate sequence similarity have been identified (T. O., unpublished data), but future studies have to elucidate the potential involvement of $p75^{NTR}$ homologous protein(s) in the signaling pathway of fish NgR.

The mRNA distribution for the zebrafish NgRs is consistent with a function in the development of CNS structures and in the regulation of axon growth and plasticity. The expression of NgR parallels the development of the nervous system, whereas NgRH1a and NgRH2a are detectable in embryos with a more mature CNS. Future immunostaining experiments will show if the NgR protein is actually present on growing axons, as would be expected. In the adult zebrafish, the expression pattern of NgR corresponds to that in mouse where it is also predominantly detected in brain (Fournier et al., 2001). Northern analysis revealed low mRNA levels also in heart and kidney, but not in other peripheral tissues. In zebrafish, NgR expression wase also observed in

heart. In addition, mRNA transcripts were detected in the eye, spinal cord and gill. As in human and rat (Pignot et al., 2003), expression of the homologs zfNgRH1a and zfNgRH2a is predominantly observed in brain, although the NgRH2a mRNA level is lower than for NgR. Low transcription of NgRH1 in muscle was observed in zebrafish as well as in rat (this study and (Pignot et al., 2003). In the spinal cord of both organisms, only low levels are detected for all three transcripts. This might result from a downregulation of the respective genes, as it was recently shown for NgR (Josephson et al., 2003; Josephson et al., 2002). Therefore, members of the zebrafish NgR family are expressed in a pattern similar to that in mammals and probably convey evolutionarily conserved functions.

Several mammalian myelin proteins have been shown to exert axonal growth inhibition via a common receptor complex comprising NgR. Since fish are capable of CNS axon regeneration but nevertheless express NgR homologs, additional, yet unidentified ligands and new functions of these receptors are expected. With the present identification of homologous NgR genes, the zebrafish is a potent model organism for *in vivo* analyses of these putative functions.

5.6 Acknowledgements

This work was supported by grants of the Deutsche Forschungsgemeinschaft (DFG) and of the Fonds der Chemischen Industrie (FCJ) to C.A.O.S.. M.K. was supported by the "Stiftung der Deutschen Wirtschaft für Qualifizierung und Kooperation e.V. (sdw)", T.O. and M.E.S. by the Swiss National Science Foundation (Grant No. 31-63633) and by the NCCR on Neural Plasticity and Repair. J.S.T. is supported by NSERC (Canada) discovery grant. We are grateful to H.-M. Pogoda for assistance in mapping zfNgR and for critical reading of the manuscript. We thank M.-A. Cahill for technical assistance, C. Haenisch for her help in the RT-PCR analysis, A.-Y. Loos for fish care, and S. Frentzel (Novartis Pharma) for sharing data prior to publication.

Published as:

Klinger, M., Taylor, J. S., Oertle, T., Schwab, M. E., Stuermer, C. A. O. and Diekmann, H. (2004). Identification of Nogo-66 Receptor (NgR) and Homologous Genes in Fish. *Mol Biol Evol* **21**, 76-85.

5.7 Supplementary data

```
HumanNgR      CPGACVCYNEPTTSCPQQGLQAVPVGIPAASQRIFLHGNRISHVPAASFLWLHSNVLARIDAAAFTGLALLEQLDLSDNA 80
MacacaNgR     CPGACVCYNEPTTSCPQQGLQAVPAGIPASSQRIFLHGNRISHVPAASFLWLHSNVLARIDAAAFAGLALLEQLDLSDNA 80
RatNgR        CPGACVCYNEPTTSCPQQGLQAVPTGIPASSQRIFLHGNRISYVPAASFLWLHSNALAGIDAAAFTGLTLLEQLDLSDNA 80
MouseNgR      CPGACVCYNEPTTSCPQQGLQAVPTGIPASSQRIFLHGNRISHVPAASFLWLHSNALARIDAAAFTGLTLLEQLDLSDNA 80
FuguNgR       CPAKCVCYSEPTVACQQQGLFSIPTEIPVRSQRIFLQSNKLTVVRSTSFLWLYSNNISYIEAGAFYGLEKLEELDIGDNS 80
DanioNgR      CPAKCVCYSEPTVACQQQGLFSIPTEIPVRSQRIFLQSNKLTVVRSTSFLWMYSNNISHIEAGAFYGLERLEELDIGDNS 80
FuguNgRH2a    CPRHCICYTAPTVSCQAHNFLTVPEGIPPDSERIFLQNNKIHRLLRGHFLWIYSNNITYIEPSTFHGFTLLEDLDLGDNR 80
DanioNgRH2a   CPRHCICYMAPTVSCQAHNFLSVPEGIPPHSERIFLQNNKIHRLLQGHFLWIYSNNITYIEPSTFQGFTLLEELDLGDNR 80
FuguNgRH2b    CPRHCICYTSPTVSCQAHNFHAVPEGIPAQSERVFLQNNKIQRLLRGHFLWLYSNNISYIQPSTFLGFDRLEELDLGDNK 80
MouseNgRH2    CPRDCVCYPAPTVSCQAHNFAAIPEGIPEDSERIFLQNNRITFLQQGHFLWIYSNNITFIAPNTFEGFVHLEELDLGDNR 80
HumanNgRH2    CPRDCVCYPAPTVSCQAHNFAAIPEGIPVDSERVFLQNNRIGLLQPGHFLWIYSNNITYIHPSTFEGFVHLEELDLGDNR 80
HumanNgRH1    CPMLCTCYSSPTVSCQANNFSSVPLSLPPSTQRLFLQNNLIRTLRPGTFLWLFSNNLSTIYPGTFRHLQALEELDLGDNR 80
MouseNgRH1    CPMLCTCYSSPTVSCQANNFSSVPLSLPPSTQRLFLQNNLIRSLRPGTFLWLFSNNLSTIHPGTFRHLQALEELDLGDNR 80
FuguNgRH1b    CPKLCVCYPTPTVSCQSQNLTIVPAGVPYNSQRVFLQNNRITELRTDSFLWLYGNNITWIEGGAFSNLRVLEELDLGDNP 80
DanioNgRH1b   CPRLCVCYHMPTVSCQSQNFTSVPAGVPYDSQRVFLQNNRITELRADSFLWLYSNNITWIEAGAFSNLRVLEELDLSDNP 80
FuguNgRH1a    CPHHCVCYPTPTVSCQAQNFTAVPAGVPYESQRVFLQNNRITELRVGSFLWLFSNNITWIEAGAFSELRDLEELDLGDNP 80
DanioNgRH1a   CPHRCVCYPTPTVSCQAQNFTIVPHGMPYESQRVFLQNNRITELRVGSFLWLFSNNITWIEAGAFSELRDLEELDLGDNP 80

HumanNgR      QLRSVDPATFHGLGRLHTLHLDRCGLQELGPGLFRGLAALQYLYLQDNALQALPDDTFRDLGNLTHLFLHGNRISSVPER 160
MacacaNgR     QLRSVDPATFHGLGRLHTLHLDRCGLQELGPGLFRGLAALQYLYLQDNALQALPDDTFRDLGNLTHLFLHGNRISSVPER 160
RatNgR        QLRVVDPTTFRGLGHLHTLHLDRCGLQELGPGLFRGLAALQYLYLQDNNLQALPDNTFRDLGNLTHLFLHGNRIPSVPEH 160
MouseNgR      QLHVVDPTTFHGLGHLHTLHLDRCGLRELGPGLFRGLAALQYLYLQDNNLQALPDNTFRDLGNLTHLFLHGNRIPSVPEH 160
FuguNgR       NLRTISPTALRGLTKLHTLHLHRCGLSELPVGVFRGMFSLQYLYLQDNNILTLQDDTFLDLANLTYLYLHNNKIKIVTDN 160
DanioNgR      NLRIISPTAFRGLTKLHTLHLHRCGLSELPVGVFRGLFSLQYLYLQDNNLLALHEDTFLDLANLTYLFLHNNKIKVVTDH 160
FuguNgRH2a    HLRSLAEDTFHGLARLNALHLYRCGLSSLPNNIFQGLRNLQYLYLQENHLKFLQDDIFMDLHNLSHLFLHGNRLWSINQN 160
DanioNgRH2a   YLRSLSAETFHGLGRLHALHLYRCGLSALPNNIFQGLRNLQYLYLQDNHLEYLQDDLFVDLHNLSHLFLHGNRLWSLHQN 160
FuguNgRH2b    HLKAVASDTFMGLGRLHALHLYHCGLISLPPGIFAGLHNLQYLYLQDNQLEFLEDDLFIDLLNLSHLFLHGNRLWSLRQN 160
MouseNgRH2    QLRTLAPETFQGLVKLHALYLYKCGLSALPAGIFGGLHSLQYLYLQDNHIEYLQDDIFVDLVNLSHLFLHGNKLWSLGQG 160
HumanNgRH2    QLRTLAPETFQGLVKLHALYLYKCGLSALPAGVFGGLHSLQYLYLQDNHIEYLQDDIFVDLVNLSHLFLHGNKLWSLGPG 160
HumanNgRH1    HLRSLEPDTFQGLERLQSLHLYRCQLSSLPGNIFRGLVSLQYLYLQENSLLHLQDDLFADLANLSHLFLHGNRLRLLTEH 160
MouseNgRH1    HLRSLEPDTFQGLERLQSLHLYRCQLSSLPGNIFRGLVSLQYLYLQENSLLHLQDDLFADLANLSHLFLHGNRLRLLTEH 160
FuguNgRH1b    -LQRLEGGAFRGLEKLQSLHMHRCKLAVLPHDLFHKLYSLQFLYLQENQLHFLQDDLFSDLVNLTHLFLHGNRIRALSEN 159
DanioNgRH1b   SLRRLDGGAFRGLERLQSLHMHRCHLTELPADLFHKLYSLQFLYLQENQLTNLPDGLFSDLVNLTHLFLHGNRIRTVSEN 160
FuguNgRH1a    GLRRLEGGAFRGLEKLQSLHMHRCRLSALPHDIFHKLYSLHFLYLQENNLHFLQDDIFSDLINLSQLFLHGNRIRTLSEN 160
DanioNgRH1a   NLHRLEGGAFRGLEKLQSLHMHRCKLAALPHDIFHKLYSLQFLYLQENQLHFIQDDLFADLINLSQLFLHGNRIRTLSEN 160

HumanNgR      AFRGLHSLDRLLLHQNRVAHVHPHAFRDLGRLMTLYLFANNLSALPTEALAPLRALQYLRLNDNPWVCDCRARPLWAWLQ 240
MacacaNgR     AFRGLHSLDRLLLHQNRVAHVHPHAFRDLGRLMTLYLFRNNLSALPAEALAPLRALQYLRLNDNPWVCDCRARPLWAWLQ 240
RatNgR        AFRGLHSLDRLLLHQNHVARVHPHAFRDLGRLMTLYLFANNLSMLPAEVLVPLRSLQYLRLNDNPWVCDCRARPLWAWLQ 240
MouseNgR      AFRGLHSLDRLLLHQNHVARVHPHAFRDLGRLMTLYLFANNLSMLPAEVLMPLRSLQYLRLNDNPWVCDCRARPLWAWLQ 240
FuguNgR       MFRGLISLDRLLLHQNRVIYVQPRAFSDLGKLKSLFLFFNNLTVLTGETMDPLVSLQYLRLNGNQWICDCRARTLWDWFK 240
DanioNgR      MLRGLVNLDRLLLHQNRIVHVQQQAFNDLSKLTTLFLFFNNLTMLTGESMNPLVSLQYLRLNGNQWICDCRARPLWDWFK 240
FuguNgRH2a    TFRGLRALDRLLLHQNQIEWVDHLAFHDLKRLTTLYLFNNSLIQLSGQCLDMLPALEYLRLNDNPWSCDCKALSLWEWLK 240
DanioNgRH2a   TFRGLGALDRLLLHHNQLQWVDRLAFHDLRRLTTLYLFNNSLTELAGECLTQLPALEYLRLNDNPWECDCKALSLWDWLK 240
FuguNgRH2b    TFRGLGVLDRLLLHQNRIQWIDRLAFHDLRRLTTLYLFNNSLTELSGGSLTLLPALEYLRLNDNPWECDCKALSLWDWLR 240
MouseNgRH2    IFRGLVNLDRLLLHENQLQWVHHKAFHDLHRLTTLFLFNNSLTELQGDCLAPLVALEFLRLNGNAWDCGCRARSLWEWLR 240
HumanNgRH2    TFRGLVNLDRLLLHENQLQWVHHKAFHDLRRLTTLFLFNNSLSELQGECLAPLGALEFLRLNGNPWDCGCRARSLWEWLQ 240
HumanNgRH1    VFRGLGSLDRLLLHGNRLQGVHRAAFRGLSRLTILYLFNNSLASLPGEALADLPSLEFLRLNANPWACDCRARPLWAWFQ 240
MouseNgRH1    VFRGLGSLDRLLLHGNRLQGVHRAAFHGLSRLTILYLFNNSLASLPGEALADLPALEFLRLNANPWACDCRARPLWAWFQ 240
FuguNgRH1b    VFRGLVNLDRLLIHDNRVRQVHRKAFRDLGRLTILYLFNNSLSELPGQAMKDTHGIQFLRLNGNPWSCGCEARALWEWFR 239
DanioNgRH1b   AFRGLVNLDRLLLHDNRIRQVHRRSFRDLGRLTILYLFNNSLQELPGQALRDTSSVQFLRLNGNPWTCGCEARSLWEWFR 240
FuguNgRH1a    VFRGLVNLDRLLLHDNRIRQVNRRAFRDLGRLTMLFLFNNSLAELPSQTLRDTQSIEFLRLNANPWSCGCESRALWEWFR 240
DanioNgRH1a   VFRGLVNLDRLLLHDNRVRQVNRRAFRDLGRLTMLFLFNNSLAELPGQAMRDVSSIEFLRLNNNPWACGCEARPLWEFFR 240

HumanNgR      KFRGSSSEVPCSLPQRLAGRDLKRLAANDLQGC 273
MacacaNgR     KFRGSSSEVPCSLPQRLAGRDLKRLAANDLQGC 273
RatNgR        KFRGSSSEVPCNLPQRLAGRDLKRLAASDLEGC 273
MouseNgR      KFRGSSSEVPCNLPQRLADRDLKRLAASDLEGC 273
FuguNgR       RFKGSSSELECSVPEFLTGKDLKRLKSEDLEGC 273
DanioNgR      RFKGSSSDLECHLPASLNGKDLKRLKSDDLEGC 273
FuguNgRH2a    RFRGSTSSVGCQAPVNMVGKDLKELRKEDFPNC 273
DanioNgRH2a   KFRGSTSSVGCVAPAELAGKDLKQLRKEDFPNC 273
FuguNgRH2b    RFRGSTSSLVCVSPPDMAGKDLKTLKKEELPSC 273
MouseNgRH2    RFRGSSSAVPCATPELRQGQDLKLLRVEDFRNC 273
HumanNgRH2    RFRGSSSAVPCVSPGLRHGQDLKLLRAEDFRNC 273
HumanNgRH1    RARVSSSDVTCATPPERQGRDLRALREADFQAC 273
MouseNgRH1    RARVSSSDVTCATPPERQGRDLRALRDSDFQAS 273
FuguNgRH1b    EARISSSELMCTSPSQRRGQDLRFLRELDFAFC 272
DanioNgRH1b   KARISSSDLTCSSPAPRKGQDLRFLRELDFALC 273
FuguNgRH1a    EARVSSSEVICASPSTRRGQDLRFLREMDFALC 273
DanioNgRH1a   GARLSSSEVLCASPASRRGQDLRFLREMDFALC 273
```

Supplementary Fig. 1: *Unambiguous alignment of 17 NgR-related sequences*

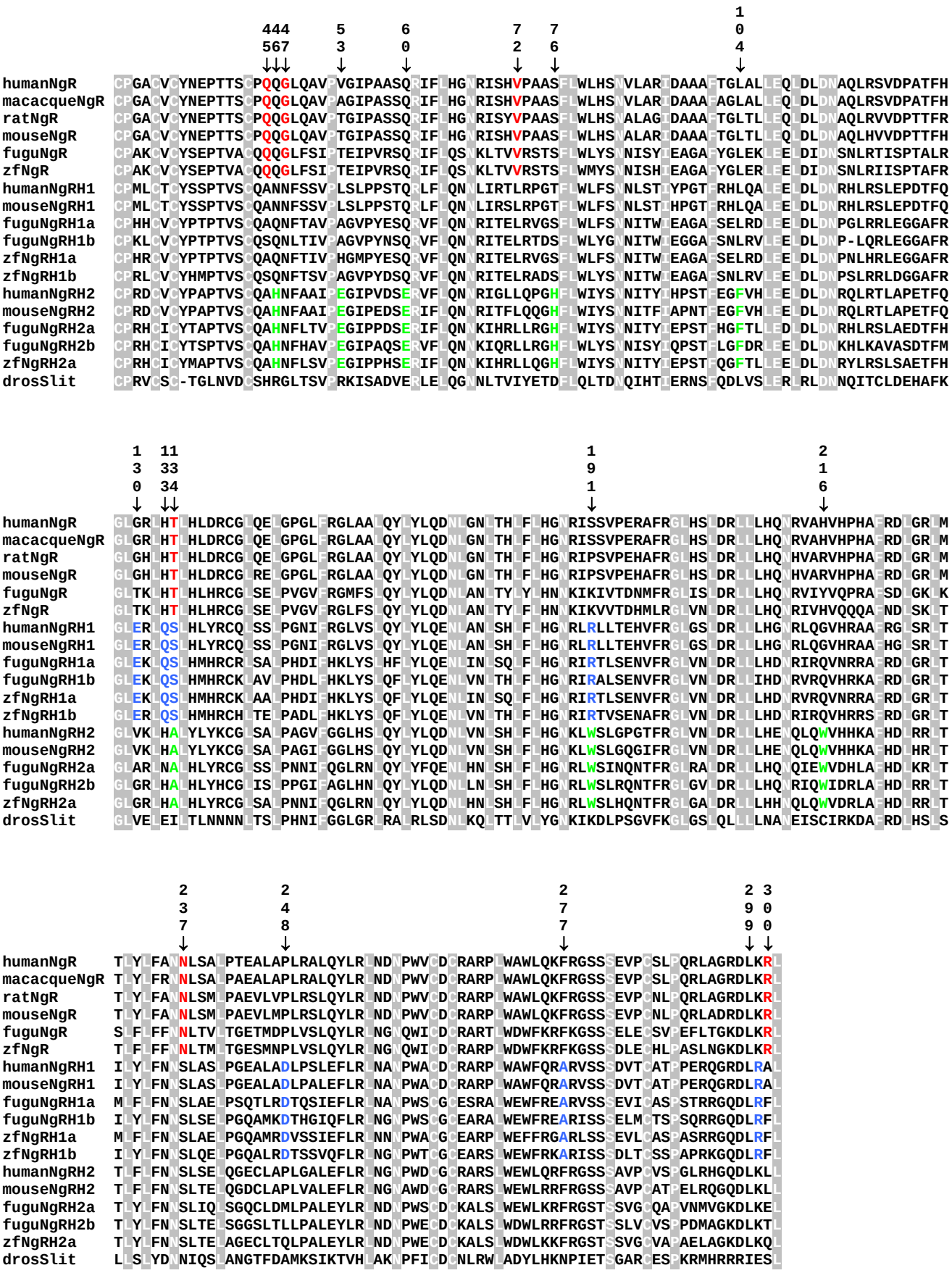
humanNgR
macacqueNgR
ratNgR
mouseNgR
fuguNgR
zfNgR
humanNgRH1
mouseNgRH1
fuguNgRH1a
fuguNgRH1b
zfNgRH1a
zfNgRH1b
humanNgRH2
mouseNgRH2
fuguNgRH2a
fuguNgRH2b
zfNgRH2a
drosSlit

Residues diagnostic for NgR

aa	aa position*	aa class	surface exposure
Q	45	polar	yes
G	47	---	yes
V	72	hydrophobic	no
T	134	polar	yes
N	237	polar	yes
R	300	charged	yes

Residues diagnostic for NgRH1

aa	aa position*	aa class	surface exposure
E	130	charged	yes
Q	133	polar	yes
S	134	polar	yes
R	191	charged	yes
D	248	charged	yes
A	277	hydrophobic	no
R	299	charged	yes

Residues diagnostic for NgRH2

aa	aa position*	aa class	surface exposure
H	46	polar	yes
E	53	charged	yes
E	60	charged	yes
H	76	polar	yes
F	104	hydrophobic	no
A	134	hydrophobic	yes
W	191	polar/aromatic	yes
W	216	polar/aromatic	yes

* with respect to human NgR

Supplementary Fig. 2: *Vertebrate NgR proteins aligned with Drosophila Slit*

Conserved residues are shaded. Residues unique to NgR subfamilies are highlighted and numbered with respect to human NgR: residues diagnostic for NgR (red), residues diagnostic for NgRH1 (blue) and residues diagnostic for NgRH2 (green).

Dros, Drosophila melanogaster; Fugu, Fugu rubripes; Human, Homo sapiens; Macaque, Macaca fascicularis; Mouse, Mus musculus; Rat, Rattus norvegicus; Zebrafish, Danio rerio.

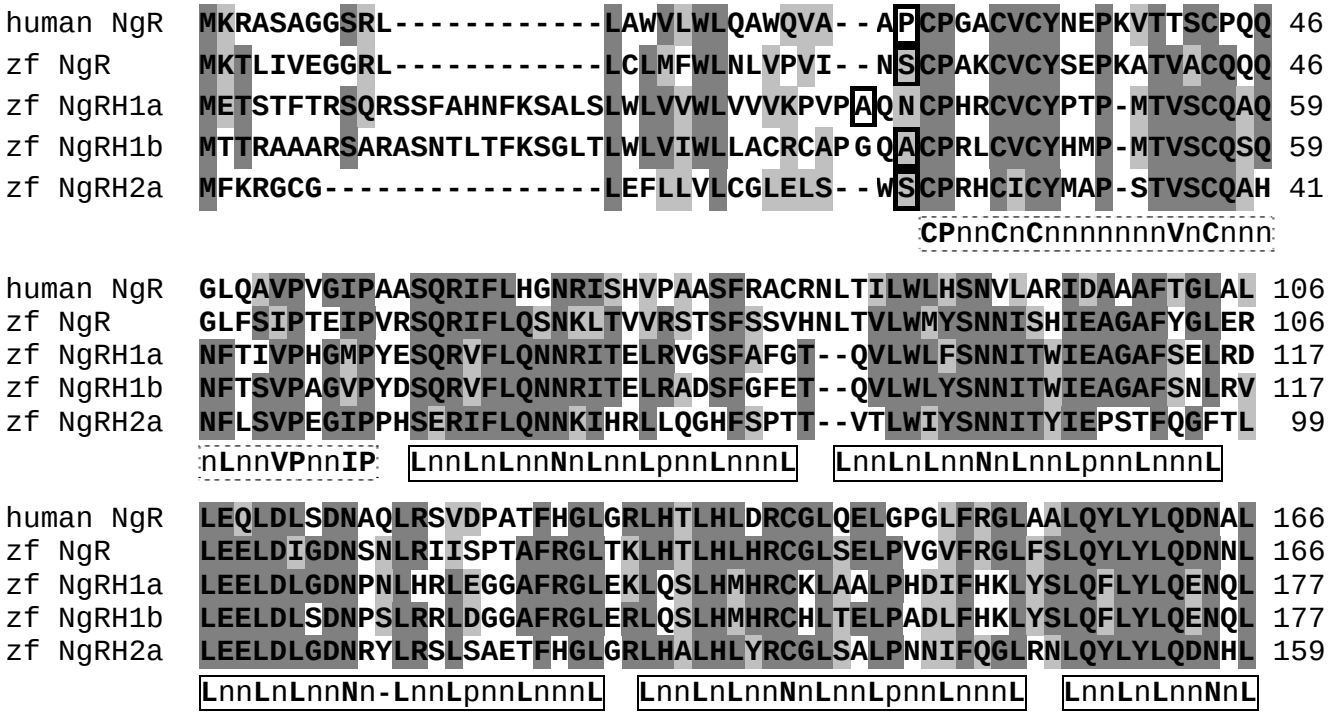

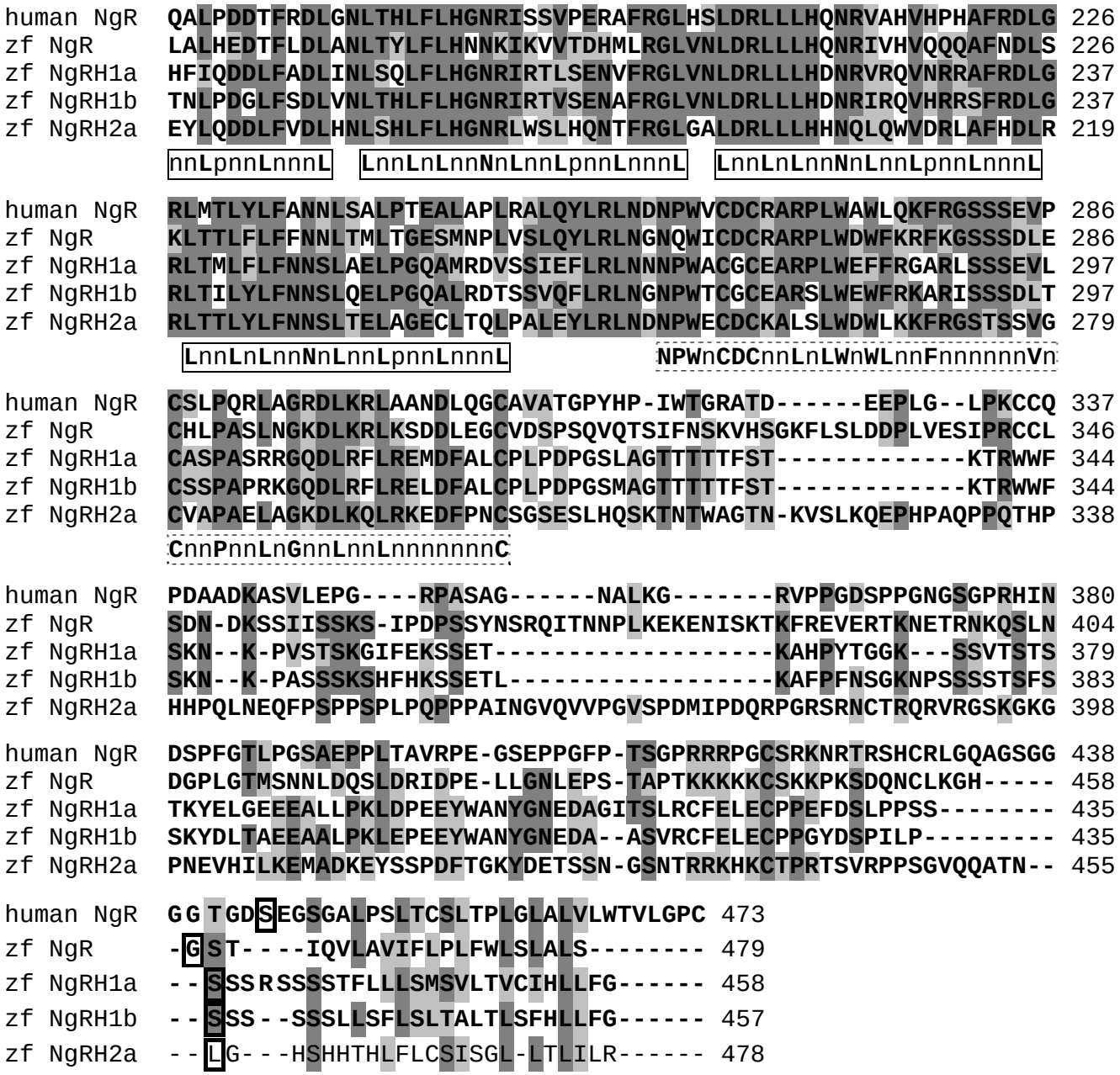

Supplementary Fig. 3: *Sequence alignment of zebrafish NgRs with human NgR*

Amino acid sequences of zfNgR, zfNgRH1a, zfNgRH1b and zfNgRH2a are aligned with the published sequence of human NgR. Identical amino acids are dark-highlighted (threshold >50%) and similar residues are shaded light grey. Predicted cleavage sites of the N-terminal signal peptides and the C-terminal GPI anchorage sites are boxed in each sequence. Consensus sequences of LRR (straight-line boxes) and of LRR amino- and carboxy-terminal flanking domains (dotted boxes) are depicted below the alignment.

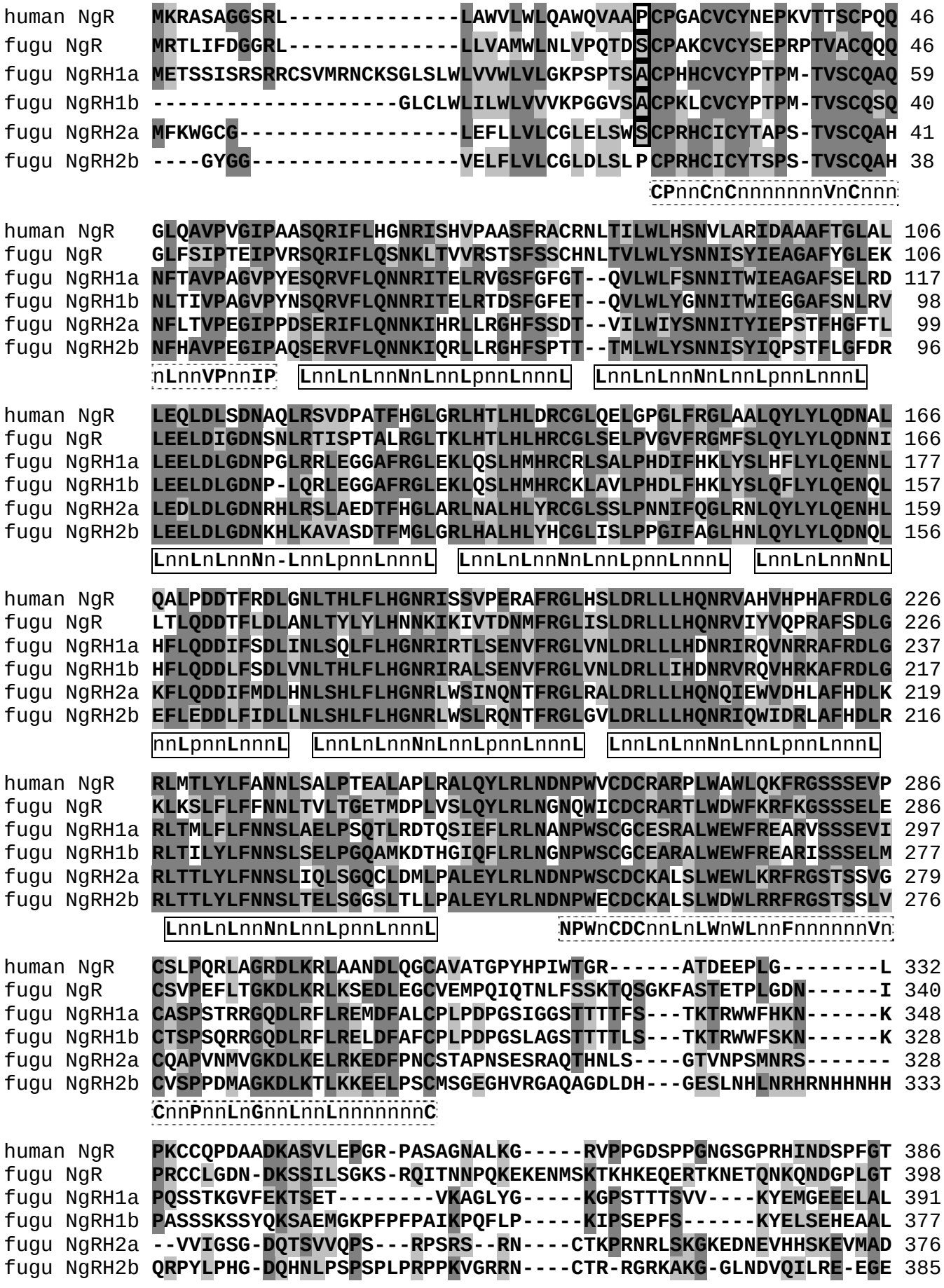
human NgR MKRASAGGSRL----------LAWVLWLQAWQVAAPCPGACVCYNEPKVTTSCPQQ 46
fugu NgR MRTLIFDGGRL----------LLVAMWLNLVPQTDSCPAKCVCYSEPRPTVACQQQ 46
fugu NgRH1a METSSISRSRRCSVMRNCKSGLSLWLVVWLVLGKPSPTSACPHHCVCYPTPM-TVSCQAQ 59
fugu NgRH1b ----------GLCLWLILWLVVVKPGGVSACPKLCVCYPTPM-TVSCQSQ 40
fugu NgRH2a MFKWGCG----------LEFLLVLCGLELSWSCPRHCICYTAPS-TVSCQAH 41
fugu NgRH2b ----GYGG----------VELFLVLCGLDLSLPCPRHCICYTSPS-TVSCQAH 38
CPnnCnCnnnnnnnVnCnnn
human NgR GLQAVPVGIPAASQRIFLHGNRISHVPAASFRACRNLTILWLHSNVLARIDAAAFTGLAL 106
fugu NgR GLFSIPTEIPVRSQRIFLQSNKLTVVRSTSFSSCHNLTVLWLYSNNISYIEAGAFYGLEK 106
fugu NgRH1a NFTAVPAGVPYESQRVFLQNNRITELRVGSFGFGT--QVLWLFSNNITWIEAGAFSELRD 117
fugu NgRH1b NLTIVPAGVPYNSQRVFLQNNRITELRTDSFGFET--QVLWLYGNNITWIEGGAFSNLRV 98
fugu NgRH2a NFLTVPEGIPPDSERIFLQNNKIHRLLRGHFSSDT--VILWIYSNNITYIEPSTFHGFTL 99
fugu NgRH2b NFHAVPEGIPAQSERVFLQNNKIQRLLRGHFSPTT--TMLWLYSNNISYIQPSTFLGFDR 96
nLnnVPnnIP LnnLnLnnNnLnnLpnnLnnnL LnnLnLnnNnLnnLpnnLnnnL
human NgR LEQLDLSDNAQLRSVDPATFHGLGRLHTLHLDRCGLQELGPGLFRGLAALQYLYLQDNAL 166
fugu NgR LEELDIGDNSNLRTISPTALRGLTKLHTLHLHRCGLSELPVGVFRGMFSLQYLYLQDNNI 166
fugu NgRH1a LEELDLGDNPGLRRLEGGAFRGLEKLQSLHMHRCRLSALPHDIFHKLYSLHFLYLQENNL 177
fugu NgRH1b LEELDLGDNP-LQRLEGGAFRGLEKLQSLHMHRCKLAVLPHDLFHKLYSLQFLYLQENQL 157
fugu NgRH2a LEDLDLGDNRHLRSLAEDTFHGLARLNALHLYRCGLSSLPNNIFQGLRNLQYLYLQENHL 159
fugu NgRH2b LEELDLGDNKHLKAVASDTFMGLGRLHALHLYHCGLISLPPGIFAGLHNLQYLYLQDNQL 156
LnnLnLnnNn-LnnLpnnLnnnL LnnLnLnnNnLnnLpnnLnnnL LnnLnLnnNnL
human NgR QALPDDTFRDLGNLTHLFLHGNRISSVPERAFRGLHSLDRLLLHQNRVAHVHPHAFRDLG 226
fugu NgR LTLQDDTFLDLANLTYLYLHNNKIKIVTDNMFRGLISLDRLLLHQNRVIYVQPRAFSDLG 226
fugu NgRH1a HFLQDDIFSDLINLSQLFLHGNRIRTLSENVFRGLVNLDRLLLHDNRIRQVNRRAFRDLG 237
fugu NgRH1b HFLQDDLFSDLVNLTHLFLHGNRIRALSENVFRGLVNLDRLLIHDNRVRQVHRKAFRDLG 217
fugu NgRH2a KFLQDDIFMDLHNLSHLFLHGNRLWSINQNTFRGLRALDRLLLHQNQIEWVDHLAFHDLK 219
fugu NgRH2b EFLEDDLFIDLLNLSHLFLHGNRLWSLRQNTFRGLGVLDRLLLHQNRIQWIDRLAFHDLR 216
nnLpnnLnnnL LnnLnLnnNnLnnLpnnLnnnL LnnLnLnnNnLnnLpnnLnnnL
human NgR RLMTLYLFANNLSALPTEALAPLRALQYLRLNDNPWVCDCRARPLWAWLQKFRGSSSEVP 286
fugu NgR KLKSLFLFFNNLTVLTGETMDPLVSLQYLRLNGNQWICDCRARTLWDWFKRFKGSSSELE 286
fugu NgRH1a RLTMLFLFNNSLAELPSQTLRDTQSIEFLRLNANPWSCGCESRALWEWFREARVSSSEVI 297
fugu NgRH1b RLTILYLFNNSLSELPGQAMKDTHGIQFLRLNGNPWSCGCEARALWEWFREARISSSELM 277
fugu NgRH2a RLTTLYLFNNSLIQLSGQCLDMLPALEYLRLNDNPWSCDCKALSLWEWLKRFRGSTSSVG 279
fugu NgRH2b RLTTLYLFNNSLTELSGGSLTLLPALEYLRLNDNPWECDCKALSLWDWLRRFRGSTSSLV 276
LnnLnLnnNnLnnLpnnLnnnL NPWnCDCnnLnLWnWLnnFnnnnnnVn
human NgR CSLPQRLAGRDLKRLAANDLQGCAVATGPYHPIWTGR------ATDEEPLG--------L 332
fugu NgR CSVPEFLTGKDLKRLKSEDLEGCVEMPQIQTNLFSSKTQSGKFASTETPLGDN------I 340
fugu NgRH1a CASPSTRRGQDLRFLREMDFALCPLPDPGSIGGSTTTTFS---TKTRWWFHKN------K 348
fugu NgRH1b CTSPSQRRGQDLRFLRELDFAFCPLPDPGSLAGSTTTTLS---TKTRWWFSKN------K 328
fugu NgRH2a CQAPVNMVGKDLKELRKEDFPNCSTAPNSESRAQTHNLS----GTVNPSMNRS------- 328
fugu NgRH2b CVSPPDMAGKDLKTLKKEELPSCMSGEGHVRGAQAGDLDH---GESLNHLNRHRNHHNHH 333
CnnPnnLnGnnLnnLnnnnnnnC
human NgR PKCCQPDAADKASVLEPGR-PASAGNALKG-----RVPPGDSPPGNGSGPRHINDSPFGT 386
fugu NgR PRCCLGDN-DKSSILSGKS-RQITNNPQKEKENMSKTKHKEQERTKNETQNKQNDGPLGT 398
fugu NgRH1a PQSSTKGVFEKTSET--------VKAGLYG-----KGPSTTTSVV----KYEMGEEELAL 391
fugu NgRH1b PASSSKSSYQKSAEMGKPFPFPAIKPQFLP-----KIPSEPFS------KYELSEHEAAL 377
fugu NgRH2a --VVIGSG-DQTSVVQPS---RPSRS--RN----CTKPRNRLSKGKEDNEVHHSKEVMAD 376
fugu NgRH2b QRPYLPHG-DQHNLPSPSPLPRPPKVGRRN----CTR-RGRKAKG-GLNDVQILRE-EGE 385

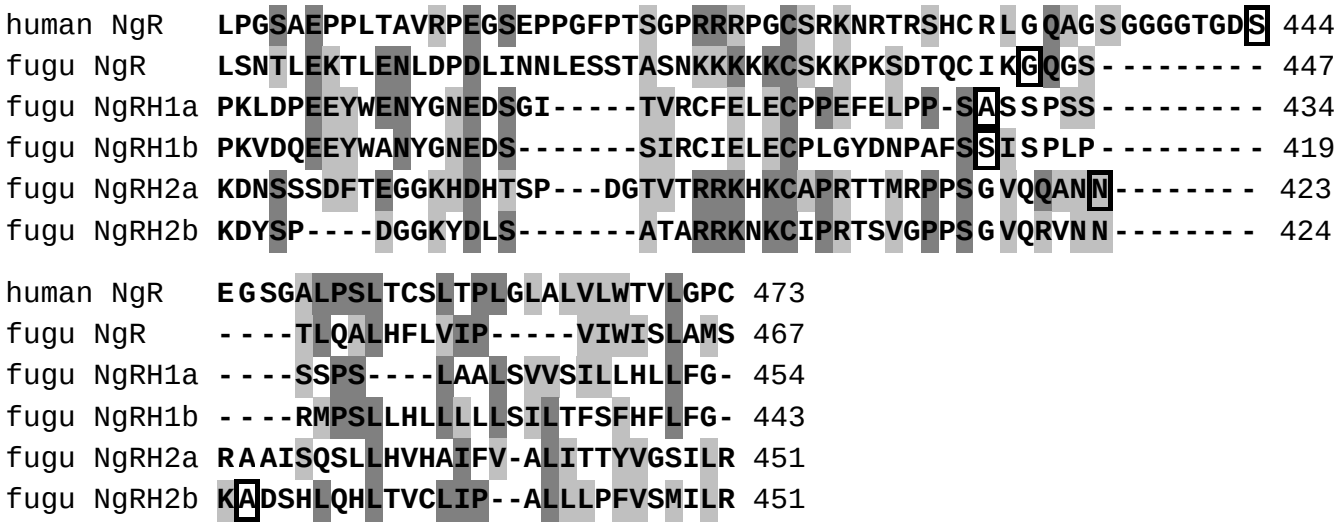

Supplementary Fig. 4: *Sequence alignment of fugu NgRs with the human NgR.*

Predicted amino acid sequences of fugu NgR, fugu NgRH1a, fugu NgRH1b, fugu NgRH2a and fugu NgRH2b are aligned with the published sequence of human NgR. Identical amino acids are dark-highlighted (threshold >50%) and similar residues are shaded light grey. Predicted cleavage sites of the signal peptides and the GPI anchorage site are boxed in each sequence. Consensus sequences of LRR; (straight-line boxes) and of LRR amino- and carboxy-terminal flanking domains (dotted boxes) are depicted below the alignment. For fugu NgRH1b and fugu NgRH2b, the sequences encoding the signal peptides could not be identified within the genomic sequences.

zf NgR	
Sequence	Project
TGC CCA GCG AAG TGC GTG TGC	Mapping sense Primer
GCA ACC TTC CAA ATC ATC GCT TTT G	Mapping antisense Primer
ATG AAG ACC TTA ATC GTG GAG	RT-PCR sense Primer
GCA ACC TTC CAA ATC ATC GCT TTT G	RT-PCR antisense Primer
TGC CCA GCG AAG TGC GTG TGC	Sense EST primer for homologue region
GCA ACC TTC CAA ATC ATC GCT TTT G	Antisense EST primer for homologue region
CCG ACC GGG AGC TCG GAC AGT CCG CAT C	5' race Primer
TGT GAC TGT CGA GCC AGG CCA CTG TGG G	3' race Primer

zf NgRH1a	
Sequence	Project
CAA GCT CTA CAG CCT GCA G	Mapping sense Primer
TGA CGC ACC CTG TTG TCA TG	Mapping antisense Primer
ACG CGG AGC CAA CGC AGC TC	RT-PCR sense Primer
TGA CGC ACC CTG TTG TCA TG	RT-PCR antisense Primer
TCG CTC CGA CTC GGG AAC	Sense primer full length amplification
GAG TTA AAC CGA GCA AAC GGG	Antisense primer full length amplification
AGC TGG CCC AGG TCC CGG AAG GCA CG	5' race Primer

zf NgRH1b	
Sequence	Project
CCTATGACTCCCAGCGTG	Mapping sense Primer
GGGAAGGtTTGTCAGCTGG	Mapping antisense Primer
TAACTCGCTCTCGGTTTG	RT-PCR sense Primer
AAGGTAGTGTAGGATAACAG	RT-PCR antisense Primer
TAACTCGCTCTCGGTTTG	Sense primer full length amplification
AAGGTAGTGTAGGATAACAG	Antisense primer full length amplification

zf NgRH2a	
Sequence	Project
GCT GTG GGC TGG AGT TCC	Mapping sense Primer
GGG TGT GTT TGT GGA GGC	Mapping antisense Primer
AAC CTG ACT GGA CAG ACA G	RT-PCR sense Primer
TTT CTG CAG ACA GCG ATC	RT-PCR antisense Primer
GCT GTG GGC TGG AGT TCC	Southern sense Primer
GGG TGT GTT TGT GGA GGC	Southern antisense Primer
GCT GTG GGC TGG AGT TCC	Sense EST primer for homologue region
GGG TGT GTT TGT GGA GGC	Antisense EST primer for homologue region
GCA TGG AGC CGG CCC AGC CCA TGA AAC G	5' race Primer
TGG CGT TCC ACG ACC TGC GAC GAC TCA CCA	3' race Primer

Actin	
Sequence	Project
GCT CAC CAT GGA TGA TGA TAT CGC	RT-PCR sense Primer
GGA GGA GCA ATG ATC TTG ATC TTC	RT-PCR antisense Primer

Supplementary Table 1: *Overview of primers and their sequences*

Supplementary Table 2a: Mapping data for the anaylsis of conserved syntenies between NgR in zebrafish and human

Accession 5'EST Accession 3'EST [1]	Zebrafish T51 LG	Zebrafish T51 Marker Symbol	Human Chr.	Human Position	Human Accession	Description
AF053632	5	tie2	9	9q21/27,340 K	I58388	protein-tyrosine kinase, receptor type tek precursor
AI882678 AI396614	5	fb15a08	12 12	12q24.2/120,163K 12q24.2/120,163K	AAH01127 R5HUP0	ribosomal protein, large, P0 acidic ribosomal protein P0, cytosolic
NM_173238	5	ars2	7	7q21/99,014K	Q9BXP5	Arsenite-resistance protein 2 hypothetical protein DKFZp564H2023.1
AI437075 AI416329	5	fb37e07	4	4q21.1/76,610 K	AAL76101 n. s. r.	ZNF363 zinc finger protein DKFZP586C1620 protein
	5		22	22q11/17,170K		NgR [2]
AW420095 AW420807	5	fj87c05	22	22q11.21/18,044K	I54388 n. s. r.	LZTR1 leucinezipperlike transcriptional regulator 1
AW280992 AW280039	5	fj48e07	12	12q24.23/117,530 K	NP_775869 n. s. r.	hypothetical protein FLJ25965
AI794374 AI667392	5	fc43f10	12	12 q24.33/133,990 K	T46399 n. s. r.	hypothetical protein DKFZp434N2420.1 CHFR checkpoint with forkhead and ring finger domains
AW175264 AW170902	5	fi34a12	12 12	12q24.33/132,833K 12q24.33/132,833K	T00354 T00354	hypothetical protein KIAA0692 hypothetical protein KIAA0692
not available AA605852	5	fa20c12	12	12q24.31/125,252 K	AAL33003	BRI3BP BRI3 binding protein , cervical cancer 1 proto-oncogene-binding protein KG19
AI353876 not available	5	zeh1094	16 22	10.9 cM/17,716K 22q11.21/17,049K	2002361A BAA07269	Ranbp1 RAN binding protein 1 RANBP1 RAN binding protein 1
AI883287 AI878513	5	fc60a02	12 12	12q24.1/108,960 K 12q24.1/108,960 K	AAH02342 T47172	CORO1C coronin, actin-binding protein, 1C hypothetical protein DKFZp762H186.1 CORO1C coronin, actin binding protein, 1C
AI437010 AI415921	5	fb36g07	17	17p13.2/7,870K	n. s. r. BAB15498	

Accession 5'EST Accession 3'EST [1]	Zebrafish LN 54 LG	Zebrafish LN 54 Marker Symbol	Human Chr.	Human Position	Human Accession	Description
AF053632	5	tie2	9	9q21/27,340 K	I58388	protein-tyrosine kinase, receptor type tek precursor
AI657571 AI641451	5	fc15c03	21 21	21q22.3/41,787K 21q22.3/41,787K	P04080 P04080	CSTB Cystatin B (Liver thiol proteinase inhibitor) (CPI-B) (stefin B) CSTB Cystatin B (Liver thiol proteinase inhibitor) (CPI-B) (stefin B)
AI437075 AI416329	5	fb37e07	4	4q21.1/76,610 K	AAL76101 n. s. r.	ZNF363 zinc finger protein DKFZP586C1620 protein
AI588598 AI588173	5	fb97b07	22 22	22q11.21/ 16,310K 22q11.21/ 16,310K	CAA61979 CAA53044	HIRA HIR histone cell cycle regulation defective homolog A (S. cerevisiae) TUP1 like enhancer of SPLIT gene 1 HIRA HIR histone cell cycle regulation defective homolog A (S. cerevisiae)
AI722961 AI722482	5	fc27h11	18	18q21.1/51,740 K	AAD50381 n. s. r.	DNA polymerase iota
AI331982 AI330561	5	fa96a09 [3]	16 [4] 22 [4]	10.9 cM/17,716K 22q11.21/17,049K	2002361A BAA07269 n. s. r.	Ranbp1 RAN binding protein 1 RANBP1 RAN binding protein 1
not available AA605852	5	fa20c12	12	12q24.31/125,252 K	AAL33003	BRI3BP BRI3 binding protein , cervical cancer 1 proto-oncogene-binding protein KG19
AI437269 AI444474	5	fb39f09	12	12q24.33 /132,853K	NP_612642 n. s. r.	hypothetical protein MGC5352
AW778141 AW777413	5	fk44h08	12 12	12q24.1/108,792K 12q24.1/108,792K	AAH01342 AAH01342 221	protein for MGC:5623 HYPE Huntingtin interacting protein E protein for MGC:5623 HYPE Huntingtin interacting protein E

[1] only one accession number for cloned genes
[2] NgR radiation hybrid PCR result: 00111010110000010000000100000000000000010000001000000010010000000100000000010000000001000000100
[3] as zeh1094 on T51 panel
[4] human Chr.al position could not be identified unequivocally
n. s. r. = no sifnificant results

Supplementary Table 2b: Mapping data for the anaylsis of conserved syntenies between NgRH1a in zebrafish and NgRH1 in human

Accession 5'EST Accession 3'EST	Zebrafish HS LG	Zebrafish HS Marker Symbol	Human Chr.	Human Position	Human Accession	Description
AW165324 AW165053	1	fd99f01	4	4q28-q32/145,980K	AAG34731 254 n. s. r.	HHIP hedgehog interacting protein
AI331170 AI330951	1	fb05f10	4	4p16.3-q21/24,882K	AAA66000 n. s. r.	SOD3 superoxide dismutase 3
AA497326 AA497251	1	fa03h10	11	11q13.3/68,950K	AAB59004 n. s. r.	immunophilin homolog ARA9 AIP aryl hydrocarbon receptor interacting protein
AI415795	1	fb30b07	11	11q13/69,497K	NP_002487	NDUFS8 NADH dehydrogenase (ubiquinone) Fe-S protein 8, 23kDa (NADH-coenzyme Q reductase)

AI437333					n. s. r.	
AI883640	1	fc68c10	10	10q24.32/104,410	BAA11502	KIAA0185, PDCD11 programmed cell death 11
AI883967			10	10q24.32/104,410	BAA11502	KIAA0185, PDCD11 programmed cell death 11
AI942795	1	fc75h02	3	3q13.33/119,780K	S51362	FSTL1 follistatin-like 1
AI884233					n. s. r.	

Accession 5'EST Accession 3'EST	Zebrafish LN54 LG	Zebrafish LN54 Marker Symbol	Human Chr.	Human Position	Human Accession	Description
AW127879	1	fi04c12	13	13q33.3/105,710K	NP_078813	FLJ12118 hypothetical protein
AW115856			13	13q33.3/105,710K	NP_078813	FLJ12118 hypothetical protein
AI477737					n. s. r.	
AI477016	1	fb54e10	17	17q11.1/28,810K	AAH00322	mitotic spindle coiled-coil related protein SPAG5 sperm associated antigen 5
AW059293	1	fe11c08	4	4q35.1/185,109K	AAH30128	ING1L inhibitor of growth family, member 1-like
AW019342					n. s. r.	
AW153435	1	fi20f07	4	4p16.3/3,430K	AAC67373	LRPAP1 low density lipoprotein-related protein-associated protein 1 (alpha-2-macroglobulin receptor-associated protein 1)
AW116851					n. s. r.	
AI545847	1	fb76b11	11	11q13.1/68,733K	BAA76848	KIAA1004, FBXL11 F-box and leucine-rich repeat protein 11
AI544518					n. s. r.	
AI415795	1	fb30b07	11	11q13/69,497K	NP_002487	NDUFS8 NADH dehydrogenase (ubiquinone) Fe-S protein 8, 23kDa (NADH-coenzyme Q reductase)
AI437333					n. s. r.	
	1		11	11q11/58,746K		NgRH1a [1]
AI545925	1	fb66a11	4	4q22-q26/109,255	AAD13581	HADHSC L-3-hydroxyacyl-Coenzyme A dehydrogenase, short chain
AI545487					n. s. r.	
AI958880	1	fd05d03	19	19q13.3 /13,076	AAC50731	ASNA1 arsA arsenite transporter, ATP-binding, homolog 1 (bacterial)
AI957759					n. s. r.	
AI330780	1	fa92h07	19	19p13.2/ 13,125	AAH09465	JUNB jun B proto-oncogene
AI330532					n. s. r.	

[1] NgRH1a radiation hybrid PCR result: 00000000000000000000001000100000010101000000000000010011000000100000000000000010010001001000000

Supplementary Table 2c: Mapping data for the anaylsis of conserved syntenies between NgRH1b in zebrafish and NgRH1 in human

Accession 5'EST Accession 3'EST[1]	Zebrafish T51 LG	Zebrafish T51 Marker Symbol	Human Chr.	Human Position	Human Accession	Description
AI396599	14	fb13d02	19	19q13.33/50,790K	P37198	NUP62 nucleoporin 62kDa
AI384234			19	19q13.33/50,790K	P37198	NUP62 nucleoporin 62kDa
AI416156	14	fb18f09	11	11q12.2/62,179 K	NP_055317	NMP200 nuclear matrix protein NMP200 related to splicing factor PRP19
AI522346			11	11q12.2/62,179 K	NP_055317	NMP200 nuclear matrix protein NMP200 related to splicing factor PRP19
AI794099	14	fc38d05	4	4p13/41,740K	BAA83054	KIAA1102 KIAA1102 protein
AI667159					n. s. r.	
AW566719	14	fk03g12	4	4p13/41,740K	BAA83054	KIAA1102 KIAA1102 protein
AW466762					n. s. r.	
AI396784	14	fb14a09	2	2q11.2/98,361K	XP_171017	LYG2 lysozyme-like
AI385012					n. s. r.	
NM_131248	14	egr1	5	5q31.1/138,478K	NP_001955	EGR1 early growth response 1
AA566458	14	zf-e549	5	5q31/138,400K	AAH00539	C5orf7 Chr. 5 open reading frame 7
not available						
NM_131309	14	ran	6	6p21/13,710K	NP_006316	RAN RAN, member RAS oncogene family
AI384316	14	fb07e04	5	5q32-q34/163,461K	AAH07093	CCNG1 cyclin G1
AI396941					n. s. r.	
AI588766	14	fb99b08	11	11q12/58,635K	NP_002550	P2RX3 purinergic receptor P2X, ligand-gated ion channel, 3
AI588308					n. s. r.	

Accession 5'EST Accession 3'EST [1]	Zebrafish LN 54 LG	Zebrafish LN 54 Marker Symbol	Human Chr.	Human Position	Human Accession	Description
AI396599	14	fb13d02	19	19q13.33/50,790K	P37198	NUP62 nucleoporin 62kDa
AI384234			19	19q13.33/50,790K	P37198	NUP62 nucleoporin 62kDa
BE016576	14	fk65d12	5	5q35.3/181,689K	NP_006089	GNB2L1 guanine nucleotide binding protein (G protein), beta polypeptide 2-like 1
BE016106			5	5q35.3/181,689K	NP_006089	GNB2L1 guanine nucleotide binding protein (G protein), beta polypeptide 2-like 1
AW018455	14	fd58c02	4	4p11/48,690K		KIAA1458 KIAA1458 protein
AW019001					n. s. r.	
not available						
AA542590	14	fa08d08	2	2p11.2/86,640 K	NP_060422	FLJ20758 hypothetical protein FLJ20758
AI723120	14	fc25g12	5	5q35/180,173K	NP_463459	MGAT4B mannosyl (alpha-1,3-)-glycoprotein beta-1,4-N-acetylglucosaminyltransferase, isoenzyme B
AI721971					n. s. r.	
	14		11	11q11/58,746K		NgRH1b [2]
not available						
AA605985	14	fa26a03	2	2p11.2/86,590K	NP_056240	DKFZP586M0122 likely ortholog of mouse RNA polymerase 1-4 (194 kDa subunit)
AI444182	14	fb44e06	11	11q13.4-q13.5/69,509K	NP_006010	TCIRG1 T-cell, immune regulator 1, ATPase, H+ transporting, lysosomal V0 protein a isoform 3
AI461380					n. s. r.	
AI721796	14	fd16e04	2	2p11.2/86,690K	BAA04656	IMMT inner membrane protein, mitochondrial (mitofilin)
AI666914					n. s. r.	
AI416156	14	fb18f09	11	11q12.2/62,179K	NP_055317	NMP200 nuclear matrix protein NMP200 related to splicing factor PRP19
AI522346			11	11q12.2/62,179K	NP_055317	NMP200 nuclear matrix protein NMP200 related to splicing factor PRP19

NM_131421	14	nkx2.5	5	5q34/173,362K	NP_004378	NKX2-5 NK2 transcription factor related, locus 5
AI558952 AI558298	14	fb78d04	5	5q31.2/139,310K	NP_061322 n. s. r.	MATR3 matrin 3
AI658062 AI641048	14	fc18d05	11	11q13.1/64,107K	NP_002687 n. s. r.	POLR2G polymerase (RNA) II (DNA directed) polypeptide G

[1] only one accession number for cloned genes
[1] NgRH1b radiation hybrid PCR result: 00100000001110221021001000000001100011001111000001010210110010111100000001111111010111201001100
n. s. r. = no sifnificant results

Supplementary Table 2d: Mapping data for the anaylsis of conserved syntenies between NgRH2a in zebrafish and human

Accession 5'EST Accession 3'EST [1]	Zebrafish T51 LG	Zebrafish T51 Marker Symbol	Human Chr.	Human Position	Human Accession	Description
AI331148 AI330892	15	fb05d08	17	17q23.2/60,300K	CAB66646 n. s. r.	VMP1 likely ortholog of rat vacuole membrane protein 1
AI558752 AI545273	15	fb80a10	3	3q13.1/104,700K	NP_001618 n. s. r.	ALCAM activated leukocyte cell adhesion molecule
AI558557 AI545015	15	fb73f06	11	11q23.3/120,511K	NP_056332 n. s. r.	DKFZP434F162 protein MIZF MBD2 (methyl-CpG-binding protein)-interacting zinc finger protein
AI331619 AI331661	15	fa99f01	19	19q13.3-q13.4/50,770K	NP_690863 n. s. r.	IL4I1 interleukin 4 induced 1
not available AI330801	15	fb02f05 [2]	11	11q23.3/120,722K	T14782 101 4e-22	hypothetical protein DKFZp586B0621.1 C1QTNF5 C1q and tumor necrosis factor related protein 5
AI794179 AI667517	15	fc41c09	17	17p13/855K	n. s. r. NP_056536	GEMIN4 gem associated protein 4
AI588538 AI588123	15	fb96d09	22	22q13/43,240K	NP_060401 n. s. r.	FLJ20699 hypothetical protein
AI546048 AI544670	15	fb77e08 [3]	17	17p13.3/2,940K	O75153 n. s. r.	Putative eukaryotic translation initiation factor 3 subunit, KIAA0664
AW174800 AW165206	15	fe05g06	17	17p13.3/2,940K	O75153 154 2e-38 n. s. r.	Putative eukaryotic translation initiation factor 3 subunit, KIAA0664
AW133613 AW116121	15	fi09d09	17	17p13.3/2,710K	AAH01213 n. s. r.	MGC3329 hypothetical protein
AI546041 AI544668	15	fb77d11	17	17p13.3/636K	NP_060759 n. s. r.	hypothetical protein FLJ10979
AI878217 AI793726	15	fc52b09	17 17	17p13.3/2,576K 17p13.3/2,576K	BAA92639 BAA92639	KIAA1401,FLJ10534 hypothetical protein KIAA1401,FLJ10534 hypothetical protein
AI330778 AI330530	15	fa92h05	21	21q11/12,570K	Q9NSI8 n. s. r.	SAMSN1 SAM domain, SH3 domain and nuclear localisation signals, 1
AI616950 not available	15	zehn0874	17	17q11.2/31,460K	P21359	NF1 neurofibromin 1 (neurofibromatosis, von Recklinghausen disease, Watson disease)
NM_131051	15	tbx2	17	17q23/61.967K	NP_005985	TBX2 T-box 2
AI558548 AI545006	15	fb73e06	17 17	17p13.3/1,910K 17p13.3/1,910K	AAC61776 AAC61776	PRPF8 PRP8 pre-mRNA processing factor 8 homolog PRPF8 PRP8 pre-mRNA processing factor 8 homolog
not available AW466839	15	fk08b02	17	17p13/7,140K	NP_112497	NIR1 PYK2 N-terminal domain-interacting receptor 1
AI877888 AI793832	15	fc54g05	17	17q11.2/29,860K	BAB21816 n. s. r.	KIAA1725, SSH2 slingshot 2

Accession 5'EST Accession 3'EST [1]	Zebrafish LN54 LG	Zebrafish LN54 Marker Symbol	Human Chr.	Human Position	Human Accession	Description
AI331148 AI330892	15	fb05d08	17	17q23.2/60,300K	CAB66646 n. s. r.	VMP1 likely ortholog of rat vacuole membrane protein 1
AW128038 AW116007	15	fi06b02	17 17	17q22-q23/ 28,568K 17q22-q23/ 28,568K	NP_066960 NP_066960	TNFAIP1 tumor necrosis factor, alpha-induced protein 1 (endothelial) TNFAIP1 tumor necrosis factor, alpha-induced protein 1 (endothelial)
not available AI331853	15	fb02c10	11	11q23.3/120,722K	T14782	hypothetical protein DKFZp586B0621.1 C1QTNF5 C1q and tumor necrosis factor related protein 5
AI723075 AI721929	15	fc25c09	17	17q21-q23/61,010K	BAA13217 n. s. r.	KIAA0228, APPBP2 amyloid beta precursor protein (cytoplasmic tail) binding protein 2
AW174800 AW165206	15	fe05g06	17	17p13.3/2,940K	O75153 n. s. r.	Putative eukaryotic translation initiation factor 3 subunit, KIAA0664
AW133613 AW116121	15	fi09d09	17	17p13.3/2,710K	AAH01213 n. s. r.	MGC3329 hypothetical protein
AI397072 AI444331	15	fb25h10	2	2q21.1/129,350K	XP_072228 n. s. r.	similar to KIAA0280 hypothetical protein LOC130074
AI558548 AI545006	15	fb73e06	17 17	17p13.3/1,910K 17p13.3/1,910K	AAC61776 AAC61776	PRPF8 PRP8 pre-mRNA processing factor 8 homolog PRPF8 PRP8 pre-mRNA processing factor 8 homolog
AW128056 AW116025	15	fi06c08	14	14q24.1/63,930K	Q92537 n. s. r.	KIAA0247gene product
	15		17	17p13.3/2,180 K		NgRH2a [4]
AI722193 AI721400	15	fd20c09	17	17q11.1/27,867K	NP_033665 n. s. r.	LGALS9 lectin, galactoside-binding, soluble, 9 (galectin 9)
BF718178	15	fd57e04	3	3q28 /188,648K	NP_001039	SST somatostatin

AW019843			3	3q28 /188,648K	NP_001039	SST somatostatin
AW153332	15	fi19d11	2	2q36/227,110K	P52594	HRB HIV-1 Rev binding protein
AW116752			2	2q36/227,110K	P52594	HRB HIV-1 Rev binding protein
AI477204	15	fb51f11	2	2q36/226,350K	NP_005535	IRS1 insulin receptor substrate 1
AI477300					n. s. r.	
AI585092	15	fb94c04	17	17p13.3/1,879K	NP_003684	SCARF1 scavenger receptor class F, member 1
AI584473					n. s. r.	

[1] only one accession number for cloned genes
[2] as fb02c10 on T51 panel
[3] as fe05g06
[4] NgR-H2 radiation hybrid PCR result: 00000100001000000000000000000000000000000010000010000000020001001001000000100100110000000010011
n. s. r. = no sifnificant results

Supplementary Table 2: *Mapping data for the analysis of conserved syntenies between NgRs in zebrafish and human*

FUGU NgR

Fugu Scaffold	Fugu Position	Ense. Peptide ID	Descri.	Human Chr	Human Position	Mouse Chr	Mouse Position	Rat Chr	Rat Position
67	0,145	SINFRUP00000136289	NgR	22	17,183	16	17,623	11	2,786
67	0,222	SINFRUP00000136291	MIT. PROLINE OXIDASE	22	17,232	16	17,554	11	2,711
67	0,234	SINFRUP00000136292	ENDOTHELIAL CELLS SCAVENGER RECEPTOR	22	17,516	16	17,277	11	2,513
67	0,270	SINFRUP00000136295	AMBIGUOUS	22	26,817	11	4,602	14	75,958
67	0,312	SINFRUP00000136298	MERLIN	22	26,743	11	4,667	14	76,027
67	0,364	SINFRUP00000136314	NIPSNAP2	n.d.r.		11	4,745	n.d.r.	

FUGU NgRH1a

Fugu Scaffold	Fugu Position	Ense. Peptide ID	Descri.	Human Chr	Human Position	Mouse Chr	Mouse Position	Rat Chr	Rat Position
1244	0,012	SINFRUP00000138764	NgRH1	(11)		2	85,780	n.d.r.	
1244	0,030	SINFRUP00000138782	UNC 93 RELATED	11	69,461	19	6,882	1	206,017
1244	0,035	SINFRUP00000138789	TIM10	11	58,810	2	85,732	3	61,601
1244	0,047	SINFRUP00000138812	PLAKOPHILIN	11	59,071	2	85,515	3	61,402
1244	0,061	SINFRUP00000138816	EMBP	11	58,688	2	85,854	3	61,728

FUGU NgRH1b

Fugu Scaffold	Fugu Position	Ense. Peptide ID	Descri.	Human Chr	Human Position	Mouse Chr	Mouse Position	Rat Chr	Rat Position
1581	2	SINFRUP00000143849	NgRH1	(11)		n.d.r.		n.d.r.	
1581	12	SINFRUP00000143850	AMBIGUOUS	11	58,940	2	85,614	3	61,501
1581	19	SINFRUP00000143852	AMBIGUOUS	11	58,965	2	85,589	3	61,479
1581	25	SINFRUP00000143854	AMBIGUOUS	11	59,008	2	85,564	3	61,451
1581	29	SINFRUP00000143866	AMBIGUOUS	11	58,989	2	85,572	3	61,459
1581	38	SINFRUP00000143872	AMBIGUOUS	11	58,781	2	85,755	3	61,633

FUGU NgRH2a

Fugu Scaffold	Fugu Position	Ense. Peptide ID	Descri.	Human Chr	Human Position	Mouse Chr	Mouse Position	Rat Chr	Rat Position
154	34	SINFRUP00000162922	SERINE/THREONINE KINASE			11	78,189	10	64,603
154	57	SINFRUP00000162936	HYPERMETHYLATED IN CANCER 1 HIC 1	17	2,301	11	75,782	10	61,003
154	143	SINFRUP00000162943	AMBIGUOUS	17	2,280	11	75,800	10	61,020
154	242	SINFRUP00000162947	NgRH2	17	2,180	n.d.r.		10	61,100
154	262	SINFRUP00000162950	REPLICATION FACTOR A 1	17	2,108	11	75,940	10	61,161
154	273	SINFRUP00000162952	ALPHA-2-PLASMIN INHIBITOR	17	1,991	11	76,050	10	61,278
154	280	SINFRUP00000162958	AMBIGUOUS	17	1,967	n.d.r.		10	61,286

FUGU NgRH2b

Fugu Scaffold	Fugu Position	Ense. Peptide ID	Descri.	Human Chr	Human Position	Mouse Chr	Mouse Position	Rat Chr	Rat Position
1111	16	SINFRUP00000148079	AMBIGUOUS	17	2,049	11	76,013	n.d.r.	
1111	32	SINFRUP00000148084	REPLICATION FACTOR A 1	17	2,108	n.d.r.		n.d.r.	
1111	61	SINFRUP00000148085	NgRH2	17	2,180	n.d.r.		10	61,100

positions are given in kilobasepairs
n.d.r. = no data retrieved with ensembl MartView
position of NgRH1 on human chromosom 11 was not retrieved from ensembl Martview, but from NCBI locuslink

Supplementary Table 3: *Mapping data for the analysis of conserved syntenies between NgRs in fugu and mammals*

Supplementary Table 4: Exon and intron sizes of NgR, NgRH1 and NgRH2

NgR

Exon	Zebrafish			Fugu			Human		
	aa	Exon (bp)	Intron (bp)	aa	Exon (bp)	Intron (bp)	aa	Exon (bp)	Intron (bp)
I	G/GT Gly	482 (22)	>6,726	G/GG Gly	(22)	>27,777	G/GG Gly	246 (22)	24,96
II		>1,701 (1,418)			(1,382)			1,695 (1,400)	

NgRH2

Exon	Zebrafish			Fugu a			Fugu b			Human		
	aa	Exon (bp)	Intron (bp)	aa	Exon (bp)	Intron (bp)	aa	Exon (bp)	Intron (bp)	aa	Exon (bp)	Intron (bp)
I	G/GC Gly	865 (13)	>75,657	G/GC (Gly)	(13)	79,123	?/GA	n.i.	n.i.	G/GG Gly	>120 (13)	>114,457
II	---	452	119	---	452	95	---	455	570	---		
III		2,192 (972)			(891)			(900)			(1,313)	

NgRH1

Exon	Zebrafish a			Zebrafish b			Fugu a			Fugu b			Human		
	aa	Exon (bp)	Intron (bp)	aa	Exon (bp)	Intron (bp)	aa	Exon (bp)	Intron (bp)	aa	Exon (bp)	Intron (bp)	aa	Exon (bp)	Intron (bp)
I	A/GC Ser	161 (58)	721	A/GT Ser	125 (58)	1,114	A/GC Ser	(58)	484	?/GT	n.i.	n.i.	G/CT Ala	387 (31)	6,716
IIa	---	227	186	---	227	97	---	227	127	---	227	84	---	482	8,073
IIb							---	234	125	---	231	851			
III		1,177 (1,092)			1,134 (1,089)			(846)			(873)			1,373 (750)	

aa = amino acid encoded by the split codon
n.i. = not identified
number in parenthesis are coding sizes of exons

6 Literature

Abi-Rached, L., Gilles, A., Shiina, T., Pontarotti, P. and Inoko, H. (2002). Evidence of en bloc duplication in vertebrate genomes. *Nat Genet* **31**, 100-5.

Altschul, S. F., Madden, T. L., Schaffer, A. A., Zhang, J., Zhang, Z., Miller, W. and Lipman, D. J. (1997). Gapped BLAST and PSI-BLAST: a new generation of protein database search programs. *Nucleic Acids Res* **25**, 3389-402.

Amores, A., Force, A., Yan, Y. L., Joly, L., Amemiya, C., Fritz, A., Ho, R. K., Langeland, J., Prince, V., Wang, Y. L. et al. (1998). Zebrafish hox clusters and vertebrate genome evolution. *Science* **282**, 1711-4.

Ankerhold, R., Leppert, C. A., Bastmeyer, M. and Stuermer, C. A. O. (1998). E587 antigen is upregulated by goldfish oligodendrocytes after optic nerve lesion and supports retinal axon regeneration. *Glia* **23**, 257-70.

Ankerhold, R. and Stuermer, C. A. O. (1999). Fate of oligodendrocytes during retinal axon degeneration and regeneration in the goldfish visual pathway. *J Neurobiol* **41**, 572-84.

Baka, I. D., Ninkina, N. N., Pinon, L. G., Adu, J., Davies, A. M., Georgiev, G. P. and Buchman, V. L. (1996). Intracellular compartmentalization of two differentially spliced s-rex/NSP mRNAs in neurons. *Mol Cell Neurosci* **7**, 289-303.

Bandtlow, C. E. and Oertle, T. (2002). Neural Regeneration. In *Enceclopedia of Cognetive Science (ECS)*. London: Nature Publishing Group.

Bapteste, E., Brinkmann, H., Lee, J. A., Moore, D. V., Sensen, C. W., Gordon, P., Durufle, L., Gaasterland, T., Lopez, P., Muller, M. et al. (2002). The analysis of 100 genes supports the grouping of three highly divergent amoebae: Dictyostelium, Entamoeba, and Mastigamoeba. *Proc Natl Acad Sci USA* **99**, 1414-9.

Barbazuk, W. B., Korf, I., Kadavi, C., Heyen, J., Tate, S., Wun, E., Bedell, J. A., McPherson, J. D. and Johnson, S. L. (2000). The syntenic relationship of the zebrafish and human genomes. *Genome Res* **10**, 1351-8.

Barton, W. A., Liu, B. P., Tzvetkova, D., Jeffrey, P. D., Fournier, A. E., Sah, D., Cate, R., Strittmatter, S. M. and Nikolov, D. B. (2003). Structure and axon outgrowth inhibitor binding of the Nogo-66 receptor and related proteins. *EMBO J.* **22**, 3291-3302.

Bartsch, U., Bandtlow, C. E., Schnell, L., Bartsch, S., Spillmann, A. A., Rubin, B. P., Hillenbrand, R., Montag, D., Schwab, M. E. and Schachner, M. (1995). Lack of evidence that myelin-associated glycoprotein is a major inhibitor of axonal regeneration in the CNS. *Neuron* **15**, 1375-81.

Bastmeyer, M., Bahr, M. and Stuermer, C. A. O. (1993). Fish optic nerve oligodendrocytes support axonal regeneration of fish and mammalian retinal ganglion cells. *Glia* **8**, 1-11.

Bastmeyer, M., Beckmann, M., Nona, S. M., Cronly-Dillon, J. R. and Stuermer, C. A. O. (1989). Identification of astrocyte- and oligodendrocyte-like cells of goldfish optic nerves in culture. *Neurosci Lett* **101**, 127-32.

Bastmeyer, M., Beckmann, M., Schwab, M. E. and Stuermer, C. A. O. (1991). Growth of regenerating goldfish axons is inhibited by rat oligodendrocytes and CNS myelin but not by goldfish optic nerve tract oligodendrocyte-like cells and fish CNS myelin. *J Neurosci* **11**, 626-40.

Beattie, M. S., Bresnahan, J. C. and Lopate, G. (1990). Metamorphosis alters the response to spinal cord transection in Xenopus laevis frogs. *J Neurobiol* **21**, 1108-22.

Becker, T. and Becker, C. G. (2001). Regenerating descending axons preferentially reroute to the gray matter in the presence of a general macrophage/microglial reaction caudal to a spinal transection in adult zebrafish. *J Comp Neurol* **433**, 131-47.

Becker, T., Bernhardt, R. R., Reinhard, E., Wullimann, M. F., Tongiorgi, E. and Schachner, M. (1998). Readiness of zebrafish brain neurons to regenerate a spinal axon correlates with differential expression of specific cell recognition molecules. *J Neurosci* **18**, 5789-803.

Bonilla, I. E., Tanabe, K. and Strittmatter, S. M. (2002). Small proline-rich repeat protein 1A is expressed by axotomized neurons and promotes axonal outgrowth. *J Neurosci* **22**, 1303-15.

Bonner, D. S., Wiley, J. E. and Farwell, M. A. (1998). Assignment1 of the mitochondrial translational initiation factor 2 gene (MTIF2) to human chromosome 2 bands p16-->p14 by in situ hybridization and with somatic cell hybrids. *Cytogenet Cell Genet* **83**, 80-1.

Bradbury, E. J., Moon, L. D., Popat, R. J., King, V. R., Bennett, G. S., Patel, P. N., Fawcett, J. W. and McMahon, S. B. (2002). Chondroitinase ABC promotes functional recovery after spinal cord injury. *Nature* **416**, 636-40.

Bregman, B. S., Kunkel-Bagden, E., Schnell, L., Dai, H. N., Gao, D. and Schwab, M. E. (1995). Recovery from spinal cord injury mediated by antibodies to neurite growth inhibitors. *Nature* **378**, 498-501.

Brittis, P. A. and Flanagan, J. G. (2001). Nogo domains and a Nogo receptor: implications for axon regeneration. *Neuron* **30**, 11-4.

Brosamle, C., Huber, A. B., Fiedler, M., Skerra, A. and Schwab, M. E. (2000). Regeneration of lesioned corticospinal tract fibers in the adult rat induced by a recombinant, humanized IN-1 antibody fragment. *J Neurosci* **20**, 8061-8.

Brose, K., Bland, K. S., Wang, K. H., Arnott, D., Henzel, W., Goodman, C. S., Tessier-Lavigne, M. and Kidd, T. (1999). Slit proteins bind Robo receptors and have an evolutionarily conserved role in repulsive axon guidance. *Cell* **96**, 795-806.

Brunelli, J. P., Robison, B. D. and Thorgaard, G. H. (2001). Ancient and recent duplications of the rainbow trout Wilms' tumor gene. *Genome* **44**, 455-62.

Burchett, S. A., Flanary, P., Aston, C., Jiang, L., Young, K. H., Uetz, P., Fields, S. and Dohlman, H. G. (2002). Regulation of stress response signaling by the N-terminal dishevelled/EGL-10/pleckstrin domain of Sst2, a regulator of G protein signaling in Saccharomyces cerevisiae. *J Biol Chem* **277**, 22156-67.

Canestro, C., Albalat, R., Hjelmqvist, L., Godoy, L., Jornvall, H. and Gonzalez-Duarte, R. (2002). Ascidian and amphioxus Adh genes correlate functional and molecular features of the ADH family expansion during vertebrate evolution. *J Mol Evol* **54**, 81-9.

Carbonetto, S., Evans, D. and Cochard, P. (1987). Nerve fiber growth in culture on tissue substrata from central and peripheral nervous systems. *J Neurosci* **7**, 610-20.

Caroni, P. and Schwab, M. E. (1988a). Antibody against myelin-associated inhibitor of neurite growth neutralizes nonpermissive substrate properties of CNS white matter. *Neuron* **1**, 85-96.

Caroni, P. and Schwab, M. E. (1988b). Two membrane protein fractions from rat central myelin with inhibitory properties for neurite growth and fibroblast spreading. *J Cell Biol* **106**, 1281-8.

Chen, M. S., Huber, A. B., van der Haar, M. E., Frank, M., Schnell, L., Spillmann, A. A., Christ, F. and Schwab, M. E. (2000). Nogo-A is a myelin-associated neurite outgrowth inhibitor and an antigen for monoclonal antibody IN-1. *Nature* **403**, 434-9.

Chomczynski, P. and Qasba, P. K. (1984). Alkaline transfer of DNA to plastic membrane. *Biochem Biophys Res Commun* **122**, 340-4.

Clarke, J. D., Alexander, R. and Holder, N. (1988). Regeneration of descending axons in the spinal cord of the axolotl. *Neurosci Lett* **89**, 1-6.

Dacks, J. B. and Doolittle, W. F. (2001). Reconstructing/deconstructing the earliest eukaryotes: how comparative genomics can help. *Cell* **107**, 419-25.

de Prat Gay, G., Johnson, C. M. and Fersht, A. R. (1994). Contribution of a proline residue and a salt bridge to the stability of a type I reverse turn in chymotrypsin inhibitor-2. *Protein Eng* **7**, 103-8.

de Souza, S. J., Long, M., Klein, R. J., Roy, S., Lin, S. and Gilbert, W. (1998). Toward a resolution of the introns early/late debate: only phase zero introns are correlated with the structure of ancient proteins. *Proc Natl Acad Sci USA* **95**, 5094-9.

Domeniconi, M., Cao, Z., Spencer, T., Sivasankaran, R., Wang, K., Nikulina, E., Kimura, N., Cai, H., Deng, K., Gao, Y. et al. (2002). Myelin-associated glycoprotein interacts with the nogo66 receptor to inhibit neurite outgrowth. *Neuron* **35**, 283.

Doolittle, R. F., Feng, D. F., Tsang, S., Cho, G. and Little, E. (1996). Determining divergence times of the major kingdoms of living organisms with a protein clock. *Science* **271**, 470-7.

Eisenhaber, B., Bork, P. and Eisenhaber, F. (1999). Prediction of potential GPI-modification sites in proprotein sequences. *J Mol Biol* **292**, 741-58.

Farber, S. A., De Rose, R. A., Olson, E. S. and Halpern, M. E. (2003). The zebrafish annexin gene family. *Genome Res* **13**, 1082-96.

Fawcett, J. W. and Asher, R. A. (1999). The glial scar and central nervous system repair. *Brain Res Bull* **49**, 377-91.

Felsenstein, J. (1985). Confidence limits on phylogenies: an approach using the bootstrap. *Evolution* **39**, 783-91.

Fink, G. R. (1987). Pseudogenes in yeast? *Cell* **49**, 5-6.

Forehand, C. J. and Farel, P. B. (1982). Anatomical and behavioral recovery from the effects of spinal cord transection: dependence on metamorphosis in anuran larvae. *J Neurosci* **2**, 654-52.

Fournier, A. E., GrandPré, T. and Strittmatter, S. M. (2001). Identification of a receptor mediating Nogo-66 inhibition of axonal regeneration. *Nature* **409**, 341-6.

Fragaki, K., Suffia, I., Ferrua, B., Rousseau, D., Le Fichoux, Y. and Kubar, J. (2001). Immunisation with DNA encoding Leishmania infantum protein papLe22 decreases the frequency of parasitemic episodes in infected hamsters. *Vaccine* **19**, 1701-9.

Gaze, R. M. (1970). The formation of nerve connections. New York: Academic Press Inc.

Geisler, J. G., Stubbs, L. J., Wasserman, W. W. and Mucenski, M. L. (1998). Molecular cloning of a novel mouse gene with predominant muscle and neural expression. *Mamm Genome* **9**, 274-82.

GrandPré, T., Li, S. and Strittmatter, S. M. (2002). Nogo-66 receptor antagonist peptide promotes axonal regeneration. *Nature* **417**, 547-51.

GrandPré, T., Nakamura, F., Vartanian, T. and Strittmatter, S. M. (2000). Identification of the Nogo inhibitor of axon regeneration as a Reticulon protein. *Nature* **403**, 439-44.

Habib, A. A., Marton, L. S., Allwardt, B., Gulcher, J. R., Mikol, D. D., Hognason, T., Chattopadhyay, N. and Stefansson, K. (1998). Expression of the oligodendrocyte-myelin glycoprotein by neurons in the mouse central nervous system. *J Neurochem* **70**, 1704-11.

Hall, T. A. (1999). BioEdit: a user-friendly biological sequence alignment editor and analysis program for Windows 95/98/NT. *Nucleic Acids Symposium Series* **41**, 95-98.

Hamada, N., Iwahashi, J., Suzuki, K., Ogi, H., Kashiwagi, T., Hara, K., Toyoda, M., Yamada, T. and Toyoda, T. (2002). Molecular cloning and characterization of the mouse reticulon 3 cDNA. *Cell Mol Biol* **48**, 163-72.

Hasegawa, M., Kishino, H. and Yano, T. (1985). Dating of the human-ape splitting by a molecular clock of mitochondrial DNA. *J Mol Evol* **22**, 160-74.

He, X. L., Bazan, J. F., McDermott, G., Park, J. B., Wang, K., Tessier-Lavigne, M., He, Z. and Garcia, K. C. (2003). Structure of the Nogo receptor ectodomain: a recognition module implicated in myelin inhibition. *Neuron* **38**, 177-85.

Henikoff, S. and Henikoff, J. G. (1992). Amino acid substitution matrices from protein blocks. *Proc Natl Acad Sci USA* **89**, 10915-9.

Ho, Y., Gruhler, A., Heilbut, A., Bader, G. D., Moore, L., Adams, S. L., Millar, A., Taylor, P., Bennett, K., Boutilier, K. et al. (2002). Systematic identification of protein complexes in Saccharomyces cerevisiae by mass spectrometry. *Nature* **415**, 180-3.

Huber, A. B., Weinmann, O., Brosamle, C., Oertle, T. and Schwab, M. E. (2002). Patterns of Nogo mRNA and protein expression in the developing and adult rat and after CNS lesions. *J Neurosci* **22**, 3553-67.

Huelsenbeck, J. P. and Ronquist, F. (2001). MRBAYES: Bayesian inference of phylogenetic trees. *Bioinformatics* **17**, 754-5.

Hughes, M. K. and Hughes, A. L. (1993). Evolution of duplicate genes in a tetraploid animal, Xenopus laevis. *Mol Biol Evol* **10**, 1360-9.

Hukriede, N. A., Joly, L., Tsang, M., Miles, J., Tellis, P., Epstein, J. A., Barbazuk, W. B., Li, F. N., Paw, B., Postlethwait, J. H. et al. (1999). Radiation hybrid mapping of the zebrafish genome. *Proc Natl Acad Sci USA* **96**, 9745-50.

Hunt, D., Coffin, R. S. and Anderson, P. N. (2002a). The Nogo receptor, its ligands and axonal regeneration in the spinal cord; a review. *J Neurocytol* **31**, 93-120.

Hunt, D., Mason, M. R., Campbell, G., Coffin, R. and Anderson, P. N. (2002b). Nogo receptor mRNA expression in intact and regenerating CNS neurons. *Mol Cell Neurosci* **20**, 537-52.

Ito, T., Chiba, T., Ozawa, R., Yoshida, M., Hattori, M. and Sakaki, Y. (2001). A comprehensive two-hybrid analysis to explore the yeast protein interactome. *Proc Natl Acad Sci USA* **98**, 4569-74.

Iwahashi, J., Kawasaki, I., Kohara, Y., Gengyo-Ando, K., Mitani, S., Ohshima, Y., Hamada, N., Hara, K., Kashiwagi, T. and Toyoda, T. (2002). Caenorhabditis elegans reticulon interacts with RME-1 during embryogenesis. *Biochem Biophys Res Commun* **293**, 698-704.

Josephson, A., Trifunovski, A., Scheele, C., Widenfalk, J., Wahlestedt, C., Brene, S., Olson, L. and Spenger, C. (2003). Activity-induced and developmental downregulation of the Nogo receptor. *Cell Tissue Research* **311**, 333-42.

Josephson, A., Trifunovski, A., Widmer, H. R., Widenfalk, J., Olson, L. and Spenger, C. (2002). Nogo-receptor gene activity: cellular localization and developmental regulation of mRNA in mice and humans. *J Comp Neurol* **453**, 292-304.

Josephson, A., Widenfalk, J., Widmer, H. W., Olson, L. and Spenger, C. (2001). NOGO mRNA expression in adult and fetal human and rat nervous tissue and in weight drop injury. *Exp Neurol* **169**, 319-28.

Kaushik, R., Lim, A. K., Morin, X., Bahri, S., Chia, W. and Yang, X. (2002). Characterisation of a novel gene CG8895 in Drosophila melanogaster. *A.Dros.Res.Conf.* **43**, 186C.

Kim, J. E., Li, S., GrandPré, T., Qiu, D. and Strittmatter, S. M. (2003). Axon regeneration in young adult mice lacking Nogo-A/B. *Neuron* **38**, 187-99.

Klinger, M., Diekmann, H., Haenisch, C., Oertle, T., Schwab, M. E. and Stuermer, C. A. O. (2002). Cloning and characterization of zebrafish reticulon genes including nogo/RTN-4. *Soc. Neurosci. Abst.* **28**, Programm No 333.14.

Klinger, M., Diekmann, H., Heinz, D., Hirsch, C., Hannbeck von Hanwehr, S., Petrausch, B., Oertle, T., Schwab, M. E. and Stuermer, C. A. O. (2004a). Identification of two nogo/rtn4 genes and analysis of Nogo-A expression in Xenopus laevis. *Mol Cell Neurosci* **25**, 205-16.

Klinger, M., Taylor, J. S., Oertle, T., Schwab, M. E., Stuermer, C. A. O. and Diekmann, H. (2004b). Identification of Nogo-66 Receptor (NgR) and Homologous Genes in Fish. *Mol Biol Evol* **21**, 76-85.

Kolkman, J. A. and Stemmer, W. P. (2001). Directed evolution of proteins by exon shuffling. *Nat Biotechnol* **19**, 423-8.

Kools, P. F., Roebroek, A. J., Van de Velde, H. J., Marynen, P., Bullerdiek, J. and Van de Ven, W. J. (1994). Regional mapping of the human NSP gene to chromosome region 14q21->q22 by fluorescence in situ hybridization analysis. *Cytogenet Cell Genet* **66**, 48-50.

Kottis, V., Thibault, P., Mikol, D., Xiao, Z. C., Zhang, R., Dergham, P. and Braun, P. E. (2002). Oligodendrocyte-myelin glycoprotein (OMgp) is an inhibitor of neurite outgrowth. *J Neurochem* **82**, 1566-9.

Kozak, M. (1996). Interpreting cDNA sequences: some insights from studies on translation. *Mamm Genome* **7**, 563-74.

Kumar, S., Tamura, K., Jakobsen, I. B. and Nei, M. (2001). MEGA2: Molecular Evolutionary Genetics Analysis software, Tempe, Arizona, USA.

Kumar, S., Tamura, K. and Nei, M. (1994). MEGA: Molecular Evolutionary Genetics Analysis software for microcomputers. *Comput Appl Biosci* **10**, 189-91.

Lang, D. M., Rubin, B. P., Schwab, M. E. and Stuermer, C. A. O. (1995). CNS myelin and oligodendrocytes of the Xenopus spinal cord - but not optic nerve - are nonpermissive for axon growth. *J Neurosci* **15**, 99-109.

Lang, D. M. and Stuermer, C. A. O. (1996). Adaptive plasticity of Xenopus glial cells in vitro and after CNS fiber tract lesions in vivo. *Glia* **18**, 92-106.

Li, Q., Qi, B., Oka, K., Shimakage, M., Yoshioka, N., Inoue, H., Hakura, A., Kodama, K., Stanbridge, E. J. and Yutsudo, M. (2001). Link of a new type of apoptosis-inducing gene ASY/Nogo-B to human cancer. *Oncogene* **20**, 3929-36.

Li, W. H., Gouy, M., Sharp, P. M., O'HUigin, C. and Yang, Y. W. (1990). Molecular phylogeny of Rodentia, Lagomorpha, Primates, Artiodactyla, and Carnivora and molecular clocks. *Proc Natl Acad Sci USA* **87**, 6703-7.

Liu, B. P., Fournier, A., GrandPré, T. and Strittmatter, S. M. (2002). Myelin-associated glycoprotein as a functional ligand for the Nogo-66 receptor. *Science* **297**, 1190-3.

Llopart, A., Comeron, J. M., Brunet, F. G., Lachaise, D. and Long, M. (2002). Intron presence-absence polymorphism in Drosophila driven by positive Darwinian selection. *Proc Natl Acad Sci USA* **99**, 8121-6.

Lockhart, P. J., Steel, M. A., Hendy, M. D. and Penny, D. (1994). Recovering Evolutionary Trees under a More Realistic Model of Sequence. *Mol Biol Evol* **11**, 605-612.

Mayor, C., Brudno, M., Schwartz, J. R., Poliakov, A., Rubin, E. M., Frazer, K. A., Pachter, L. S. and Dubchak, I. (2000). VISTA : visualizing global DNA sequence alignments of arbitrary length. *Bioinformatics* **16**, 1046-7.

McKerracher, L., David, S., Jackson, D. L., Kottis, V., Dunn, R. J. and Braun, P. E. (1994). Identification of myelin-associated glycoprotein as a major myelin- derived inhibitor of neurite growth. *Neuron* **13**, 805-11.

Meyer, A. and Schartl, M. (1999). Gene and genome duplications in vertebrates: the one-to-four (-to-eight in fish) rule and the evolution of novel gene functions. *Curr Opin Cell Biol* **11**, 699-704.

Mi, S., Lee, X., Shao, Z., Thill, G., Ji, B., Relton, J., Levesque, M., Allaire, N., Perrin, S., Sands, B. et al. (2004). LINGO-1 is a component of the Nogo-66 receptor/p75 signaling complex. *Nat Neurosci* **7**, 221-8.

Moreira, E. F., Jaworski, C. J. and Rodriguez, I. R. (1999). Cloning of a novel member of the reticulon gene family (RTN3): gene structure and chromosomal localization to 11q13. *Genomics* **58**, 73-81.

Morgenstern, D. A., Asher, R. A. and Fawcett, J. W. (2002). Chondroitin sulphate proteoglycans in the CNS injury response. *Prog Brain Res* **137**, 313-32.

Morin, X., Daneman, R., Zavortink, M. and Chia, W. (2001). A protein trap strategy to detect GFP-tagged proteins expressed from their endogenous loci in Drosophila. *Proc Natl Acad Sci USA* **98**, 15050-5.

Morris, N. J., Ross, S. A., Neveu, J. M., Lane, W. S. and Lienhard, G. E. (1999). Cloning and characterization of a 22 kDa protein from rat adipocytes: a new member of the reticulon family. *Biochim Biophys Acta* **1450**, 68-76.

Mukhopadhyay, G., Doherty, P., Walsh, F. S., Crocker, P. R. and Filbin, M. T. (1994). A novel role for myelin-associated glycoprotein as an inhibitor of axonal regeneration. *Neuron* **13**, 757-67.

Nagase, T., Ishikawa, K., Miyajima, N., Tanaka, A., Kotani, H., Nomura, N. and Ohara, O. (1998). Prediction of the coding sequences of unidentified human genes. IX. The complete sequences of 100 new cDNA clones from brain which can code for large proteins in vitro. *DNA Res* **5**, 31-9.

Nei, M. and Gojobori, T. (1986). Simple methods for estimating the numbers of synonymous and nonsynonymous nucleotide substitutions. *Mol Biol Evol* **3**, 418-26.

Neumann, S. and Woolf, C. J. (1999). Regeneration of dorsal column fibers into and beyond the lesion site following adult spinal cord injury. *Neuron* **23**, 83-91.

Niederost, B., Oertle, T., Fritsche, J., McKinney, R. A. and Bandtlow, C. E. (2002). Nogo-A and myelin-associated glycoprotein mediate neurite growth inhibition by antagonistic regulation of RhoA and Rac1. *J Neurosci* **22**, 10368-76.

Nielsen, H., Engelbrecht, J., Brunak, S. and von Heijne, G. (1997). Identification of prokaryotic and eukaryotic signal peptides and prediction of their cleavage sites. *Protein Eng* **10**, 1-6.

Ninkina, N. N., Baka, I. D. and Buchman, V. L. (1997). Rat and chicken s-rex/NSP mRNA: nucleotide sequence of main transcripts and expression of splice variants in rat tissues. *Gene* **184**, 205-10.

Oertle, T., Huber, C., van der Putten, H. and Schwab, M. E. (2003a). Genomic Structure and Functional Characterisation of the Promoters of Human and Mouse nogo/rtn4. *J Mol Biol* **325**, 299-323.

Oertle, T., Klinger, M., Stuermer, C. A. O. and Schwab, M. E. (2003b). A reticular rhapsody: phylogenic evolution and nomenclature of the RTN/Nogo gene family. *FASEB J.* **17**, 1238-1247.

Oertle, T., Merkler, D. and Schwab, M. E. (2003c). Do cancer cells die because of Nogo-B? *Oncogene* **22**, 1390-9.

Oertle, T. and Schwab, M. E. (2003). Nogo and its paRTNers. *Trends Cell Biol* **13**, 187-94.

Oertle, T., van der Haar, M. E., Bandtlow, C. E., Robeva, A., Burfeind, P., Buss, A., Huber, A. B., Simonen, M., Schnell, L., Brosamle, C. et al. (2003d). Nogo-A Inhibits Neurite Outgrowth and Cell Spreading with Three Discrete Regions. *J Neurosci* **23**, 5393-5406.

Paschke, K. A., Lottspeich, F. and Stuermer, C. A. O. (1992). Neurolin, a cell surface glycoprotein on growing retinal axons in the goldfish visual system, is reexpressed during retinal axonal regeneration. *J Cell Biol* **117**, 863-75.

Pasterkamp, R. J., Giger, R. J., Ruitenberg, M. J., Holtmaat, A. J., De Wit, J., De Winter, F. and Verhaagen, J. (1999). Expression of the gene encoding the chemorepellent semaphorin III is induced in the fibroblast component of neural scar tissue formed following injuries of adult but not neonatal CNS. *Mol Cell Neurosci* **13**, 143-66.

Patthy, L. (1999). Genome evolution and the evolution of exon-shuffling--a review. *Gene* **238**, 103-14.

Pearce, E. J. and MacDonald, A. S. (2002). The immunobiology of schistosomiasis. *Nat Rev Immunol* **2**, 499-511.

Pignot, V., Hein, A. E., Barske, C., Wiessner, C., Walmsley, A. R., Kaupmann, K., Mayeur, H., Sommer, B., Mir, A. K. and Frentzel, S. (2003). Characterisation of two novel proteins, NgRH1 and NgRH2, structurally and biochemically homologous to the Nogo-66 receptor (NgR). *J Neurochem* **85**, 717-28.

Prinjha, R., Moore, S. E., Vinson, M., Blake, S., Morrow, R., Christie, G., Michalovich, D., Simmons, D. L. and Walsh, F. S. (2000). Inhibitor of neurite outgrowth in humans. *Nature* **403**, 383-4.

Ramón y Cajal, S. (1928). Cajal's Degeneration and Regeneration of the Nervous System, (ed. J. DeFelipe and E. G. Jones): Oxford Univ. Press, Oxford.

Rise, M. L., von Schalburg, K. R., Brown, G. D., Mawer, M. A., Devlin, R. H., Kuipers, N., Busby, M., Beetz-Sargent, M., Alberto, R., Gibbs, A. R. et al. (2004). Development and application of a salmonid EST database and cDNA microarray: data mining and interspecific hybridization characteristics. *Genome Res* **14**, 478-90.

Roebroek, A. J., Ayoubi, T. A., Van de Velde, H. J., Schoenmakers, E. F., Pauli, I. G. and Van de Ven, W. J. (1996). Genomic organization of the human NSP gene, prototype of a novel gene family encoding reticulons. *Genomics* **32**, 191-9.

Roebroek, A. J., Contreras, B., Pauli, I. G. and Van de Ven, W. J. (1998). cDNA cloning, genomic organization, and expression of the human RTN2 gene, a member of a gene family encoding reticulons. *Genomics* **51**, 98-106.

Roebroek, A. J., van de Velde, H. J., Van Bokhoven, A., Broers, J. L., Ramaekers, F. C. and Van de Ven, W. J. (1993). Cloning and expression of alternative transcripts of a novel neuroendocrine-specific gene and identification of its 135-kDa translational product. *J Biol Chem* **268**, 13439-47.

Saitou, N. and Nei, M. (1987). The neighbor-joining method: a new method for reconstructing phylogenetic trees. *Mol Biol Evol* **4**, 406-25.

Schnell, L. and Schwab, M. E. (1990). Axonal regeneration in the rat spinal cord produced by an antibody against myelin-associated neurite growth inhibitors. *Nature* **343**, 269-72.

Schwab, M. E. and Bartholdi, D. (1996). Degeneration and regeneration of axons in the lesioned spinal cord. *Physiol Rev* **76**, 319-70.

Schwab, M. E. and Caroni, P. (1988). Oligodendrocytes and CNS myelin are nonpermissive substrates for neurite growth and fibroblast spreading in vitro. *J Neurosci* **8**, 2381-93.

Schwartz, S., Zhang, Z., Frazer, K. A., Smit, A., Riemer, C., Bouck, J., Gibbs, R., Hardison, R. and Miller, W. (2000). PipMaker - a web server for aligning two genomic DNA sequences. *Genome Res* **10**, 577-86.

Senden, N. H., Timmer, E. D., Boers, J. E., van de Velde, H. J., Roebroek, A. J., Van de Ven, W. J., Broers, J. L. and Ramaekers, F. C. (1996). Neuroendocrine-specific protein C (NSP-C): subcellular localization and differential expression in relation to NSP-A. *Eur J Cell Biol* **69**, 197-213.

Simonen, M., Pedersen, V., Weinmann, O., Schnell, L., Buss, A., Ledermann, B., Christ, F., Sansig, G., van der Putten, H. and Schwab, M. E. (2003). Systemic deletion of the myelin-associated outgrowth inhibitor Nogo-A improves regenerative and plastic responses after spinal cord injury. *Neuron* **38**, 201-11.

Sipiczki, M. (2000). Where does fission yeast sit on the tree of life? *Genome Biol* **1**, Reviews 1011.

Spillmann, A. A., Bandtlow, C. E., Lottspeich, F., Keller, F. and Schwab, M. E. (1998). Identification and characterization of a bovine neurite growth inhibitor (bNI-220). *J Biol Chem* **273**, 19283-93.

Spring, J. (1997). Vertebrate evolution by interspecific hybridisation - are we polyploid? *FEBS Lett* **400**, 2-8.

Steen, P., Kalghatgi, L. and Constantine-Paton, M. (1989). Monoclonal antibody markers for amphibian oligodendrocytes and neurons. *J Comp Neurol* **289**, 467-80.

Stubbs, L., Carver, E. A., Shannon, M. E., Kim, J., Geisler, J., Generoso, E. E., Stanford, B. G., Dunn, W. C., Mohrenweiser, H., Zimmermann, W. et al. (1996). Detailed comparative map of human chromosome 19q and related regions of the mouse genome. *Genomics* **35**, 499-508.

Stuermer, C. A. O., Bastmeyer, M., Bahr, M., Strobel, G. and Paschke, K. (1992). Trying to understand axonal regeneration in the CNS of fish. *J Neurobiol* **23**, 537-50.

Stuermer, C. A. O. (1988a). Trajectories of regenerating retinal axons in the goldfish tectum: I. A comparison of normal and regenerated axons at late regeneration stages. *J Comp Neurol* **267**, 55-68.

Stuermer, C. A. O. (1988b). Trajectories of regenerating retinal axons in the goldfish tectum: II. Exploratory branches and growth cones on axons at early regeneration stages. *J Comp Neurol* **267**, 69-91.

Stuermer, C. A. O. (1995). Glial cells and axonal regeneration in the central nervous system, pp. 905-915: Oxford Univ. Press.

Suffia, I., Ferrua, B., Stien, X., Mograbi, B., Marty, P., Rousseau, D., Fragaki, K. and Kubar, J. (2000). A novel Leishmania infantum recombinant antigen which elicits interleukin 10 production by peripheral blood mononuclear cells of patients with visceral leishmaniasis. *Infect Immun* **68**, 630-6.

Swofford, D. L. (2002). PAUP* Phylogenetic Analysis Using Parsimony (*and other methods). Version 4. *Sinauer Associates,* Sunderland, Massachusetts.

Tagami, S., Eguchi, Y., Kinoshita, M., Takeda, M. and Tsujimoto, Y. (2000). A novel protein, RTN-XS, interacts with both Bcl-XL and Bcl-2 on endoplasmic reticulum and reduces their anti-apoptotic activity. *Oncogene* **19**, 5736-46.

Tajima, F. (1993). Simple methods for testing the molecular evolutionary clock hypothesis. *Genetics* **135**, 599-607.

Tavare, S. (1986). Some probabilistic and statistical problems on the analysis of DNA sequences. *Lect Math Life Sci* **17**, 57-86.

Taylor, J. S., Braasch, I., Frickey, T., Meyer, A. and Van De Peer, Y. (2003). Genome duplication, a trait shared by 22,000 species of ray-finned fish. *Genome Res* **13**, 382-90.

Thompson, J. D., Higgins, D. G. and Gibson, T. J. (1994). CLUSTAL W: improving the sensitivity of progressive multiple sequence alignment through sequence weighting, position-specific gap penalties and weight matrix choice. *Nucleic Acids Res* **22**, 4673-80.

Van de Peer, Y., Taylor, J. S., Braasch, I. and Meyer, A. (2001). The ghost of selection past: rates of evolution and functional divergence of anciently duplicated genes. *J Mol Evol* **53**, 436-46.

Van de Velde, H. J., Roebroek, A. J., Senden, N. H., Ramaekers, F. C. and Van de Ven, W. J. (1994). NSP-encoded reticulons, neuroendocrine proteins of a novel gene family associated with membranes of the endoplasmic reticulum. *J Cell Sci* **107**, 2403-16.

Wang, K. C., Kim, J. A., Sivasankaran, R., Segal, R. and He, Z. (2002a). P75 interacts with the Nogo receptor as a co-receptor for Nogo, MAG and OMgp. *Nature* **420**, 74-8.

Wang, K. C., Koprivica, V., Kim, J. A., Sivasankaran, R., Guo, Y., Neve, R. L. and He, Z. (2002b). Oligodendrocyte-myelin glycoprotein is a Nogo receptor ligand that inhibits neurite outgrowth. *Nature* **417**, 941-4.

Wang, X., Chun, S. J., Treloar, H., Vartanian, T., Greer, C. A. and Strittmatter, S. M. (2002c). Localization of Nogo-A and Nogo-66 receptor proteins at sites of axon- myelin and synaptic contact. *J Neurosci* **22**, 5505-15.

Wanner, M., Lang, D. M., Bandtlow, C. E., Schwab, M. E., Bastmeyer, M. and Stuermer, C. A. O. (1995). Reevaluation of the growth-permissive substrate properties of goldfish optic nerve myelin and myelin proteins. *J Neurosci* **15**, 7500-8.

Wendland, B. (2001). Round-trip ticket: recycling to the plasma membrane requires RME-1. *Nat Cell Biol* **3**, E133-5.

Winzeler, E. A., Shoemaker, D. D., Astromoff, A., Liang, H., Anderson, K., Andre, B., Bangham, R., Benito, R., Boeke, J. D., Bussey, H. et al. (1999). Functional characterization of the S. cerevisiae genome by gene deletion and parallel analysis. *Science* **285**, 901-6.

Wood, M. R. and Cohen, M. J. (1979). Synaptic regeneration in identified neurons of the lamprey spinal cords. *Science* **206**, 344-7.

Wood, V. Gwilliam, R. Rajandream, M. A. Lyne, M. Lyne, R. Stewart, A. Sgouros, J. Peat, N. Hayles, J. Baker, S. et al. (2002). The genome sequence of Schizosaccharomyces pombe. *Nature* **415**, 871-80.

Woods, I. G., Kelly, P. D., Chu, F., Ngo-Hazelett, P., Yan, Y. L., Huang, H., Postlethwait, J. H. and Talbot, W. S. (2000). A comparative map of the zebrafish genome. *Genome Res* **10**, 1903-14.

Yang, J., Yu, L., Bi, A. D. and Zhao, S. Y. (2000). Assignment of the human reticulon 4 gene (RTN4) to chromosome 2p14 -->2p13 by radiation hybrid mapping. *Cytogenet Cell Genet* **88**, 101-2.

Yang, Z. (1993). Maximum-likelihood estimation of phylogeny from DNA sequences when substitution rates differ over sites. *Mol Biol Evol* **10**, 1396-401.

Yoder, J. A. and Litman, G. W. (2000). The zebrafish fth1, slc3a2, men1, pc, fgf3 and cycd1 genes define two regions of conserved synteny between linkage group 7 and human chromosome 11q13. *Gene* **261**, 235-42.

Zhang, Z., Harrison, P. and Gerstein, M. (2002). Identification and analysis of over 2000 ribosomal protein pseudogenes in the human genome. *Genome Res* **12**, 1466-82.

Zhou, Z. M., Sha, J. H., Li, J. M., Lin, M., Zhu, H., Zhou, Y. D., Wang, L. R., Wang, Y. Q. and Zhou, K. Y. (2002). Expression of a novel reticulon-like gene in human testis. *Reproduction* **123**, 227-34.

Zupanc, G. K., Clint, S. C., Takimoto, N., Hughes, A. T., Wellbrock, U. M. and Meissner, D. (2003). Spatio-temporal distribution of microglia/macrophages during regeneration in the cerebellum of adult teleost fish, Apteronotus leptorhynchus: a quantitative analysis. *Brain Behav Evol* **62**, 31-42.

7 List of publications

Research Articles:

- **Weidinger, G., Wolke, U., Koprunner, M., Klinger, M. and Raz, E.** (1999). Identification of tissues and patterning events required for distinct steps in early migration of zebrafish primordial germ cells. *Development* **126**, 5295-307.

- **Oertle, T., Klinger, M., Stuermer, C. A. O. and Schwab, M. E.** (2003). A reticular rhapsody: phylogenic evolution and nomenclature of the RTN/Nogo gene family. *FASEB J.* **17**, 1238-1247.

- **Klinger, M., Taylor, J. S., Oertle, T., Schwab, M. E., Stuermer, C. A. O. and Diekmann, H.** (2004). Identification of Nogo-66 Receptor (NgR) and Homologous Genes in Fish. *Mol Biol Evol* **21**, 76-85.

- **Klinger, M., Diekmann, H., Heinz, D., Hirsch, C., Hannbeck von Hanwehr, S., Petrausch, B., Oertle, T., Schwab, M. E. and Stuermer, C. A. O.** (2004). Identification of two nogo/rtn4 genes and analysis of Nogo-A expression in Xenopus laevis. *Mol Cell Neurosci* **25**, 205-16.

- **Haenisch, C., Diekmann, H., Klinger, M., Gennarini, G., Kuwada, J. Y. and Stuermer, C. A. O.** (2004) Identification and characterization of the neuronal growth and regeneration associated molecule Cntn1 (Contactin/F3/F11) in fish: potential subfunctionalization of paralogous genes *Mol Cell Neurosci* **in press**.

- **Klinger, M., Diekmann, H., Oertle, T., Pogoda, H.-M.,. Schwab, M. E. and Stuermer C. A. O.** Analysis of the reticulon gene family demonstrates the absence of Nogo-A in fish (2004) **submitted**

Poster Presentations:

- **Klinger, M., Weidinger, G. and Raz, E.** (1999). Function of IRES sequences in zebrafish. *First european meeting on Zebrafish Genetics and Development, Tübingen*.

- **Klinger, M., Motz, C., Diekmann, H., Oertle, T., Schwab, M. E. and Stuermer, C. A.** (2001). Identification of two Nogo-A encoding genes in Xenopus Laevis. *Soc. Neurosci. Abst.* **27**, Programm No 572.14.

- **Diekmann, H., Klinger, M. and Stuermer, C. A. O.** (2002). Impairment of Zebrafish Retina Development by Neurolin-Morpholino Injection. *Soc. Neurosci. Abst.* **28**, Programm No 236.15.

- **Klinger, M., Diekmann, H., Haenisch, C., Oertle, T., Schwab, M. E. and Stuermer, C. A. O.** (2002). Cloning and characterization of zebrafish reticulon genes including nogo/RTN-4. *Soc. Neurosci. Abst.* **28**, Programm No 333.14.

- **Stuermer, C. A. O, Klinger, M., Heinz, D., Diekmann, H.,** (2003). Nogo-A and *RTN4/nogo* gene transcripts in fish and frogs. *Begutachtung zum Transregio SFB Konstanz Zürich.*

- **Klinger, M., Heinz, D., Diekmann, H., Petrausch, B., Hannbeck von Hanwehr, S., Haenisch, C., Oertle, T., Schwab, M. E. and Stuermer, C. A. O.** (2004). Cloning and characterization of Xenopus and fish reticulon genes including nogo/RTN-4. *Leopoldina Symposium "From Bench to Bedside in the Neurosciences" Kartause Ittingen, Switzerland* **6th - 8th May, 2004**

Talks:

- **Race (Rapid amplification of cDNA ends) and DNA Sequencing** Vortrag im Rahmen des interdisziplinären Methodenseminars (Chemie / Biologie / Physik, 2000)

- **Regeneration im ZNS** Vortrag im Rahmen des Doktorandenkolloquiums der "Stiftung der Deutschen Wirtschaft für Qualifizierung und Kooperation e.V." (Berlin, 2002)

8 Abbreviations

aa	amino acids
AS	antiserum
B	brainstem
bp	base pair
br	brain
BS	bootstrap
cDNA	copy DNA
Chr	chromosome
cM	centimorgan
CNS	central nervous system
cR	centiray
CSPG	chondroitine sulfate proteoglycane
+ct	positive control
-ct	negative control
C-terminus	carboxy terminus
d_N	numbers of nonsynonymous nucleotidsubstitutions per nonsynonymous site
DNA	desoxyribonuleic acid
d_S	umbers of synonymous nucleotide substitutions per synonymous site
ER	endoplasmatic reticulum
ERC	endocytic recycling compartment
EST	expressed sequence tag
ey	eye
fb or F	forebrain
Fig.	Figure
gi	gill
GPI	glycosylphosphatidylinositol
he	heart
hpf	hours post fertilization
HS	heat shock
hv	higher vertebrates
HYK	Hasegawa, Kishino and Yan
K	kilobasepairs
kb	kilobases
ki	kidney
LG	linkage group
liv	liver
LRR	leucine rich repeat
LRRCT	LRR C-terminal
LRRNT	LRR N-terminal
lu	lung
Lv	lower vertebrates
M	marker

M	midbrain
mAb	monoclonal antibody
MAG	myelin associated glycoprotein
mg	milligramm
ML	maximum likelihood
ml	milliliter
mM	millimolar (mmol/l)
MP	maximum parsimony
ML	maximum likelyhood
mRNA	messenger RNA
mu	muscle
MYA	million years ago
µl	microliter
µm	micrometer
ng	nanogramm
NgR	Nogo-66 receptor
NgRH	NgR homolog
Nogo-66	66 amino acids long loop in the RHD of the Nogo proteins
N-terminus	amino terminus
OMgp	oligodendrocyte-myelin glycoprotein
PCR	polymerase chain reaction
PIP	percent identity plot
PNS	peripheral nervous system
PS	pseudogene
RACE	rapid amplification of cDNA ends
RDH	radiation hybrid mapping
ret	retina
RGC	retinal ganglion cell
RNA	ribonukleic acid
RT	room temperatur
RTN	reticulon
RTNL	reticulon-like
RT-PCR	reverse transcriptase polymerase chain reaction
sc	spinal cord
SE	standard error
sec	second
sn	sciatic nerve
SP	southern probe
te or T	tectum opticum
UTR	untranslated region
v/v	volume per volume
w/v	weight per volume
wt	wildtype
zf	zebrafish

9 Index of figures and tables

A reticular rhapsody: phylogenic evolution and nomenclature of the RTN/Nogo gene family

Analysis of the reticulon gene family demonstrates the absence of Nogo-A in fish

Identification of two nogo/rtn4 genes and analysis of Nogo-A expression in Xenopus laevis

Identification of Nogo-66 receptor (NgR) and homologous genes in fish

10 Index of supplementary material

A reticular rhapsody: phylogenic evolution and nomenclature of the RTN/Nogo gene family

Analysis of the reticulon gene family demonstrates the absence of Nogo-A in fish

Identification of two nogo/rtn4 genes and analysis of Nogo-A expression in Xenopus laevis

Identification of Nogo-66 receptor (NgR) and homologous genes in fish

11 Summary

In the mammalian nervous system, axons of the PNS can regrow upon lesion, while axons of the CNS lack this regenerative capacity. In stark contrast, CNS axons readily regenerate in fish and urodeles. Anura, like *Xenopus laevis*, take an intermediate position: retinal ganglion cell axons are capable of lifelong regeneration but spinal cord fiber tracts fail to do so after metamorphosis. Mammalian Nogo-A, a member of the reticulon family, has been shown to exert neurite growth inhibition *in vitro* via two distinct domains (one in the Nogo-A specific N-terminus and the second in the conserved C-terminus) and to restrict axonal regeneration after injury in the CNS of 'higher vertebrates'. The aim of this study was to get insights into the evolution of reticulon genes in order to clarify, whether fish and anura possess a Nogo-A homolog and if so, what its function might be in these organisms.

All proteins of the reticulon gene family contain a highly conserved carboxy-terminal reticulon homology domain (RHD) and a variable amino-terminus. This conserved RHD allowed database searches and the prediction of 300 previously unknown reticulon proteins. Reticulon-like genes were identified in deeply diverging eukaryotes, fungi, plants and animals and a systematic nomenclature for all genes has been introduced. This detailed investigation suggested that the RTNs arose during early eukaryotic evolution in paralell to the development of the ER. In vertebrates, four reticulon genes are present (RTN1-RTN4) with Nogo beeing RTN4. The analysis of exon-intron structures indicates that the exceptionally large RTN4-A-specific exon 3, that harbours one of the two axon outgrowth inhibitory sites, may has evolved *de novo* during the transition to land vertebrates.

To proof this hypothesis and to determine whether fish express an rtn4 ortholog at all, detailed analysis of fish rtns was performed. In fish, more RTN genes were observed than in mammals, which is in accordance with the prediction of a genome duplication in ray-finned fish. Phylogenetic analyses revealed that all fish sequences are orthologous to mammalian RTN1, RTN2, RTN3 and RTN4/Nogo and that two fish rtn4 orthologs (e.g. rtn4 and rtn6) were identified. The expression of various rtn4 and rtn6 splice forms was prooven by RT-PCR. Comparison of the genomic organisations and analyses of the variable N-terminal sequences argue for fundamental differences in the evolution of rtn1-rtn3 and rtn4: the specific N-termini of fish and mammalian rtn1, rtn2 and rtn3, respectively, evolved from a common ancestor, whereas the rtn4 N-termini have been acquired independently. Thus, the neurite outgrowth inhibitory region of the N-terminus of RTN4-A/Nogo-A is not present in zebrafish. This result is in accordance with earlier functional data showing that axon growth inhibitory molecules are absent from fish oligodendrocytes and CNS myelin.

In *Xenopus laevis,* I identified two independent rtn4 genes (rtn4.1 and rtn4.2) that resulted from the tetraploidization of the *Xenopus* genome. To date, the frog is therefore the 'lowest' vertebrate, in which RTN4-A/Nogo-A transcripts have been found. As in mammals, differential splicing and alternative promoter usage, give rise to *Xenopus* nogo-A, -B, -C and to a new isoform, rtn4-N/nogo-N. *Xenopus*

RTN4-A/Nogo-A is predominantly expressed in the nervous system, whereas the other isoforms mainly occur in non-neuronal tissues. The expression pattern is consistent with that observed for rat Nogo-A and suggests similar functions. Nogo-A in *Xenopus* myelin might therefore contribute to the failure of spinal cord regeneration in frogs - a feature that has evolved during the transition from fish to land vertebrates.

In mammals, no Nogo-A specific receptor, mediating the inhibitory effect of this domain, has been identified so far. On the other hand, the Nogo-66 receptor (NgR), which binds to a 66 aa loop in the RHD of RTN4, has been proposed to play an important role in axonal growth inhibition. It is an intriguing question whether fish posses an NgR ortholog. Because fish CNS axons regenerate, the functions of prospective fish NgR proteins are likely to differ from the mammalian function. In this context, I set out to identify NgR homologs in fish. Four different NgR-related genes were cloned and sequenced from zebrafish and five genes were uncovered in the fugu genome. Synteny between fish and human, comparable intron-exon structures and phylogenetic analyses provide convincing evidence that true fish NgR orthologs were identified. Phylogenetic trees show that the extra fish genes were produced by duplication events that occurred in ray-finned fishes similar to the duplication of fish rtns. Expression of zebrafish NgR homologs was detected relatively late in development and prominently in the adult brain suggesting functions in axon growth, guidance or plasticity.

These extensive analyses of gene structures, evolution and expression of NgR in fish and rtns in fish and frogs is the bases for further investigation of their function in lower vertebrates.

12 Zusammenfassung

Im Nervensystem von Säugern können Axone des PNS nach einer Verletzung wieder auswachsen, während Axone des ZNS diese Regenerationsfähigkeit nicht aufweisen. Im Gegensatz dazu regenerieren ZNS Axone von Fischen und Urodelen problemlos. Anuren wie *Xenopus laevis* haben eine Zwischenstellung: Axone retinaler Ganglienzellen können lebenslang regenerieren, wohingegen Fasertrakte des Rückenmarks diese Fähigkeit nach der Metamorphose verlieren. Säuger Nogo-A, ein Mitglied der Reticulon Familie, in der Lage ist, das Auswachsen von Neutiten *in vitro* durch zwei umgrenzte Domänen (davon eine im Nogo-A spezifischen Amino-Ende und die zweite im konservierten Carboxy-Ende) zu unterdrücken. Auch bei der Beschränkung der Axonregeneration nach der Verletzung des ZNS von „höheren" Wirbeltieren spielt Nogo-A eine Rolle. Das Ziel der vorliegenden Doktorarbeit war es, die Evolution der Reticulongene zu untersuchen. Es soll geklärt werden, ob auch Fische und Anuren ein Nogo-A verwandtes Protein besitzen und falls dies so ist, welche Funktion es in diesen Tiergruppen hat.

Die Proteine der Reticulon Familie weisen alle eine hoch konservierte carboxy-terminale Reticulon Homologie Domäne (RHD) und ein variables Amino-Ende auf. Diese konservierte RHD ermöglichte die Datenbank-Suche nach und die Herleitung von 300 bislang unbekannten Reticulonproteinen. Reticulon-artige Gene wurden in primitiven Eukaryoten, Pilzen, Pflanzen und Tieren gefunden und eine systemati-sche Benennung aller Gene wurde eingeführt. Detaillierte Untersuchungen lassen den Schluss zu, dass die RTN Familie während der frühen Eukarioten-Evolution parallel zur der Entwicklung des ER entstanden ist. In Wirbeltieren gibt es vier Reticulon-Gene, RTN1-RTN3 und RTN4/Nogo. Analysen der Exon-Intron Struktur legen nahe, dass das außergewöhnlich große, dritte Exon von Nogo-A, in dem eine der beiden Axonwachstum-inhibierenden Stellen liegt, in Landwirbeltiere neu entstanden ist.

Um diese Hypothese zu überprüfen und um festzustellen, ob Fische überhaupt ein RTN4 orthologes Gen haben, wurden die RTN-Gene in Fischen näher untersucht. Aufgrund der Genomduplikation, die höchstwahrscheinlich in Strahlen-Flossern stattgefunden hat, wurden mehr RTN Gene in Fischen als in Säugern gefunden. Stammbaumanalysen zeigten auf, dass alle Fischsequenzen entweder zu RTN1, RTN2, RTN3 oder RTN4/Nogo ortholog sind und dass zwei Fischorthologe von rtn4 (rtn4, rtn6) identifiziert wurden. Die Expression verschiedener Spliceformen von rtn4 und rtn6 wurde mittels RT-PCR überprüft. Vergleiche der genomischen Organisation und die Analyse der variablen amino-terminalen Sequenzen sprechen für einen fundamentalen Unterschied in der Evolution von rtn1-rtn3 und rtn4: die spezifischen Amino-termini von rtn1, rtn2 und rtn3 in Fischen und Säugern lassen sich jeweils von einem gemeinsamen Vorfahren ableiten, wohingegen die unterschiedlichen amino-terminalen rtn4 Enden von Fischen und Säugern unabhängig entstanden sind. Folglich ist die Region im Amino-Terminus von RTN4-A/Nogo-A, die das Auswachsen von Neuriten verhindert, in Zebrafischen nicht vorhanden. Dieser Befund stimmt mit früheren funktionellen Daten überein, die gezeigt haben, dass Axonwachstum unterdrückende Moleküle in Oligodendrocyten und Myelin von Fischen nicht vorhanden sind.

In *Xenopus laevis* habe ich zwei unabhängige rtn4 Gene (rtn4.1 und rtn4.2) identifiziert, die während der Tetraploidisierung des *Xenopus* Genoms entstanden sind. Der Frosch ist damit bislang das „niederste" Wirbeltier, in dem RTN4-A/Nogo-A Transkripte nachgewiesen werden konnten. Wie in Säugern werden alternative Transkripte sowohl durch differentielles Splicen als auch durch die Benutzung alternativer Promotoren generiert. So entstehen nogo-A, -B, und C sowie eine neue Isoform, nogo-N/rtn4-N. *Xenopus* Nogo-A/RTN4-A wird hauptsächlich im Nervensystem exprimiert, während die anderen Formen überwiegend in nicht neuronalen Geweben vorkommen. Das Expressionsmuster stimmt gut mit dem Expressionsmuster, das in Ratten beobachtet wurde, überein und legt ähnliche Funktionen nahe.

Bis dato wurde in Säugetieren noch kein Nogo-A spezifischer Rezeptor identifiziert, der den inhibierenden Effekt dieser Proteindomäne vermitteln würde. Der Nogo-66 Rezeptor (NgR), der an die 66 Aminosäuren lange Schleife in der konservierten RHD von RTN4 bindet, spielt dagegen nachweislich eine wichtige Rolle bei der Vermittlung der Inhibition des Axon-Wachstums. In diesem Zusammenhang stellt sich die interessante Frage, ob Fische auch ein NgR Ortholog haben. Da Fischaxone im ZNS regene-rieren können, ist es wahrscheinlich, dass sich die Funktion der Fisch NgR-Proteine von denen der Säugerproteine unterscheidet. Vor diesem Hintergrund habe ich begonnen, NgR homologe Gene in Fischen zu identifizieren und ich konnte vier verschiedene Zebrafischgene klonieren und sequenzieren sowie fünf Gene im Fugugenom nachweisen. Synteny-Beziehungen zwischen Fischen und Menschen, vergleichbare Exon-Intron Strukturen und Stammbaum-Analysen zeigten auf, dass zusätzliche Fisch NgR-Gene genauso wie die RTN-Gene durch Duplikationen entstanden sind. Die Expression der Zebrafisch NgR homologen Gene konnte relativ spät in der Entwicklung und in ausgewachsenen Fischen hautsächlich im Gehirn nachgewiesen werden, was Funktionen beim Wachstum, der Richtungslenkung oder der Plasti-zität von Axonen nahe legt.

Diese weitreichenden Analysen der Genstrukturen, Evolution und Expression von NgR in Fischen sowie von rtns in Fischen und Fröschen ist die Grundlage für weitergehenden Untersuchungen zu ihrer Funktion in „niederen" Wirbeltieren.

Dank

Die vorliegende Arbeit wurde in der Arbeitsgruppe von Frau Prof. Dr. Claudia A. O. Stürmer am Lehrstuhl für Entwicklungsneurobiologie an der Universität Konstanz angefertigt. Ich danke Frau Prof. Dr. Claudia A. O. Stürmer für die Bereitstellung des Themas und für ihr Vertrauen und den Freiraum, den sie mir gewährt hat. Außerdem danke ich ihr für die stets gute Ausstattung des Labors und die Möglichkeit, an Kongressen teilzunehmen.

Mein besondere Dank gilt Christina Haenisch und vor allem Heike Diekmann, mit denen ich über Jahre das Labor, die täglichen Probleme, Erfolge und Rückschläge aber auch viele schöne private Stunden geteilt habe. Unsere Diskussionen waren stets anregend und haben maßgeblich dazu beigetragen, alle unsere Projekte gemeinsam voranzubringen und publikationsreif zu machen. Das Arbeitsklima im "Nordlabor" war stets optimal.

Ich danke Thomas Oertle, mit dem ich über Jahre wunderbar kooperieren konnte. Seine stets prompten Email-Antworten, sein unerschütterlicher Optimismus und die vielen Stunden, die wir gemeinsam beim Formulieren vor dem Computer verbracht haben, waren eine große Hilfe beim Verfassen der Publikations-Manuskripte und haben mir geholfen, auch zähe Momente zu überwinden.

Ulrike Binkle, Silvia Hannbeck und Bunny Cahill haben mich bei meiner täglichen Laborarbeit unterstützt und dadurch zum Gelingen meiner Arbeit beigetragen.

Ich danke allen, die durch ihre vielfältige Unterstützung und Rücksichtnahme dazu beigetragen haben, daß ich neben der Dissertation auch meinen kommunalpolitischen Aktivitäten und Verpflichtungen nachgehen konnte.

Bei meinen Eltern möchte ich mich für ihre Unterstützung und ihr unerschütterliches Vertrauen in mich bedanken.

Ganz besonders danke ich Sibylle. Sie hat mich die ganze lange Zeit dieser Doktorarbeit unterstützt, aufgerichtet und auch in schwierigen Phasen begleitet. Danke!

Während der Zeit meiner Dissertation wurde ich von zwei Stiftungen gefördert. Mein besondere Danke gilt der "Stiftung der Deutschen Wirtschaft für Qualifizierung und Kooperation e.V. (sdw)", deren Stipendiat ich über Jahre war. Von der sdw habe ich nicht nur finanzielle Förderung, sondern auch über die Wissenschaft hinaus viele Anregungen und Hilfestellung für meinen Berufsweg erhalten. "e-fellows-net" hat mich mit einem Online-Stipendium gefördert.